https://doi.org/10.35662/unine-thesis-2887

UNIVERSITÉ DE NEUCHÂTEL

Functions of RMR proteins in intracellular trafficking in the moss *Physcomitrium patens* Mitten (previously *Physcomitrella patens*)

A dissertation submitted to the Faculty of Science of the University of Neuchâtel

For the degree of Doctor in Sciences by

Carla Coppola

Institute of Biology - Laboratory of Cell and Molecular Biology

University of Neuchâtel

Thesis committee

Prof. Jean-Marc Neuhaus (Thesis Director) - University of Neuchâtel, CH

Prof. Felix Kessler (Thesis Co-director) - University of Neuchâtel, CH

Prof. Erika Isono - University of Konstanz, DE

Defended on December 16th, 2020

Faculté des Sciences
Secrétariat-décanat de Faculté
Rue Emile-Argand 11
2000 Neuchâtel – Suisse
Tél : + 41 (0)32 718 21 00
E-mail: secretariat.sciences@unine.ch

IMPRIMATUR POUR THESE DE DOCTORAT

La Faculté des sciences de l'Université de Neuchâtel autorise l'impression de la présente thèse soutenue par

Madame Carla COPPOLA

Titre:

"Functions of RMR proteins in intracellular trafficking in the moss *Physcomitrium patens* Mitten (previously *Physcomitrella patens*)"

sur le rapport des membres du jury composé comme suit:

- Prof. Jean-Marc Neuhaus, directeur de thèse, Université de Neuchâtel, Suisse
- Prof. Felix Kessler, co-directeur de thèse, Université de Neuchâtel, Suisse
- Prof. Erika Isono, Université de Constance, Allemagne

Neuchâtel, le 15 janvier 2021

Le Doyen, Prof. A. Bangerter

Keywords: RMR, moss, vacuole, *Physcomitrium patens* Mitten, *Physcomitrella patens*, ubiquitylation, E3 ligase, phenotype, confocal microscopy, *in vitro* assay, salt stress

Mots-clés: RMR, mousse, vacuole, *Physcomitrium patens* Mitten, *Physcomitrella patens*, ubiquitination, E3 ligase, phénotype, microscopie confocale, test *in vitro*, stress salin

Table of Contents

Abbreviations

% v/v: volume/volume (ml/100 ml)
% w/v: weight/volume (g/100 ml)
µg: microgram
µl: microliter
µM: micromolar
aa: amino acid
ABA: Abscisic Acid
ADP: Adenosine Diphosphate
Amp R: Ampicillin Resistance
AP: Aspartic Proteinase
ARF: ADP Ribosylation Factor
Arg: Arginine
Asn: Asparagine
At: Arabidopsis thaliana
ATP: Adenosine Triphosphate
ATPase: Adenosine Triphosphate hydrolase
BARD1: BRCA1 Associated RING Domain 1
BFA: Brefeldin A
BiP: Binding immunoglobulin Protein
BIRC7: Baculoviral Inhibitor of apoptosis Repeat Containing protein 7
bp: base pair
BP-80: Binding Protein of 80 KDa
BRCA1: Breast Cancergene 1
BRI1: Brassinosteroid-Insensitive 1
BSA: Bovine Serum Albumin
BY-2: Bright Yellow-2
C-ter: Carboxyl-terminus
CCP: Clathrin-Coated Pit
CCV: Clathrin-Coated Vesicle
CD40: Cluster of Differentiation 40
CHIP: Carboxyl-terminus of Hsc70-Interacting Protein
Ci-Card: Citrine-Cardosin
cIAP: cellular Inhibitor of Apoptosis Protein
CME: Clathrin-Mediated Endocytosis
COPI: Coat Protein I
COPII: Coat Protein II
COPG: Coatomer Protein complex subunit Gamma
CP: Core Protease
CTPP: Carboxyl-Terminal Propeptide
ctVSD: c-terminal Vacuolar Sorting Determinant
ddH_2O: double distilled water
DDM: n-Dodecyl-β-D-Maltoside
DIP: Dark Intrinsic Protein
DMSO: Dimethyl Sulfoxide
DNA: Deoxyribonucleic Acid

dNTPs: Deoxynucleotide Triphosphates
DTT: Dithiothreitol
DUB: Deubiquitylating enzyme
DUSP: Dual-Specificity Phosphatase
DV: Dense Vesicle
E. coli: Escherichia coli
e.g.: *exempli gratia*
EDTA: Ethylenediaminetetraacetic Acid
EE: Early Endosome
EF-1α: Elongation Factor-1 alpha
EGF: Epidermal Growth Factor
ER: Endoplasmic Reticulum
ERAD: Endoplasmic Reticulum-Associated protein Degradation
ERD2: ER Retention Defective 2
ERES: Endoplasmic Reticulum Exit Sites
ESCRT: Endosomal Sorting Complexes Required for Transport
FT: Flow-Through
fw: forward
g: gram
GA: Golgi Apparatus
GAP: GTPase-Activating Protein
gDNA: genomic DNA
GDP: Guanosine Diphosphate
GEF: GTP Exchange Factor
GFP: Green Fluorescent Protein
Gly: Glycine
GRAIL: Gene Related to Anergy In Lymphocytes
GST: Glutathione-S-Transferase
GTP: Guanosine Triphosphate
GTPase: Guanosine Triphosphate hydrolase
h: hour
HdmX: Human homolog of murine double minute X
HECT: Homologous to the E6-AP (E6-associated protein) Carboxyl Terminus
His: Histidine
HR: Homologous Recombination
HS: Heat-Shock
HSP70: Heat-Shock Protein of 70 KiloDalton
Hygro R: Hygromycin Resistance
i.e.: *id est*
IDOL: Inducible Degrader Of LDLR (Low-Density Lipoprotein Receptor)
Ile: Isoleucine
IPTG: Isopropyl β-D-1-Thiogalactopyranoside
IRT1: Iron-Regulated Transporter 1
Kan: Kanamycin
Kb: Kilobase
KDa: KiloDalton
KO: Knock-Out
L: Liter

LB: Luria-Bertani
LC-MS: Liquid Chromatography - Mass Spectrometry
LE: Late Endosome
Leu: Leucine
LV: Lytic Vacuole
Lys: Lysine
M: Molar
MAPK: Mitogen-Activated Protein Kinase
Mdm2/MdmX: Murine double minute 2/Murine double minute X
MES: 2-(N-Morpholino)ethanesulfonic acid
mg: milligram
min: minute
ml: milliliter
mM: millimolar
mRNA: messenger RNA
MS: Mass Spectrometry
MVB: Multivesicular Body
MW: Molecular Weight
N. benthamiana: Nicotiana benthamiana
N. tabacum: Nicotiana tabacum
N-ter: amino-terminus, NH_2-terminus
NEDD8: Neural precursor cell-Expressed Developmentally Down-regulated 8
ng: nanogram
Ni-NTA: Nickel-Nitrilotriacetic Acid
nm: nanometer
nM: nanomolar
NR: Neutral Red
NSF: N-ethylmaleimide-Sensitive Factor
NV: Neutral Vacuole
OD: Optical Density
Os: *Oryza sativa*
PA: Protease-Associated (domain)
PAC: Precursor-Accumulating vesicles
PBS: Phosphate-Buffered Saline
PCR: Polymerase Chain Reaction
PEG: Polyethylene Glycol
Phe: Phenilalanine
PI 3-kinase: Phosphatidylinositol 3-kinase
Pic: Protease inhibitor cocktail
PIP: Phosphatidylinositol Phosphate
PIP2: Phosphatidylinositol-4,5-bisphosphate
PM: Plasma Membrane
Pp: Physcomitrium (or *Physcomitrella*) *patens*
Pro: Promoter
Prp19: Pre-mRNA-processing factor 19
PSI: Plant-Specific Insert
PSV: Protein Storage Vacuole
psVSD: physical structure Vacuolar Sorting Determinant

PVC: Prevacuolar Compartment
PVPP: Poly(vinylpolypyrrolidone)
Rab: Ras (Rat Sarcoma)-related in brain
rbcS: ribulose-1,5-bisphosphate carboxylase/oxygenase small subunit
RBR: RING-in-Between-RING
RE: Recycling Endosome
rev: reverse
RFP: Red Fluorescent Protein
RING: Really Interesting New Gene
RMR: Receptor-like Membrane RING-H2
RNA: Ribonucleic Acid
RNAse: Ribonuclease
RNC: Ribosome-Nascent Chain Complex
RNF: RING Finger protein
RP: Regulatory Particle
RT: Room Temperature
SB: Sample Buffer
SDS: Sodium Dodecyl Sulfate
SDS-PAGE: SDS-Polyacrylamide Gel Electrophoresis
sec: second
Ser-Rich: Serine-Rich (motif)
SH-EP: Sulfhydryl-Endopeptidase
SMURF1: Smad Ubiquitination Regulatory Factor 1
SNARE: Soluble NSF Attachment protein Receptor
SP: Signal Peptide
SRP: Signal Recognition Particle
ssVSD: sequence-specific Vacuolar Sorting Determinant
TBE: Tris-Borate-EDTA
TBS: Tris-Buffered Saline
TEMED: Tetramethylethylenediamine
Ter: Terminator
TGN: *Trans*-Golgi Network
TIP: Tonoplast Intrinsic Protein
TM: Transmembrane
TMD: Transmembrane Domain
Trp: Tryptophan
Tyr: Tyrosine
Ub: Ubiquitin
UBL: Ubiquitin-Like
VAMP3: Vesicle-Associated Membrane Protein 3
VCP: Valosin-Containing Protein
Vps4p/SKD1: Vacuolar protein sorting 4/Suppressor of K^+ transport growth Defect 1
VSD: Vacuolar Sorting Determinant
VSR: Vacuolar Sorting Receptor
WT: Wild Type
Y2H: Yeast Two-Hybrid
YFP: Yellow Fluorescent Protein

Abstract

In this study, I focused on a new family of receptors, called RMRs (Receptor-like Membrane RING-H2) and I tried to investigate their role in the moss *Physcomitrium patens* Mitten (previously *Physcomitrella patens*).

There is some evidence that in Angiosperms, RMRs are vacuolar receptors for the neutral/storage vacuole that is a compartment where storage proteins and metabolites are accumulated during seeds development or in somatic tissues. It is distinguished from lytic vacuole which has the same functions as animal lysosomes.

The five *Pp*RMR genes have been knocked-out, yielding viable material without visible phenotype (Ayachi, 2012). A trafficking phenotype was described by Fahr (2017) who generated the construct Citrine-Cardosin (Ci-Card) composed of the fluorescent protein Citrine fused to the C-terminal vacuolar sorting determinant (ctVSD) from cardosin A (cardosin is addressed to the vacuole in higher plants — Pereira *et al.*, 2013). The fusion protein was delivered to the central vacuole of *Pp*WT but mistargeted in *Pp*RMR-KO lines, indicating that the targeting of this protein to the vacuole depends on *Pp*RMRs.

The introduction of this thesis presents the plant endomembrane system, with particular attention to vacuolar transport and ubiquitylation.

In the second chapter, I show the techniques used to attempt to detect *Pp*RMRs by Western Blot: our failure may be due to a rapid degradation of these proteins, which could prevent their detection.

In the third chapter, I focused on *Pp*RMR2 involvement in ubiquitylation. We hypothesize that *Pp*RMRs are E3 ligases because they are members of the PA-TM-RING protein family. Most of these proteins have an E3 ubiquitin ligase activity in animals (Seroogy *et al.*, 2004; Borchers *et al.*, 2002), for this reason, we think that plant *Pp*RMRs could have this function as well, which could contribute to vacuolar targeting. Indeed, I could confirm that *Pp*RMR2 has an E3 ubiquitin ligase activity.

*Pp*RMRs substrates are still unknown in moss thus we have analysed putative candidates supposing that they could be ubiquitylated by *Pp*RMRs. We have tested this hypothesis through *in vitro* ubiquitylation assays, obtaining ambiguous results.

In the fourth chapter, I show preliminary results about the visible phenotype of *Pp*RMR-KO mutants: *Pp*WT and *Pp*RMR-KO lines displayed phenotypic differences in leafy gametophores, which were accentuated upon salt stress exposure.

Lastly, I transformed the transgenic lines *Pp*WT/Ci-Card and *Pp*5KO/Ci-Card with mutated versions of *Pp*RMR2 and analysed their effect on vacuolar transport by confocal microscopy. For most of the constructions tested, the trafficking was perturbed in both lines. Only *Pp*WT/Ci-Card expressing *Pp*RMR2ΔSer (lacking the Serine-Rich motif) displayed a typical vacuolar pattern.

Résumé

Dans cette étude, je me suis concentrée sur une nouvelle famille des récepteurs, appelés RMRs (Receptor-like Membrane RING-H2) et j'ai essayé d'étudier leur rôle dans la mousse *Physcomitrium patens* Mitten (précédemment *Physcomitrella patens*).

Chez les Angiospermes, les protéines RMRs sont considérées des récepteurs vacuolaires pour la vacuole neutre/de stockage, un compartiment où les protéines de stockage et les métabolites s'accumulent pendant le développement des graines mais aussi dans des tissues somatiques. Elle se distingue de la vacuole lytique qui a les mêmes fonctions que les lysosomes animaux.

Les cinq gènes RMRs de la mousse ont été éliminés en produisant un matériel viable sans phénotype visible (Ayachi, 2012). Un phénotype intracellulaire a été décrit par Fahr (2017) qui a généré la construction Citrine-Cardosin (Ci-Card) composée de la protéine fluorescente Citrine fusionnée au déterminant d'adressage vacuolaire C-terminal (ctVSD) de la "cardosin A" (la cardosine est adressée à la vacuole chez les plantes supérieures — Pereira *et al.*, 2013). La fluorescence a été détectée dans la vacuole centrale de *P. patens* sauvage mais faussement adressée au réticulum endoplasmique chez les lignées *Pp*RMR-KO en indiquant que l'adressage à la vacuole de cette protéine dépend des *Pp*RMRs.

L'introduction de cette thèse traite du système endomembranaire des plantes, avec une attention particulière au transport vacuolaire et à l'ubiquitination.

Dans le deuxième chapitre, je montre les techniques utilisées pour tenter de détecter les *Pp*RMRs par immunotransfert: l'échec de détection est probablement dû à une dégradation rapide de ces protéines qui pourrait empêcher leur détection.

Dans le troisième chapitre, je me suis intéressée à l'implication des *Pp*RMRs dans l'ubiquitination. Nous supposons que les *Pp*RMRs sont des E3 ligases parce-qu'elles sont membres de la famille des protéines PA-TM-RING. La plupart de ces protéines ont une activité de E3 ligase chez les animaux (Seroogy *et al.*, 2004; Borchers *et al.*, 2002), c'est pourquoi nous avons pensé que les *Pp*RMRs pourraient également avoir cette fonction chez le plantes en contribuant ainsi au ciblage vacuolaire.

Les partenaires de *Pp*RMRs étant inconnus dans la mousse, nous avons analysé des candidats en supposant qu'ils pourraient être ubiquitinés. Nous avons testé cette hypothèse par des tests d'ubiquitination par *Pp*RMR2 *in vitro*, n'obtenant que des résultats ambigus.

Dans le quatrième chapitre, je montre des résultats préliminaires sur le phénotype visible de mutants KO des RMRs de la mousse: les lignées *Pp*WT et *Pp*RMR-KO ont montré des différences phénotypiques à niveau des gamétophores qui ont été accentuées lors d'une exposition au stress salin.

Enfin, j'ai transformé les lignées transgéniques *Pp*WT/Ci-Card et *Pp*5KO/Ci-Card avec des versions mutées de *Pp*RMR2, et j'ai analysé leur effet sur le transport vacuolaire par microscopie confocale. Pour la plupart des constructions testées, le trafic a été perturbé dans les deux lignées. Seule la ligne *Pp*WT/Ci-Card exprimant *Pp*RMR2ΔSer (sans le motif riche en sérine) présentait un phénotype vacuolaire sauvage typique.

Chapter 1

General Introduction

1.1 The plant endomembrane system

The eukaryotic endomembrane system is a complex network of membrane-bounded organelles involved in production, maturation, storage and turnover of macromolecules such as lipids and proteins.

In plants it is composed of: nuclear envelope, endoplasmic reticulum (ER), Golgi apparatus (GA), *trans*-Golgi network (TGN), endosomes, multivesicular bodies (MVBs)/prevacuolar compartments (PVCs), vacuoles, plasma membrane (PM) (**Figure 1.1**). These compartments can be directly connected to each other, such as the nuclear envelope and the ER, or physically separated: in this case, they communicate via trafficking vesicles or by a maturation process (Robinson and Neuhaus, 2016).

Molecules are shuttled in vesicles that bud from a donor membrane compartment and are transported through the cytoplasm thanks to the involvement of the cytoskeleton. When vesicles reach their destination, they fuse with the membrane of the acceptor organelle where the cargo is released.

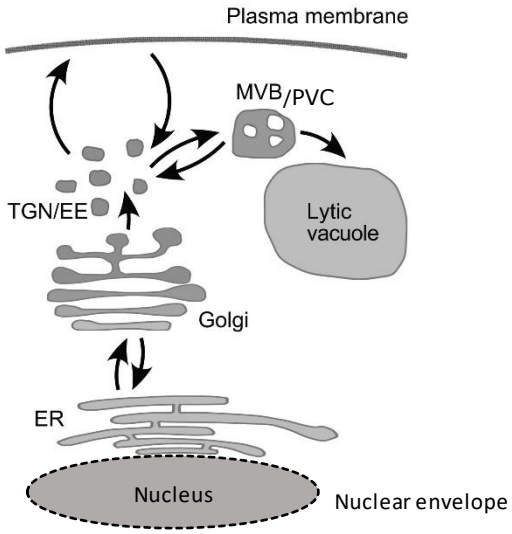

Figure 1.1. Trafficking routes for plasma membrane and vacuolar proteins in plants. The outer nuclear membrane is continuous with the endoplasmic reticulum (ER). *De novo* synthesized plasma membrane proteins are translocated into the ER, sorted through the Golgi, then carried into the *trans*-Golgi network/early endosome (TGN/EE). Vesicular trafficking mediates the transport of cargo either to the plasma membrane or via multivesicular body (MVB) compartment into the vacuole. Proteins that are endocytosed from the plasma membrane can be recycled via TGN/EE compartments, or transported to the lytic vacuole to be degraded (adapted from Luschnig and Vert, 2014).

Two different pathways exist in the cell: in the biosynthetic pathway, the proteins are synthesized in the ER, modified in the GA and transported to a final compartment (PM, lysosomes in animals or vacuoles in plants). Some proteins synthesized in the ER as well as complex polysaccharides synthesized in the GA, can be secreted from the cell, for this reason the biosynthetic pathway is also known as secretory pathway. In the opposite direction, material follows the endocytic pathway moving from the cell surface to the internal compartments of the cytoplasm (endosomes, lysosomes/vacuoles).

In plants, these two pathways have been studied as separated (Lam *et al.*, 2007) but the study of vacuolar sorting receptors in *N. tabacum* BY-2 cells revealed that the two routes converge to vacuoles. In this study (Tze *et al.*, 2004), a typical reporter of PVCs, named YFP-80, was used. The cells expressing this reporter were treated with FM4-64, a styryl dye useful to study endosomal compartments in plants (Kim *et al.*, 2001; Bolte *et al.*, 2004); it is also employed to follow bulk membrane internalization and vacuolar transport in yeast (Vida and Emr, 1995). Tze *et al.* (2004) observed that 15-30 minutes after FM-64 addition to BY-2 cells, all the YFP-positive organelles accumulated the dye, including the PVC, thus they concluded that this is an endocytic compartment.

Both pathways lead to the early endosome (which is also the TGN in plants). From there, cargo can be transported to the PM, to the Golgi apparatus, or to the PVC/MVB, and then to the vacuoles.

1.1.1 The secretory pathway

Endoplasmic Reticulum

The endoplasmic reticulum (ER) is a dynamic compartment composed of distinct domains such as the nuclear envelope, sheets (also called *cisternae*; Park and Blackstone, 2010) and a tubular network that forms membrane contact sites (MCS) with diverse organelles and with the PM (Wu *et al.*, 2018). These domains are involved in the synthesis of proteins and lipids, proteins folding, quality control, carbohydrates metabolism, maintenance of calcium homeostasis and materials exchange with other organelles (Reid and Nicchitta, 2015; Westrate *et al.*, 2015).

This multifunctional organelle is subdivided into two types, both present in animal and plant cells: the rough ER and the smooth ER. The rough ER is so-called because of the presence of ribosomes bound on its cytosolic face, which are engaged in the synthesis of secretory and membrane proteins, whereas free ribosomes synthesize soluble proteins (Lerner *et al.*, 2003). Lipids and steroid hormones are produced in the smooth ER (Sparkes *et al.*, 2009; Lynes and Simmen, 2011) that has no ribosomes on its surface.

Protein translation starts in the cytosol: here the free ribosomes are addressed to the ER membrane via a signal peptide (SP) of 16-30 residues present at the N-terminus of the nascent polypeptide. In this

process, the SP allows the targeting of the ribosome-nascent chain complex (RNC) to the ER membrane, where the SP is bound by the signal recognition particle (SRP) which also pauses translation. Some studies have shown that SRP binds to RNC only when the nascent hydrophobic N-terminal motif emerges from the ribosome (Luirink and Sinning, 2004), but according to other works, this recognition may occur in the earlier stages of the translation (Chartron *et al.*, 2016; Voorhees and Hegde, 2015). The binding of SRP to its receptor (SR) leads to the dissociation of SRP from the ribosome, and following GTP hydrolysis, SRP and SR dissociate from each other (Shan *et al.*, 2009). Therefore, the ribosome can bind to the translocon channel (called Sec61 in eukaryotes and SecY in prokaryotes) which is a heterotrimeric complex composed of α- (forming the pore of the channel), β- and ɣ- subunits. Translation resumes and the polypeptide is translocated through the ER membrane. After translocation of the protein across the membrane, the signal peptide is cleaved by a signal peptidase in the ER lumen, and degraded, while the protein synthesis continues until it reaches its final conformation (Nam and Paetzel, 2013; Voss *et al.*, 2013). If the signal peptide is not cleaved, the protein will be anchored in the membrane. This process is called co-translational translocation because it is concurrent with the protein synthesis by the ribosome, and it is distinguished from post-translational translocation in which the protein is translated in the cytosol and later transferred into ER (Ellgaard *et al.*, 2016). In this case, the SRP is not required: the Sec61 complex and other receptor proteins (Sec62/63 complex) recognize the signal peptide, while cytosolic chaperones maintain the unfolded conformation of the polypeptide chain during its entry in the Sec61 channel; the receptor BiP (binding immunoglobulin protein) intervenes to pull the protein into the channel and into the ER (Cooper, 2000). In eukaryotes, post-translational translocation has mostly been observed in yeast.

Quality Control

In plants, stress conditions due to abiotic and biotic agents may prevent the correct folding causing an accumulation of aberrant proteins in the ER (Liu and Howell 2010; Verchot, 2016). Here, molecular chaperones (luminal binding protein BiP, calnexin, calreticulins, protein disulfide isomerase PDI) ensure the proper folding of the proteins and prevent the aggregation of the misfolded ones (Nawkar *et al.*, 2018). A cytoprotective response called UPR (unfolded protein response) is invoked by the cell to overcome the ER stress: when this happens, the level of molecular chaperones increases and the ER-associated protein degradation (ERAD) is enhanced (Liu and Howell, 2016). The aberrant proteins are then addressed to the cytosol for proteasomal degradation (McCaffrey and Braakman, 2016) or targeted to lysosomal/vacuolar degradation mediated by endosomal sorting complexes required for transport (ESCRT) (Inada and Ueda, 2014).

ERAD

Misfolded proteins are retained in the ER and then eliminated by the ERAD machinery: first, they are retro-translocated to the cytosol, then polyubiquitylated and degraded by the 26S proteasome, that is composed of a cylindrical 20S core protease (CP) capped on each end by a 19S regulatory particle (RP) (Inada and Ueda, 2014; Moon *et al.*, 2004). The CP is an ATP-dependent complex, also involved in ubiquitin independent proteolysis; the RP receives the ubiquitylated proteins, assists in deubiquitylation, and opens the channel of the CP allowing the unfolded substrate to enter and be degraded (Smalle and Vierstra, 2004). Depending on the location of the folding defect, different ERAD pathways have been described in *S. cerevisiae*: defects in the cytosolic domain of membrane proteins (ERAD-C) are detected by the DOA10 complex; if the lesion is located in the luminal domain (ERAD-L) or in the transmembrane domain of proteins (ERAD-M), the HRD1 complex will be invoked for the degradation pathway (Carvalho *et al.*, 2006). The aberrant substrates detected by HRD1 or DOA10 complexes are retro-translocated across the ER membrane, ubiquitylated and transferred by the AAA-ATPase VCP/Cdc48 into the cytoplasm; from here, they are delivered in a soluble state to the proteasome, where they are degraded (Hiller *et al.*, 1996; Jarosch *et al.*, 2002; Wu and Rapoport, 2018).

In *A. thaliana*, the HRD1 complex is involved in abiotic and ER stress responses (Hüttner and Strasser, 2012; Van Hoewyk, 2018) while in rice it is implicated in the formation of protein bodies in the endosperm (Ohta and Takaiwa, 2015). Together with HRD1, the E3 ligase DOA10 negatively regulates thermotolerance in *A. thaliana* (Li LM *et al.*, 2017).

It has been shown that BRI1-5 and BRI1-9 (variants of the heavily glycosylated receptor brassinosteroid insensitive 1) with misfolded luminal domains, undergo glycan-dependent ERAD (Jin *et al.*, 2007; Hong *et al.*, 2008).

A ubiquitin-independent proteasomal degradation pathway has been described in animals: in this case, proteins are degraded by 20S proteasomes (Asher *et al.*, 2006). Among them, the ornithine decarboxylase (ODC) has been identified, together with cellular proteins called p21, p73, BIMEL (Asher *et al.*, 2005; Wiggins *et al.*, 2011) and highly oxidized proteins (Shringarpure *et al.*, 2003). In animals, the regulator of cell cycle, p53, is subjected to both ubiquitin-dependent and independent degradation (Asher and Shaul, 2005).

Trafficking from ER to Golgi

In the early secretory pathway, all the proteins that have passed the ER quality control, initiate an anterograde transport from ER exit sites (ERES) to the GA through the coat protein complex II (COPII), while all the proteins that need to travel back from GA to ER are transported in COPI vesicles (daSilva *et al.,* 2004; Matheson *et al.,* 2006) (**Figure 1.2**).

COPII is formed by three cytosolic components: the GTPase Sar1 and the two heterodimers Sec 23/24 and Sec 13/31 (Barlowe *et al*., 1994). It is not clear how the ER and the Golgi are connected, but it is thought that there are closed compartments such vesicles and tubules that allow the transport of cargoes from ER to Golgi (Hanton *et al*., 2006).

The mechanism of export of soluble cargoes needs to be elucidated: probably they are transported by means of a bulk flow (Phillipson *et al*., 2001). For other proteins such transmembrane proteins, the process could also be dependent on specific motifs recognized by COPII proteins (Robinson *et al*., 2015), but it is not known yet whether these signals recruit or are recruited by COPII (Contreras *et al*., 2004; Hanton *et al*., 2005).

The recruitment of COPII begins with the activation of the small GTPase Sar1 (Nakano and Muramatsu, 1989): in this process, the complex Sar1-GDP is converted in Sar1-GTP by the guanine nucleotide exchange factor GEF-Sec12 (Nakano *et al*., 1988). Once Sar1 binds to GTP, it exposes its N-terminal amphipathic tail which penetrates the lipid bilayer (Bielli *et al*., 2005). The bond of Sar1-GTP to the membrane allows the recruitment of Sec23/24 heterodimer (Barlowe *et al.,* 1994; Hicke *et al.,* 1992). The Sec23/24-Sar1 is then ready to select and bind the cargo, forming the so-called prebudding complex (Aridor *et al*., 1998). This complex recruits the heterotetramer Sec13/31 permitting the formation of a scaffold for the outer layer of the COPII coat (Lederkremer *et al*., 2001; Fath *et al*., 2007). COPII vesicles (70-80 nm in diameter) bud from the donor membrane and mediate the transport of the cargo to either the ER-Golgi-intermediate compartment (ERGIC) or the Golgi complex (Sato and Nakano, 2007). Sec23 activates the hydrolysis of Sar1-GTP and the consequent disassembly of COPII coat (Kurokawa *et al*., 2016).

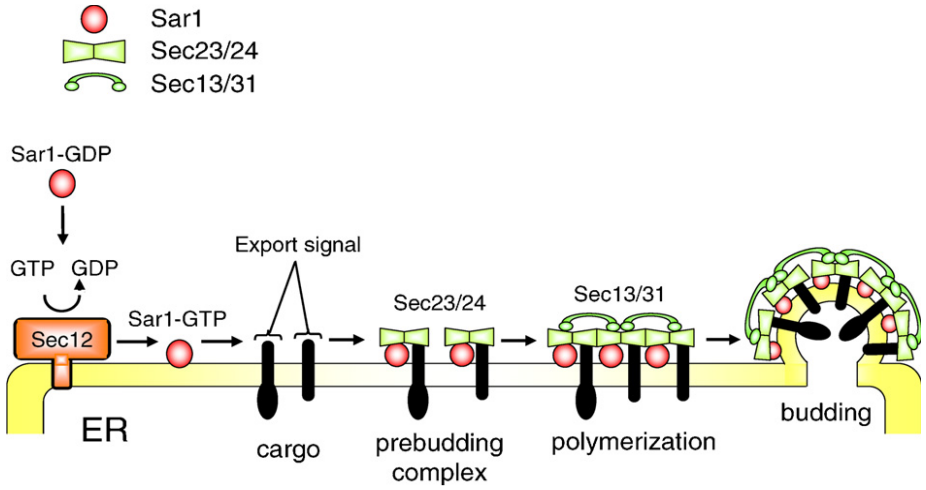

Figure 1.2. COPII vesicle formation and the selective uptake of cargo proteins. GDP-GTP exchange on Sar1 is catalysed by the transmembrane guanine nucleotide exchange factor Sec12. Sar1-GTP binds to the ER membrane and recruits the Sec23/24 subcomplex. The transmembrane cargo exposes its signal into the cytosol which is captured by Sec24. The newly formed "prebudding complex'' is clustered by the Sec13/31 subcomplex, generating COPII coated vesicles (adapted from Sato and Nakano, 2007).

The retrograde transport of the escaped ER resident proteins is mediated by the COPI complex, also called coatomer (**Figure 1.3**). This is composed of a GTPase ADP-ribosylation factor 1 (ARF1) and a heptameric complex divided in a B-subcomplex (α, β' and ε subunits) and a F-subcomplex (β, γ, δ and ζ subunits; Waters *et al.*, 1991; Rothman and Wieland 1996; Eugster *et al.*, 2000). GDP-ARF1 is recruited to the Golgi membrane by a guanine nucleotide exchange factor (GEF) that catalyses the loading of GTP on ARF1 (Donaldson *et al.*, 1992). This causes a conformational change of ARF1 so that it can anchors into the membrane through its myristoylated N-terminal amphipathic helix (Antonny *et al.*, 1997; Liu *et al.*, 2009). ARF1-GTP recruits the coatomer to the Golgi membrane: during this recruitment, a type I transmembrane protein p23 participates in the COPI coat assembly (Sohn *et al.*, 1996; Bremser *et al.*, 1999); p23, a member of p24 protein family (Gommel *et al.*, 2001), was identified as ARF1-GDP receptor. Once COPI-coated vesicle is formed, the Arf1 GTPase-activating proteins (ArfGAPs) catalyse the GTP hydrolysis inducing the dissociation of ARF1 from GTP and the uncoating of the COPI vesicle (Tanigawa *et al.*, 1993; Beck *et al.*, 2009).

Homologues of COPI complex components have been found in plants (Hanton *et al.*, 2005). It has been shown that if COPI is inhibited, the ER export is impaired and the ERES disrupted (Stefano *et al.*, 2006), leading to the hypothesis that ARF1 plays a role in both retrograde and anterograde transport.

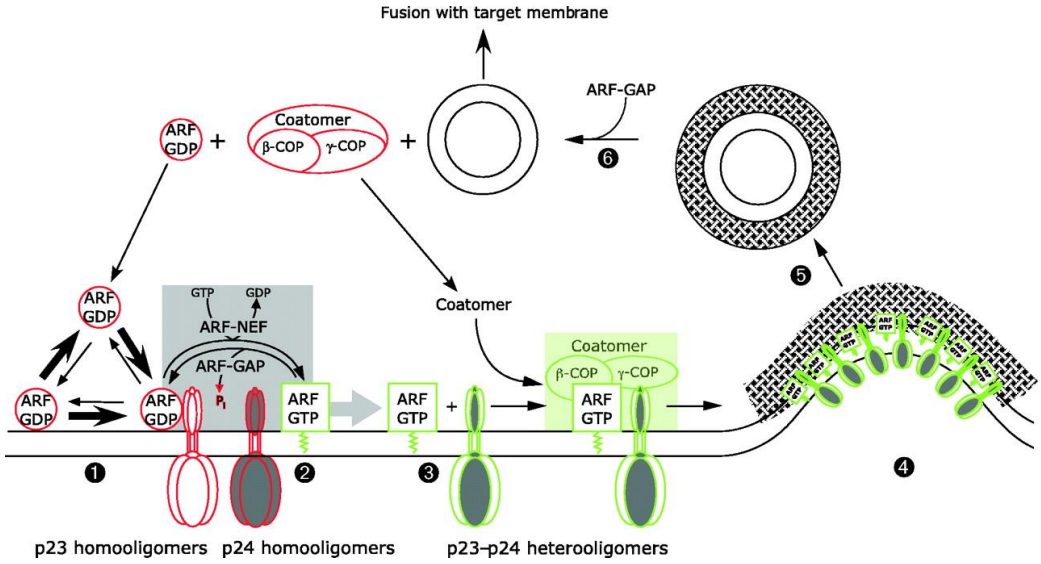

Figure 1.3. The core machinery of COPI recruitment to membranes, coat polymerization, vesicular budding and uncoating. The bond of ARF-GDP to p23 is the first step for the recruitment of coat proteins (**1**). Following nucleotide exchange, ARF-GTP dissociates from p23 and binds to the membrane (**2**). GDP to GTP exchange (grey box) causes rearrangements of p23/p24 oligomers (**3**). ARF-GTP and presumably a p23/p24 heterooligomer are generated from this process, thus activating coatomer binding and coat polymerization (**4**). Following budding (**5**), the catalytic domain of ARF-GAP triggers uncoating (**6**). Active components are shown in green; inactive components are shown in red (adapted from Nickel *et al.*, 2002).

COPI vesicles are engaged in the transport of soluble proteins such as the escaped resident ER glycoproteins, many of which have a C-terminal KDEL sequence (HDEL in yeast) that prevents their secretion (Munro and Pelham, 1987). In yeast, it has been shown that the transport of HDEL proteins from Golgi to ER is mediated by ERD2 receptor (HDELR). *In vivo* studies showed that ERD2 localizes to the *cis*-Golgi apparatus (Silva-Alvim *et al.*, 2018). The interaction between ERD2 and HDEL-ligands occurs in the Golgi due to the acidic pH in this compartment. The bond causes the dimerization and a conformational change of ERD2 leading to the generation of a COPI binding motif. Once HDEL ligands are retrieved to the ER, the neutral pH of this compartment causes their dissociation from ERD2 (Robinson and Aniento, 2020).

A Golgi independent pathway

In the cotyledon cells of mung bean seedlings, the KDEL-tailed cysteine proteinase SH-EP reaches the protein storage vacuole (PSV) bypassing the Golgi apparatus (Toyooka *et al.*, 2000). This result has been obtained by performing an immunogold assay with an anti-SH-EP antibody: it was shown that ER and KDEL-vesicles were labelled but the GA was not. On the other side, the antibody against the vacuolar protease asparginyl endopeptidase labelled the Golgi and the vacuoles, but not the KDEL-vesicles (KVs). This indicates that KDEL vesicles bypass the Golgi and fuse with PSV (Okamoto, 2006).

In the maturing seeds, it was also found that the precursor-accumulating (PAC) vesicles mediate protein transport directly to PSV (Hara-Nishimura *et al.*, 1998). On the periphery of PAC vesicles, storage glycoproteins were found, suggesting that the vesicles which transport these proteins, bud from Golgi and fuse with PAC vesicles on the way to the PSV (Hanton *et al.*, 2005). It might also be possible that these glycoproteins are transported to Golgi to be processed, then they would be recycled to ER for packaging into PAC vesicles, and transported to PSV (Hanton *et al.*, 2005).
In developing wheat seeds, the storage proteins aggregate in the ER, and budding from here, they form protein bodies which are internalized in the PSV through a mechanism similar to autophagy (Ibl and Stoger, 2011; Herman, 2008).

Golgi Apparatus

The plant GA has the function to modify, sort and package the macromolecules, thus representing an important traffic point between ER, vacuoles and plasma membrane.
Plant and animal GA have a different structure. In animal cells, the GA occupies a stationary perinuclear position, while in plant cells the GA is divided into individual and functionally independent Golgi stacks, distributed all over the cytoplasm (Vildanova *et al.*, 2014); each stack is made up of four - eight *cisternae* organized in *cis*-Golgi (near to ER), medial-Golgi (central) and *trans*-Golgi (far from ER). Proteins and lipids coming from ER, are packaged into transport vesicles, enter the *cis* face and exit from the *trans* face to reach their final destination (Foresti and Denecke, 2008).
The GA is also involved in the biosynthesis of hemicellulose and acidic pectic polysaccharides which are very important components of the cell wall matrix (Driouich *et al.*, 2012).
In animals, proteins and lipids arrive at the *cis*-Golgi in clusters of fused vesicles that migrate through microtubules forming the vesicular tubular cluster (Martínez-Menárguez *et al.*, 1999).
In the GA, the molecules undergo modifications, including cleavage or addition of short chains of sugars moieties, addition of fatty acids or phosphate groups (Ruiz-May *et al.*, 2012; Stanley, 2011). The enzymes responsible for these modifications are found in the different compartments of the GA, for example, the mannose moieties are cleaved in *cis* and medial *cisternae*, while the galactose or the sulphate are added in the *trans cisternae* (Stanley, 2011). All the modified proteins and lipids reach the *trans*-Golgi network (TGN) where they are packaged into vesicles at the *trans* face, and from here, they are transported to their final destination (lysosomes or vacuoles, cell membrane).
It is still unclear how proteins and lipids move from *cis*- to *trans*-Golgi, but two prevailing models have been suggested (Emr *et al.*, 2009; Pelham and Rothman, 2000). According to the first one, called "vesicle-transport model", the vesicles bud off from a cisterna and fuse to the next one, or carry the molecules back to the ER; this model proposes the GA as a stationary compartment. In the other model named "cisternal progression model", the cargo would remain in a compartment while specific

enzymes convert the *cis* cisterna into a medial one, or the medial cisterna into a *trans* one. It implies retrograde transport of cisternal specific enzymes as part of the maturation process. This indicates that the GA is a dynamic organelle (Pfeffer, 2010).

Trans-Golgi Network (TGN)

The TGN is found on the *trans* side of GA and is involved in cargo sorting, packaging and delivering to the PM or lysosomes/vacuoles (Griffiths and Simons, 1986).

The plant TGN is important for the assembly of the cell wall and the organization of the traffic to and from the PM, whereas in animal cells, these two pathways are separately confined to TGN and endosomes (Rosquete *et al.*, 2018).

In plant cells, the TGN is also called early endosome (EE) because it plays a role in trafficking and recycling of endosomal material (Dettmer *et al.*, 2006; Viotti *et al.*, 2010). A model for TGN biogenesis in plants was proposed by Kang *et al*. (2011).

Studies of cell fractionation and electron microscopy/tomography demonstrated that two types of TGN exist: the Golgi-associated TGN (GA-TGN) *cisternae* which are attached to the *trans* side of Golgi, and the free TGN *cisternae*, that are detached. Clathrin-coated vesicles (CCVs) and secretory vesicles (SVs) buds were found in both fractions, but they were more abundant in the free TGN *cisternae* (Rosquete *et al.*, 2018).

Treating *N. tabacum* BY-2 cells with the fungal inhibitor brefeldin A (BFA), the TGN, endosomal and Golgi material undergo aggregation in large intracellular bodies (Langhans *et al.*, 2011) but when BFA is removed, Golgi and TGN population regenerate independently, indicating that plant TGN is an independent compartment (Ito *et al.*, 2017).

Endosomes

Endosome trafficking in plants is essential for the composition and the structure of the plasma membrane and cell wall (Toyooka *et al.*, 2009), for the maintenance of the vacuole and cell growth (*e.g.* pollen tube growth; Richter *et al.*, 2012; Šamaj *et al.*, 2006). Endosomes have also a key role in generating cell polarity and in hormonal and defense signaling (Contento and Bassham, 2012).

Proteins coming from both biosynthetic and endocytic pathways converge in the endosomes. Endocytosed plasma membrane proteins have two possible destinies: they can be recycled back to PM by means of early and recycling endosomes (EE and RE) or can be targeted for degradation through internalization in intermediate/late endosomes (LE), also called multivesicular bodies (MVBs, spherical compartments containing internal vesicles; Otegui and Reyes, 2010).

Different marker proteins such as the Rab GTPases can be found in these compartments: EE contain RAB4 and RAB5; in the RE, RAB11 is more abundant, while RAB7 or mannose6-phosphate (in animals) might be detected in LE (Huotari and Helenius, 2011).

The most important plant endosomal compartments are identified as TGN or EE, and MVB or LE; the MVB is also called prevacuolar compartment (PVC) because here, endocytic and biosynthetic vacuolar trafficking meet (Tse *et al.*, 2004). When receptors gradually decrease, the PVC matures into a late PVC that is found between the PVC and the vacuole (Foresti *et al.*, 2010). Other types of endosomes could exist, but more investigations need to be done (Contento and Bassham 2012).

The endosomal trafficking in plants is essential for signaling, and requires several plasma membrane kinase receptors: the steroidal plant hormone receptor brassinosteroid insensitive 1 (BRI1), responsible for cell expansion and division, has been shown to localize to both PM and EE in *A. thaliana* (Geldner *et al.*, 2007).

A model proposed by Scheuring *et al*. (2011) shows that in *Arabidopsis thaliana*, the TGN matures into MVB which finally fuses with the tonoplast of the vacuole to release the cargo.

In plant cells, proteins are exchanged between PM and endosomes in a process called "constitutive cycling", so that the cells are able to easily control the rapid changes in plasma membrane composition: examples of these proteins are the auxin carrier PIN-FORMED1 (PIN1), the water channel PIP2 and the K^+ channel KAT1 (Otegui and Reyes, 2010). The auxin regulates many growth and developmental processes, thus having an inhibitory effect on endocytosis (Paciorek *et al.*, 2005); the abscisic acid induces the endocytosis and the recycling of KAT1 that is an important channel for the regulation of stomatal opening (Sutter *et al.*, 2007).

Endosomes play an essential role in the degradation of membrane proteins. While soluble proteins are degraded by the cytosolic 26S proteasome, the plasma membrane proteins, once ubiquitylated, are delivered to endosomes where they are recognized by endosomal protein complexes and sorted into vesicles, generating the MVBs; this is a quite unique endosomal invagination in which a small vesicle forms inside the endosome, but in most cases, the vesiculating membrane buds away from the cytoplasm. ESCRT also generates exosomes and ectosomes in animals but their biogenesis in plants is still not clear.

The fusion of MVBs with vacuoles/lysosomes causes the release of the endosomal vesicles in the lumen where they are degraded by hydrolytic enzymes (Otegui and Reyes, 2010).

A crucial role in this process is played by the complexes ESCRT-0, -I, -II and -III.

ECRT-I, II and -III were identified because of their involvement in the biogenesis of intraluminal vesicles (ILV) of MVB (Bassham *et al.*, 2008); ESCRT-0 was discovered later, and it is so-called because it acts upstream of ESCRT-I (Raiborg and Stenmark, 2009). ESCRT-0, ESCRT-I and ESCRT-II contain ubiquitin-binding subunits through which they bind the ubiquitylated transmembrane cargo at the late

endosome membrane, and initiate membrane invagination (Frankel and Audhya, 2018). In yeast, ESCRT-III is composed of Vps20, Snf7, Vps24, and Vps2 subunits. It drives membrane budding and scission of vesicles (Schöneberg *et al.*, 2017). It represents the main complex responsible for the formation of ILVs and participates also in virus budding, cytokinesis reactions (Raiborg and Stenmark, 2009) and autophagy (Rusten and Stenmark, 2009). The energy necessary to form MVB vesicles comes from the ATPase activity of Vps4p/SKD1 which is also required in the disassembly and recycling of ESCRT coat (Schmidt and Teis, 2012).

Protists and plants lack ESCRT-0 which is replaced by TOM1 proteins: these are involved in ubiquitylated cargo sorting and recruitment of ESCRT-I components from the cytoplasm (Richardson *et al.*, 2011; Wang T *et al.*, 2010). As in yeast, ESCRT-III forms stable protein complexes in the cytoplasm, and together with the ATPase Vps4p/SKD1, it is required for membrane fission and the releasing of the nascent vesicle in the MVB lumen.

Vacuoles

Vacuoles are dynamic multifunctional compartments surrounded by a membrane, the tonoplast. More than one kind of vacuole can be found in one single plant cell (Paris *et al.*, 1996; Epimashko *et al.*, 2004) but, depending on the cell types, vacuoles can fuse to form a unique large central compartment which can occupy more than the 80% of the total cell volume (Marty, 1999). Plant vacuoles are involved in nutrient accumulation, turgor maintenance, pH balancing, homeostasis, defense.

They can be subdivided into three different types: the acidic vacuole, named also lytic vacuole (LV) is equivalent to animal lysosomes; it is abundant in vegetative organs and contains hydrolytic enzymes involved in digestion and turnover of several compounds. The neutral vacuole (NV) is found in vegetative tissues; the protein storage vacuole (PSV) instead is involved in the accumulation of storage proteins (Marty, 1999; Frigerio *et al.*, 2008) and is located in seeds, in leaf cells, and in specialized vegetative cells in response to wounding or to developmental switches (Jauh *et al.*, 1998). LV and NV have different pH which can be visualized using probes sensitive to acidic environments (Swanson *et al.*, 1998). Lytic vacuoles accumulate the pH-sensitive dye Neutral Red, neutral vacuoles do not (Di Sansebastiano *et al.*, 2001).

Xiang *et al*. (2013) described a classical Golgi route, showing that vacuolar proteins are packaged into vesicles and pass through the Golgi before being delivered to the vacuole.

A Golgi-independent pathway is preferred (unconventional route) in particular conditions such as plant development, stress conditions, storage protein accumulation in seeds, upregulation of protein expression. In these situations, the unconventional route is faster and more efficient (De Marchis *et al.*, 2013).

Insoluble protein aggregates, soluble and tonoplast proteins can bypass the Golgi and directly reach the vacuole (Herman, 2008; De Marchis *et al*., 2013).

1.1.2 Vesicle transport pathway in plants

As mentioned above, the transport of cargoes to their final destination is mediated by three important coated vesicles: COPI, COPII and clathrin-coated vesicles, helped by small GTPases (**Figure 1.4**). According to the classical model, after the formation of the bud in the donor compartment, the vesicle containing the cargo is delivered to the acceptor compartment where it fuses with the target membrane allowing the subsequent release of the content (Paul and Frigerio, 2007).

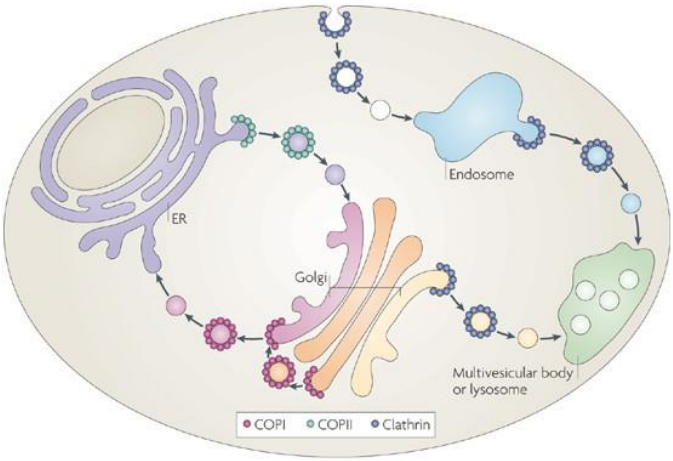

Figure 1.4. The coated vesicles. COPII and COPI deliver proteins between ER and Golgi by anterograde and retrograde transport, respectively. Clathrin-coated vesicles mediate protein transport between TGN and endosomes (adapted from Hsu *et al*., 2009).

SNAREs (Soluble NSF Attachment Protein Receptors)

A regulatory machinery composed of GTPases, tethering factors, and SNAREs, is necessary to control vesicle trafficking. The SNARE complexes, responsible for the final membrane fusion, comprise four SNAREs: three have a glutamine residue in the SNARE motif (Q-SNAREs) and reside on the target membrane, in fact they are also called t-SNAREs; one has a central arginine (R-SNARE) in the SNARE motif and is found on the transport vesicle, thus it is called v-SNARE. The v-SNARE and t-SNAREs create a kind of bridge between the transport vesicle and the target membrane, then by forming a 4-helix bundle, they induce their fusion (Saito and Ueda, 2009). After membrane fusion, the N-ethylmaleimide-sensitive factor (NSF) and the alpha-soluble NSF attachment protein (α-SNAP) are involved in the dissociation and recycling of the SNARE complex (Gu *et al*., 2017).

1.1.3 The endocytic pathway

In the endocytosis process, the cells take up macromolecules and particulate substances enclosing them in an endocytic vesicle through the invagination of the plasma membrane.

A well-known form of endocytosis is the receptor-mediated endocytosis, essential in mammal cells for the uptake of cholesterol and other macromolecules. These need to bind to specific receptors of the plasma membrane, often located in clathrin-coated pits (CCPs). After budding from the membrane, they give rise to clathrin-coated vesicles (CCVs) in which the receptors and their ligands are incorporated; vesicles fuse to early endosomes where the content is released and then transported to lysosomes or vacuoles (Chen *et al.*, 2011).

Clathrin consists of three heavy and three light chains forming a triskelion which assembles in a basket-like "clathrin lattice" (Kirchhausen, 2000; Wilbur *et al.*, 2005). The formation of the clathrin lattice (**Figure 1.5**) requires the accumulation of phosphatidylinositol-4,5-bisphosphate (PIP2) and several proteins, including the adaptor protein complexes (AP1, AP3, AP4 at TGN, AP2 at PM, AP5 in the LE) at the pinching site (Mousavi *et al.*, 2004; Park and Guo 2014; Hirst *et al.*, 2011). Once the cargoes have been selected by the clathrin adaptors, the clathrin coat grows and forms a CCP: the assembly of CCP requires the participation of PIP2 and several actin-binding proteins, such as the ones belonging to the BAR (Bin-Amphiphysin-Rvs167) superfamily. These BAR proteins are involved in membrane deformation and promote its tabulation (Yoshida *et al.*, 2018). The CCP invaginates until it forms a thin membrane neck: here, the GTPase dynamin assembles into helical polymers, promoting the scission from the plasma membrane (Hinshaw, 2000). The generated free endocytic vesicle will transport its cargo to TGN or EE. The cargo can be carried to the PM or targeted to the vacuole where it is degraded (Viotti *et al.*, 2010; Reynolds *et al.*, 2018).

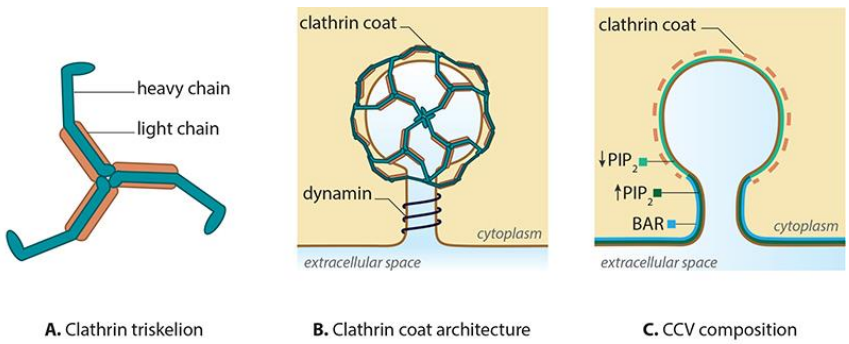

Figure 1.5. Clathrin-Coated Vesicles. Clathrin is assembled in a triskelion (**A**). Clathrin forms a coat around the vesicle (**B**). PIP2 levels and BAR protein binding are necessary for membrane curvature and thus for the formation of the clathrin-coated vesicle (**C**) (adapted from www.mechanobio.info).

In plants, besides the clathrin-mediated endocytosis (CME), an alternative route exists, the so-called membrane microdomain-associated endocytosis, that is clathrin-independent (**Figure 1.6**). Two membrane microdomain marker proteins are involved in this route: flotillin and remorin, the first one containing a stomatin/prohibitin/flotillin/HflK/C (SPFH) domain (Haney and Long, 2010). In *Arabidopsis thaliana*, Flotillin1 (Flot1) is required for seedlings development (Li R *et al.*, 2012) and the regulation of signal transduction via endocytosis (Wang *et al.*, 2013). Remorin has no SPFH domains and is an important component of plasmodesmata and PM (Raffaele *et al.*, 2009; Jarsch *et al.*, 2014).
In tomato, the sucrose transporter SlSUT2 is thought to be internalized into the cell through the membrane microdomain-associated pathway (Bitterlich *et al.*, 2014). In tobacco BY-2 cells, glucose is also taken up via clathrin-independent endocytosis (Bandmann and Homann, 2012).

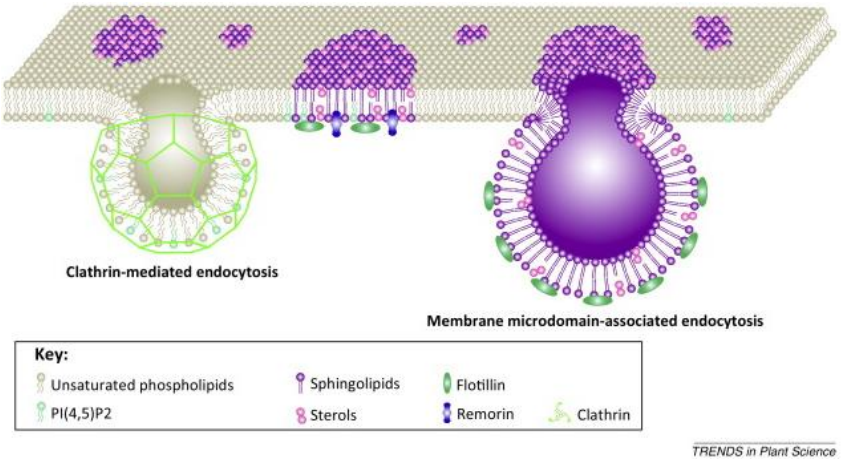

Figure 1.6. Endocytic pathways identified in plants. Clathrin-mediated endocytosis (CME) and membrane microdomain-associated endocytosis have been described in plants. CME is essential for the entry of extracellular material into plant cells. Membrane microdomains are nanodomains at the plasma membrane (PM) mainly composed of sterol and sphingolipids. Two membrane microdomain marker proteins, flotillin and remorin, have been identified: flotillin participates in the clathrin-independent endocytic pathway (adapted from Fan *et al*., 2015).

1.1.3.1 Endocytosis and ubiquitylation

The studies on IRT1 root iron transporter, BOR1 boron transporter, and PIN2 auxin efflux carrier, elucidated the role played by ubiquitin (Ub) in plant PM protein endocytosis and vacuolar degradation (Barberon *et al.*, 2014; Leitner *et al.*, 2012). These proteins are post-translationally modified by ubiquitylation of lysine residues in their cytosolic loops. An important study showed that if the target lysines were substituted by non-ubiquitinatable arginine residues, the three proteins were expressed but not endocytosed, leading to their accumulation at the plasma membrane and preventing their degradation in the vacuole in response to gravistimulation or boron excess (Barberon *et al.*, 2014;

Leitner *et al*, 2012). These results were supported by other studies demonstrating that the presence of Ub on an artificially ubiquitylated PM protein cargo (carrying in-frame fusion with Ub) was a sufficient signal for its transport to the vacuolar lumen (Herberth *et al.*, 2012; Scheuring *et al.*, 2012).
Other PM proteins that undergo ubiquitin-mediated endocytosis (UbME) are the brassinosteroid insensitive receptor BRI1 (Martins *et al.*, 2015), the phosphate transporter PHT1-1 (Scheuring *et al.*, 2012; Cardona-López *et al.*, 2015), and the membrane-associated ABA receptors PYL4/PYR1 (Bueso *et al.*, 2014).
In this process, endocytic adaptor proteins recruit the Ub cargoes into clathrin-coated pits. Epsins for instance, are well-known adaptors containing Ub-interacting motifs. They are characterized by the epsin N-terminal homology (ENTH) and the AP180 N-terminal homology (ANTH) domains that associate with clathrin, AP2 adaptor complex and PIP2 (Traub, 2009).
While Ub-mediated endocytosis occurs mainly via the clathrin-dependent endocytosis (Barberon *et al.*, 2011; Scheuring *et al.*, 2012), the work of Sigismund *et al.*, (2013) describes the Ub-dependent but clathrin-independent internalization of the mammalian EGF receptor. This mechanism needs to be elucidated in plants where the internalization mechanisms and the internalization pathways do not always match: this is the case of some cargoes that undergo UbME (such as BRI1) but are internalized via clathrin-independent processes (Wang *et al.*, 2015).

1.2 Different types of vacuoles in plants

The different vacuolar types are defined by specific membrane markers, the tonoplast intrinsic proteins (TIPs). It has been shown that the isoforms α-TIP and δ-TIP are the markers for PSV (Jauh *et al.*, 1998), whereas γ-TIP is the marker for LV (Jauh *et al.*, 1999).
In barley and pea root tips, two different vacuoles were described in the same cell near the meristem: a PSV characterized by the presence of α-TIP and the storage protein barley lectin; an LV labeled by γ-TIP and aleurain (Paris *et al.*, 1996).
The *A. thaliana* genome encodes 10 TIP isoforms: 3 γ-TIP, 3 δ-TIP, 1 α-TIP, 1 β-TIP, 1 ε-TIP, 1 ζ-TIP (Johanson *et al.*, 2001). The ε-TIP and δ-TIP are mostly found in roots and floral organs; γ-TIP and ζ-TIP are abundant in flowers; α-TIP and β-TIP are mainly expressed during seed maturation (Frigerio *et al.*, 2008). Hunter *et al.* (2007) showed that α, γ or δ-TIP fused to YFP, localized to the tonoplast of the central vacuole of transgenic *A. thaliana* leaves, mature roots and root tips; all the three TIPs localized to the tonoplast of PSV in the embryos of developing, germinating and mature seeds. These results show that LV and PSV are present at particular stages of plant development and that TIPs exhibit tissue-specificity: in particular, γ-TIP and δ-TIP are expressed in vegetative tissues except in root tips, α-TIP in seeds during germination. This suggests that in root tips, leaves and seeds of *A. thaliana*, there is a

single type of vacuole, but this does not exclude that two separated vacuoles may coexist in other cell types (Frigerio *et al.*, 2008).
The two vacuoles LV and PSV can also be differentiated using soluble markers: vacuolar proteins with a sequence-specific vacuolar sorting determinant (ssVSD) for LV, and vacuolar proteins with C-terminal vacuolar sorting determinants (ctVSD) for PSV (Di Sansebastiano *et al.*, 1998).

1.2.1 Vacuolar Sorting Determinants (VSD)

Soluble proteins that are sorted to the vacuole contain in their sequence the vacuolar sorting determinant (VSD), while proteins addressed to the apoplast do not have such a signal (Pereira *et al.*, 2014). This motif can be found within a protein, at its N-terminal or C-terminal end, and it is removed by vacuolar proteases after vacuolar sorting (Xiang *et al.*, 2013).

Protein precursors may contain sequence-specific (ssVSD), C-terminal (ctVSD), or physical structure-dependent VSD (psVSD) (Xiang *et al.*, 2013).

ssVSD are found in proteins delivered to LV. They were identified in N-terminal propeptides (NTPP) of barley aleurain and sweet potato sporamin, both characterized by an NPIR motif (Holwerda *et al.*, 1992) that binds to the vacuolar sorting receptor BP-80; similar motifs were later found in internal propeptides (castor bean ricin; Frigerio *et al.*, 2001) and C-terminal propeptides (castor bean 2S albumin; Brown *et al.*, 2003). In each case, Ile or Leu residues are essential for transport and for *in vitro* binding to putative receptors (Cao *et al.*, 2000). Sorting receptors that bind to NPIR-containing peptides were first described in pea (Kirsch *et al.*, 1994; Paris *et al.*, 1997), *A. thaliana* (Ahmed *et al.*, 1997) and pumpkin (Shimada *et al.*, 1997).

Proteins containing a ctVSD are addressed to PSV. The C-terminal propeptide (CTPP) of barley lectin (Bednarek and Raikhel 1991), tobacco chitinase A (Neuhaus *et al.*, 1991), β-1,3-glucanase (Sticher *et al.*, 1992) or bean phaseolin (Frigerio *et al.*, 1998) is necessary and sufficient for the correct vacuolar targeting. The introduction of C-terminal glycosylation sites as well as the addition of extra-glycine stretches at the C-terminus, block the function of the VSD, leading to cell surface secretion (Bednarek and Raikhel 1991; Neuhaus *et al.*, 1994).

The third class of VSD depends on the physical structure of the proteins (psVSD). These signals are located in the center of the protein and have a particular three-dimensional structure, as observed in legumin (Saalbach *et al.*, 1991). They are common in storage proteins, and their sorting to vacuole is

probably based on protein aggregation (Neuhaus and Rogers 1998; Vitale and Chrispeels, 1992). For instance, cereals prolamins can aggregate in the ER to form protein bodies (Okita and Rogers 1996).

VSDs were also studied in two aspartic proteinases (APs) cardosin A and B from cardoon flower (*Cynara cardunculus* L.), which are used in Portugal in artisanal cheese manufacture. Cardosin A accumulates in PSV of stigmatic papillae (Ramalho-Santos *et al*., 1997), while cardosin B is found in the extracellular matrix of floral transmitting tissues (Vieira *et al*., 2001).

The most studied ctVSDs in plants are:

ctVSD of tobacco chitinase A: chitin is a polymer of N-acetylglucosamine, abundant in the exoskeleton of insects, algae, yeast, fungi, marine resources, and in the internal structures of vertebrates (Hamid *et al*., 2013). This polysaccharide is degraded by the enzymes chitinases which are essential for the recycling of carbon and nitrogen in the ecosystem. In plants, chitinases are important defense enzymes against fungal pathogens.
Neuhaus *et al.* (1991) demonstrated that the C-terminal sequence of tobacco chitinase A is essential for the proper vacuolar sorting. They expressed two different chitinases in tobacco cells and observed that the tobacco class I chitinase A accumulated in vacuoles, but the deletion of the C-terminal propeptide led to its secretion. On the other hand, the cucumber class III chitinase was secreted, while it accumulated in vacuoles if the C-terminal propeptide of chitinase A was added to its sequence.
Fluorescent neutral vacuoles were observed by Di Sansebastiano *et al.* (1998) who fused the C-terminal VSD of tobacco chitinase A to the fluorescent marker GFP.

ctVSD of barley lectin: this is a typical *Gramineae* lectin that accumulates in vacuoles/protein bodies of embryonic and adult root cap cells of barley (Mishkind *et al*., 1983; Lerner and Raikhel, 1989). It binds specifically to chitin and like most of the lectins, it has several functions such as plant defense against predators and pathogens, and participation in symbiotic interaction between plants and microbes (De Hoff *et al*., 2009). It has been demonstrated that the C-terminal propeptide (GVFAEAIAANSTLVAE) is necessary for proper sorting of barley lectin to vacuoles (Bednarek *et al*., 1990). The lectin is synthesized as a preproprotein containing a 15-amino acids-glycosylated carboxyl-terminal propeptide (CTPP). The mutant version, lacking the CTPP, was expressed in tobacco protoplasts, suspension-cultured cells, and transgenic plants. In each case, the wild-type barley lectin was addressed to the vacuoles, while the mutant version was secreted from the cells. These results showed that the C-terminal domain of the barley lectin preprotein is necessary for its sorting to vacuoles (Bednarek *et al.,* 1990).

ctVSD of phaseolin: the phaseolin is the principal globulin seed storage protein of the French bean *Phaseolus vulgaris.* The expression of the bean phaseolin in transgenic tobacco causes its binding to membranes in ER/Golgi fractions, and leads to the formation of SDS-resistant aggregates (Castelli and Vitale, 2005). If the C-terminal AFVY motif of phaseolin is deleted, the aggregates are not produced and the mutated protein is transported to the cell wall rather than to the vacuole (Castelli and Vitale, 2005).

ctVSD of cardosin A and B: in 1998, Runeberg-Roos and Saarma identified in barley, the AP phytepsin that is highly homologous to mammalian cathepsin D and yeast vacuolar proteinase A. The two aspartic proteinases cardosin A and B are involved in degradation, biotic and abiotic stress response, programmed cell death, reproduction (Simões and Faro, 2004). Their structure is composed of an N-terminal region, a saposin-like PSI (plant-specific insert) domain, and a C-terminal region. The PSI, about 100 aa, is unique to plant cells and it is supposed to be involved in both host defense and vacuolar targeting (Muñoz *et al.*, 2010). In the heterodimeric form of plant APs, the PSI domain is partially or completely removed during the maturation process of the protein, whereas in the monomeric form, the PSI is retained (Bryksa *et al.*, 2011). The role of PSI in vacuolar targeting is well described by Kervinen *et al.* (1999) who determined its crystal structure. A study performed in tobacco protoplasts showed that the truncated PhytepsinΔ(PSI) is secreted into the culture medium (Törmäkangas *et al.*, 2001).
The cDNA encoding an aspartic proteinase in *P. patens* (called *Pp*AP1), was isolated and fused to GFP, showing a vacuolar fluorescence in transiently transfected protoplasts (Schaaf *et al.*, 2004), but this could not be reproduced in our laboratory.

1.2.2 Vacuolar Sorting Receptors (VSR)

VSR are type I transmembrane proteins involved in the transport of vacuolar soluble proteins to LV (daSilva *et al.*, 2006; Zouhar *et al.*, 2010) and were first identified in CCV fraction from pea (*Pisum sativum* L.) cotyledons (Kirsch *et al.*, 1994). It has been thought for years that the interaction between VSRs and their ligands occurs in the TGN and that the VSR-ligand complex is engulfed into CCVs which fuse with MVB/PVC. In these organelles, the VSR-ligand dissociation occurs, then VSR is recycled to the TGN. This model is in contrast with more recent studies according to which the VSRs and their ligands may interact earlier in the secretory pathway, already in the lumen of the ER, and dissociate in the TGN (Robinson and Neuhaus, 2016).

VSR are composed of: an N-terminal luminal domain which binds the ssVSD (Cao *et al.*, 2000), a single transmembrane domain (TMD) and a C-terminal cytoplasmic tail (CT) (Khirsh *et al.*, 1994) (**Figure 1.7**).

The luminal region contains a protease-associated (PA) domain at its N-terminus, a central domain, and three epidermal growth factor repeats (EGF) (Luo *et al.*, 2014). The CT is involved in the formation of clathrin-coated vesicles (daSilva *et al.*, 2006), and together with the TMD, it is responsible for targeting the VSR to the vacuole (daSilva *et al.*, 2006; Foresti *et al.*, 2010).

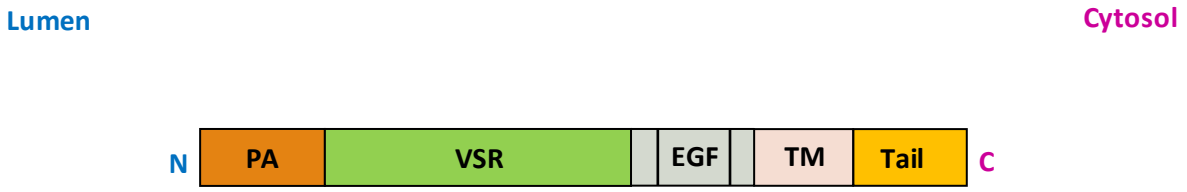

Figure 1.7. Structure of plant VSR. N: N-terminal end; PA: protease-associated domain; VSR: vacuolar sorting receptor; EGF: epidermal growth factor repeats; TM: transmembrane domain; C: C-terminal end.

The VSR sequences from *Arabidopsis*, rice and poplar genome were aligned with the VSR sequence of pea (BP-80) and pumpkin (PV72) using the fastDNAmL program (Olsen *et al.*, 1994) which allowed to obtain a phylogenetic tree for Angiosperms, including three subfamilies VSR1, VSR2, VSR3.

The phylogenetic tree (**Figure 1.8**) published in the work of De Marcos Lousa *et al.* (2012) includes the VSR sequences from *Arabidopsis thaliana* and other flowering plants (the dicot soybean *Glycine max,* the monocot rice *Oryza sativa*, the gymnosperm spruce *Picea sitchensis*). The authors also added the VSR sequences of other organisms: the moss *Physcomitrella patens*, the green unicellular algae *Ostreococcus tauri, Micromonas sp* RCC299 and *Chlamydomonas reinhardtii*, the diatom *Phaeodactylum tricornutum*, and the oomycete *Phytophthora infestans.*

The VSRs of *P. patens* form a separate clade, different from the classes 1 and 2 of flowering plants.

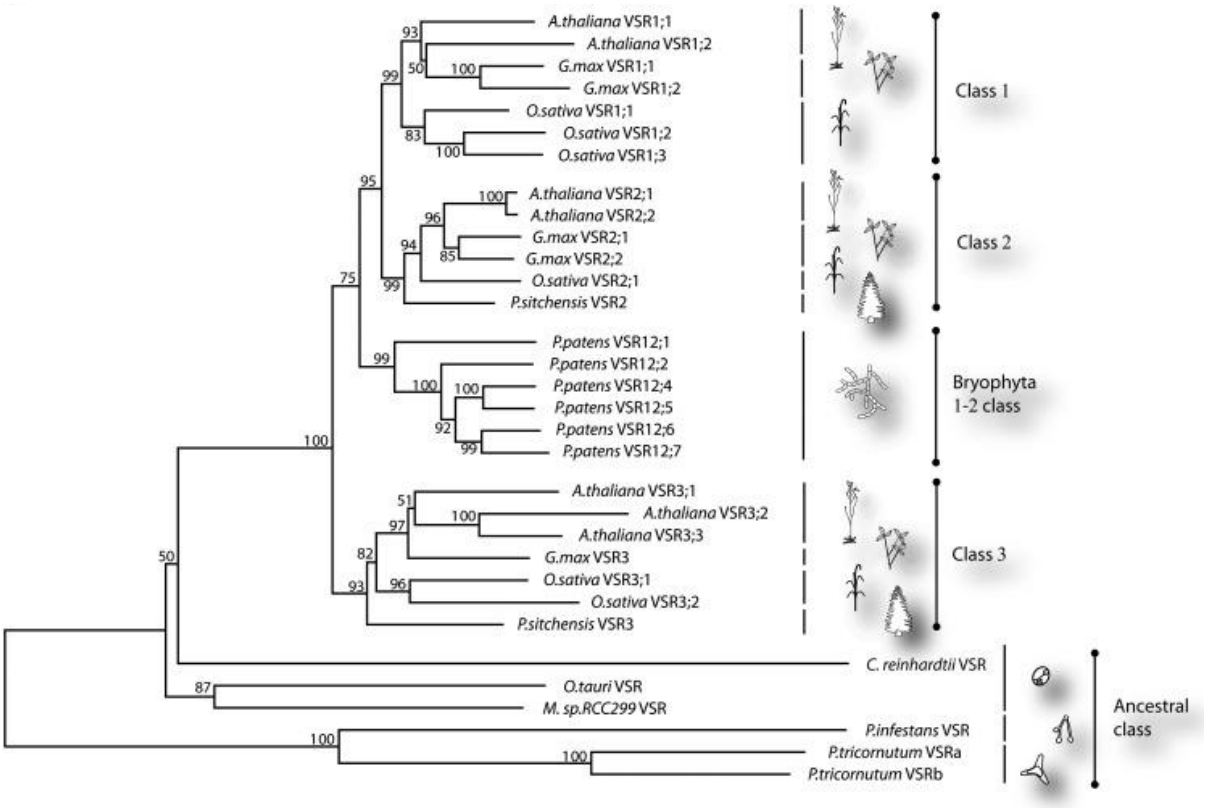

Figure 1.8. VSR phylogenetic tree and nomenclature (De Marcos Lousa *et al*., 2012).

The seven VSR of *A. thaliana* (Avila *et al*., 2008) were localized to the TGN and PVC (Sanderfoot *et al*., 1998), but it is s still unclear if their main function is the trafficking to PSV or LV (or both). *At*VSR1 seems to be involved in 2S albumin transport to PSV in developing seeds (Shimada *et al*., 2003).

The first VSR, BP-80 (80 KDa), was isolated from clathrin-coated vesicle extracts of *Pisum sativum* cotyledons (Kirsch *et al*., 1994). It binds to the motif NPIR identified in the N-terminal region of barley aleurain (Holwerda *et al.,* 1992) and is involved in protein sorting to LV. This receptor acts in a pH or Ca^{2+}-dependent manner and it has been found in the *trans cisternae* of GA, in the TGN, and the prevacuolar compartment (Paris *et al*., 1997). daSilva *et al*. (2006) hypothesized that after cargo release, BP-80 is recycled from PVC to Golgi. In 2016 Robinson and Neuhaus suggested that in plants, the interaction between the VSR and the ligand starts in the ER or the *cis*-Golgi, and terminates in the TGN/EE but the pH of these compartments is almost the same (around 5.5), indicating that the release of the cargo cannot be pH-dependent, but more likely is Ca^{2+} dependent.

1.2.3 A putative vacuolar receptor family: the RMRs

A second family of proteins called RMR (Receptor-like Membrane RING-H2) was proposed to mediate protein sorting to PSV (Park *et al.*, 2007; Park *et al.*, 2005).

RMRs are type I transmembrane proteins which contain a luminal N-terminal side mainly composed of a PA domain involved in cargo recognition; a single TMD; a linker; a cytosolic RING-H2 domain (Really Interesting New Gene, with two histidines, $C_3H_2C_3$) and a C-terminal Serine-Rich tail (**Figure 1.9**).

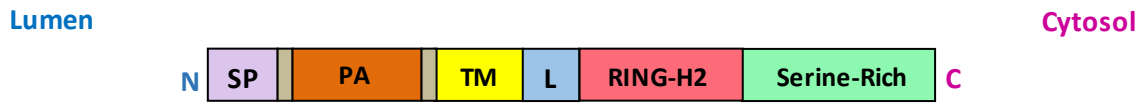

Figure 1.9. Structure of plant RMR. N: N-terminal end; SP: signal peptide; PA: protease-associated domain; TM: transmembrane domain; L: linker; RING-H2 domain; Serine-Rich cytosolic tail; C: C-terminal end.

In *At*RMR2 (*A. thaliana*), the linker is involved in the targeting to TGN and in the formation of homodimers and heterodimers (with *At*RMR1) (Occhialini *et al.*, 2016). The structure of RING-H2 is related to zinc finger in which histidine and cysteine residues coordinate zinc ions (Stone *et al.*, 2005), but unlike zinc finger domains which can bind DNA (Lovering *et al.*, 1993), RING-H2 domains function exclusively in protein-protein interaction.

The luminal domain of plant RMRs is similar to the PA domain of VSR BP-80 (Hinz *et al.*, 2007), and this homology allowed to clone and characterize JR700 (*At*RMR1) and JR702 (*At*RMR2) from *A. thaliana* (Jiang *et al.*, 2000).

It has been thought that RMRs are putative receptors for proteins which carry a C-terminal vacuolar sorting determinant (ctVSD) and are destined to PSV (Park *et al.*, 2007).

The **figure 1.10** shows a trafficking model of plant RMRs.

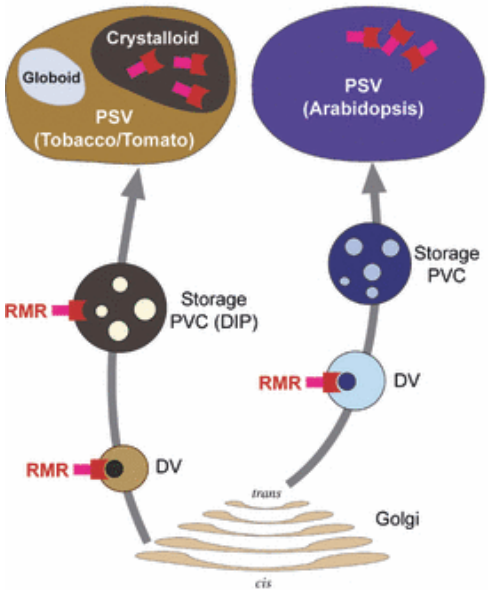

Figure 1.10. Working model of RMR proteins in plants. In developing tomato and tobacco seeds, RMR is found in the crystalloid of PSV, the storage PVC or DIP organelle; in developing *Arabidopsis* seeds, RMR is found in DVs (adapted from Wang *et al*., 2011).

The similar structure between plant RMRs and animal PA-TM-RING proteins suggests that they also have similar functions, especially because their transmembrane domain and RING-H2 domain are quite conserved (Wang *et al.*, 2011). In mammalian cells, the RING-H2 domain may function as transcriptional regulator (Tranque *et al.*, 1996) or as a ubiquitin-ligase (Bocock *et al.*, 2009; Stone *et al.*, 2006). Its role is better known in animals (Jin *et al.*, 2011; Whiting *et al.*, 2011), while in plants it is still elusive.

By immunogold electron microscopy, Shen *et al.* (2011) found the rice RMR1 (*Os*RMR1) in the GA, TGN, and in an organelle called storage prevacuolar compartment (sPVC), precursor of one of the two types of protein storage vacuoles.

In *A. thaliana*, the RMR family is composed of six members and is subdivided into two different subfamilies, *At*RMR1 and *At*RMR2-6 (from *At*RMR2 to *At*RMR6). The *At*RMR1, 5 and 6 lack the cytosolic Serine-Rich tail.

*At*RMR1 was found to sort the bean storage protein phaseolin to the PSV in *A. thaliana* leaf protoplasts (Park *et al.*, 2005), while *At*RMR2, *in vitro*, binds the ctVSD of tobacco chitinase and barley lectin (Park *et al.*, 2007), proving that in plants, the PA domain can serve as a ligand-binding domain. *At*RMR1 has been found in PVC (Park *et al.*, 2005) or vacuoles (Scabone *et al.*, 2011), *At*RMR2 in the GA, dense vesicles (DV) and PSV in *A. thaliana* embryos (Hinz *et al.*, 2007).

P. patens genome encodes 5 RMRs with a short Serine-Rich tail, but their localization needs to be elucidated.

1.2.4 PA-TM-RING proteins

Proteins having a similar structure as RMRs are called PA-TM-RING proteins and contain a PA domain and a RING finger domain separated by a transmembrane (TM) domain (Bocock *et al*., 2009). The PA domain, composed of 100-120 aa, is involved in protein-protein interaction, recognition of the substrate/ligand, and could also function as a protease regulatory region (Mahon and Bateman, 2000). The PA has also been found in the transferrin receptor, in the prostate-specific membrane antigen (Davis *et al*., 2005), in the human Golgi/endosomal signal peptidase-like proteins SPPL2a and SPPL2b (Krawitz *et al*., 2005), and in the streptococcal C5a peptidase (Brown *et al*., 2005).

GRAIL

The RNF128/GRAIL (RING finger protein 128/gene related to anergy in lymphocytes) is a member of the PA-TM-RING family in mammals. It acts as E3 ligase and localizes to recycling endosomes; when overexpressed, it inhibits the proliferation of anergic $CD4^+$ T-cells which are unresponsive to antigen rechallenge (Aziz *et al*., 2014). The mutation of the RING-H2 domain of GRAIL leads to the disruption of its E3 ligase activity (Anandasabapathy *et al*., 2003). As GRAIL, other E3 ubiquitin ligases play a functional role in T cell anergy, such as Cbl-b and Itch (Liu, 2007). A defective expression of these E3 ligases is linked to autoimmune or inflammatory diseases in experimental murine and human models (Whiting *et al*., 2011; Lin *et al*., 2009).

In vitro studies showed that GRAIL's substrates include CD40 ligand (CD40L) and Rho GDP-dissociation inhibitor (Su *et al*., 2006). Lineberry NB *et al*. (2008) found that GRAIL interacts with the transmembrane proteins tetraspanins CD151 and CD81, and ubiquitylates them: their luminal/extracellular domain is captured by the PA domain of GRAIL, whereas the ubiquitylation of the cytosolic tail is mediated by the RING-H2 finger.

Goliath

Goliath is a ubiquitin ligase composed of a signal peptide (a.a. 1-25), a PA domain (a.a. 98-207), a TM domain (a.a. 235-257) and a RING-H2 domain (a.a. 303-343) (Yamazaki *et al*., 2013).

d-Goliath was first identified in the mesoderm of *Drosophila melanogaster* (Bouchard and Côté, 1993). Later, also mouse-goliath (Baker and Reddy, 2000) and human-goliath (Guais *et al*., 2006) were described.

In the fly, it is located on recycling endosomes where it plays a role in regulating trafficking via ubiquitylation of the VAMP3 SNARE protein (Yamazaki *et al*., 2013). Another member of the same family is called Godzilla: like Goliath, it regulates the endosomal processes in *Drosophila.* Mutations of

either key histidine residues in RING finger domain of Goliath and Godzilla or of the target lysines on VAMP3, prevented the formation of giant endosome (Yamazaki *et al.*, 2013).

RING Finger protein 13 (RNF13)

The RNF13 or chicken-RING zinc finger (C-RZF) is expressed in different tissues of chicken, mouse and humans (Zhang *et al.*, 2009, 2010; Bocock *et al.*, 2009) where it acts as E3 ubiquitin ligase and may play a critical role in the development and the regulation of diseases like myogenesis and tumorigenesis (Jin *et al.*, 2011). In the chicken embryo brain, where it was first identified, the expression of RNF13 increases in presence of the extracellular matrix component tenascin-C (Tranque *et al.*, 1996).

Synthesized as an integral membrane protein, the RNF13 is located in ER, GA and endosome membranes. Performing an *in vitro* ubiquitylation assay, Bocock *et al.* (2009) showed that RNF13 is able to ubiquitylate itself; moreover, they demonstrated that the C-terminal domain, containing the RING-H2 motif, is released into the cytoplasm by proteolytic cleavage. In response to protein kinase C activation, the cleavage is inhibited, and the more stable protein is transported to the inner nuclear membrane via recycling endosomes, exposing the RING-H2 domain to the nucleoplasm. This suggests that RNF13 can mediate ubiquitylation in endosomes, on the plasma membrane, in the cytoplasm, in the nucleoplasm, or on the inner nuclear membrane, depending on various stimuli (Bocock *et al.*, 2010). RNF13 also shows a PEST sequence adjacent to the RING domain, that represents a signal for degradation (Bocock *et al.*, 2009). It is enriched in proline (P), glutamic acid (E), serine (S), threonine (T).

RING Finger protein 167 (RNF167)

The human RNF167 has been detected at the PM, in endosomes and lysosomes (Yamazaki *et al.*, 2013; Lussier *et al.*, 2012; van Dijk *et al.*, 2014). It ubiquitylates the tumor-suppressing subchromosomal transferable fragment cDNA 5 (TSSC5) (Yamada and Gorbsky, 2006), the vesicle-associated membrane protein 3 (VAMP3) (Yamazaki *et al.*, 2013), and the α-amino-3-hydroxy-5-methyl-4-isoxazole propionate (AMPA) receptor (Lussier *et al.*, 2012). It inhibits the cell cycle progression and is involved in the recycling endosome trafficking. Recent studies have shown that RNF167 colocalizes with the E2 ubiquitin-conjugating enzyme UBE2N in HEK293 cells (probably in endosomal vesicles or in lysosomes; Ghilarducci, 2019). It has also been demonstrated its involvement in the regulation of lysosomes positioning and endocytic trafficking via ubiquitylation of the GTPase Arl8B (ADP-ribosylation factor-like 8B; Deshar *et al.*, 2016).

The **figure 1.11** from Wang *et al.*'s publication (2011) shows a comparison between plant RMRs and mammalian PA-TM-RING proteins.

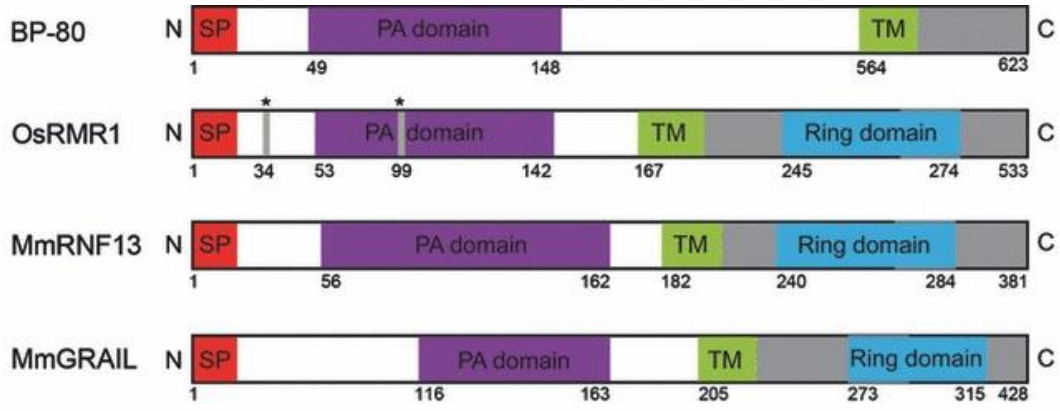

Figure 1.11. Comparison between plant RMR proteins and mammalian PA-TM-RING proteins. Structures of rice *Os*RMR1, BP-80, the pea VSR, two mammalian PA-TM-RING proteins MmRNF13 and MmGRAIL. The conserved PA and RING domains among the plant RMRs and the mammalian PA-TM-RING family proteins are highlighted in boxes. The asterisks indicate the two conserved Asn-linked glycosylation sites in the lumenal domain of the plant RMR (*Os*RMR1) (adapted from Wang *et al*., 2011).

1.3 The Ubiquitin System

Ubiquitin (Ub) is a small protein of 76 amino acids (8.5 KDa) involved in ubiquitylation that gets attached to other proteins in a process that regulates degradation, protein-protein interaction and subcellular localization in eukaryotes (Sadowski and Sarcevic, 2010). In this process of ubiquitylation, three classes of enzymes are involved (**Figure 1.12**): E1 ubiquitin-activating enzyme, E2 ubiquitin-conjugating enzyme and E3 ubiquitin ligase. The free C-terminus of the glycine (Gly76) of Ub protein forms a thioester bond with the catalytic cysteine of E1 in an ATP-dependent reaction. Ub is then transferred from E1 to the catalytic cysteine of E2. Finally, E3 transfers Ub from E2 to a lysine of the target protein forming a bond with the C-terminal glycine of ubiquitin. In monoubiquitylation, a single ubiquitin is attached to the lysine residue of the target protein; in multiubiquitylation, one molecule of Ub is attached to several lysines of the target protein (Petroski and Deshaies, 2005); polyubiquitylation occurs when the lysine residue of the target protein is tagged with a Ub chain (Pickart and Eddins, 2004); in the polyubiquitin chain, each Ub molecule is bound to one of the seven lysine residues of the previously added ubiquitin (K6, K27, K29, K33, K11, K48, K63, depending on the E3 ligase). Mono- and multiubiquitylation are specific for cargo membrane proteins that are internalized in vesicles, and via the endocytic pathway, reach the lysosomes/vacuoles for degradation (d'Azzo *et al*., 2005). A chain of at least 4 Ubs linked at K48, and K11-linked polyubiquitylation (Jin *et al*., 2008) are signals for proteasomal degradation of soluble proteins (Thrower *et al*., 2000).

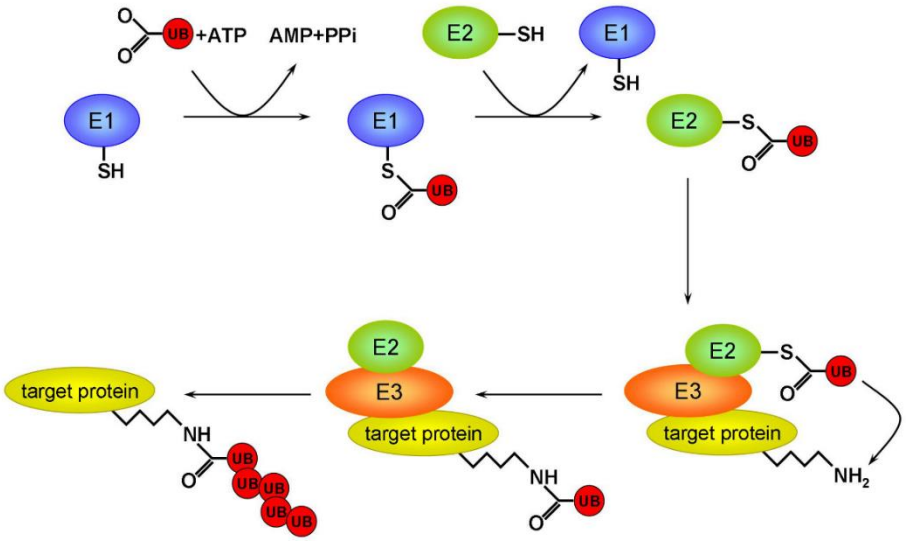

Figure 1.12. The ubiquitylation pathway. The activating enzyme (E1) binds to ubiquitin's C-terminus in an ATP-dependent reaction. The ubiquitin is transferred to the cysteine residue of the ubiquitin-conjugating enzyme (E2) which interacts with E3 ubiquitin ligases. E2-E3 complexes bind to substrates and catalyze the transfer of ubiquitin to a lysine on the substrate protein (adapted from "Identification of ubiquitinated proteins"– www.labome.com).

Ubiquitin participates not only in proteolytic processes: monoubiquitylation and multiubiquitylation for instance regulate DNA repair (Hofmann, 2009), gene expression, receptor endocytosis. Polyubiquitylation through K63 of ubiquitin can regulate kinase activation and endocytosis (Passmore and Barford, 2004) (**Figure 1.13**); polyubiquitylation on the α-amino group of the N-terminal methionine (M) residue of ubiquitin, regulates nuclear factor-kB activation (Rahighi *et al.*, 2009).

The role of K6-, K27-, K29-, K33-linked Ub chains needs to be elucidated.

Many E3 ubiquitin ligases are RING finger proteins (Joazeiro and Weissman, 2000). The RING family of E3 ligases contains either the classical RING domain (with one histidine) or a RING-H2 domain with two histidines (Mazzucotelli *et al.*, 2006).

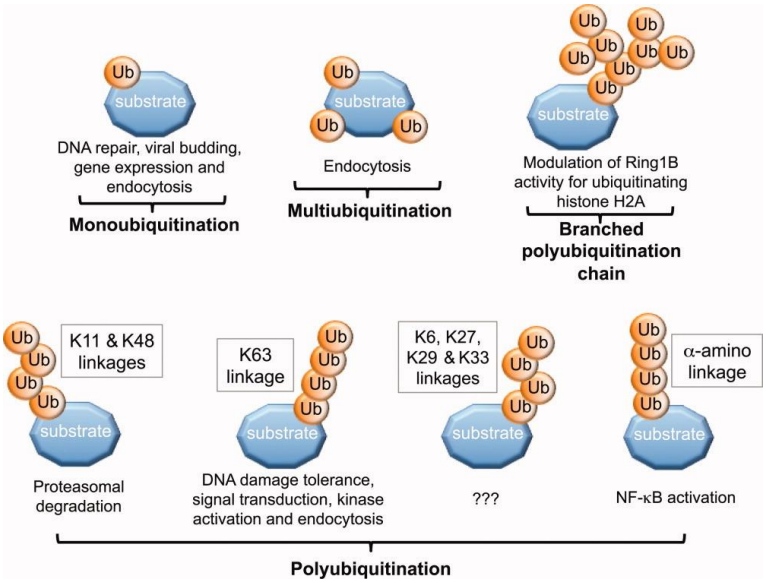

Figure 1.13. Different modes of ubiquitylation lead to different substrate fates. Ub can be linked to proteins as a monomer on one (monoubiquitylation) or more substrate lysines (multiubiquitylation) or as a polymer (polyubiquitylation) by the sequential addition of further Ubs to each other through Ub lysines. Monoubiquitylation regulates DNA repair, viral budding, gene expression. Multiubiquitylation regulates receptor endocytosis. Polyubiquitylation through K11 or K48 of Ub is generally a signal for proteasomal degradation. K63-linked Ub chains can work in signaling and endocytosis. A polyubiquitin chain can also be generated through the α-amino group of the N-terminal methionine residue, to regulate NF-kB activation. The role of K6-, K27-, K29-, K33-linked Ub chains needs to be elucidated (adapted from Sadowski *et al.*, 2012).

In vivo and *in vitro* assays are commonly used to elucidate the different biochemical functions mediated by E3 ligases. *In vitro* autoubiquitylation tests are useful to determine the E2-E3 pairing, nevertheless, it may happen that the *in vivo* selectivity is not completely reflected by the *in vitro* activity tested through autoubiquitylation (Turek *et al.*, 2018). In our work, several *in vitro* assays have been done, E2 and E3 enzymes have been tested, hence the choice to briefly describe these classes of enzymes in the next paragraphs.

1.3.1 E2 ubiquitin-conjugating enzymes

Ubiquitin-conjugating enzymes (UBC-E2s) have important functions in the ubiquitylation process: they accept Ub from E1 via a transthiolation reaction (Stewart *et al.*, 2016), carry the activated Ub (or Ub-like proteins such as SUMO and NEDD8) and finally pass it to the E3 ligase. The conserved region containing the cysteinyl residue is composed of about 140-150 amino acids and is called UBC (ubiquitin conjugation) domain. This can interact with the E3 enzymes or with the substrate (Kalchman *et al.*, 1996). The formation of the E2-ubiquitin intermediate may require other conserved amino acids (Wu *et al.*, 2003).

About 40 human E2s have been found (Bachmair *et al.*, 2001; Jiang and Beaudet, 2004); in plants, few E2s have been described at the beginning because it was thought they only had an auxiliary role in ubiquitylation, instead they were later shown to be not just simply carriers of Ub. All E2s can interact with one or more E3s, playing more than one role: they act during the initiation and the elongation of ubiquitin chain, control the chain formation (Stewart *et al.*, 2016), and regulate other enzymes activity (Wiener *et al.*, 2013; Pruneda *et al.*, 2011).
Detailed studies led to discover 48 E2s in rice (Bae and Kim, 2014), 75 in maize (Jue *et al.*, 2015), 37 in *A. thaliana* (Kraft *et al.,* 2005).

1.3.2 The E3 ligases classification

The RING E3 ligases are the most abundant known E3 ligases. Their structure contains a zinc-binding domain called RING (really interesting new gene).
They are grouped in:

- ✓ monomeric RING finger E3 ligases
- ✓ multimeric RING finger E3 ligases (cullin-based)
- ✓ U-box E3 ligases (RING finger-like ubiquitin ligases)

The RING domain, 40-60 amino acids, resembles the classical zinc finger domain with cysteine and histidine residues. It creates a platform for binding E2s through a Zn^{2+} ions coordination and a central α-helix. Proteins containing a zinc finger domain, generally interact with DNA and RNA, instead the RING motif seems to be only involved in protein-protein interaction (Lovering *et al.*, 1993).
An important zinc finger-RING E3 ligase is UBR4, involved in the N-end rule pathway where single N-terminal amino acids, called N-degrons, act as degradation signals (Bachmair *et al.*, 1986; Tasaki *et al.*, 2012). Among N-degrons, there are Arg, Lys, His (type-1, positively charged), Trp, Phe, Tyr, Leu, and Ile (type-2, bulky hydrophobic) found at the N-termini of human proteins (Kwon *et al.*, 1998; 1999). These residues determine the half-life of the protein and are recognized by N-recognins (UBR1, UBR2, UBR4/p600, and UBR5/EDD; Tasaki *et al.*, 2005). The target protein is then degraded by either the ubiquitin proteasome system (UPS) or the autophagy-lysosome system. In *A. thaliana*, the UBR-type E3 ligase called BIG, is an auxin transport protein involved in developmental processes, light and phytohormones pathways (Kanyuka *et al.*, 2003). The work of Kim *et al.* (2018) shows that in UBR4-knockout mice, the generation of multivesicular bodies is inhibited.

Some RING E3s have multiple subunits, such as the cullin-RING ligases (CRLs; Petroski and Deshaies, 2005) whose structure is composed of a scaffold protein called cullin (Cul-1, 2, 3, 4a, 4b, 5, or 7), a

RING-box protein at its N terminus, and a C terminus consisting of an adaptor protein Skp1 and a F-box protein which recognizes the substrates (Sarikas *et al.*, 2011). A well-studied CRL superfamily is the Skp1-Cul1-F-box protein (SCF) family (**Figure 1.14**), in which the exchange of F-box proteins in the SCF scaffold is controlled by cycles of attachment and removal of the ubiquitin-like protein NEDD8 (Duda *et al.*, 2011), in a process called NEDDylation.

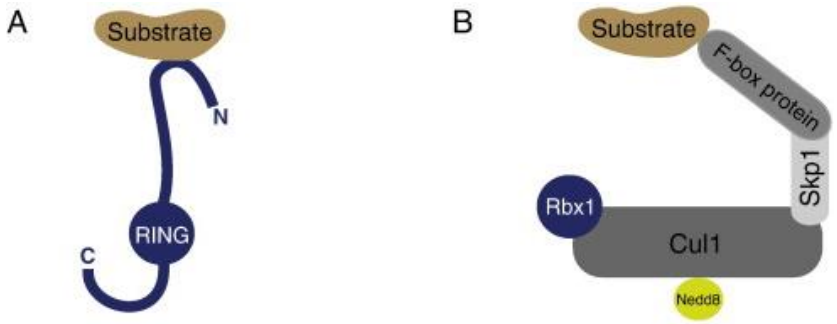

Figure 1.14. Architecture of RING-type E3s. (**A**) In the monomeric RING-type E3 model, the RING domain would mediate binding to E2 thioester-linked to ubiquitin. (**B**) Model of a multi-subunit RING E3 of the cullin RING ligase (CRL) superfamily, *e.g.* SCF (CRL1) family. SCF is composed of a cullin protein (Cul1), a RING finger protein (Rbx1), and an adaptor protein (Skp1) that binds F-box proteins. The ubiquitin-like molecule Nedd8 is reversibly conjugated to cullins and associated with activation of CRLs (adapted from Metzger *et al.*, 2014).

The human anaphase-promoting complex/cyclosome (APC/C) is a multi-subunit culling-RING E3 ligase which consists of 13 core subunits including a cullin-like protein and a small RING protein. Its interchangeable co-activator subunits, Cdc20 and Cdh1, recognize different substrates and are involved in several phases of cell cycle (Schreiber *et al.*, 2011).

The U-box domain, composed of approximately 70 amino acids, resembles the structure of RING finger motif. It does not contain zinc but it utilizes hydrogen bonds (Hatakeyama and Kei-ichi, 2003). Both domains are involved in binding the ubiquitin-loaded E2 and in stimulating the ubiquitin transfer to the substrate (Metzger *et al.*, 2014).

RING E3 ligases are known to form homodimers and heterodimers. The first ones include cIAP, RNF4, BIRC7, IDOL, and the U-box proteins CHIP and Prp19 (Mace *et al.*, 2008; Vander Kooi *et al.*, 2006); the other ones include BRCA1-BARD1, Mdm2-MdmX (or HdmX/Hdm4 in humans) and RING1B-Bmi1. In the homodimeric form, the RING E3 ligases functionally interact with E2s (binding one E2 per each monomer), whereas in the heterodimeric form, this is not possible. For instance, BRCA1 and RING1B each function with E2, whereas their partner (BARD1 or Bmi1) enhances the activity or interacts with the substrate (Joukov *et al.*, 2001). In the complex BRCA1-BARD1, the loss of a portion of the central

α-helix could explain the inability of BARD1 to interact with E2s (Brzovic *et al.*, 2001). On the other side, in the complex Mdm2-MdmX, the Mdm2 can form an active homodimer, instead the MdmX can generate an inactive homodimer: the two RINGs can form an active heterodimer (Uldrijan *et al.*, 2007; Poyurovsky *et al.*, 2007) and this highlights the importance of RING dimerization in promoting substrate ubiquitylation (Choo and Hagen, 2012).

RING E3s can ubiquitylate themselves *in vivo* (Lorick *et al.*, 1999). Moreover, they may be ubiquitylated by other RING- or HECT-type E3 ligases (Weissman *et al.*, 2011). There is evidence that post-translational modifications, such as phosphorylation, regulate the RING-type E3 ligase activity. For instance, the recognition of receptor tyrosine kinases (RTKs) by the Cbl RING E3s, is facilitated if tyrosine is phosphorylated (Ryan *et al.*, 2006).

Not all the RING domains have an E3 ligase activity, some are involved in transcription and other protein-protein interactions (Deshaies and Joazeiro, 2009; Borden and Freemont, 1996).

In *A. thaliana* there are more than 460 RING-type proteins (Lee and Kim, 2011-review).

Plant RING E3 ligases are involved in biotic and abiotic stress tolerance (Marino *et al.*, 2012; Duplan and Rivas, 2014), gravitropism, metabolism (Nakamura *et al.*, 2011; Sakai *et al.*, 2012), circadian rhythm (Han *et al.*, 2004; Harmon *et al.*, 2008), cell division (del Pozo *et al.*, 2002; Kim *et al.*, 2008), phytohormone signal transduction (An *et al.*, 2010; Ariizumi *et al.*, 2011). However, their substrates are not well known yet (Metzger *et al.*, 2014).

The HECT (Homologous to E6AP Carboxyl-Terminus) E3 ligases: in mammals, ~30 HECT domain E3s have been found. They are involved in protein trafficking, immune response, cellular growth and proliferation (Rotin and Kumar, 2009).

The first described member of the HECT family is the E6-associated protein (E6-AP) that interacts with the E6 protein of the cancer-associated human papillomavirus types 16 and 18 (Huibregtse *et al.*, 1995). The HECT domain, about 350 amino acids, is composed of a large N-terminal lobe ("N-lobe") containing the E2-binding domain, connected to a smaller C-terminal lobe ("C-lobe") by a short linker essential for catalysis (Verdecia *et al.*, 2003). A catalytic cysteine residue contained in the C-lobe, interacts with ubiquitin during the transfer reaction from E3 to the target protein. The C-tail region of the C-lobe plays a role, not yet clarified, in catalysis (Salvat *et al.*, 2004; Kamadurai *et al.*, 2013; Maspero *et al.*, 2013), whereas the N-terminal region recognizes the target proteins. It is known that the zinc finger domain of RING E3 ligases interacts with the complex ubiquitin-E2 permitting the Ub transfer from E2 to a target protein in a single step, whereas the HECT- (and RBR-) type E3s form a thioester-linked complex with ubiquitin, before transferring it to the target protein (Huibregtse *et al.*, 1995; Scheffner *et al.*, 1993; Wenzel *et al.*, 2011).

In humans there are 28 members of the HECT E3 ubiquitin ligase family, while *Saccharomyces cerevisiae* and *Arabidopsis* only have three and seven members respectively (Huibregtse *et al.*, 1995; Downes *et al.*, 2003).

Three subfamilies of human HECT E3 enzymes can be distinguished: the HERC subfamily is composed of 6 members (HERC1-6); the NEDD4 subfamily consists of 9 members (NEDD4-1, NEDD4-2, ITCH, WWP1, WWP2, SMURF1, SMURF2, HECW1, HECW2); 13 heterogeneous members are classified as "other HECTs" including HUWE1, UBR5, TRIPC, AREL1, UBE3A, UBE3B and UBE3C (Lorenz, 2018).

In *Arabidopsis*, the seven identified E3 ligases are called UPL (ubiquitin-protein ligase; Downes *et al.*, 2003) and are divided into four subfamilies (UPL1/2, UPL3/4, UPL5, and UPL6/7; Huibregtse *et al.*, 1995; Downes *et al.*, 2003), but their role needs to be elucidated; it is known that UPL3 acts in trichome development (Downes *et al.*, 2003; Perazza *et al.*, 1999) and UPL5 is involved in regulating leaf senescence (Miao and Zentgraf, 2010).

RBR (RING-in-Between-RING) E3 ligases: RBR E3s have a tripartite motif of three Zn^{2+}-binding domains: two RING domains (RING1 and RING2) connected via an in-between-RING (IBR) domain (Morett and Bork, 1999; van der Reijden *et al.*, 1999). Once discovered, RBR E3s were classified as a subfamily of RING-type E3s (Imai *et al.*, 2000) but it was later shown that they have an active site which instead lacks in all the RING E3 ligases. Like RINGs, the RING1 domain of RBR binds the complex E2~Ubs. RING2, instead, exhibits an active cysteine that receives Ub from the E2~Ub complex, thus promoting the formation of the covalent E3~Ub thioester intermediate, which also occurs in HECT-type E3s (Wenzel *et al.*, 2011). The IBR and the RING2 domains coordinate two zinc ions but they do not have a RING fold. For all these features, RBR E3s are also named RING-HECT-hybrids (Dove and Klevit, 2017).

In humans, there are 14 RBR E3s (Marín *et al.*, 2004) involved in diverse cellular processes that have not been defined yet. A well-studied enzyme is Parkin which participates in the autophagic degradation of dysfunctional mitochondria, a process called mitophagy (Pickrell and Youle, 2015; Eiyama and Okamoto, 2015).

In *A. thaliana*, there are more RBR genes than in animals and three times more than in humans (Marín and Ferrús, 2002).

Plant RBR proteins are grouped into four subfamilies: Ariadne, ARA54, Plant I/Helicase and Plant II (Marín *et al.*, 2004; Marín and Ferrús, 2002; Lucas *et al.*, 2006). The first three are found in unikonts and bikonts (Marín and Ferrús, 2002; Marín, 2009), the fourth one only in higher plants.

1.4 The moss *Physcomitrium patens* Mitten

P. patens is a bryophyte of the *Funariaceae* family. Its life cycle comprises a dominant haploid gametophytic generation and a simple diploid sporophyte. The haploid gametophyte consists of two distinct developmental stages (**Figure 1.15**):

1. the protonema, composed of a filamentous network of chloronemal cells, rich in chloroplasts, and caulonemal cells where chloroplasts are less abundant (Prigge and Bezanilla 2010);

2. the gametophore or leafy shoot, from which rhizoid filaments differentiate ensuring soil anchoring and nutrient uptake (Hoffmann *et al.*, 2014). The sexual organs antheridia and archegonia form on the top of the gametophores. Spermatozoids are produced in the antheridia and fertilize the egg cell in the archegonium (Prigge and Bezanilla 2010).

P. patens plantlets grow easily on a mineral solid medium in *Petri* dishes, in a growth chamber at 25 °C under a 16/8 h light/dark photoperiod. In 8-10 weeks, the gametophyte reaches the complete development, whereas the spores are produced in 3-4 months (Schaefer and Zrÿd, 2001).
The moss has several advantages that make it a model system: it has a simple developmental pattern, it is suitable for cell lineage analysis, it shares many biological features with flowering plants: for instance, it uses the same phytohormones (*e.g.* auxin, abscisic acid and gibberellins) and mechanisms of intracellular messaging (*e.g.* Ca^{2+}) (Reski, 1998; Quatrano *et al.*, 2007). *P. patens* provides an excellent experimental material for genetic transformation, due to the high frequency and rapidity of protoplasts regeneration. An efficient method to transform protoplasts is based on PEG-mediated DNA uptake which allows to obtain more stable transformants if the plasmid DNA is linearized (Hohe *et al.*, 2004).
The moss genome (27 small chromosomes), with 35000 protein-coding genes, was sequenced in 2008 by Rensing *et al.*, and it represents a valuable means to understand the evolution and the adaptation of flowering plants.

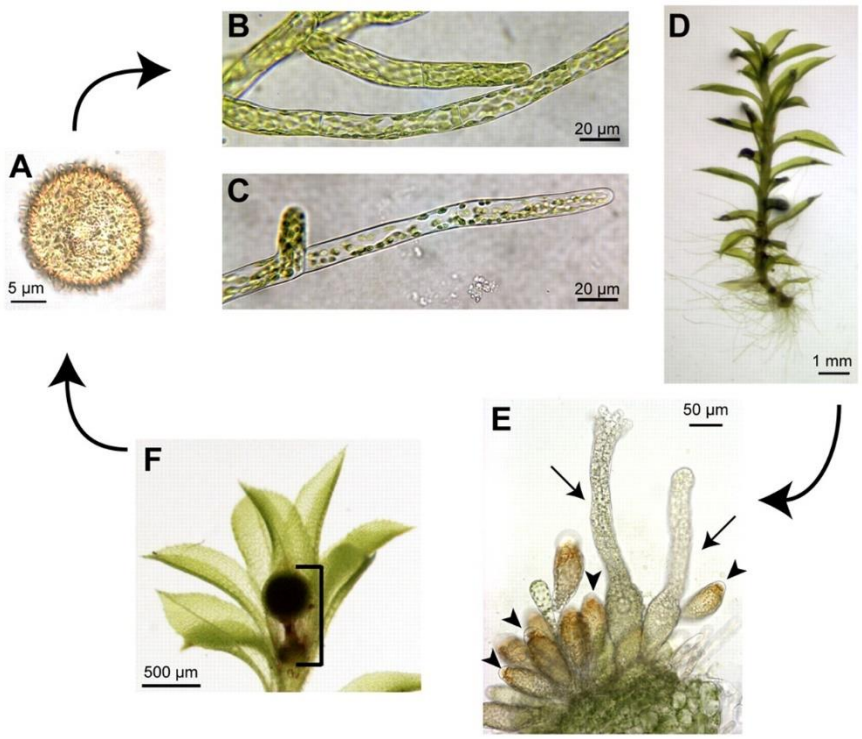

Figure 1.15. *P. patens* life cycle. (**A**) A haploid spore germinates into (**B**) chloronemal cells, which continue to grow and differentiate into (**C**) caulonemal cells. (**D**) Gametophores, or shoots, emerge off protonemal filaments and are ultimately anchored by rhizoids that grow by tip growth from the base of the gametophore. (**E**) At the apex of the gametophore, both female archegonia (arrows), and male antheridia (arrowheads) organs form. A motile flagellate sperm fertilizes the egg and the (**F**) sporophyte (marked with a bracket) develops at the apex of the gametophore (image and text from Prigge and Bezanilla, 2010).

1.4.1 Homologous recombination in *P. patens*

Unlike other land plants, a unique advantage of *P. patens* is the highly efficient integration of foreign DNA by homologous recombination (HR) which enables gene targeting to study the functions of the genes (Schaefer and Zrÿd 1997; Kamisugi *et al.*, 2006). DNA constructs used in HR must contain sequences homologous to the targeted genomic locus. The gene can be either mutated, deleted and consequently inactivated (Knock-Out), or it can be modified if a foreign sequence is inserted (Knock-In) (**Figure 1.16**).

In addition, it is possible to use the Cre/Lox system to insert site-specific mutations in the genome of *P. patens* or to excise markers. This system, naturally present in the bacteriophage P1 genome, consists of a Cre recombinase and a DNA target site, the LoxP site (34 bp sequences composed of two 13 bp recognition sites and an 8 bp spacer region between them). The genome of yeast and mouse have been manipulated by Cre/Lox system (Sauer, 1987; Schaefer and Zrÿd, 2001); in plant biotechnology, the Cre/Lox has been used to excise selectable markers and plasmid sequences in genetically modified crops (Dale and Ow, 1991).

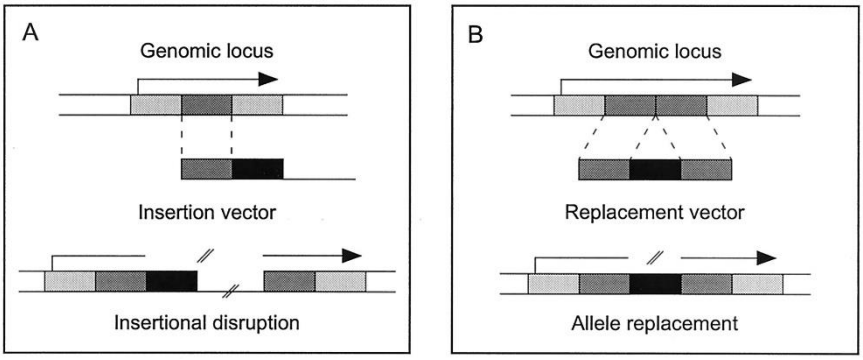

Figure 1.16. Typical vector design used in *P. patens* transformation. (**A**) The insertion vector carries a genomic fragment (dark gray) beside a selectable marker (black). Targeted integration is characterized by the insertion of one or several copies of the vector through homologous recombination with the genomic sequences. The resulting mutation is a gene inactivation by insertion. (**B**) A replacement vector carries a selectable marker (black) inserted between two genomic sequences. Integration occurs through two homologous recombination events. The result is a loss-of-gene function through allele replacement (image and text from Schaefer and Zrÿd, 2001).

1.4.2 The moss vacuoles

In the work of Oda *et al.* (2009), the morphology of the moss vacuoles in chloronemata was described using a fusion construct composed of GFP and the *A. thaliana* t-SNARE *At*VAM3 (**Figure 1.17**). This tonoplast marker allowed to show that in the apical chloronemata, the vacuoles are highly dynamic and complex, characterized by tubular protrusions, while their structure in sub-apical cells is simpler. These structures are maintained by the microtubules rather than actin microfilaments; thus, it has been thought that vacuolar distribution could be regulated by the interaction between microtubules and vacuolar membranes.

Dynamic tubular vacuoles were observed in the chloronema cell cortex and the rhizoid cells; dynamic vacuoles have been also found in the root hair cells and the pollen tubules of higher plants, indicating that vacuoles could play a key role in the tip-growing cells (Hepler *et al.*, 2001; Hicks *et al.*, 2004; Ovecka *et al.*, 2005).

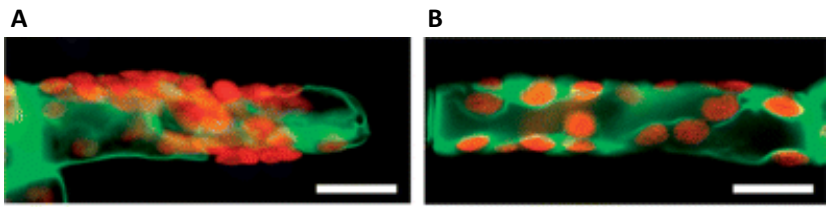

Figure 1.17. Visualization of vacuolar membranes by stable expression of GFP-*At*VAM3 fusion protein. Fluorescent images of a chloronema apical cell (**A**) and a non-apical cell (**B**) of a transgenic line expressing GFP-*At*VAM3 fusion protein. Green represents GFP, red signals indicate autofluorescence of chloroplasts (adapted from Oda *et al.*, 2009).

In the same cell of moss chloronema, two vacuoles can coexist, as well as in flowering plants (Epimashko *et al.*, 2004): acidic vacuoles accumulate the dye Neutral Red (NR) and appear red, while neutral vacuoles do not accumulate the dye (Fahr, 2017). NR is also a pH indicator that turns yellow when the pH increases (pH range: 6.8-8.0) and it becomes positively charged when protonated. It can then no more cross membranes. This means it accumulates in acidic compartments which turn red. NR is also used as lysosomes/vacuoles stain for live cells (Repetto *et al.,* 2008): when these are going to die, they are no more able to accumulate the NR.

1.5 Aims

Because in Angiosperms it was not yet possible to eliminate or replace target genes, our laboratory switched to *P. patens* which has been used as model plant to study RMRs using gene targeting, replacement or Knock-Out by homologous recombination.
Single RMR-KO did not show any phenotype in *A. thaliana* which has six RMR genes. On the contrary, the generation of targeted *P. patens* mutants is feasible, for this reason, Sanaa Ayachi, who worked in our laboratory (2012), deleted sequentially all five moss RMR genes. The single and multiple *Pp*RMR-KO lines generated, were not distinguishable from *Pp*WT, thus they did not lead to any visible phenotype.
The 5 *Pp*RMRs show similar levels of RNA expression, but unfortunately, the localization of the proteins in moss is not known.

The first aim of this work is the detection of endogenous *Pp*RMRs. This is done by Western Blot using various antibodies and methods, such as protein extraction in DDM, or the microsomal fractionation (chapter 2).

By analogy with the related animal PA-TM-RING proteins, plant RMRs may also function as E3 ubiquitin ligases, contributing to vacuolar protein transport. The second aim is to determine if *Pp*RMRs (using *Pp*RMR2 as model) are indeed E3 ligases. Their autoubiquitylation, common in several E3 ligases, can be tested *in vitro* using a commercial E2 screening kit (chapter 3).

The third aim is to test candidate interactors of *Pp*RMR2 for ubiquitylation by *Pp*RMR2. Putative cytosolic candidates of *Pp*RMR2 have been identified by yeast two-hybrid screening (Hybrigenics company). Their interaction with *Pp*RMR2 can be tested through *in vitro* ubiquitylation assays (chapter 3).

The last aim is to identify phenotypes of the *Pp*RMR-KO mutants: about the visible phenotype, we will analyse the moss development under normal and salt stress conditions which could give us more information about the role of *Pp*RMRs. Concerning the intracellular phenotype, we will test for complementation of *Pp*KO mutants by overexpression of WT or mutant *Pp*RMR2. We will also test for dominant-positive or -negative effects of these mutants (chapter 4).

Chapter 2

*Pp*RMRs: unstable proteins?

In *P. patens*, 5 RMRs were identified, grouped into two sub-families, one including RMR1 and 2, the other one including RMR3, 4 and 5. The 5 genes are expressed at the same level but in different proportions depending on the tissues and the organs. While all the organs show the same expression level of RMR4, the other RMRs are differently distributed: high levels of RMR1, 3 and 5 are found in sporophytes and spores, whereas RMR2 is mainly expressed in protonema and gametophores (*Physcomitrella* eFP browser).

Localization of RMRs in moss is still unknown. The previous PhD student Fahr (2017) generated a construct containing the full sequence of *Pp*RMR2, C-terminally fused with a blue variant of GFP, named Cerulean, under the control of the HSP (heat-shock protein) promoter. The transgenic *Pp*WT line transformed with this construct did not display any fluorescence under confocal microscope, suggesting a gene silencing. This experiment was not repeated, and we focused on other methods for protein detection, using the antibodies anti-RMR available in our laboratory. Here we describe the techniques used for detection, from genomic DNA (by PCR) to proteins (by Western Blot analysis).

2.1 Results

2.1.1 Detection of *Pp*RMR genes by PCR

After genomic DNA extraction from *Pp*WT and *Pp*5KO, all five RMRs were detected by PCR in *Pp*WT and none in the *Pp*5KO DNA (**Figure 2.1**).

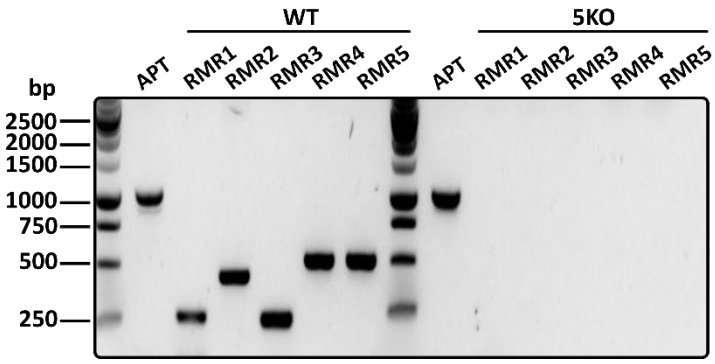

Figure 2.1. Genotyping of 5 *Pp*RMR genes by PCR. gDNA was extracted from *Pp*WT and *Pp*5KO protonema cultures. The five genes (RMR1: 250 bp; RMR2: 432 bp; RMR3: 236 bp; RMR4: 512 bp; RMR5: 522 bp) were detected in *Pp*WT, not in *Pp*5KO as expected. APT (Adenine Phosphoribosyl Transferase: ~ 1 Kb) was used as positive control.

2.1.2 Attempted detection of *Pp*RMR proteins — extraction in SDS-Sample Buffer

Since the detergent sodium dodecyl sulfate (SDS) is widely employed for the solubilization of membrane proteins, we used the 2X SDS-sample buffer (SB) to homogenize moss total proteins in the attempt to isolate RMRs. After SDS-PAGE, immunodetection was performed using different antibodies. Those against rice and *Arabidopsis* RMRs did not detect any RMR. We also tested antipeptide antibodies against moss RMR2 and RMR4, targeted to a region of the cytosolic tail. We tested several bleedings for each rabbit and the only antibody which detected a band on the nitrocellulose membrane was the one against *Pp*RMR2/*Pp*RMR4 – "final day". However, the band did not correspond to any RMR (~ 40 KDa) either in *Pp*WT or in *Pp*3KO samples (where RMR2 and RMR4 are remaining), and the same band was present even in the 5KO moss. The **figure 2.2** shows a Western Blot of total protein extracts after incubation with anti-RMR2 antibody (final day): only non-specific bands appeared on the blot.

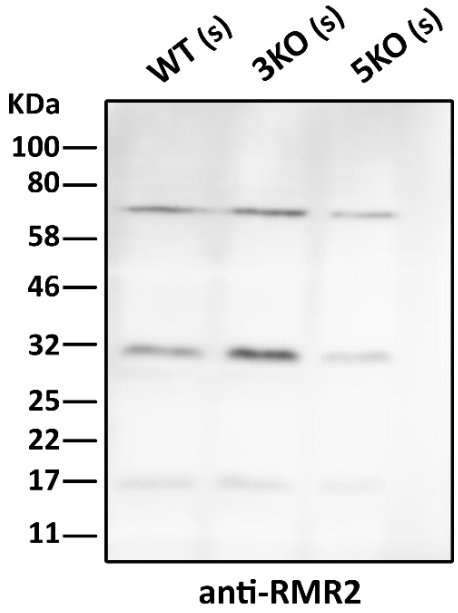

Figure 2.2. Western Blot of moss total proteins extracted in 2X SDS-SB. Total proteins were extracted from *Pp*WT, *Pp*3KO and *Pp*5KO protonema. Supernatant (**s**) fractions were collected and loaded on polyacrylamide gel for Western Blot analysis. Anti-RMR2 antibody (final day) detected the same band in all *Pp* strains, which did not correspond to the right MW of *Pp*RMR2 (~ 40 KDa).

On the other hand, the recombinant GST-*Pp*RMR2 produced by the previous PhD student Fahr (2017) was instead properly recognized at 42 KDa by both anti-RMR2 final day (**Figure 2.3 A**) and anti-GST antibodies (**Figure 2.3 B**). This recombinant protein is the fusion of the 26 KDa GST and the 16 KDa cytosolic side of *Pp*RMR2.

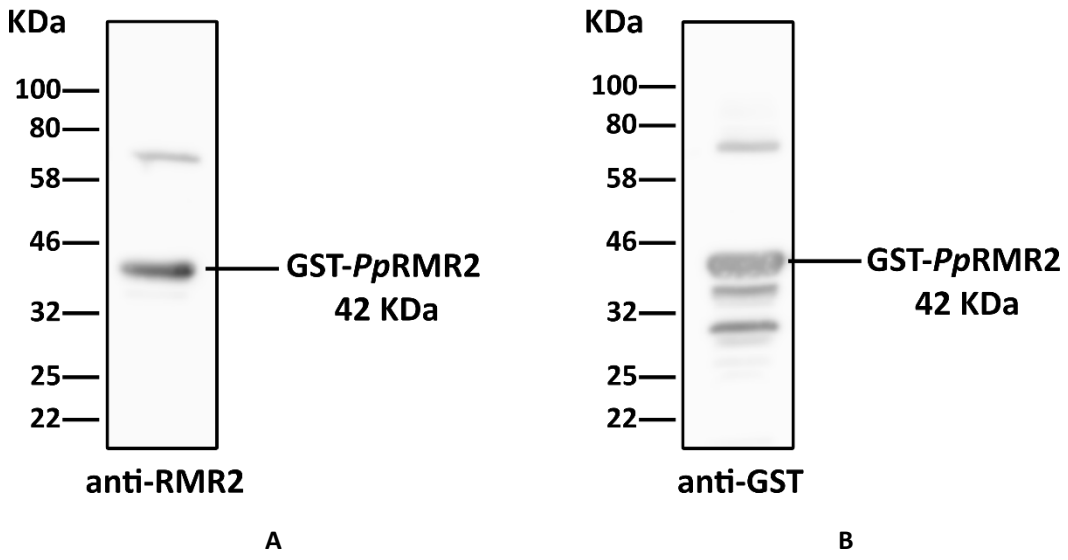

Figure 2.3. Western Blot of recombinant GST-*Pp*RMR2 expressed in *E. coli* and purified. Anti-RMR2 (**A**) and anti-GST (**B**) antibodies detected GST-*Pp*RMR2 at 42 KDa.

2.1.3 Attempted detection of *Pp*RMR proteins — extraction with the detergent DDM

Besides 2X SDS-SB, another detergent was tested, the n-dodecyl-β-D-maltoside (DDM) which is useful for the solubilization of membrane protein complexes (Liu *et al*., 2015). This nonionic detergent is composed of a lauryl hydrophobic chain and a maltose hydrophilic part. It is employed to purify membrane proteins (Loo and Clarke, 1995; Hazard and Montemagno, 2002) and to solubilize hydrophobic proteins keeping intact their structure, thus it is considered a mild detergent (Whitelegge *et al*., 1999; Lee *et al*., 2013).

0 .5% DMM was added to the total protein extraction buffer (Tris-HCl, pH 7.5). Protonema cultures of *Pp*WT, *Pp*3KO and *Pp*5KO were homogenized, centrifuged and the supernatant fractions were analysed by Western Bot: the anti-RMR2/RMR4 antibodies did not detect any RMR2/RMR4 in the total protein extracts from *Pp*WT and *Pp*3KO lines (the **figure 2.4** shows the immunodetection by anti-RMR2 antibody).

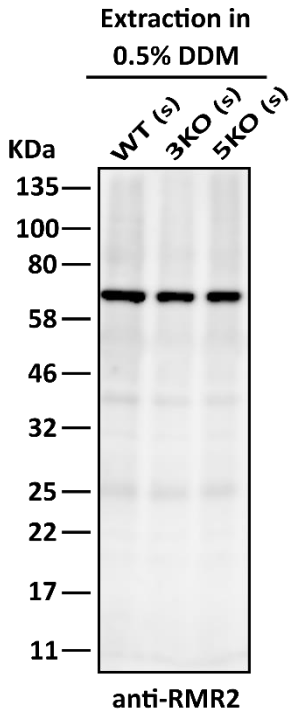

Figure 2.4. Western Blot of moss total proteins extracted in 0.5% DDM. Total proteins were extracted from *Pp*WT, *Pp*3KO and *Pp*5KO protonema. Supernatant (**s**) fractions were collected and loaded on polyacrylamide gel for Western Blot analysis. Anti-RMR2 antibody only detected non-specific bands in all the samples.

2.1.4 Attempted detection of *Pp*RMR proteins in a microsomal fraction

Microsomal fractionation was performed to make *Pp*RMRs detection easier: microsomes are vesicle-like structures formed during cell lysis. In plants, they consist of pieces of the ER, GA, TGN and tonoplast. As well described by LaMontagne *et al*. (2016), the microsomal fractionation consists of an initial low-speed centrifugation where nuclei, chloroplasts and mitochondria are removed, while microsomes are separated from cytosolic and soluble proteins by ultracentrifugation.

Total proteins were extracted from *Pp*WT, *Pp*3KO and *Pp*5KO lines and a Western Blot was performed using anti-RMR2/RMR4 antibodies. The **figure 2.5** shows non-specific bands detected by anti-RMR2 antibody, either in the pellet, where the microsomal fraction is supposed to be, or in the supernatant fractions, loaded as controls.

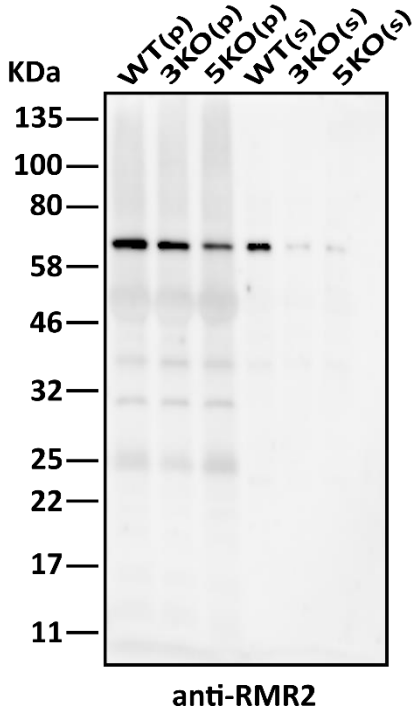

Figure 2.5. Western Blot after microsomal fractionation. *Pp*WT, *Pp*3KO and *Pp*5KO underwent microsomal fractionation; pellet (**p**) and supernatant (**s**) were collected and loaded on polyacrylamide gel for Western Blot analysis. Anti-RMR2 antibody only detected non-specific bands.

2.2 Discussion

Localization of RMRs has been investigated in higher plants. In 2000, Jiang *et al*. found RMRs in the PSV crystalloid of tomato cells. In *A. thaliana*, *At*RMR1 has been found in PVC (Park *et al*., 2005) or in vacuoles (Scabone *et al*., 2011), *At*RMR2 in the GA, dense vesicles (DV) and PSV of *A. thaliana* embryos (Hinz *et al*., 2007). Later, *At*RMR1 was mainly localized to the ER and *At*RMR2 to the TGN of tobacco leaves (Occhialini *et al*., 2016). In rice cultured cells and in developing rice seeds, *Os*RMR1 was identified in GA, TGN and PVC-like organelles; in developing rice seeds, *Os*RMR1 was also detected in the protein body type II (PBII) or PSV (Shen *et al*., 2011).

In the moss *Physcomitrella patens*, RMRs localization is still unknown.

In this chapter, we have shown that the 5 moss RMR genes were easily detected by genotyping, but protein detection in the moss total protein extracts was unsuccessful. The unstable nature of *Pp*RMRs or their short half-life could explain the issues encountered in detection.

We expected to detect moss RMR2 or RMR4 at ~ 40 KDa, but only unspecific bands of ~ 30 KDa were found in *Pp*WT, *Pp*3KO (where RMR2 and RMR4 are remaining) and *Pp*5KO. Different conditions were tested: antibody dilution was decreased, different exposure times and/or temperatures were performed during the blocking step (30 minutes, 1 hour, 2 hours at room temperature, overnight at 4°C), either milk or BSA were used as blocking solution, but even the use of a strong detergent such as 0.5% DDM did not help us to detect *Pp*RMRs.

We also performed a microsomal fractionation where the last pellet collected at 150000 x g, called microsomal fraction, is enriched in plasma membranes, endoplasmic reticulum, Golgi apparatus, vacuolar membranes and diverse endosomal vesicles and compartments, but no *Pp*RMRs were found in our samples.

If the endogenous *Pp*RMRs were not detected, on the other side, the recombinant GST-*Pp*RMR2 was recognized by anti-RMR2 antibody, therefore we can assume that endogenous *Pp*RMRs have a short half-life. The Serine-Rich motif present in the cytosolic tail of *Pp*RMRs could be the reason for their rapid degradation, in fact it is known that serine/tyrosine-rich domains undergo phosphorylation which is a post-translational modification involved in protein stability and endurance (Varedi *et al*., 2010).

Proteins can be degraded by proteasomes (which capture the ubiquitylated proteins in the cytosol; Vierstra, 2009), or through autophagy of cytosolic complexes, or by lysosomes/lytic vacuoles (Araújo *et al*., 2011) and a network of organelle-localized proteases (Janska *et al*., 2013; van Wijk, 2015). Isotopic labelling and mass spectrometry allowed to measure protein degradation rates and half-lives in yeast, mammalian cell cultures, and intact animals using single labelled amino acids (Price *et al*., 2010; Schwanhäusser *et al*., 2011). This technique, known as stable isotope labelling by amino acids in

cell culture (SILAC) is possible if the cell line tested is auxotrophic for the amino acid used for labelling, therefore plants are unsuitable because they are autotrophic. In this case, different metabolic labels such as ^{2}H, ^{13}C, and ^{15}N have been used by researchers to show the presence of proteins with a short half-life in plants (Yang *et al.*, 2010; Li L *et al.*, 2012).

A very important feature that could affect a protein half-life, relies on its structure: it has been proved that the presence of disordered regions in proteins of yeast, mouse and human cells, affects protein half-life. Disordered regions are referred to polypeptide regions that do not possess a defined 3D structure; van der Lee *et al.* (2014) demonstrated that proteins containing a long (> 30 residues) terminal region or internal disordered segments have a short half-life. The most used tools to predict disordered regions are DISOPRED2 (Ward *et al.*, 2004), IUPred (Dosztányi *et al.*, 2005), and PONDR® VLS1 (Obradovic *et al.*, 2005).

We have used PrDOS tool to show that all five *Pp*RMR sequences exhibit a disordered region (> 50 residues) in the C-terminal side, therefore these proteins could have a short half-life, and this would explain why we could not detect them.

Chapter 3

*Pp*RMR2 involvement in ubiquitylation: an *in vitro* study

We have decided to continue the work of the previous PhD students, focusing our study on *Pp*RMR2: Ayachi (2012) generated the *Pp*1KO mutant (Δrmr2) and Fahr (2017) transformed it with the fluorescent construct Citrine-Cardosin (Ci-Card) carrying out studies on the sorting phenotype (details in chapter 4). She also fused the C-terminal part of *Pp*RMR2 to GST-tag, in order to identify putative binding partners by mass spectrometry: it is known that the cytosolic part of *Pp*RMR2 contains the RING-H2 domain, probably involved in protein-protein interaction. This domain is conserved in the homologues of RMRs which belong to PA-TM-RING protein group (GRAIL, Goliath, RFN13, RNF167) and are supposed to function as E3 ubiquitin ligases.

It is known that the ubiquitin pathways are essential for the function of the eukaryotic cell (Joazeiro and Weissman, 2000; Denison *et al.*, 2005). Several cellular processes depend on ubiquitylation, such as trafficking, protein turnover, protein localization, regulation of protein function (Sawasdikosol *et al.*, 2000; Marmor and Yarden, 2004). The ubiquitylation process involves E1, E2 and E3 enzymes. First, ubiquitin is activated in an ATP-dependent reaction by the E1 activating enzyme. The activated ubiquitin is transferred to the E2 conjugating enzyme which interacts with a specific E3 ligase promoting the autoubiquitylation of the E3 or ubiquitylation of the lysine residues of specific target proteins (Fang and Weissman, 2004). The two major classes of E3 enzymes are the HECT-type E3 ubiquitin ligases and the E3 enzymes RING finger domain proteins.

3.1 Inhibition of degradation

Lineberry N *et al*. (2008) found that the RING-H2 domain of GRAIL ubiquitylates lysines on the cytosolic side of target proteins such as tetraspanins CD151 and CD81. To show this, they used specific inhibitors E64, ALLN and MG132. These potent molecules are generally used to inhibit the degradation of polyubiquitylated proteins which are known to have a short half-life.

Because we suppose that *Pp*RMRs are E3 ligases, we have repeated the same experiment in moss, in order to find potential partners that could be ubiquitylated by *Pp*RMRs.

3.1.1 Results

We have treated WT and 5KO moss liquid cultures for 4 hours in presence of 2.5 µM ALLN (proteasome and lysosomal cathepsins inhibitor), 2.5 µM MG132 (proteasome inhibitor) and 2.5 µM E64 (lysosomal cysteine proteases inhibitor). The treatment was performed at 15 °C in order to slow down the vesicular trafficking. Total protein extracts from protonema were then immunoprecipitated using the anti-Ub antibody. Ubiquitylation patterns were compared in WT and 5KO mosses by Western Blot. In the **figure 3.1 A**, a significant pattern was observed: *Pp*WT treated with MG132 showed an accumulation of ubiquitylated proteins. This result was not confirmed in the second assay where the WT and 5KO moss cultures were also treated with all the three inhibitors mixed. No obvious difference was visible between *Pp*WT and *Pp*5KO, only the heavy chain of anti-Ub antibody (~ 50 KDa) was detected (**Figure 3.1 B**). Overnight incubation with the inhibitors was also tested but the results did not change.

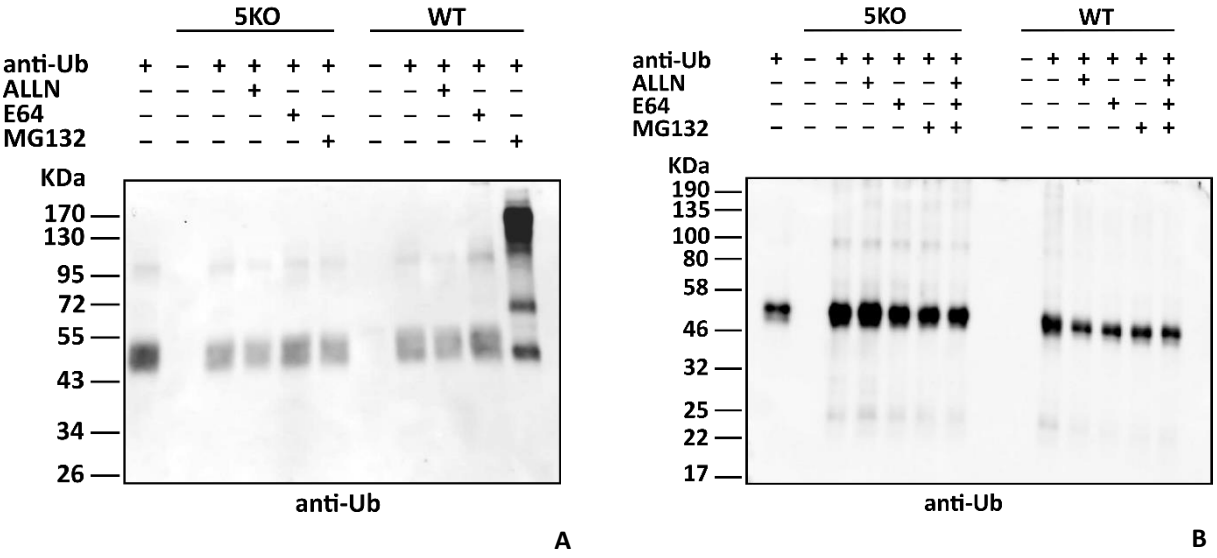

Figure 3.1. Western Blot of total protein extracts from 5KO and WT moss protonema after treatment with inhibitors. Total protein extracts from protonema were immunoprecipitated in presence of anti-Ub antibody and protein A sepharose beads, 4 hours after moss treatment with inhibitors of degradation ALLN, E64, MG132 at 15°C. Immunoprecipitation was followed by Western Blot using anti-Ub antibody. A pattern of ubiquitylation was detected in the total proteins extracted from *Pp*WT treated with MG132 (**A**). The experiment was repeated respecting the same conditions: new samples were prepared adding the one containing all the three inhibitors. No pattern of ubiquitylation was detected this time (**B**).

3.2 *Pp*RMR2 autoubiquitylation

It is possible to monitor the enzymatic activity of the RING E3 ligase through an *in vitro* autoubiquitylation assay, in which the E3 ligase adds ubiquitin moieties to itself (Amemiya *et al.*, 2008). GRAIL for instance is autoubiquitylated (Whiting *et al.,* 2011), hence we used GST-*Pp*RMR2 (cytosolic domain only) to test its autoubiquitylation *in vitro*.

The construct GST-*Pp*RMR2 was previously cloned into pGEX vector by Fahr (2017). I expressed it in *E. coli* BL21 strain, I purified, dialyzed the protein and tested its autoubiquitylation *in vitro*, following the protocols of Choo and Zhang (2009) and Stone *et al.* (2005). A kit containing 29 different E2 ubiquitin-conjugating human enzymes (UBPBio company; Zhang Q *et al.*, 2015) was tested since we know that the activity of an E3 ligase, including its autoubiquitylation, depends on a compatible combination of E2/E3.

Some E2s can function with different types of E3s (Stewart *et al.*, 2016), although it is not clear how they affect ubiquitylation outcomes. For a long time, researchers only tested the E2 named Ube2D1 (or UbcH5a) to study ubiquitylation activity. Indeed, the type of ubiquitylation produced by U-box and RING domain-containing E3 ligases is determined by the identity of E2, therefore other E2s have been tested, and consistent differences in ubiquitylation outcomes have been observed (Windheim *et al.*, 2008; Christensen *et al.*, 2007; Soss *et al.*, 2011).

In 2009, Markson *et al.* used the yeast two-hybrid (Y2H) screening to show that most of RING domain-E3 ligases enzymes bind a small number of E2 conjugating enzymes and that few E2 enzymes bind almost every E3 enzyme.

In vivo the ubiquitylation status is also controlled by the deubiquitylating enzymes (DUBs) which remove the ubiquitin moieties from the substrates, hydrolysing the bond between the ubiquitins. It is known that in *A. thaliana* there are more than 1500 E3s and about 50 DUBs: DUBs in fact, only interact with ubiquitin chains, not with the substrate (Isono and Nagel, 2014).

3.2.1 Results

The reagents involved in ubiquitylation were used at the following concentrations: 100 nM E1, 2 µM E2, 2 µM E3, 50 µM ubiquitin, 2 mM ATP, 10 X ubiquitylation buffer, in 20 µl final volume adjusted with Milli-Q H_2O.

The following reactions were set up for each of the 29 E2 enzymes:

- ✓ All the reagents except E1 activating enzyme (control)
- ✓ All the reagents except E2 ubiquitin-conjugating enzyme (control)
- ✓ All the reagents except GST-*Pp*RMR2 (E3 ligase) (control)
- ✓ All the reagents except ubiquitin (control)
- ✓ All the reagents

After 2 hours at 25 °C, the reaction was stopped by adding 2X SB. Samples were heated at 100 °C for 5 minutes and loaded on a polyacrylamide gel. Anti-Ub, anti-GST and anti-His antibodies were used for the immunodetection. Besides the ubiquitin (8.5 KDa), the first antibody (**Figure 3.2**) detected a polyubiquitin (poly-Ub) chain in the samples where all the reagents were present for five of the 29 E2 conjugating enzymes tested. These five E2 enzymes are known to catalyse Lys 11 and Lys 48-linked polyubiquitylation *in vitro*, and are: Ube2D1 (UbcH5A), Ube2D2 (UbcH5B), Ube2D3 (UbcH5C), Ube2D4 (UbcH5D), Ube2E1 (UbcH6), all 6xHis-tagged.

The anti-GST antibody detected GST-*Pp*RMR2 (42 KDa) but not the poly-Ub chain, therefore we cannot assume that GST-*Pp*RMR2 ubiquitylates itself.

A test with anti-His antibody was performed as we thought that, if GST-*Pp*RMR2 did not ubiquitylate itself, it might ubiquitylate one of the His-E2 enzymes. We were encouraged in doing this assay after having received a list by the Hybrigenics company which identified, through the Y2H screening, a huge number of putative candidates interacting with *Pp*RMR2. Among them there were three E2 ubiquitin-conjugating enzymes [one E2-W and two E2-D/E (family not specified)] which were supposed to interact with the cytosolic side of *Pp*RMR2, thus we thought they could be ubiquitylated by *Pp*RMR2, but we did not confirm this hypothesis in our *in vitro* ubiquitylation assay, because the anti-His antibody only detected the 6xHis-E2, not the poly-Ub chain (Ube2D1 is shown in the **figure 3.2**).

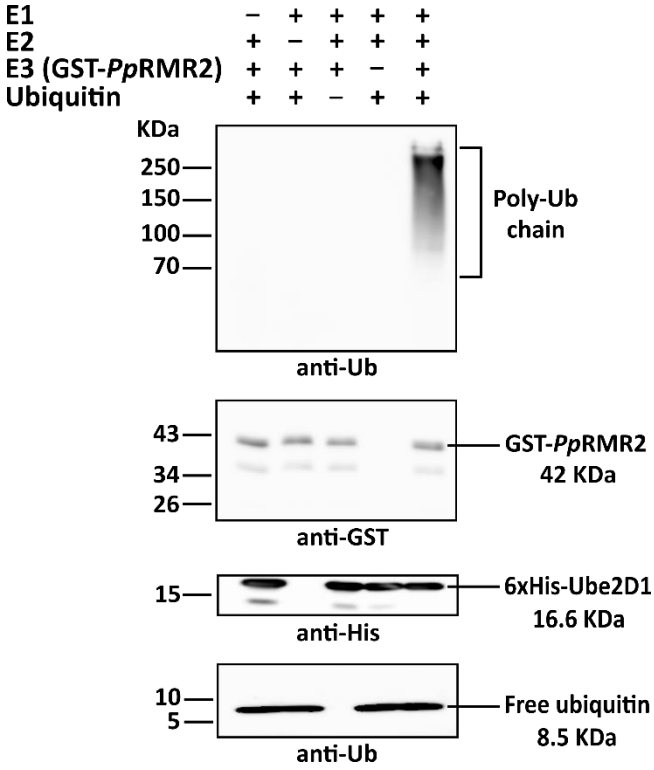

Figure 3.2. Western Blot after *in vitro* GST-*Pp*RMR2 autoubiquitylation assay. Three Western Blots were performed: the anti-Ub antibody detected the free ubiquitin (8.5 KDa) and a poly-Ub chain on GST-*Pp*RMR2 in the sample where all the reagents were present; anti-GST and anti-His antibodies detected GST-*Pp*RMR2 (42 KDa) and 6xHis-Ube2D1 (16.6 KDa) respectively, without detecting the poly-Ub chain. Ubiquitylation reactions were resolved in an 8%, 10% and 18% Tris-glycine PAGE.

3.3 *Pp*RMR2's cytosolic interacting proteins

We hired the French company Hybrigenics in order to find possible partners of *Pp*RMR2. For this aim, the company, through the Y2H system, screened the luminal and cytosolic sides of *Pp*RMR2 against a library of cDNA from *P. patens*, providing us with a list of interacting proteins that we have analysed. Some of them are supposed to be found in the nucleus or other cell compartments: molecular chaperones, transcription factors, splicing factors, heat-shock proteins, ATP binding proteins and molecules involved in glycolysis or photosynthesis processes were identified, but we have decided to keep the ones which have a high confidence in interaction with the cytosolic side of *Pp*RMR2 because this part of the protein could work as E3 ubiquitin ligase. The proteins listed in the **table 3.1** represent the cytosolic candidates that we have kept: the same candidates were also identified by mass spectrometry after a pull-down assay (Fahr, 2017) and this result encouraged us to focus on them. The purpose was finding the proteins eligible for ubiquitylation, and at the same time understanding whether vacuolar transport in moss is controlled by ubiquitylation (chapter 4).

Putative partners (Accession Number)	Functions
Dual-specificity phosphatase (Pp1s172_76V6.1)	Phosphorylation tyrosine or serine/threonine residues
Cytosolic ubiquitin ligases HUWE1-type (Pp1s138_130V6.1) UBR4-type (Pp1s131_210V6.1)	Proteasomal degradation N-end rule
26S proteasome subunits N2 (Pp1s114_55V6.1), N3 (Pp1s65_153V6.1), N9 (Pp1s131_74V6.1)	Protein degradation
Coatomer subunits α (Pp1s135_34V6.1), β (Pp1s168_28V6.1), γ (Pp1s276_96V6.1)	Intra-Golgi transport and from Golgi to ER and in endosomes (?)

Table 3.1. Some of *Pp*RMR2's cytosolic putative partners found by Y2H screening and mass spectrometry.

We have chosen to clone these partners, induce protein expression in *E. coli* BL21 strain, and study their involvement in ubiquitylation through *in vitro* assays.

3.3.1 Cytosolic ubiquitin ligases

Because of the big size of HUWE1 (CDS = 11.7 Kb) and UBR4 (CDS= 15.6 Kb), we have thought to knockout them using the CRISPR/Cas9 technology to verify whether the loss of these genes would affect the trafficking in *Pp*WT/Ci-Card. This line displays a fluorescent vacuolar pattern imputable to the targeting of Citrine-Cardosin to the vacuole (details in chapter 4): if the Knock-Out of the genes HUWE1 or UBR4 affects vacuolar transport in *Pp*WT/Ci-Card, we could suppose that the targeting of Citrine-Cardosin to the vacuole depends on the interaction between two E3 ligases such as *Pp*RMR and HUWE1 or UBR4. Unfortunately, we failed in obtaining the constructs, then we could not proceed with the CRISPR/Cas9 technology.

3.3.2 Dual-Specificity Phosphatase

The dual-specificity phosphatases (DUSPs) regulate MAPK activity by dephosphorylating both tyrosine and serine/threonine residues (Keyse, 1995). Their structure, similar to that of dual-specificity tyrosine phosphatase, contains a tensin-like domain and a catalytic domain, conserved in all DUSPs, which includes aspartic acid, cysteine and arginine residues (Huang and Tan, 2012).

They have been found in the nucleus or cytoplasm (or both) of yeast and other eukaryotes, including plants.

The MAPK pathways in animals are involved in inflammation and cancer diseases (Dhillon *et al.*, 2007; Kyriakis and Avruch, 2001) as well as in gene transcription, protein stability and localization, regulation of cell proliferation and cell death (Wada and Penninger, 2004; Turjanski *et al.,* 2007). *At*DsPTP1 (*Arabidopsis thaliana* dual-specificity protein tyrosine phosphatase) was demonstrated to dephosphorylate and inactivate the chinase *At*MPK4 (Gupta *et al.*, 1998).

The activity of DUSPs is regulated by post-translational modifications such as ubiquitylation, acetylation, phosphorylation, methylation. Ubiquitylation, for example, leads to the degradation of eight DUSPs in animals: DUSP1, DUSP4, DUSP5, DUSP6, DUSP7, DUSP8, DUSP9 and DUSP16; phosphorylation enhances the stability of DUSP2 and DUSP10 (Chen *et al.*, 2019-review). Yang *et al*. (2018) hypothesized that methylation of DUSP14 regulated its ubiquitylation and this might be induced by the interaction between the methylated DUSP14 and the E3 ligase TRAF2.

3.3.3 Proteasome subunits N2 (Rpn2), N3 (Rpn3), N9 (Rpn9)

The 26S proteasome is a compartment involved in diverse functions: protein degradation, cell differentiation, stress signaling, apoptosis. It is found in the cytosol and in the nucleus, and it contains a catalytic core called CP or 20S particle, and two 19S regulatory particles or RP, that allow the degradation of ubiquitylated proteins in an ATP-dependent reaction (**Figure 3.3**). In many eukaryotes, such as yeast and mammals, the 20S proteasome has a cylindrical structure, composed of two outer β-rings and two inner α-rings which are made up of seven α and β subunits, respectively; these rings form a complex called α1–7β1–7β1–7α1–7 (Tanaka, 2009-review). When the 20S proteasome degrades proteins, it generates oligopeptides of 3-15 amino acid residues which are hydrolysed into amino acids by oligopeptidases and/or amino-carboxyl peptidases. The RP recognizes polyubiquitylated proteins, and after removing the ubiquitin chain, it opens the α-ring allowing the CP to degrade the unfolded substrate.

The 19S RP (also called PA700) is composed of two sub-complexes: the lid and the base (Glickman *et al.*, 1998; Hanna and Finley, 2007). It is formed by about 20 subunits divided into two groups:

regulatory particle of triple-ATPase (Rpt) subunits and regulatory particle of non-ATPase (Rpn) subunits.

In the lid complex there are nine non-ATPase subunits: Rpn3, Rpn5, Rpn6, Rpn7, Rpn8, Rpn9, Rpn11, Rpn12 and Rpn15. The lid forms a horseshoe-like structure to position the deubiquitinase Rpn11, a metalloprotease which hydrolyses the isopeptide bond and releases Ub (Verma *et al.*, 2002; Worden *et al.*, 2017).

The base complex is formed by six homologous AAA-(ATPases associated with diverse cellular activities)-ATPase subunits, (Rpt1–Rpt6), and four regulatory particle non-ATPase subunits (Rpn1, Rpn2, Rpn10 and Rpn13). The Rpt1-Rpt6 subunits have the function to capture, unfold the ubiquitylated protein and open the α-ring of the channel. Rpn10 and Rpn13 bind polyUb, while the large subunits Rpn1 (110 KDa) and Rpn2 (104 kDa) show an affinity for ubiquitin-like (UBL) domains (Rosenzweig *et al.*, 2012). In plants, Rpn1 is important for *Arabidopsis* embryogenesis (Brukhin *et al.*, 2005), Rpn10 regulates ABA signaling (Smalle *et al.*, 2003); *Arabidopsis* Rpn12 is involved in cytokinin responses (Smalle *et al.*, 2002; Smalle and Vierstra, 2004).

The function of regulatory particle non-ATPase subunits in plants is poorly understood. Their deletion causes cell death, and their mutation in yeast determines the accumulation of polyubiquitylated proteins and proteasome malfunctioning (DeMarini *et al.*, 1995; Wang *et al.*, 2009). The sequences of Rpn1 and Rpn2 show 40% identity and contain 11 helix-turn-helix pseudo-repeats (Kajava *et al.*, 2004) composed of 35-40 amino acids. These repeats are largely distributed, and different subclasses are known, such as HEAT [huntingtin, elongation factor 3 (EF3), protein phosphatase 2A (PP2A), PI 3-kinase TOR1], tetratricopeptide repeat (TPR) and armadillo (arm) repeats (Andrade *et al.*, 2001).

The Rpn1 and Rpn2 pseudo-repeats belong to a subclass of subunits connected to proteasome and cyclosome, thus they are called “PC repeats” whose structure is a curved concave toroid (Kajava, 2002; Effantin *et al.*, 2009; He *et al.*, 2012). The central PC repeats form a closed toroidal structure, flanked by flexible N and C-terminal domain (Effantin *et al.*, 2009; Rosenzweig *et al.*, 2008).

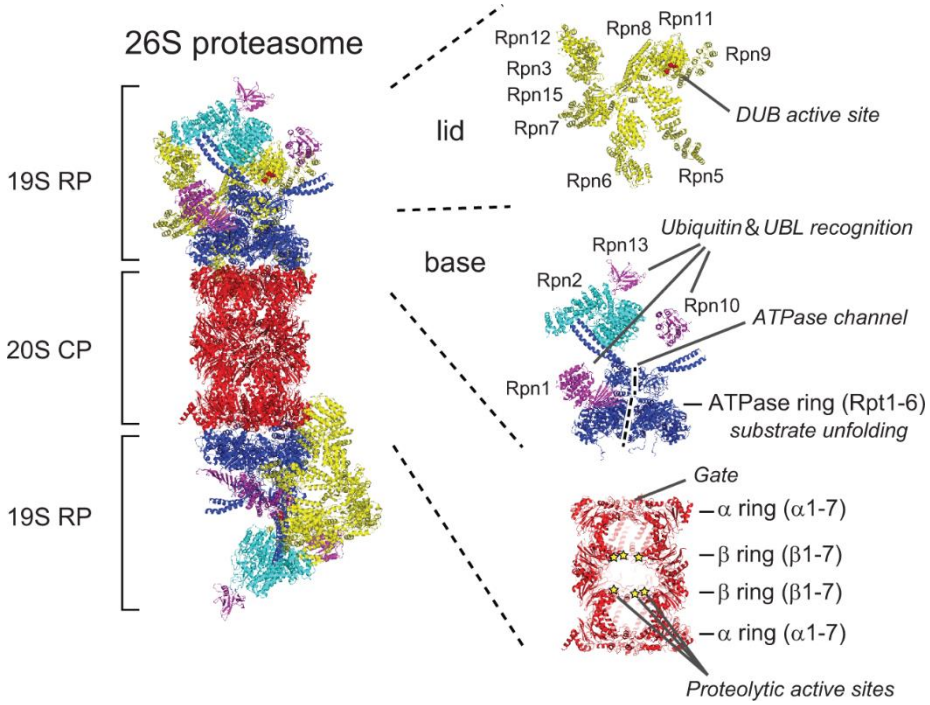

Figure 3.3. Structure and key subunits of the 26S proteasome. The 26S proteasome consists of a 20S core particle (CP) and one or two 19S regulatory particles (RP). The RP is composed of three ubiquitin/UBL receptors, deubiquitylating (DUB) enzymes, and hexameric ATPase enzymes involved in processing substrate proteins; these represent the components of two sub-assemblies called the lid and base. Proteins targeted for degradation are unfolded by ATPase enzymes and translocated into the proteolytic active sites through the CP channels (adapted from Saeki, 2017).

The activity of proteasome subunits is modulated by post-translational modifications such as phosphorylation, myristoylation, ubiquitylation, acetylation, methylation (reviewed by Kors *et al.*, 2019). Monoubiquitylation of Rpn10 in human cells prevented its capacity to interact with polyubiquitylated substrates (Isasa *et al.,* 2010) whereas in yeast, it caused the 26S proteasome dissociation (Keren-Kaplan *et al.*, 2016). Polyubiquitylation of Rpn10 led to its degradation in *Drosophila* (Lee *et al.*, 2014). An increased polyubiquitylation of Rpn13 was observed in human cells during stress conditions (heat-shock, oxidative or proteotoxic stress; Besche *et al.*, 2014): this event led to an accumulation of polyubiquitylated and/or damaged proteins thus suppressing their degradation.

It is known that proteasomes are found in the cytoplasm and in the nucleus, but an interesting work of Albert *et al.* (2017) revealed a different distribution of proteasomes in *Chlamydomonas reinhardtii* cells, analysed by tomography. These organelles were shown to be highly concentrated in the inner nuclear membrane and in the nuclear pore complex areas, whereas they were scattered in the cytoplasm.

N2 (Rpn2)

It interacts, together with Rpn1, with ubiquitin-binding proteins and proteasome auxiliary factors (Rosenzweig *et al*., 2008; Fatimababy *et al*., 2010) which belong to the UBL-domain containing proteins (UDPs). The solenoid portions of Rpn1 and Rpn2 are required for their mutual interaction, and for binding the ubiquitin receptor Rpn10 and the ATPases (Gorbea *et al*., 2000). These flexible extensions are probably involved in maintaining the stability of 19S RP-20S CP association (Marques *et al*., 2007) and may contribute to the proper nuclear localization of proteasome in yeast (Wendler *et al*., 2004).

N3 (Rpn3)

Interesting works revealed that this protein plays a role in cell cycle transition and in the mitosis process in budding yeast (Kominami *et al.,* 1997; Bailly and Reed, 1999): in temperature-sensitive mutant alleles, the essential non-ATPase Rpn3/Sun2 subunit, if mutated, causes a metaphase arrest without preventing the G1/S transition. In these mutants, the ubiquitin-dependent proteolysis of diverse substrates is compromised, and the half-life of Clb2 (B-type cyclin involved in cell cycle progression) is severely increased during the G1 phase. The arrest of rpn3 mutants prior to anaphase, impairs the proteolysis of the anaphase inhibitor Pds1, meaning that Rpn3 is essential in the destruction of Pds1 at the metaphase/anaphase transition.

N9 (Rpn9)

This nonessential subunit is needed at high temperatures for the proper functioning of the yeast proteasome (Takeuchi *et al*., 1999). The deletion of this gene leads to a temperature-sensitive growth and to a multi-ubiquitylated proteins accumulation.

Jin *et al*. (2006) showed that the silencing of the gene Rpn9 in *Nicotiana benthamiana*, inhibits the systemic transport of *Tobacco mosaic virus* and *Turnip mosaic virus*, due to an altered vascular tissue. The Rpn9 silenced plants were characterized by an extra leaf vein formation, an increased xylem, and a decreased phloem. These plants also displayed a reduced auxin transport and an alteration of brassinosteroid signaling which are two essential processes occurring in vascular formation. The authors proposed that Rpn9 controls vascular formation by targeting specific regulatory proteins for degradation, including the brassinosteroid-signaling protein BZR1.

3.3.4 Coatomer subunits

In 1991, the first studies about coated vesicles allowed to identify in animals, four large protein subunits (α-, β-, γ- and δ-COP) (Serafini *et al.*, 1991; Duden *et al.*, 1991). In the same year, a complex composed of these and other subunits was isolated from the cytosol, and it was called coatomer (Waters *et al.*, 1991). Later, new subunits were identified and termed β'-COP (Stenbeck *et al.*, 1993; Harrison-Lavoie *et al.*, 1993), ε-COP (Hara-Kuge *et al.*, 1994) and ζ-COP (Kuge *et al.*, 1993), thus the complete structure resulted to be a heptameric coat complex. It has been described a model of the organization of the COPI coatomer complex in which the α, β' and ε subunits form the B-subcomplex while the β, γ, δ and ζ subunits form the F-subcomplex (Faulstich *et al.*, 1996; Fiedler *et al.*, 1996).

Coated vesicles (COPI, COPII, CCVs) allow protein trafficking throughout the endomembrane system (Paul and Frigerio, 2007). COPII vesicles are responsible for the anterograde transport from ER to GA; CCVs mediate endocytosis and deliver proteins out of the TGN; COPI-coated vesicles mediate protein transport in the early secretory pathway (Rothman, 1994) in particular the intra-Golgi transport and the retrograde transport of proteins from the GA to the ER (Paul and Frigerio, 2007).

Using immunolabeling and *in vitro* reconstitution techniques, plant γ-COP proteins were found in the vesicles proximal to the GA (Pimpl *et al.*, 2000).

The work of Ahn *et al.* (2015) shows that in *N. benthamiana*, the β'-, γ- and δ-COP subunits interact with each other in the GA. The silencing of β'-, γ-, and δ-COP genes by VIGS (virus-induced gene silencing) caused the disassembly of GA and the accumulation of autolysosome-like structures. Moreover, DEX-inducible RNAi of β'-COP in tobacco BY-2 cells, affected cell plate formation. This suggests that the COPI coatomer complex is involved in plant growth and survival (Ahn *et al.*, 2015).

During the formation of COPI vesicles, the coat protein coatomer can interact either with membrane cargo proteins that should come back to the ER, or with membrane proteins that cycle between the ER and the GA.

In mammals and yeast, the mechanism through which ER-resident proteins bind to coatomer has been described: the C-terminal side of their cytoplasmic tail exhibits a conserved KKXX motif that is recognized by the coatomer complex (Cosson and Letourneur, 1994).

The work of Harter and Wieland (1998) describes the binding of the cycling p24 proteins to the coatomer in animals. p24 proteins represent the major transmembrane proteins of COPI-coated transport vesicles (Nickel *et al.*, 1997). It has been shown that they must dimerize in order to interact with two independent binding sites located on the trunk and on the appendage domain of γ-COP. This mechanism is different from the one adopted by ER-resident cargoes which instead bind as monomers to α- and β'-COP (Eugster *et al.*, 2004).

Xu *et al*. (2017) demonstrated that the specific recycling of an exocytic SNARE from the PM by COPI in yeast is mediated by ubiquitylation, particularly by recognition of a polyubiquitin chain on cargoes. Furthermore, the mammalian ε-COP ubiquitylation, mediated by the E3 ligase PIRH2, resulted in its proteasomal degradation (Maruyama *et al*., 2008). These results indicate that COPI activity is regulated by post-translational modifications, particularly by ubiquitylation.

3.3.5 Results

3.3.5.1 Cloning and protein purification

We encountered several issues during DNA cloning and protein purification, because of the huge size of most sequences. The CDS of each putative candidate was first subcloned in pJET1.2 vector then in pET21b containing 6xHis-tag for protein expression in *E. coli* BL21 strain. The His-tag was placed at the C-terminus of each protein sequence.

The **figure 3.4** shows the results of cloning in pET21b vector. The expected sizes are:
DUSP ~ 2 Kb (**A**); N2 ~ 3 Kb (**B**); N3 ~ 1.5 Kb (**C**); N9 ~ 1.2 Kb (**C**); Coatomer subunit γ (COPG) ~ 2.7 Kb (**D**).

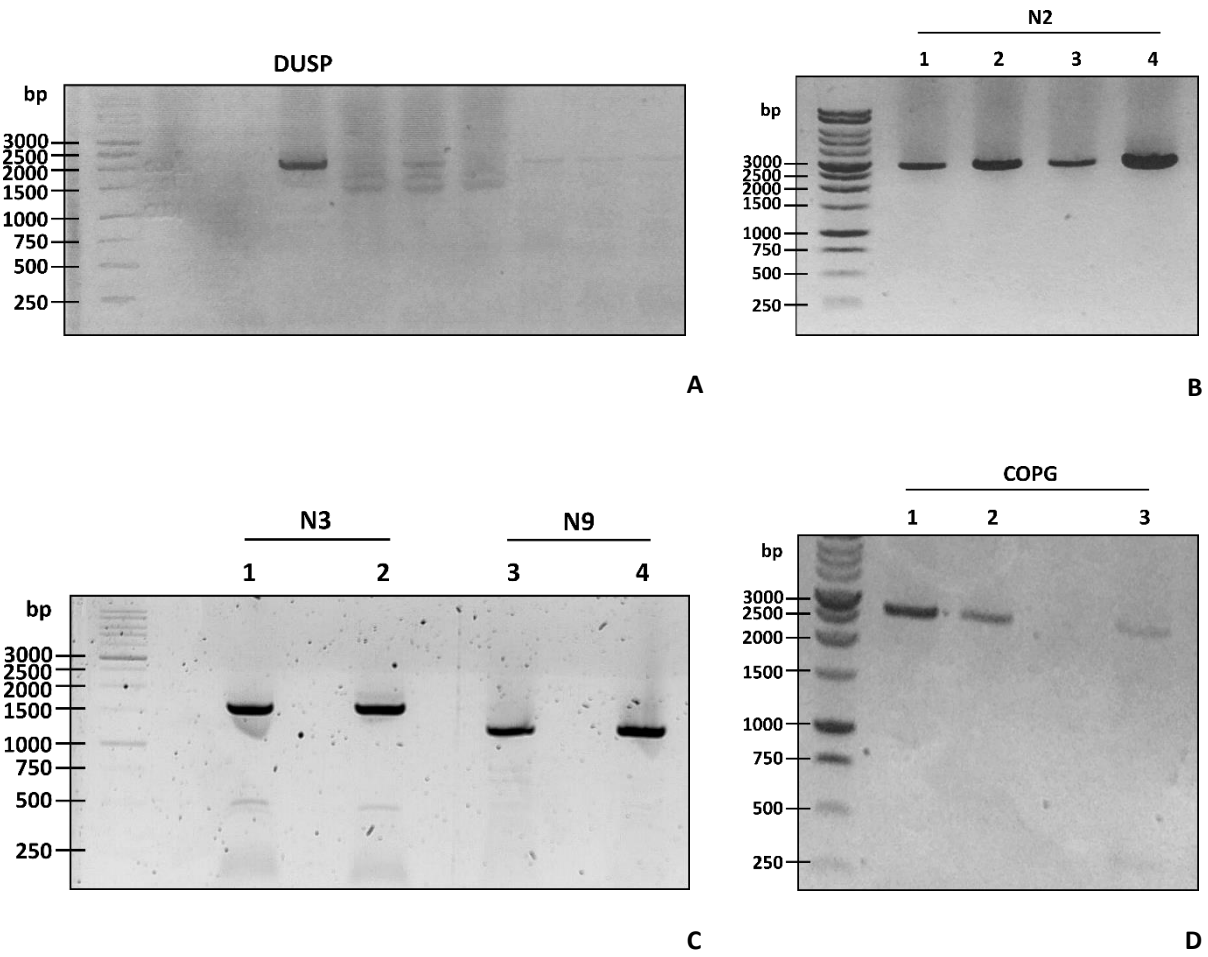

Figure 3.4. PCR of the five genes cloned in the final vector pET21b. A: Dual-specificity phosphatase (DUSP = ~ 2 Kb); **B:** N2 (~ 3 Kb); **C:** N3 (~ 1.5 Kb); N9 (~ 1.2 Kb); **D:** Coatomer subunit γ (COPG = ~ 2.7 Kb).

After cloning, the competent bacteria *E. coli* BL21 (D3) were employed for protein expression and purification. Each protein was purified in native conditions, using a Poly-Prep® chromatography column packed with Ni-NTA agarose resin, and dialyzed in an Amicon® Ultra centrifugal filter or using a regenerated cellulose (RC) membrane.

A Western Blot of all the collected samples was performed. The dialyzed proteins-His (10 µg loaded) were detected by anti-His antibody.

DUSP-His

We obtained the protein (even if not pure) after several assays due to a weak expression and degradation. We tested three IPTG concentrations (0.25 - 0.5 -1 mM) and collected samples every 15 minutes during 3 hours of induction. We found that DUSP-His expression was induced in 1h15min with 0.5 mM IPTG; afterwards, it was weakly expressed and undetectable by anti-His antibody. Nevertheless, the protein (~ 70 KDa) appeared degraded as shown in the **figure 3.5**.

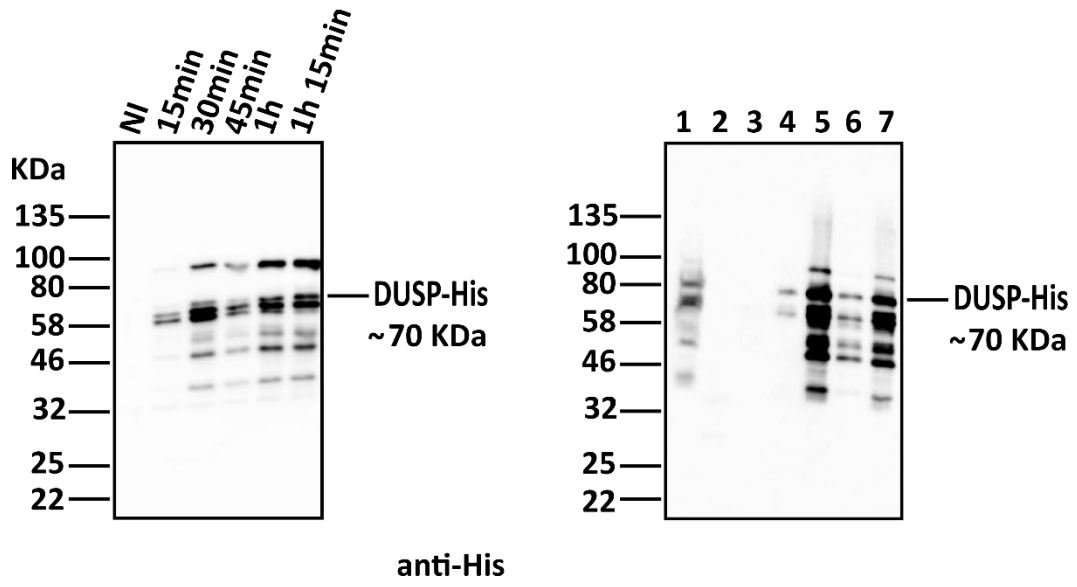

Figure 3.5. Western Blot of protein fractions from DUSP-His purification. NI: fraction of pellet from not induced bacterial culture. Fractions of pellet from IPTG-induced bacterial culture were collected every 15 minutes for 3 hours. The fraction collected after 1h15min was considered as optimal for the remaining purification steps. **Lane 1:** aliquot of supernatant collected after lysis (by French press) and centrifugation of the induced bacterial culture. **Lane 2:** aliquot of pellet collected after lysis (by French press) and centrifugation of the induced bacterial culture. **Lane 3:** flow-through (FT) collected after adding the cell lysate mixture into the column packed with Ni-NTA agarose resin. **Lane 4:** aliquot of fifth wash of the resin. **Lane 5:** eluted fraction. **Lane 6:** aliquot of resin after application of elution buffer. **Lane 7:** dialyzed fraction. Protein was detected at ~ 70 KDa by anti-His antibody.

N2-His

The purification of the insoluble protein N2-His, after several attempts, was not successful because of the huge molecular weight (110 KDa) and the presence of a TM domain.

N3-His

The expression of the soluble protein N3-His (~ 56 KDa) was induced by 0.5 mM IPTG for 1h15min, but the dialyzed protein resulted degraded when detected by anti-His antibody (**Figure 3.6**).

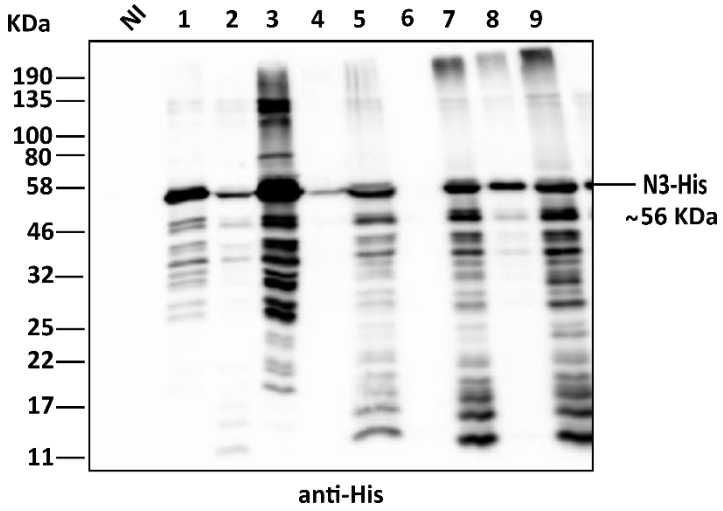

Figure 3.6. Western Blot of protein fractions from N3-His purification. NI: fraction of pellet from not induced bacterial culture. **Lane 1:** fraction of pellet from IPTG-induced bacterial culture collected after 1h15min. **Lane 2:** aliquot of supernatant collected after lysis (by French press) and centrifugation of the induced bacterial culture. **Lane 3:** aliquot of pellet collected after lysis (by French press) and centrifugation of the induced bacterial culture. **Lane 4:** flow-through (FT) collected after adding the cell lysate mixture into the column packed with Ni-NTA agarose resin. **Lane 5:** fraction of the resin after FT passed through the column. **Lane 6:** aliquot of fifth wash of the resin. **Lane 7:** eluted fraction. **Lane 8:** aliquot of resin after application of elution buffer. **Lane 9:** dialyzed fraction. Protein was detected at ~ 56 KDa by anti-His antibody.

N9-His

The soluble protein N9-His was purified, dialyzed and detected with anti-His antibody at the size of 45 KDa (**Figure 3.7**). The IPTG induction (0.5 mM) was stopped after 3 hours without any degradation issues.

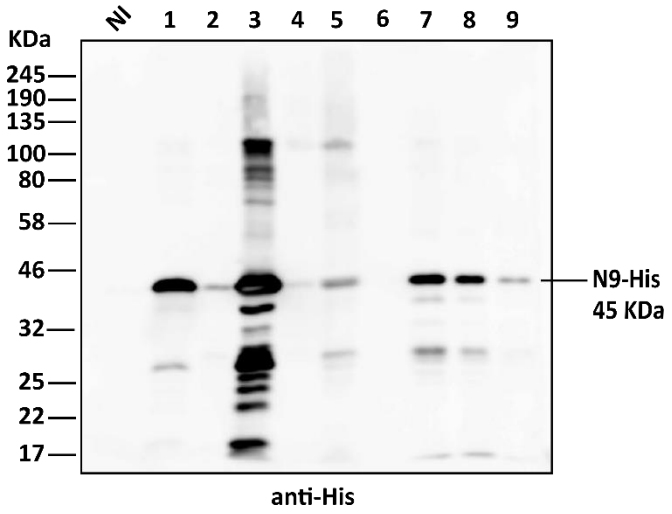

Figure 3.7. Western Blot of protein fractions from N9-His purification. NI: fraction of pellet from not induced bacterial culture. **Lane 1:** fraction of pellet from IPTG-induced bacterial culture collected after 3 hours. **Lane 2:** aliquot of supernatant collected after lysis (by sonication) and centrifugation of the induced bacterial culture. **Lane 3:** aliquot of pellet collected after lysis (by sonication) and centrifugation of the induced bacterial culture. **Lane 4:** flow-through (FT) collected after adding the cell lysate mixture into the column packed with Ni-NTA agarose resin. **Lane 5:** fraction of the resin after FT passed through the column. **Lane 6:** aliquot of fifth wash of the resin. **Lane 7:** eluted fraction. **Lane 8:** dialyzed fraction. **Lane 9:** aliquot of resin after application of elution buffer. Protein was detected at 45 KDa by anti-His antibody.

γ-coatomer subunit COPG-His

This soluble protein was correctly detected by anti-His antibody at 100 KDa (**Figure 3.8**). IPTG induction (0.5 mM) was stopped in 45 minutes to avoid degradation.

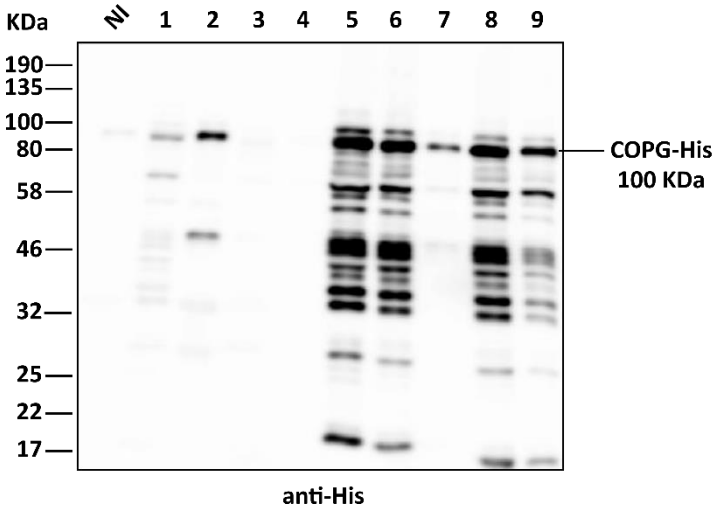

Figure 3.8. Western Blot of protein fractions from COPG-His purification. NI: fraction of pellet from not induced bacterial culture. **Lane 1:** fraction of pellet from IPTG-induced bacterial culture collected after 45 minutes. **Lane 2:** aliquot of supernatant collected after lysis (by French press) and centrifugation of the induced bacterial culture. **Lane 3:** aliquot of pellet collected after lysis (by French press) and centrifugation of the induced bacterial culture. **Lane 4:** flow-through (FT) collected after adding the cell lysate mixture into the column packed with Ni-NTA agarose resin. **Lane 5:** fraction of the resin after FT passed through the column. **Lane 6:** aliquot of fifth wash of the resin. **Lane 7:** eluted fraction. **Lane 8:** aliquot of resin after application of elution buffer. **Lane 9:** dialyzed fraction. Protein was detected at 100 KDa by anti-His antibody.

3.3.5.2 *In vitro* ubiquitylation assay between GST-*Pp*RMR2 and its putative candidates

The UbiSite tool was used to predict the presence of ubiquitylation sites in each putative candidate. For all the substrates that we have cloned and purified, we tested the American UBPBio kit and we have chosen the same E2s that gave us a pattern in the GST-*Pp*RMR2 autoubiquitylation assay [Ube2D1 (UbcH5A), Ube2D2 (UbcH5B), Ube2D3 (UbcH5C), Ube2D4 (UbcH5D), Ube2E1 (UbcH6)].

The ubiquitylation mix was composed of 100 nM E1, 2 µM E2, 2 µM E3, 2 µM substrate, 50 µM ubiquitin, 2 mM ATP, 10 X ubiquitylation buffer, in 20 µl final volume adjusted with Milli-Q H_2O.

GST-*Pp*RMR2 was used as E3 ligase. The negative controls were not prepared for each of the five E2 enzymes but only for Ube2D1, because the amount of the reagents was not enough to perform several assays.

The following reactions were set up:

- ✓ All the reagents without the E1 activating enzyme
- ✓ All the reagents without the E2 ubiquitin-conjugating enzyme
- ✓ All the reagents without the E3 ligase (GST-*Pp*RMR2)
- ✓ All the reagents without the substrate
- ✓ All the reagents without the ubiquitin
- ✓ All the reagents

This list has been used for all the putative candidates. After an incubation of 2 hours at 25 °C, the samples were collected for a Western Blot analysis.

DUSP-His + GST-PpRMR2

We have supposed that DUSP could be ubiquitylated by *Pp*RMR2 because its sequence (662 aa) contains 13 ubiquitylation sites (lysines) with a high confidence score (0.75).

The **figure 3.9** shows a poly-Ub chain detected by anti-Ub antibody. This is evident in presence of each E2 enzyme tested, but we cannot assume that DUSP-His is ubiquitylated by GST-*Pp*RMR2 *in vitro*, because the pattern was not confirmed by anti-His antibody which detected properly the protein (~70 KDa) but not the poly-Ub chain.

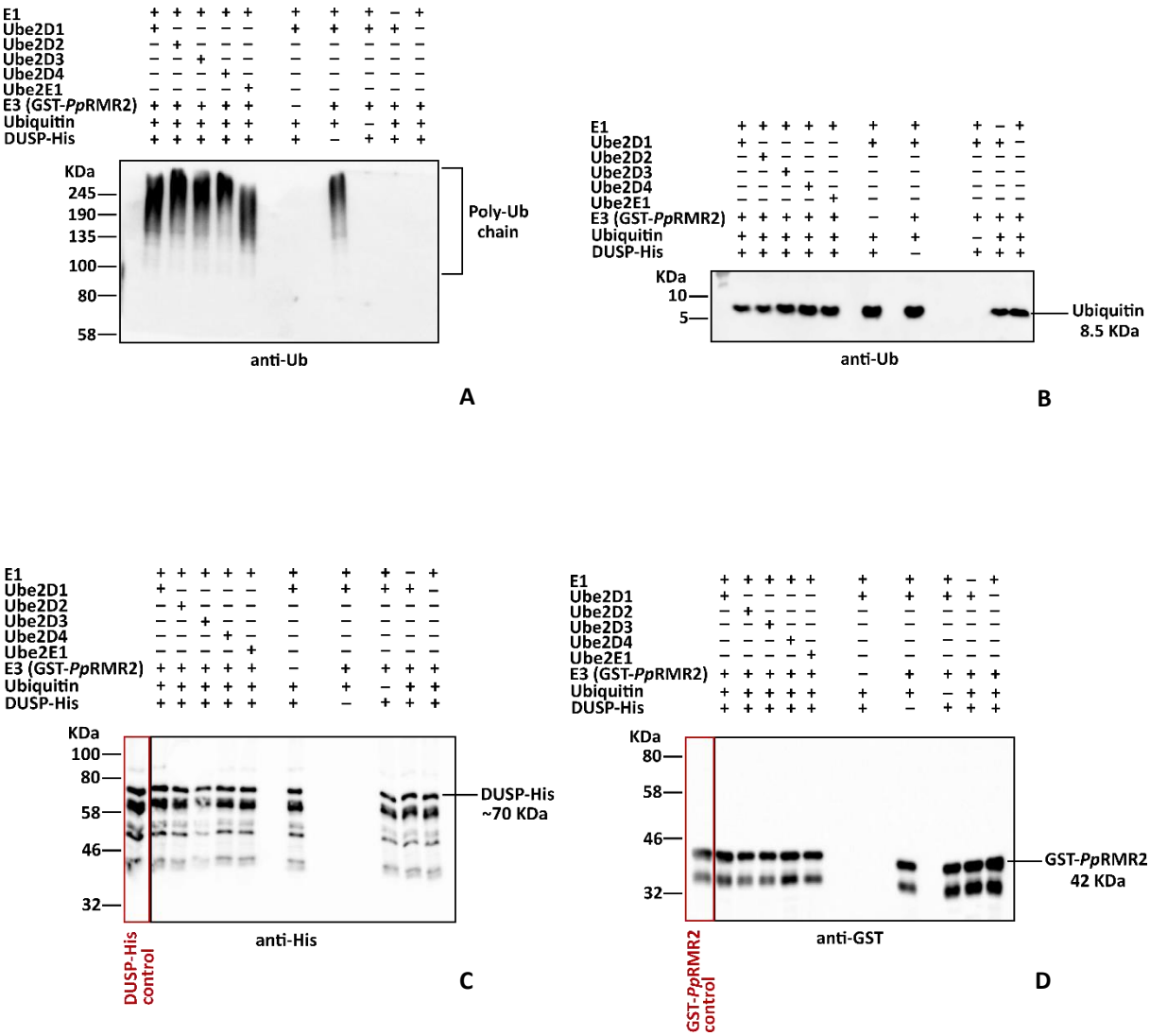

Figure 3.9. Western Blot after *in vitro* ubiquitylation test between DUSP-His and GST-*Pp*RMR2. GST-*Pp*RMR2 and DUSP-His were used as E3 ligase and putative candidate respectively, in presence of the E2 conjugating enzymes Ube2D1/Ube2D2/Ube2D3/Ube2D4/Ube2E1. Anti-Ub antibody detected a poly-Ub chain (**A**) and the free ubiquitin (8.5 KDa) (**B**). The detection of the chain was not confirmed by anti-His antibody which only recognized DUSP-His (~ 70 KDa) (**C**). GST-*Pp*RMR2 (42 KDa) was detected by anti-GST antibody (**D**). Ubiquitylation reactions were resolved in an 8%, 10% and 18% Tris-glycine PAGE.

N3-His + GST-PpRMR2

N3 (~ 56 KDa) is composed of 493 amino acids, and 5 lysines are predicted to be ubiquitinatable, with a score of 0.75 (high confidence). The results of Western Blot after the *in vitro* test, show the same patterns observed in the previous assay: a poly-Ub chain was only detected by anti-Ub, not by anti-His antibody (**Figure 3.10**).

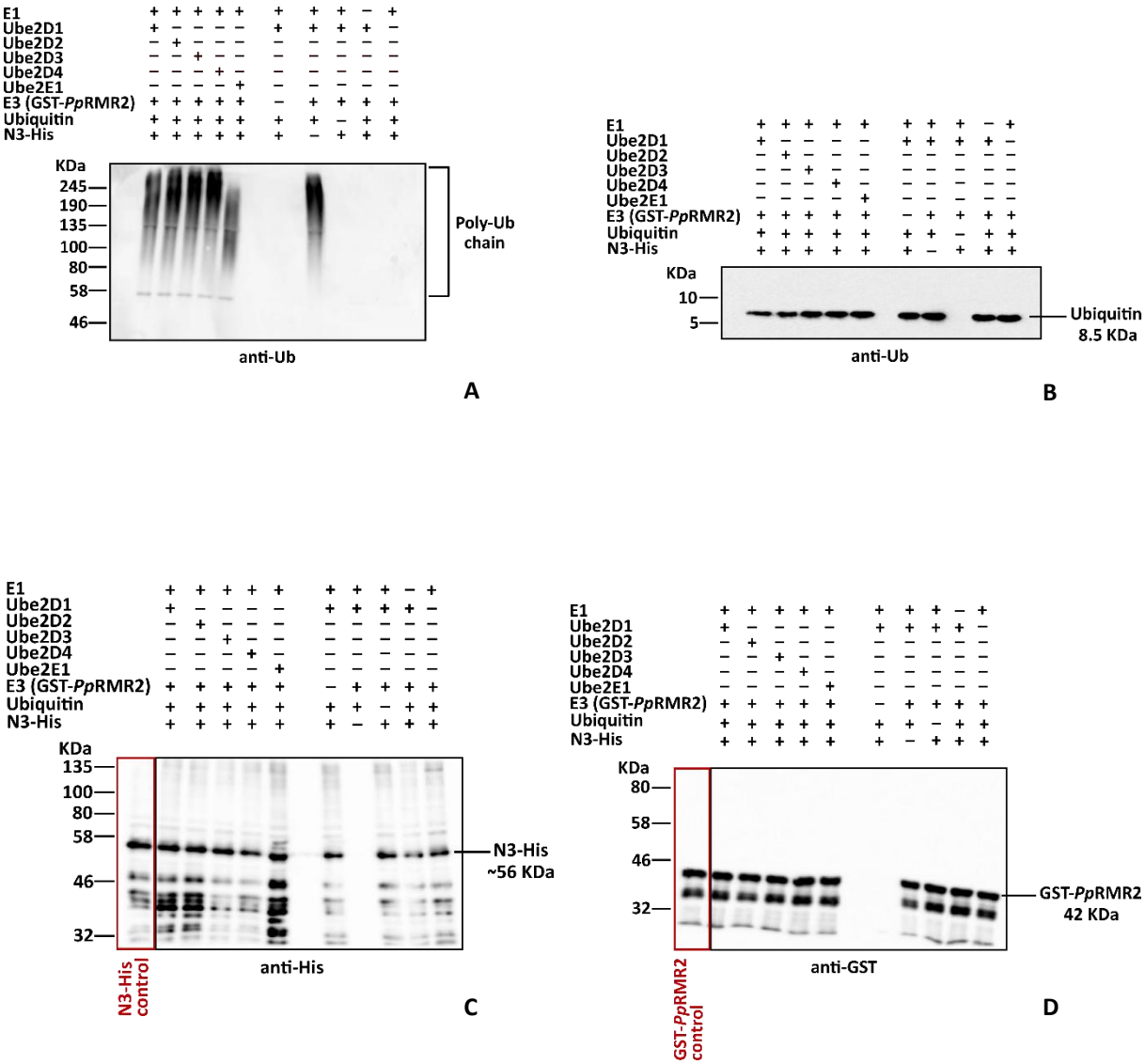

Figure 3.10. Western Blot after *in vitro* ubiquitylation test between N3-His and GST-*Pp*RMR2. GST-*Pp*RMR2 and N3-His were used as E3 ligase and putative candidate respectively, in presence of the E2 conjugating enzymes Ube2D1/Ube2D2/Ube2D3/Ube2D4/Ube2E1. Anti-Ub antibody detected a poly-Ub chain (**A**) and the free ubiquitin (8.5 KDa) (**B**). The detection of the chain was not confirmed by anti-His antibody which only recognized N3-His (~ 56 KDa) (**C**). GST-*Pp*RMR2 (42 KDa) was detected by anti-GST antibody (**D**). Ubiquitylation reactions were resolved in an 8%, 10% and 18% Tris-glycine PAGE.

N9-His + GST-PpRMR2

In N9 sequence (386 amino acids), 8 lysines are predicted to be ubiquitylation sites (score 0.75). In the **figure 3.11**, we can observe a poly-Ub chain in the samples where all the reagents are present. This has occurred for each E2 tested, except for Ube2D3 (very weak signal). The pattern was not reproduced by anti-His antibody which only detected N9-His (45 KDa) but not the poly-Ub chain. Therefore N9-His is not ubiquitylated by GST-*Pp*RMR2.

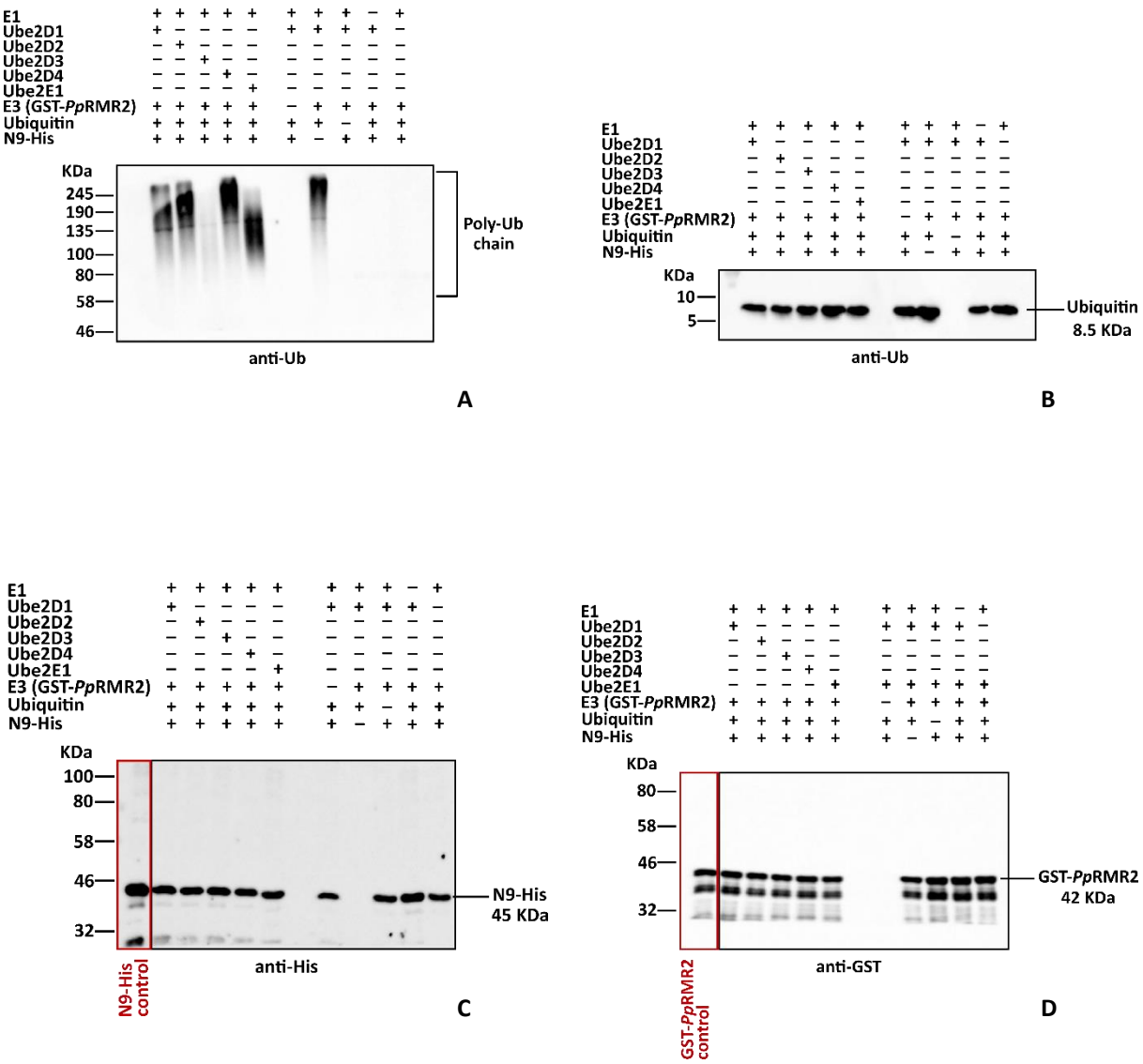

Figure 3.11. Western Blot after *in vitro* ubiquitylation test between N9-His and GST-*Pp*RMR2. N9-His was supposed to be the substrate of GST-*Pp*RMR2. Anti-Ub antibody detected a poly-Ub chain (**A**) and the free ubiquitin (8.5 KDa) (**B**) in presence of the five E2s tested. Anti-His only detected N9-His (45 KDa) (**C**), not the poly-Ub chain. GST-*Pp*RMR2 (42 KDa) was properly recognized by anti-GST antibody (**D**). Ubiquitylation reactions were resolved in an 8%, 10% and 18% Tris-glycine PAGE.

COPG-His + GST-PpRMR2

The 892 amino acids sequence of COPG contains 17 lysines that could be ubiquitylated. Even in this case, we cannot assume that COPG-His is ubiquitylated by GST-*Pp*RMR2 because the poly-Ub chain generated is only detected by anti-Ub antibody (**figure 3.12**).

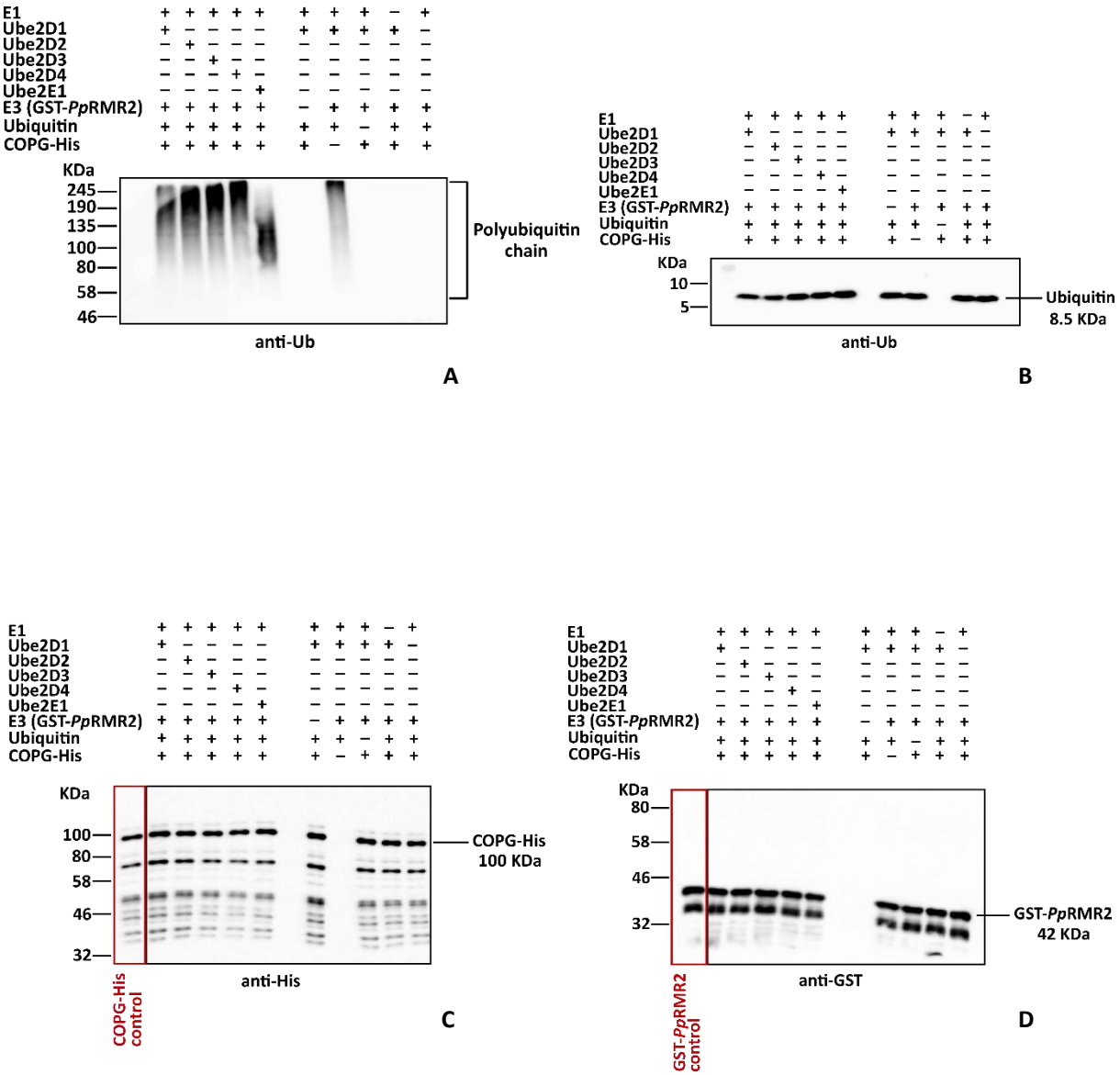

Figure 3.12. Western Blot after *in vitro* ubiquitylation test between COPG-His and GST-*Pp*RMR2. COPG-His was used as putative candidate of GST-*Pp*RMR2. Anti-Ub antibody detected a poly-Ub chain (**A**) and the free ubiquitin (8.5 KDa) (**B**) in presence of the five E2s tested. Anti-His only detected COPG-His (100 KDa) (**C**), not the poly-Ub chain. GST-*Pp*RMR2 (42 KDa) was properly recognized by anti-GST antibody (**D**). Ubiquitylation reactions were resolved in an 8%, 10% and 18% Tris-glycine PAGE.

3.4 Discussion

An important part of this project consisted in testing the hypothesis of a ubiquitylation activity of *Pp*RMRs. The similar structure between plant and animal RMRs suggests that they have similar functions, especially because their transmembrane domain and RING-H2 domain are quite conserved (Wang H *et al.*, 2010). Animal proteins having a similar structure as RMRs are called PA-TM-RING, and some of them act as E3 ligases. Many E3 ubiquitin ligases are RING finger proteins (Joazeiro and Weissman, 2000) whose stability is frequently controlled by self-ubiquitylation and protein-protein interaction (Huibregtse *et al.*, 1995; Lorick *et al.*, 1999).

As we could not detect *Pp*RMR proteins, we have focused our study on finding out their potential substrates, supposing that *Pp*RMRs are E3 ubiquitin ligases.
We have tried to discover putative candidates that would be ubiquitylated by *Pp*RMRs, treating *Pp*WT and *Pp*5KO with three inhibitors of proteasomal/vacuolar degradation: ALLN, MG132 and E64. We detected a ubiquitylation pattern in *Pp*WT treated with 2.5 µM MG132, but this was not reproduced when we have repeated the assay at the same conditions. This could be attributed to the short half-life and rapid degradation of *Pp*RMRs in the cell, thus we were not able to detect *Pp*RMRs' ubiquitylated substrates.

The more conserved lysines (K) in the cytosolic tail of *Pp*RMRs could be good candidates for ubiquitylation by *Pp*RMRs themselves, thus we performed an *in vitro* assay using the recombinant protein GST-*Pp*RMR2 as E3 ligase.
We tested the American UBPBio kit containing 29 human E2s, and for five of them (Ube2D1, Ube2D2, Ube2D3, Ube2D4, Ube2DE1), we obtained a ubiquitylation pattern on GST-*Pp*RMR2, detected by anti-Ub antibody. We could not show if this was a self-ubiquitylation of GST-*Pp*RMR2 neither if GST-*Pp*RMR2 ubiquitylated another target protein in the mix. On the other hand, the results by Y2H screening revealed that three E2 ubiquitin-conjugating enzymes (two type D, one type W) and three ubiquitin-like proteins interact with GST-*Pp*RMR2. This is interesting because the E3 ligases containing U-box and RING domain need to bind both substrate and E2-Ub conjugates in order to promote the ubiquitin transfer (Soss *et al.*, 2011). Thus, we have had good reasons to believe that *Pp*RMR2 is an E3 ubiquitin ligase, although we were not able to show the ubiquitylation of another protein *in vitro* by GST-*Pp*RMR2.
Another question is still open: which are *Pp*RMR2's potential substrates? We have focused on 5 candidates provided by the Hybrigenics company. These partners are supposed to interact with the

cytosolic side of *Pp*RMR2, and are: DUSP, the proteasome subunits N2, N3, N9 and the coatomer subunits α, β, γ.

Except for N9, we have encountered several issues in cloning the genes as well as in protein-His purification. Because of the huge size of α and β coatomer subunits (3.6 Kb and 2.9 Kb), the cloning of these genes was not completed.

The amino acid sequence of all these proteins exhibits ubiquitylation sites (lysines) with a high score of 0.75, according to UbiSite tool, hence, after cloning, we have purified them and tested their ubiquitylation *in vitro* using GST-*Pp*RMR2 as putative E3 ligase.

The experiment was performed in presence of the five E2 enzymes previously tested in the *in vitro* autoubiquitylation test of GST-*Pp*RMR2. Surprisingly, our Western Blot results revealed a polyubiquitin chain for each His-tagged candidate. The chain was only detected by anti-Ub antibody but not reproduced by anti-His antibody. Thus, we have concluded that no one of these substrates is ubiquitylated by GST-*Pp*RMR2, although this protein seemed to show an E3 ligase activity.

A very important aspect we need to highlight is that some conditions cannot be reproduced *in vitro*: it is known that the specificity of E2-E3 pairing is determined *in vivo* by diverse factors, such as post-translational modifications and additional interacting proteins. Moreover, the high concentration of recombinant proteins employed in these *in vitro* assays might cause unspecific E2-E3 interactions (Turek *et al.*, 2018).

Probably the proteins we have chosen are not eligible for ubiquitylation by *Pp*RMR2, but our results demonstrated that a ubiquitylation pattern was detected when GST-*Pp*RMR2 was present in the mix and no pattern was detected when GST-*Pp*RMR2 was absent, therefore we think that it is the only responsible for ubiquitylation in the reaction mix. Have we obtained just artifacts in each assay? Could GST-*Pp*RMR2 act as an E3 ligase towards another target in the mix? These aspects need to be investigated.

Chapter 4

Study of moss phenotype and characterization of *Pp*RMR2 mutants

We have decided to use the moss as plant model because one of its biggest advantages is the high frequency of integration of a foreign DNA in its genome, by homologous recombination. Moreover, working on moss protonema allowed us to study the phenotype at sub-cellular level and to easily observe our samples under the microscope. Our study focused on vacuoles, which are not investigated yet in seedless plants. In the secretory pathway, soluble vacuolar proteins are addressed to lytic vacuole or protein storage vacuole, depending on specific sequence motifs called vacuolar sorting determinants (VSD).

RMRs are expected to be vacuolar receptors (Jiang *et al.*, 2000; Park *et al.*, 2005; Hinz *et al.*, 2007). The 5 RMR genes were knocked-out in moss by the previous collaborator Ayachi (2012) without detecting any visible phenotype, leading us to think that the loss of all *Pp*RMRs does not affect moss development. Only later it was observed that leafy gametophores developed differently in the mutant lines, compared to *Pp*WT (Fahr, 2017).

Exposition of *Pp*WT and *Pp*RMR-KO lines to salt stress could help us to understand which function RMRs have in moss: besides their involvement in vacuolar transport, we hypothesize a role as E3 ubiquitin ligases that are known to participate in plant development and stress responses such as high salinity and drought (Cho *et al.*, 2017; Stone, 2018).

Vacuolar trafficking in moss was also described by Fahr (2017) who generated fluorescent markers and confirmed that the ctVSD of tobacco chitinase, cardosin A and *Pp*AP1 addresses a fluorescent reporter to the central vacuole, as it happens in flowering plants (Di Sansebastiano *et al.*, 1998; Flückiger *et al.*, 2003; Pereira *et al.*, 2013). In particular, a vacuolar pattern was observed in *Pp*WT expressing the construction Citrine-Cardosin (Ci-Card) in which the ctVSD of cardosin A was fused to the C-terminus of the fluorescent protein Citrine. In *Pp*RMR-KO lines, instead, the fusion protein was ER-retained. Hence, I transformed the lines *Pp*WT/Ci-Card and *Pp*5KO/Ci-Card with the overexpressed WT *Pp*RMR2 or its mutated versions to test their effect on vacuolar trafficking.

4.1 Visible phenotype in *Pp*WT and *Pp*RMR-KO lines

The loss of single or multiple RMR genes did not cause any phenotypic changes in moss (Ayachi, 2012). The **figure 4.1** shows 10-day-old protonema of *Pp*WT, *Pp*1KO, *Pp*3KO, *Pp*5KO which all exhibit the same shape and colour.

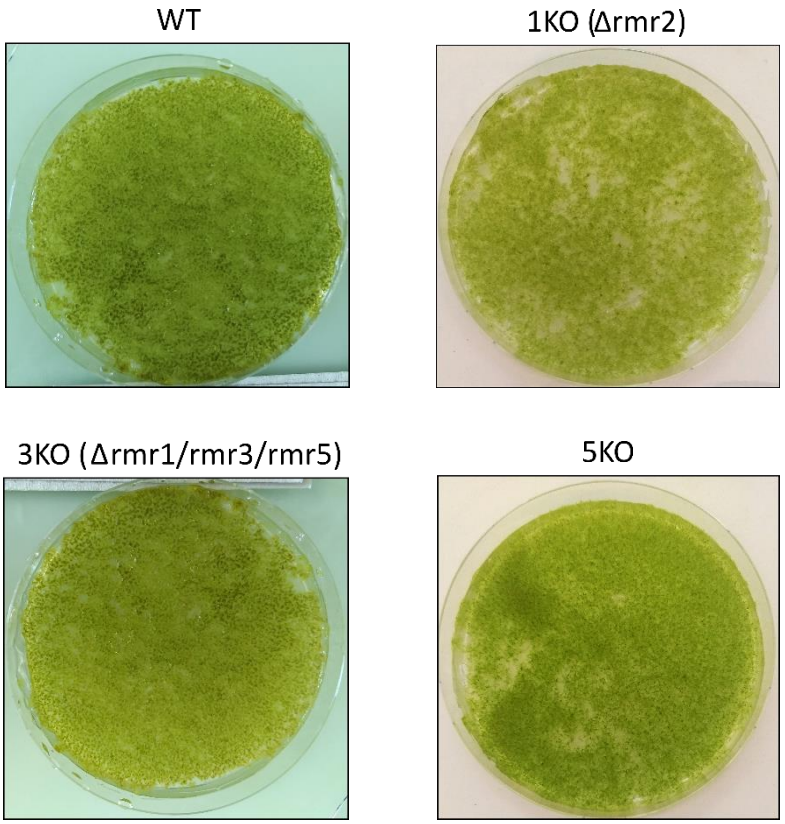

Figure 4.1. *In vitro* 10-day-old moss protonema on NH_4 medium. Moss protonema was grown in the phytotron for 10 days on standard NH_4 medium. No phenotypic differences were observed between *Pp*WT and the mutant lines *Pp*1KO, *Pp*3KO, *Pp*5KO.

A phenotypic difference between *Pp*WT and mutants has been observed in protonema grown on NH_4 medium for 3 weeks. The results of Fahr (2017) showed that moss mutants developed more leafy gametophores than *Pp*WT. I did not confirm these results: I rather found that leafy shoots were small and short in *Pp*WT, bigger and elongated in mutants. The method described by Fahr needed to be slightly modified: I could not let the moss on the same medium for 3 weeks because it turned brown.

4.1.1 Results

Extended growth of PpWT and PpRMR-KO lines on NH_4 medium

WT, 1KO, 3KO and 5KO moss protonema were grown for 2 weeks in *Petri* dishes containing NH_4 medium, discs (diameter 2.5 cm) were then cut and transferred onto fresh medium. The discs corresponding to each line were placed distant from each other in the same plate. Duplicates of each disc were prepared. Every 14 days, for 2 months, the discs were moved to a fresh NH_4 medium.

Data were not collected after short-term because morphogenetic parameters were visible only after 4 weeks whereas drastic phenotypic differences between *Pp*WT and *Pp*KO lines were observed after 2 months, that is the exact time when photos were taken. The results showed that *Pp*WT developed many small and short leafy gametophores which were instead bigger and longer in *Pp*KO mutants (**Figure 4.2**).

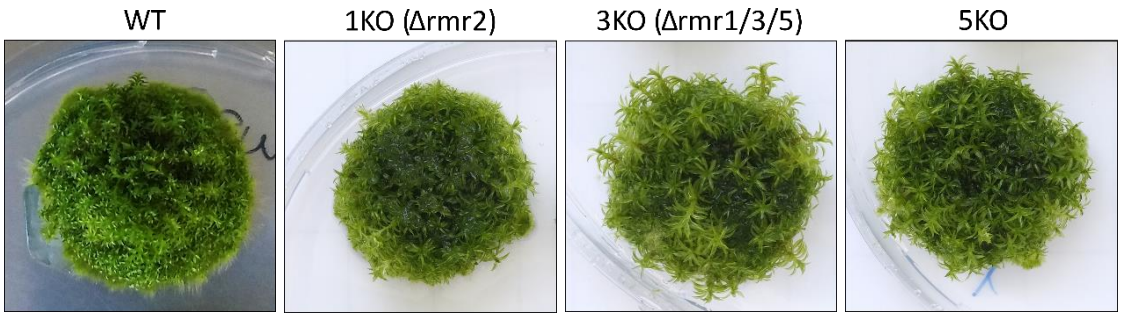

Figure 4.2. Leafy gametophores of *Pp* mutant lines displayed a visible phenotype. *Pp*WT and mutants protonema were grown for two weeks on standard NH_4 medium, then discs of each line were cut and transferred to a fresh medium. Every 14 days, for 2 months, the discs were moved to a fresh NH_4 medium. The leafy shoots developed in *Pp*WT were smaller and shorter than in *Pp*KO lines.

4.2 Abiotic stress response

It is known that vacuoles are important for resistance to drought stress (Marty, 1999) and that proteins having an E3 ligase activity, can negatively regulate drought stress response (Cheng *et al.*, 2012). The experiments performed by our previous collaborator Ayachi (2012) showed that *Pp*WT and *Pp*KO lines coped with severe water loss in the same manner, and no significant differences were observed in the mutant lines after recovering from desiccation.

Other studies have demonstrated a relationship between ubiquitylation and abiotic stress responses, such as dark and high salinity. For instance, the RING-type E3 ligase COP1 in *A. thaliana* negatively regulates roots elongation, promoting the degradation of SCAR1 in dark-grown roots (Dyachok *et al.*, 2011). The E3 ligase *At*RDUF1 instead positively regulates plant response to salt stress (Li *et al.*, 2013).

Salt stress response

All the researchers who have tested abiotic stress conditions agree that moss exhibits a high degree of tolerance against salt stress (Wang *et al*., 2008; Frank *et al*., 2005; Ćosić *et al*., 2020). This happens because of the presence of a Na^+-pump ATPase which flowering plants do not possess (Pedersen and Palmgren, 2017-review).

Frank *et al*. (2005) treated *P. patens* with increasing concentrations of NaCl added to a regular growth medium (Knop medium). After 3 days of treatments, plants were transferred to a standard medium for recovery. The samples exposed to 250, 300 and 350 mM NaCl survived and recovered successfully, while the ones treated with 500 mM NaCl were bleached 2 weeks after the treatment.

I also treated *Pp*WT and *Pp*KO lines with increasing concentrations of NaCl, following the same method as described in figure 4.2.

4.2.1 Results

*Pp*WT and *Pp*KO were grown on NH_4 medium supplemented with 50, 100, 200, 350 or 500 mM NaCl. In each case, the assay was carried out for 2 months. These are preliminary results: the pictures below show how the development of gametophores is globally affected under salt stress conditions. The assay should be repeated, and a detailed analysis should be done.

NH_4 medium supplemented with 50/100/200/350/500 mM NaCl

The protonema of *Pp*WT, *Pp*1KO, *Pp*3KO and *Pp*5KO was grown on NH_4 medium supplemented with increasing concentrations of NaCl. After 14 days of growth, protonema discs were cut and transferred to a fresh NH_4-NaCl medium. In 2 months, the medium was changed every 14 days. Results showed that the mutant lines grown in 50 mM NaCl developed smaller gametophores compared to the respective controls. In *Pp*WT instead, gametophores did not develop at all, compared to the untreated one (**Figure 4.3**).

The plants treated with 100 mM NaCl displayed a different phenotype, compared to the controls: they were characterized by a darker green colour. *Pp* mutants developed fewer leafy shoots. *Pp*WT, again, did not exhibit any leafy gametophores (**Figure 4.3**).

The plants treated with 200 mM NaCl appeared smaller and dark green-coloured compared to the ones grown on salt-free medium, with no developed leafy shoots either in *Pp*WT or mutants (**Figure 4.4**).

Similar results have been also demonstrated by Ćosić *et al*. (2020) who tested even lower concentrations of NaCl and found that at 5 and 10 mM NaCl, new gametophores developed in three

different moss species, including *P. patens.* Instead, at higher salt concentrations, the formation of new buds was inhibited.

In my assay, I did not measure the index of multiplication, but it is clear from the pictures, that the development of gametophores is more affected in *Pp*WT than in *Pp*KO lines.

Lastly, *P. patens* growth on NH_4 medium supplemented with 350 or 500 mM NaCl was seriously affected: after 2 weeks all the lines were completely bleached, thus discs were cut and moved to a standard NH_4 medium for the recovery. Small green spots were visible after 20 days (the **figure 4.5** shows how moss looks like 20 days after recovery from 500 mM NaCl) and it took about 2 months for a complete recovery, at the end of which, only the samples exposed to 350 mM NaCl, looked like the respective controls (**Figure 4.6**). The plantlets treated with 500 mM NaCl showed a different phenotype compared to the controls, with less developed gametophores. *Pp*WT was more affected than mutants after recovery from 500 mM NaCl (**Figure 4.6**).

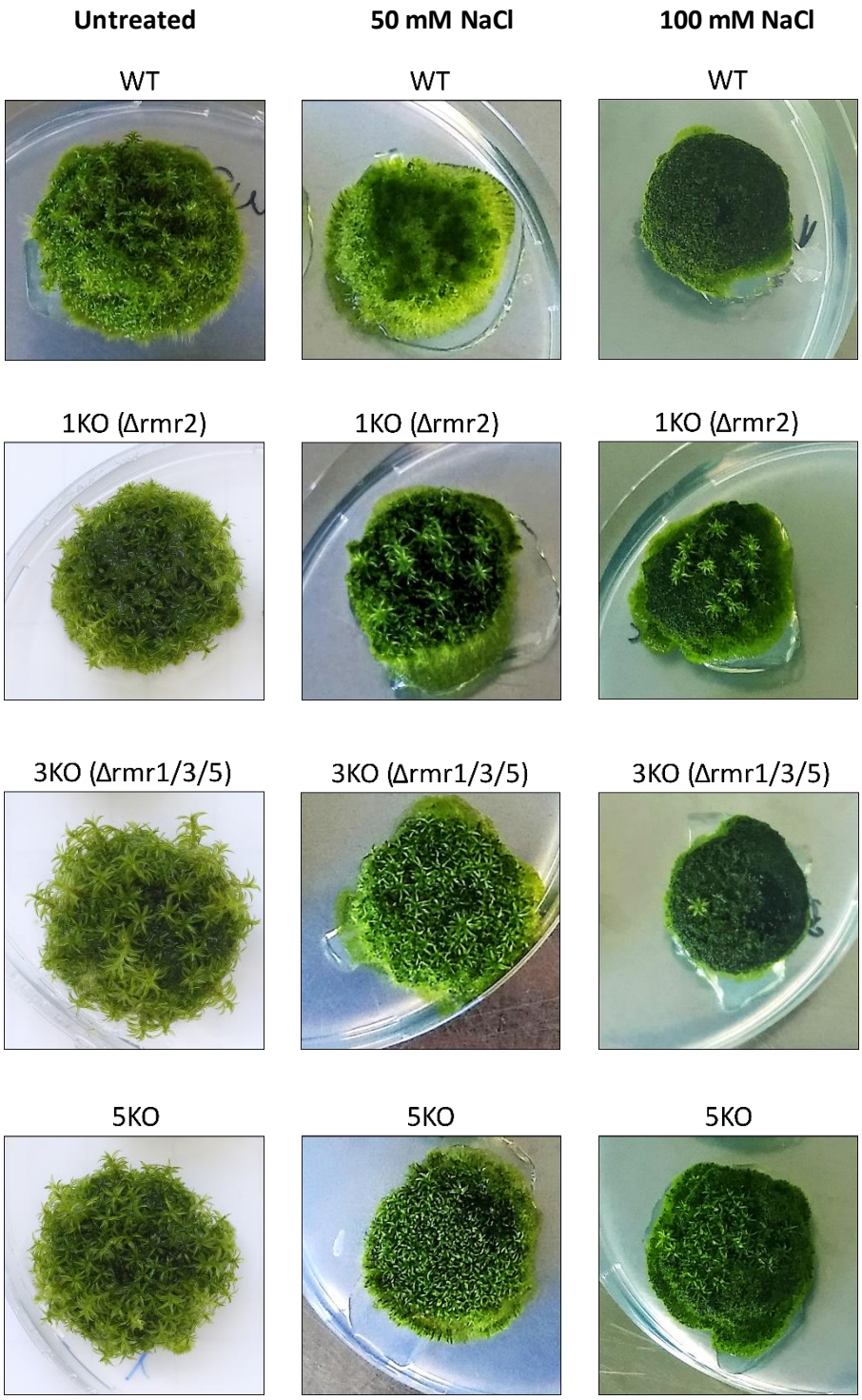

Figure 4.3. *Pp*WT and *Pp*KO lines were grown on NH_4-50/100 mM NaCl medium. *Pp*WT was affected in 50 and 100 mM NaCl. In 50 mM NaCl, gametophores did not develop in *Pp*WT, whereas the mutant lines displayed smaller gametophores than the untreated plants. In 100 mM NaCl, *Pp*WT showed no leafy gametophores, while in mutants, the number of shoots decreased. Pictures were taken 2 months after treatment.

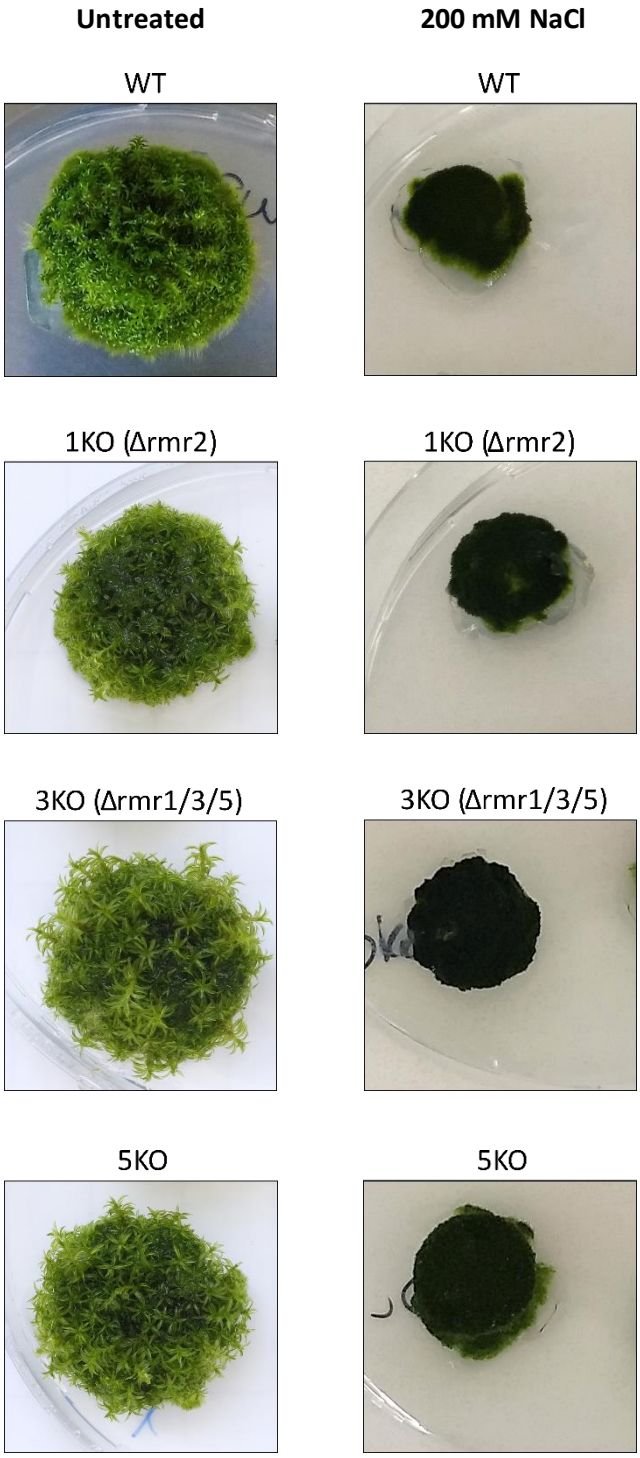

Figure 4.4. *Pp*WT and *Pp*KO lines were grown on NH_4-200 mM NaCl medium. All the lines were affected in 200 mM NaCl. They were smaller than the controls, and the leafy gametophores did not develop at all, either in *Pp*WT or in mutants. Pictures were taken 2 months after treatment.

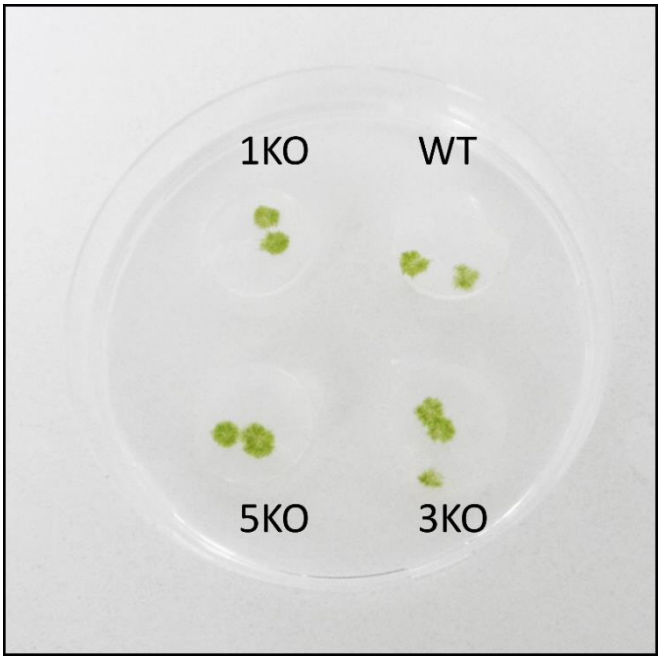

Figure 4.5. Moss recovery from 500 mM NaCl. 20 days after recovery from 500 mM NaCl, small green colonies grew on standard NH_4 medium. *Pp*WT and mutant lines looked alike.

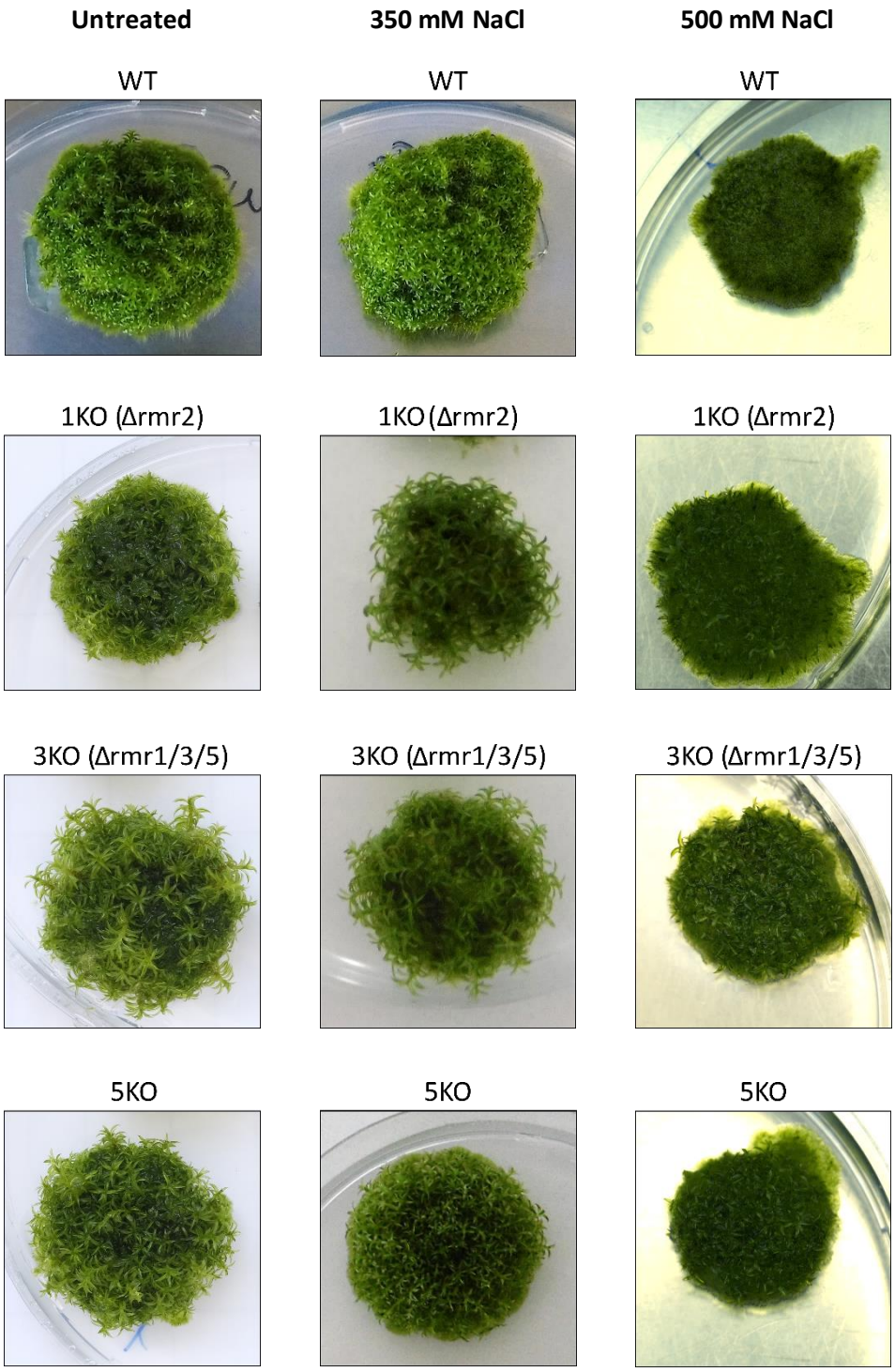

Figure 4.6. Recovery of *Pp*WT and KO lines from growth on NH_4-350/500 mM NaCl medium. On NH_4-350/500 mM NaCl medium, all the lines were bleached after 2 weeks of salt stress treatment. Recovery in standard NH_4 medium was run for 2 months. No significant differences were observed between the recovered samples from 350 mM NaCl and the controls. The recovered plantlets from 500 mM NaCl developed fewer leafy shoots compared to the controls. *Pp*WT was more affected than mutants. Pictures were taken 2 months after recovery.

4.3 Production of constructs to study vacuolar targeting in *P. patens*

The construction which allowed to reveal an intracellular phenotype in *Pp*RMR-KO lines was the Citrine-Cardosin (Ci-Card), composed of the fluorescent protein Citrine C-terminally fused to the ctVSD (VGFAEAA) of cardosin A (Fahr, 2017). The Citrine was used instead of GFP because it is more resistant to acidic pH. The ctVSD of cardosin A had been previously demonstrated to sort the reporter m-Cherry to the vacuoles of *Nicotiana tabacum* leaves (Pereira *et al*., 2013).

The construction Ci-Card was tested in *Pp*WT, *Pp*1KO (Δrmr2 or Δrmr5), *Pp*3KO (RMR2 and RMR4 remaining) and *Pp*5KO. The heat-shock (HS) promoter facilitated the observation of protein transport in the cell.

In *Pp* mutant lines, 24 hours after heat-shock induction, the construct was blocked in the ER, while in *Pp*WT, the pattern was vacuolar (Fahr, 2017; **Figure 4.7**).

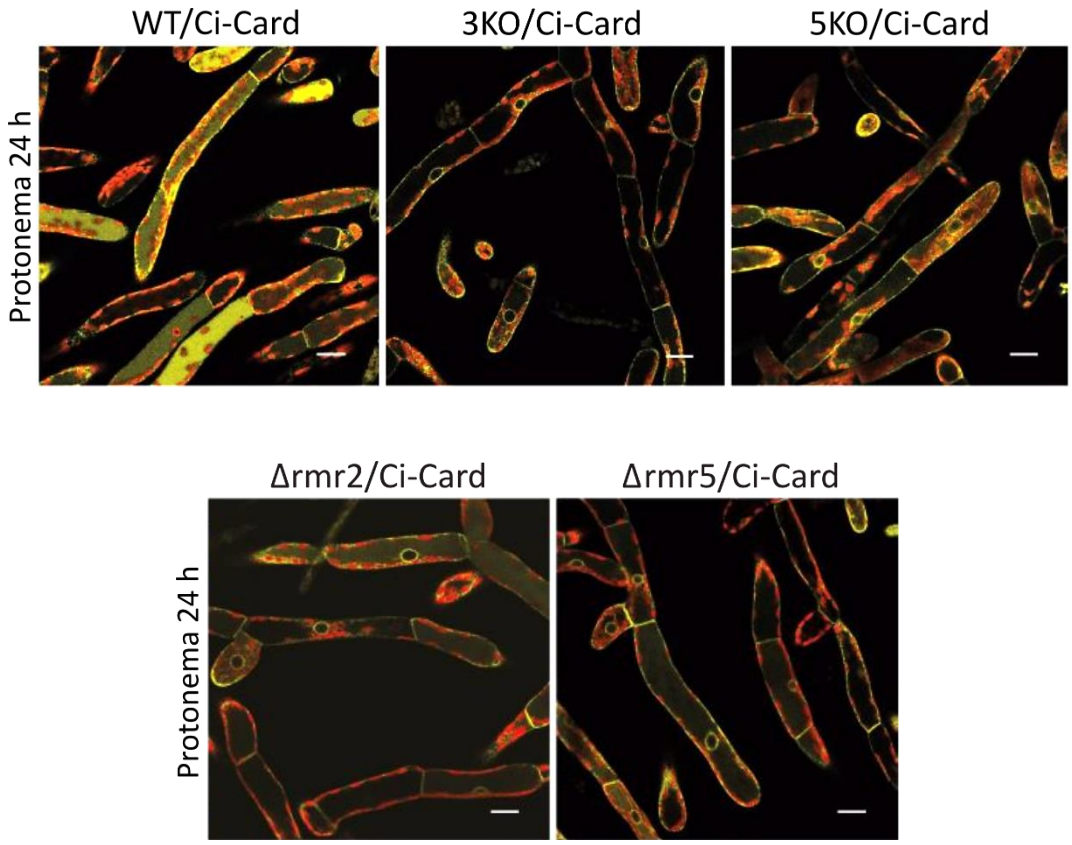

Figure 4.7. The Ci-Card construct was mistargeted in *Pp*RMR-KO lines 24 hours after heat-shock induction. A vacuolar fluorescence was observed in *Pp*WT whereas the fusion protein was mistargeted in all the *Pp*KO lines. In this typical ER pattern, the nuclear envelope is well visible. Ci-Card: Citrine-Cardosin. Scale bar = 20 µm (adapted from Fahr, 2017).

4.3.1 *Pp*RMR2 overexpression and characterization of mutants

The observations made by Fahr (2017) had shown that the line *Pp*Δrmr2/Ci-Card has a similar phenotype as *Pp*5KO/Ci-Card, but so far, we cannot assume that vacuolar targeting requires the work in concert of the 5 *Pp*RMRs, and we do not know yet whether this process is controlled by ubiquitylation. Our aim is to answer these questions.

As explained in chapter 2, *Pp*RMR2 is highly expressed in protonema and gametophores, whereas the other *Pp*RMRs are prevalently expressed in sporophytes and spores. Our experiments were performed on protonema, therefore our studies focused on *Pp*RMR2 also because in our laboratory we had an antipeptide antibody available against this protein.

We focused on *Pp*RMR2 function as E3 ligase because of its homology to animal PA-TM-RING proteins such as Goliath and Godzilla which are E3 ligases as well. The work of Yamazaki *et al*. (2013) describes the function of these two proteins as key regulators of the recycling endosomes pathway in *Drosophila*. The replacement of two key histidines by two arginine residues in their RING finger domain prevented the generation of large endosomes induced by both E3 ligases. Moreover, the replacement of three lysines by arginine residues in the SNARE protein VAMP3 led to the abrogation of recycling endosome trafficking. This means that VAMP3 is a target of Goliath and Godzilla and that its ubiquitylation regulates recycling endosome trafficking (Yamazaki *et al*., 2013).

Thus, I decided to transform both *Pp*WT/Ci-Card and *Pp*5KO/Ci-Card with the overexpressed WT or mutated versions of *Pp*RMR2, in order to test whether the deletion of certain domains or mutation of particular amino acids probably involved in ubiquitylation, would affect vacuolar trafficking. If this is perturbed, we could hypothesize that protein transport to the vacuole is mediated by ubiquitylation. The constructions obtained are:

- ✓ ***Pp*RMR2_ΔSer**: the Serine-Rich motif following the RING-H2 domain could be involved in selecting the target proteins for ubiquitylation. Without this domain, *Pp*RMR2 would then lose the E3 ubiquitin ligase activity.
- ✓ ***Pp*RMR2_RINGR2**: the two histidines (H) of the RING-H2 domain have been replaced by arginines (R). These amino acids have similar chemical properties, but a RING domain cannot be formed if contains arginines, thus *Pp*RMR2 would become an E3 ligase dead-mutant. If *Pp*RMR2 is involved in ubiquitylation, the loss of this function (either ubiquitylation of target proteins or autoubiquitylation) might cause an abnormal accumulation or a mistargeting of *Pp*RMR2. The RING-H2 domain is thought to be involved in protein-protein interaction, thus this mutation should prevent *Pp*RMR2 from selecting the target to ubiquitylate.

- ✓ ***Pp*RMR2_KtoR**: in the cytosolic tail of *Pp*RMR2 there are three lysines to which ubiquitin may bind. The lysine K295 (position 295 in the protein sequence) is conserved in all moss RMRs, whereas the lysines K301 and K304 show a high score of ubiquitylation (according to UbPred prediction tool), hence they are good candidates for ubiquitylation by *Pp*RMR2 itself or by other E3 ligases. Replacing each of these lysines by arginines, *Pp*RMR2 could not be ubiquitylated: will this mutation perturb vacuolar trafficking?
- ✓ Furthermore, if the over-expression of **WT *Pp*RMR2** (**Figure 4.8**) restores the phenotype in *Pp*5KO/Ci-Card we could finally assume that *Pp*RMR2 alone is able to mediate vacuolar transport.

MPSLVVETGLVSRIMNHRELMISLAGLSLVLLTLLLGRVNSAVILLTESNESWSFPDTEASFSPRIPTTGIVGVLHASNP
LDACSPLTNVSRQGQTLFSDFLLVERGVCNFEVKVWNAQEAGFEAVIIYNNQNDHELVTMSGSSNDIHAYSVFVSK
VTGEFLLKYADDKGATCYIMPAFENTAWSVMAVSFISLLAVSSVLVTFFFVRQHRIQHLSARFLPKEPAGMSVKEVN
TLPSFVFKHIEDGKGTSETCAICLEDYVAGEKLRLLPCQ**H**EF**H**LDCIDQWLTTRKPFCPVC**K**RDAQS**K**VD**K**PVATETT
PLLAAVGRALGVGESRVGTPMNSSPLFAPTGASPDETTDTRIFSLSSPDGSEDLC

Signal Peptide (1-42 aa)
Protease-Associated domain (43-183 aa)
Transmembrane domain (184-206 aa)
Linker (207-252 aa)
RING-H2 motif (253 - 296 aa)
Serine-Rich motif (297-366 aa)

Figure 4.8. Amino acid sequence of *Pp*RMR2. The different domains are shown in different colours. The two histidines of the RING-H2 domain and the three lysines that were mutated are underlined in bold.

4.3.1.2 Results

*Pp*RMR2 cDNA was subcloned in pGEM®-T easy vector, then in POG1. The latter contains a strong endogenous promoter EF-1α (elongation factor-1 αlpha) to overexpress RMR2. From the construct called POG1-RMR2, I produced the individual mutated versions using the Q5® Site-directed mutagenesis. Each construct was targeted to PIG1 loci in the moss genome. For the K to R mutants, we failed to replace K304, while the other two K295 and K301 were mutated.

Protoplasts of *Pp*WT/Ci-Card and *Pp*5KO/Ci-Card were transformed with the above-mentioned constructions, and stable transgenic lines were obtained. The correct DNA insertion in moss was confirmed by genotyping, then total proteins were extracted, and a Western Blot was performed using the anti-RMR2 antipeptide antibody available in our laboratory. We thought that at least the overexpressed WT *Pp*RMR2 could be detectable, but unfortunately, no signal was found.

The lines were observed by confocal microscopy 24 hours and 48 hours after heat-shock induction.

A comparison between Fahr's results (**Figure 4.7**) and mine, shows that after 24 h, for 4 of the constructions used, no vacuolar fluorescence was detected in *Pp*WT/Ci-Card. Only when *Pp*RMR2ΔSer was expressed, few cells displayed a faint vacuolar pattern 24 hours after HS induction (**Figure 4.9**).

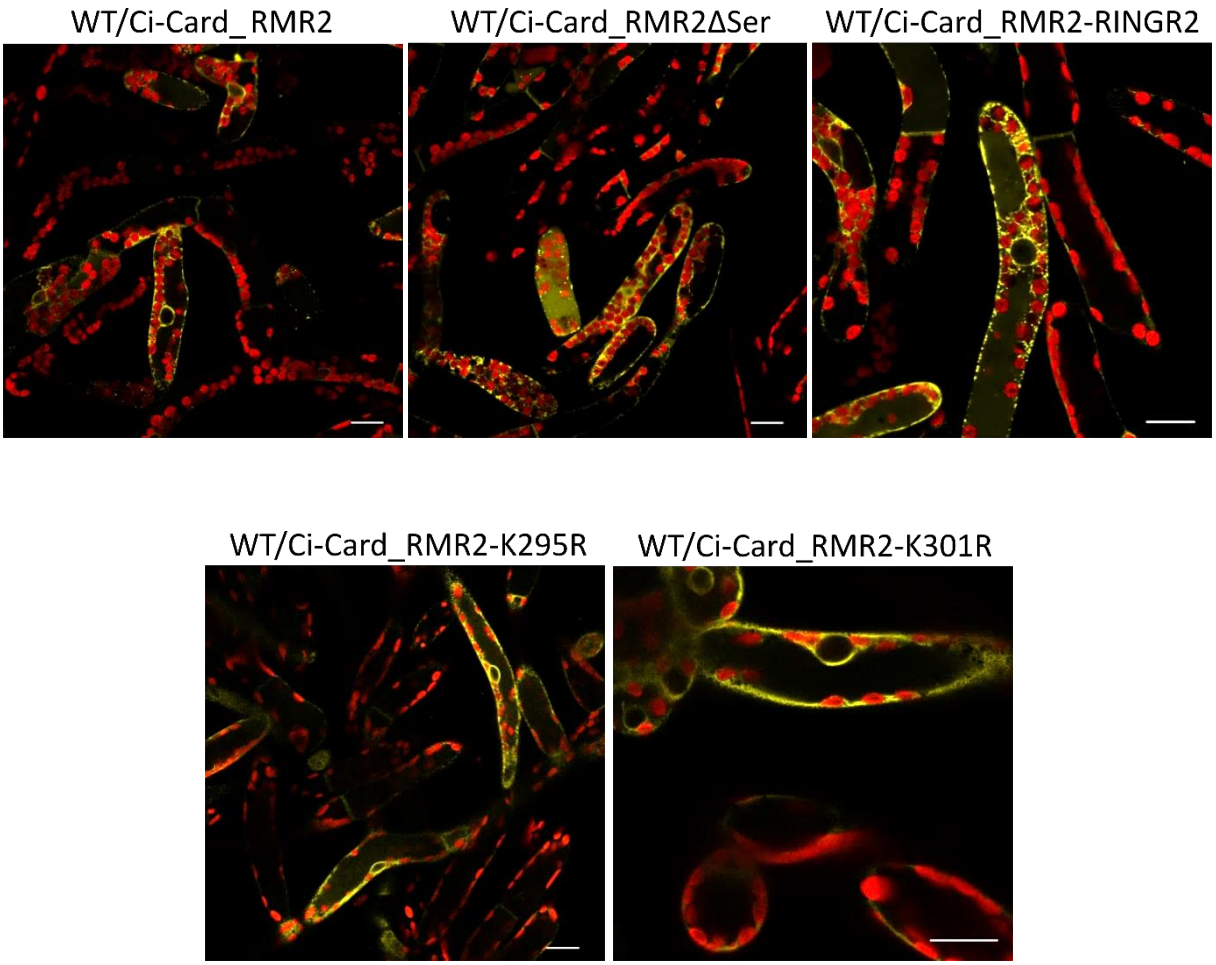

Figure 4.9. Protonema cells of *Pp*WT/Ci-Card transformed with different versions of *Pp*RMR2 did not show any vacuolar fluorescence 24 hours after HS induction. The fusion protein Ci-Card was blocked in the ER of *Pp*WT/Ci-Card expressing either WT *Pp*RMR2 or its mutated versions. WT/Ci-Card_RMR2ΔSer showed a faint vacuolar fluorescence in a few cells. Scale bar = 25 µm.

48 hours after HS induction, a typical vacuolar pattern was observed in the line *Pp*WT/Ci-Card expressing the mutated version *Pp*RMR2ΔSer (**Figure 4.10**).

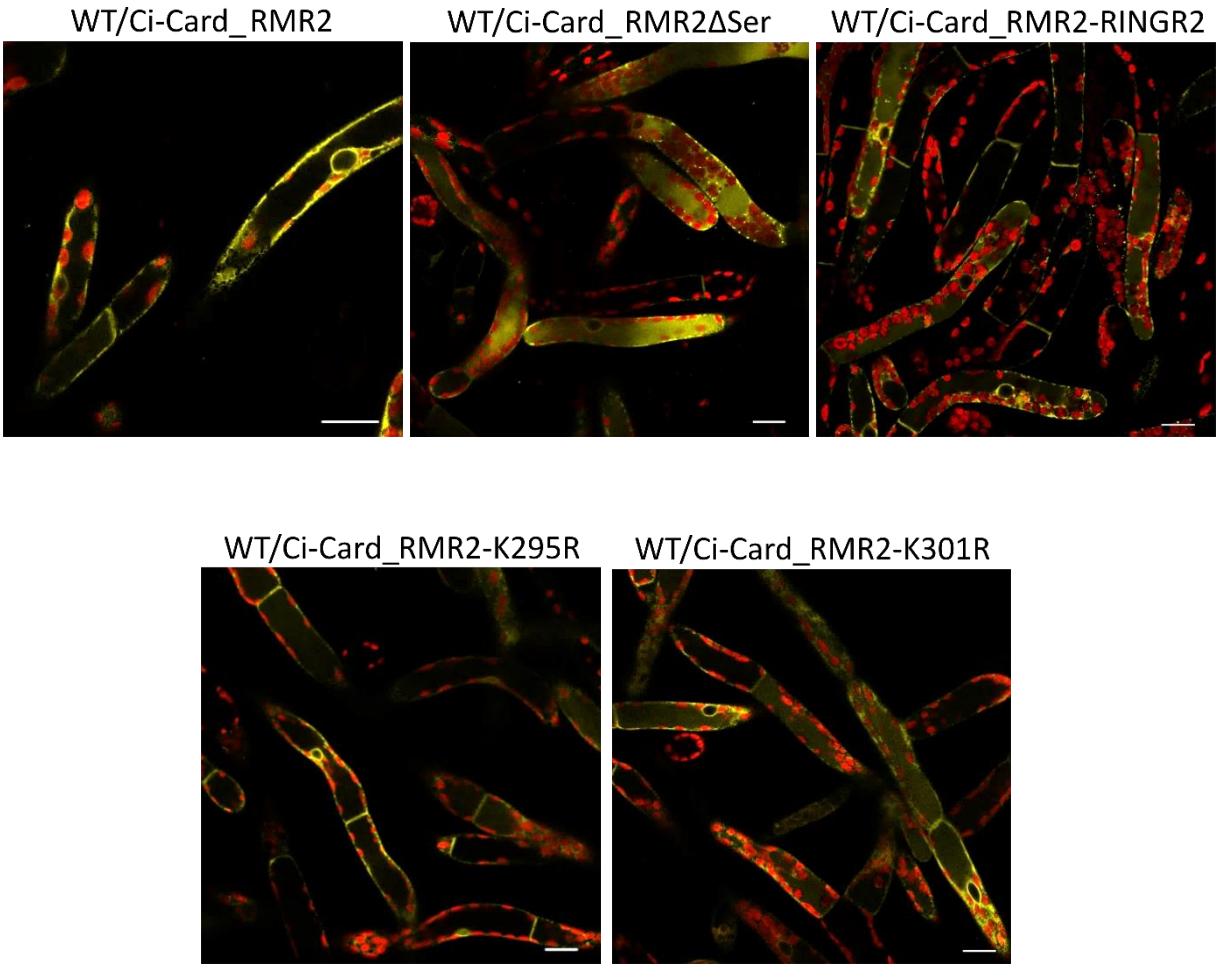

Figure 4.10. Protonema cells of *Pp*WT/Ci-Card transformed with *Pp*RMR2ΔSer showed a vacuolar fluorescence 48 hours after HS induction. The fusion protein Ci-Card was addressed to the central vacuole of the line expressing *Pp*RMR2ΔSer, but mistargeted in the lines expressing either the other mutated versions or WT *Pp*RMR2. Scale bar = 25 µm.

On the other side, we expected that the overexpressed WT *Pp*RMR2 could restore the phenotype in *Pp*5KO/Ci-Card line, but the complementation did not occur (**Figures 4.11-4.12**).

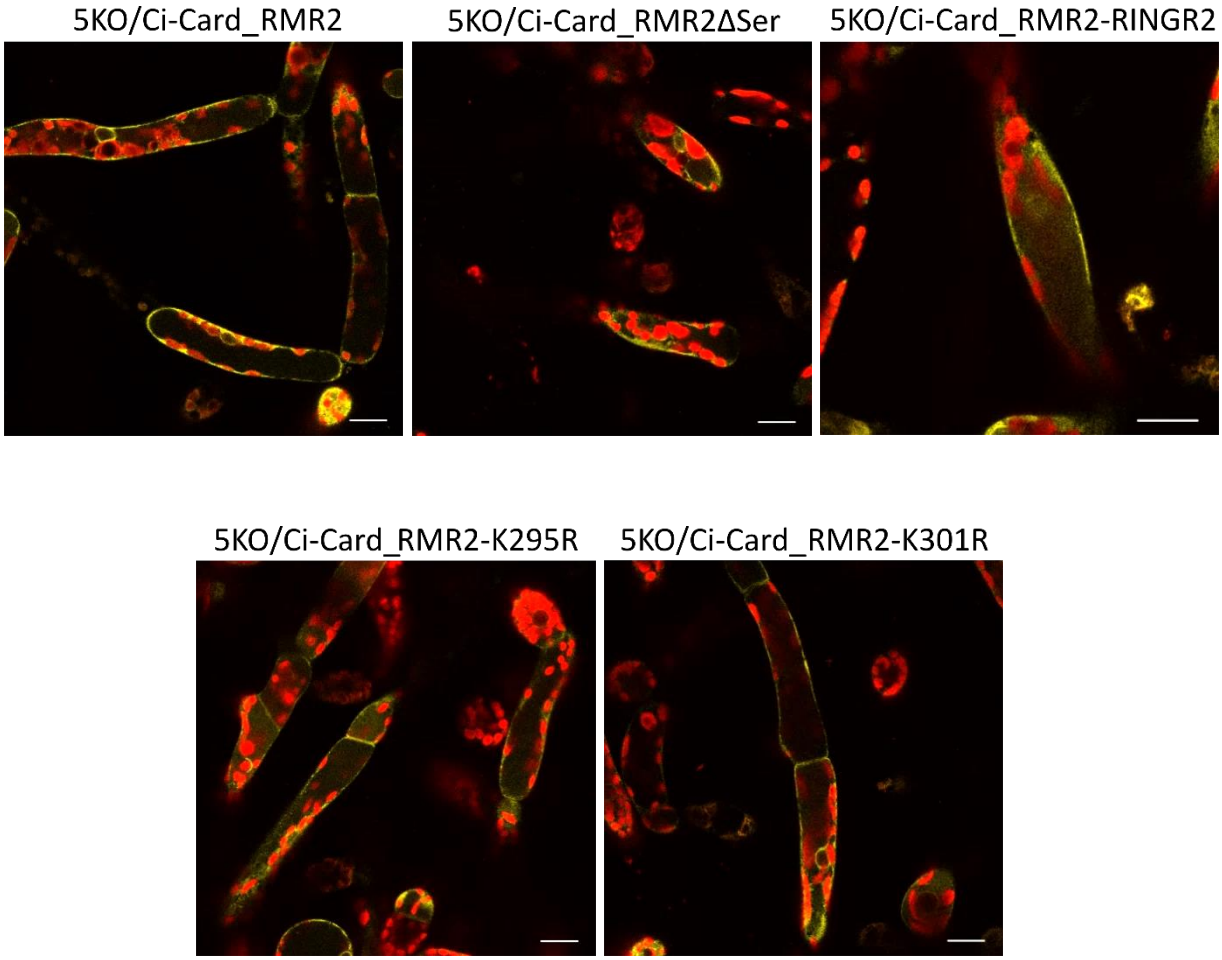

Figure 4.11. 24 hours after HS induction, the vacuolar phenotype was not restored in *Pp*5KO/Ci-Card transformed with different versions of *Pp*RMR2. The fusion protein Ci-Card was mistargeted in *Pp*5KO/Ci-Card expressing either WT *Pp*RMR2 or its mutated versions. Observations were made on protonema 24 hours after HS induction. Scale bar = 25 µm.

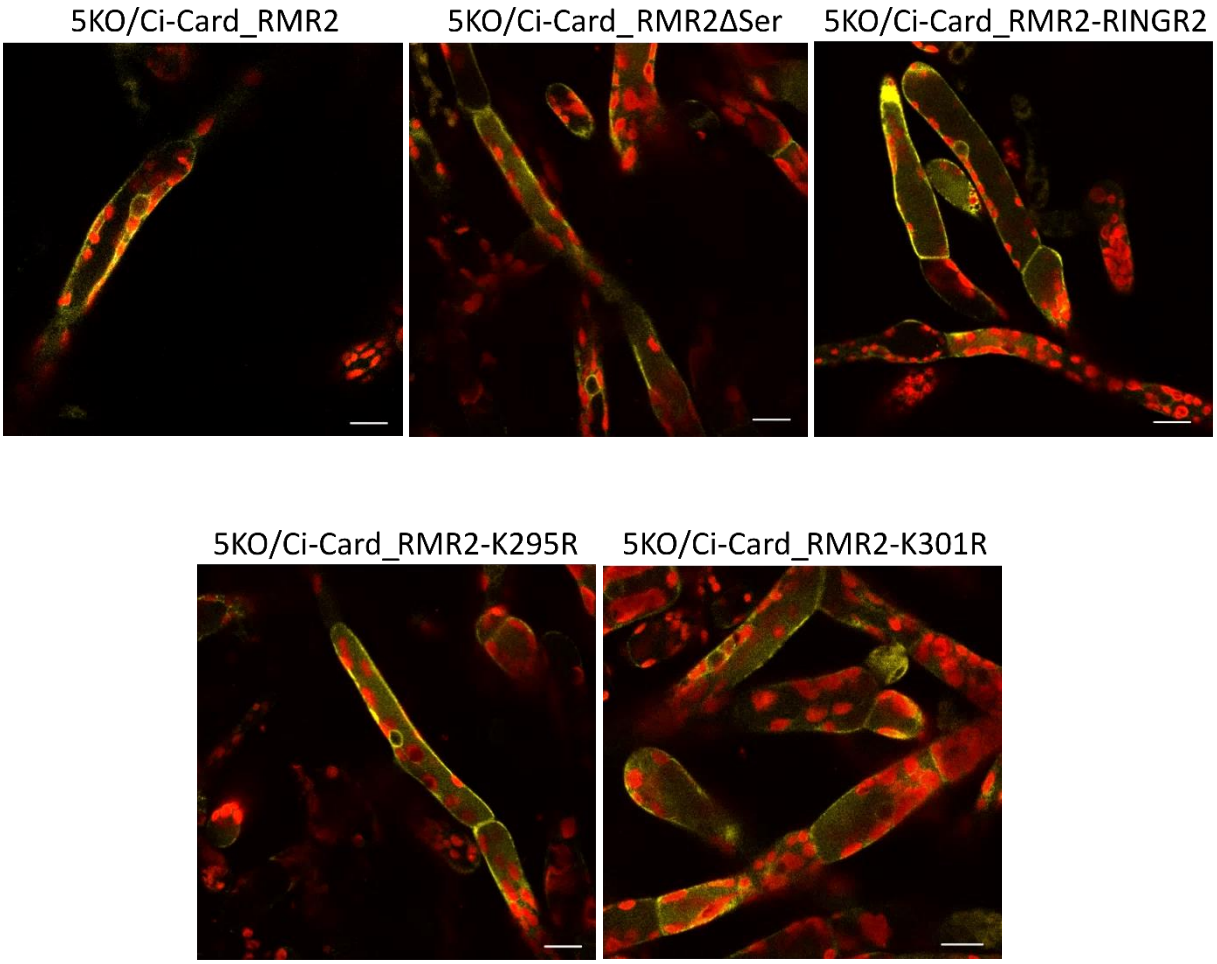

Figure 4.12. 48 hours after HS induction, the vacuolar phenotype was not restored in *Pp*5KO/Ci-Card transformed with different versions of *Pp*RMR2. The fusion protein Ci-Card was mistargeted in *Pp*5KO/Ci-Card expressing either WT *Pp*RMR2 or its mutated versions. Observations were made on protonema 48 hours after HS induction. Scale bar = 25 µm.

4.4 Discussion

In the first part of this chapter, I showed preliminary results about the visible phenotype of *Pp* mutants. In 2012, Ayachi had observed the same shape and colour for *Pp*WT as for *Pp*RMR-KO lines.

Instead, phenotypic differences were observed in leafy gametophores. In standard NH_4 medium, *Pp*WT developed many small and short leafy gametophores compared to the numerous bigger and elongated ones of the *Pp*KO lines. Furthermore, salt stress conditions affected the development of the shoots, particularly in *Pp*WT: in 50 mM NaCl, *Pp*WT did not develop gametophores at all, while the mutant lines developed smaller gametophores than the controls. In 100 mM NaCl, fewer gametophores were observed in the mutants, and again, none in *Pp*WT. At 200 mM NaCl, the development of leafy gametophores was inhibited in both *Pp*WT and mutants, but all the lines still survived.

In 350 and 500 mM NaCl, moss growth was seriously altered, in fact all the lines were completely bleached 2 weeks after treatment. The recovery on standard NH_4 medium was necessary to detect how the plantlets coped with high salinity stress. The recovered plants from 350 mM NaCl looked like the controls, while the ones recovered from 500 mM NaCl, especially *Pp*WT, developed fewer gametophores compared to the untreated plants. We can thus confirm that *P. patens* is resistant to salt stress conditions, and that it shows an excellent ability to recover. This is not surprising, in fact it is known that certain moss plantlets exposed to high NaCl concentrations are able to regenerate on a salt-free medium because they maintained their viability (Ćosić *et al.*, 2020). Moreover, some species of bryophytes, known to be non-halophytes, have already shown to tolerate high salt concentrations (Sabovljević M and Sabovljević A, 2007).

These results suggest that *Pp*RMRs, maybe acting as E3 ligases, negatively regulate the development of leafy gametophores and this is more evident upon salt stress. Is there any relationship between *Pp*RMRs (as E3 ligases) and leafy shoots development? There is evidence of several RING-type E3 ligases involved in plant development and stress responses, even if their substrates are not known yet. For instance, the *A. thaliana* E3 DA2 negatively regulates seed size (Xia *et al.*, 2013; Li N and Li Y, 2016) as well as the rice RING-type E3 *Os*GW2 (*Oryza sativa* grain width 2), the latter also causes a delay of seed growth in *Arabidopsis* (Xia *et al.*, 2013). Moreover, in *A. thaliana*, the interaction between some ubiquitin receptors and RING-type E3 ligases leads to the restriction of the organ size (Xia *et al.*, 2013). Other studies have demonstrated that RING-type E3s are involved in plant salt stress responses, acting as positive or negative regulators. For example, SDIR1 (salt-and drought-induced RING finger 1) RING-type E3 ligase confers drought tolerance and regulates ABA-mediated responses to salt stress (Zhang H *et al.*, 2015).

In the last part of this chapter, I tested the effect that mutated versions of *Pp*RMR2 have on vacuolar trafficking. It is widely demonstrated that neutral/storage and lytic vacuoles can coexist in plant cells, but the existence of a storage vacuole in moss has not been proven yet.

The localization of several fluorescent markers was described in *Pp*WT and *Pp*RMR-KO mutants (Fahr, 2017). In particular, the construction Ci-Card was addressed to *Pp*WT central vacuole, while it was blocked in the ER of *Pp*1KO (either Δrmr2 or Δrmr5), *Pp*3KO (Δrmr1/3/5) and *Pp*5KO lines. This suggested that the loss of one *Pp*RMR is sufficient to disturb vacuolar trafficking. The global RMR level could be just sufficient for their function and the loss of any RMR could lead to a too low level. The similar phenotype displayed by *Pp*1KO/Ci-Card (either Δrmr2 or Δrmr5) and *Pp*3KO/Ci-Card indicated that *Pp*RMRs could work together and maybe dimerize or form heterodimers to work properly.

Occhialini *et al*. (2016) demonstrated that the vacuolar *A. thaliana* receptor *At*RMR2 forms homodimers but also forms heterodimers with *At*RMR1; dimerization allowed to localize these proteins to the TGN.

To better understand the function of *Pp*RMRs, I generated 5 constructions to overexpress either WT *Pp*RMR2 or several mutated versions. The latter included: deletion of Ser-Rich motif, replacement of two histidines by arginines in the RING-H2 domain, replacement of two potentially ubiquitinatable lysines by arginines in the cytosolic tail.

After transformation of the transgenic lines *Pp*WT/Ci-Card and *Pp*5KO/Ci-Card, results showed that for 4 of the constructions tested, no vacuolar fluorescence was detected in *Pp*WT/Ci-Card, and even the overexpression of WT *Pp*RMR2 surprisingly impaired the vacuolar trafficking of Ci-Card. This is consistent with some research studies which demonstrated that protein overexpression can be harmful to cell (Stoebel *et al.*, 2008; Vavouri *et al.*, 2009; Tang and Amon, 2013).

Only the line *Pp*WT/Ci-Card_RMR2ΔSer displayed a weak vacuolar pattern 24 hours after HS induction (the marker remained mostly in ER), and a stronger vacuolar fluorescence 48 hours after HS induction. Our results showed that when WT *Pp*RMR2 is overexpressed in *Pp*WT/Ci-Card, protein function is impaired as well as vacuolar transport, which could suggest a co-suppression of *Pp*RMR genes. Instead, the truncated *Pp*RMR2ΔSer does not affect vacuolar trafficking, indicating that this mutation makes RMR2 itself still able to work with the other RMRs.

In 2016 Occhialini *et al.* showed that *At*RMR2 cycles between PSV and TGN in *N. benthamiana* but the protein was not detected in transgenic *A. thaliana* plants. Instead, the truncated version of *At*RMR2, lacking the Ser-Rich domain, was more expressed in PSV and TGN of *A. thaliana* transgenic plants than the wild type protein in *N. benthamiana.* Moreover, *At*RMR1 which possesses a very short C-terminal Serine-Rich domain, was shown to be an ER-resident protein in *N. benthamiana*.

The mutated versions *Pp*RMR2-RINGR2, *Pp*RMR2-K295R, *Pp*RMR2-K301R affected vacuolar transport in *Pp*WT/Ci-Card, suggesting that the replacement of particular amino acids disrupts *Pp*RMR2 function,

and this is sufficient to affect vacuolar trafficking. This confirms our hypothesis that *Pp*RMRs need to cooperate to work correctly. We could also suppose that those amino acids are crucial for promoting ubiquitylation events and that their replacement prevents vacuolar trafficking because the function of *Pp*RMR2 as E3 ligase or as target of other E3 ligases, is impaired. These results also indicate that the mutation of critical amino acids in just one RMR, is sufficient to affect the functioning of the others, and that vacuolar trafficking might be regulated by *Pp*RMR2 involvement in ubiquitylation.

On the other hand, the vacuolar phenotype was not restored in the *Pp*5KO/Ci-Card line transformed with WT *Pp*RMR2. Indeed, there is evidence that the overexpression of a wild-type gene can impair the function of the protein, leading to the same phenotype as loss-of-function mutations (Prelich, 2012).

These results confirm again the hypothesis that *Pp*RMRs work together, in fact, neither *Pp*5KO/Ci-Card_RMR2ΔSer showed a vacuolar pattern, indicating that the truncated *Pp*RMR2ΔSer, which seems more stable in *Pp*WT/Ci-Card, is not able alone to promote vacuolar transport. Therefore, the other mutated versions of *Pp*RMR2 did not lead to any vacuolar phenotype in *Pp*5KO/Ci-Card as well.

Chapter 5

Conclusions and outlooks

The study of moss RMRs has turned out to be very difficult and despite the competent technical support of our technician, many experiments did not work as expected. In the end, I have obtained few results. Since the project ended with the retirement of Prof. Neuhaus and then the financial support also ended, I discuss here what could be done to continue this work if it should be taken up by another research group.

5.1 *Pp*RMR proteins detection

In this work, I have tried to detect *Pp*RMRs by Western Blot using the antibodies against *Arabidopsis* or rice RMRs and the antipeptide antibodies against *Pp*RMR2/RMR4 available in our laboratory. The use of common detergents such as SDS or DDM did not allow us any detection of *Pp*RMRs, neither the microsomal fractionation has been successful. This is a major problem as *Pp*RMRs detection would have been extremely useful for the rest of my experiments. Here I try to explain how this detection could be improved.

Total proteins have been always extracted from moss protonema, but protein extraction from leafy gametophores would also be suggested since *Pp*RMR2 and 4 are highly expressed in these organs as well. However, a more efficient antibody should be tested.

Although the use of detergents has been for years a valid alternative for membrane proteins solubilization, it has been shown that they can affect membrane proteins isolation: the subunits of membrane protein complexes, for instance, may not interact in presence of the detergent (Breyton *et al.*, 1997; Esmann, 1986). For this reason, some researchers have recommended to isolate membrane proteins keeping their lipid environment: lipids in fact are important for protein function and structure, and their removal could make the protein unfolded and inactive (Dawaliby *et al.*, 2016; Zoghbi *et al.*, 2016; Debnath *et al.*, 2011). In 2009, Knowles *et al.* demonstrated that the styrene maleic acid (SMA) copolymer could be used to extract membrane proteins in self-assembled styrene maleic acid lipid particles (SMALPs, *i.e.* SMA lipid particles, also called native nanodiscs or lipodisqs), without using any detergent. This method allows to extract membrane proteins still surrounded by their lipid environment. It has been successfully used to purify ABC transporters (Gulati *et al.*, 2014), a tetrameric K^+ channel (Dörr *et al.*, 2014) and a seven-transmembrane receptor protein (Orwick-Rydmark *et al.*,

2012). SMALPs can then be purified by affinity chromatography and analysed by Western Blot. Nevertheless, this technology revealed some limitations such as the sensitivity of SMALPs to the divalent cations magnesium and calcium which cause SMA precipitation (Morrison *et al.*, 2016; Oluwole *et al.*, 2017). SMALPs and SMA are also sensitive to low pH (below 7) which leads to their precipitation. Another limiting factor is represented by the size of the discs (10-12 nm) that is too small for proteins with large membrane domains (Lee *et al.*, 2016).

Because we cannot detect endogenous *Pp*RMRs by Western Blot, this could mean either that the epitope is masked or that the proteins have a too short half-life. The 70 amino acids long Ser-Rich domain of *Pp*RMR2 contains 9 serines which are all potential phosphorylation sites (NetPhos 3.1 Server). Phosphorylation is the most common post-translational modification, and there are examples where multisite phosphorylation is responsible for protein degradation (Varedi *et al.*, 2010).
The green fluorescent protein GFP from the jellyfish *Aequorea victoria* is used not only for the study of gene expression and protein localization, but also for monitoring protein degradation, allowing rapid and precise assays. Jiang *et al.* (2004) screened mammalian cells expressing a GFP-cDNA expression library, and monitored the ones in which the fluorescence diminished because of protein synthesis inhibition. In this way, they could study the short half-life and the regulation of these proteins.
Metabolic labels (^{2}H, ^{13}C, ^{15}N) also allowed to measure protein degradation rate in *A. thaliana* cell cultures (Yang *et al.*, 2010; Li L *et al.*, 2012; Nelson *et al.*, 2013) and to identify protease substrates in *A. thaliana* leaf mitochondria (Li L *et al.*, 2017; Huang *et al.*, 2015).

5.2 *Pp*RMRs as E3 ubiquitin ligases: which connection with moss development?

I could demonstrate that *Pp*RMR2 has an E3 ubiquitin ligase activity.
The experiment with the inhibitors of degradation ALLN, E64, MG132 did not allow us to identify putative candidates ubiquitylated by *Pp*RMRs. If we had obtained a ubiquitylation pattern, we would have analysed our samples by mass spectrometry (MS) or by LC-MS/MS-based multidimensional protein identification technology (MudPIT) which are the methods mainly used to identify ubiquitylated proteins (Maor *et al.*, 2007; Kim *et al.*, 2013).
We could also have tested another potent specific proteasome inhibitor, the Syringolin A, which allowed to determine protein abundance levels and to identify ubiquitylated targets in *A. thaliana* leaves, revealing that the regulation of certain proteins can occur at transcriptional and post-transcriptional level (Svozil *et al.*, 2014).

The Hybrigenics company (France) identified for us putative cytosolic candidates of *Pp*RMR2. We have decided to clone some of them, choosing the ones which had a high score of interaction with *Pp*RMR2 and a strong ubiquitylation prediction score. The proteins that we chose could be thus regulated by ubiquitylation, as explained in chapter 3, hence we hypothesized that they could be regulated by *Pp*RMR2. The ambiguous results that we have obtained *in vitro* did not confirm our hypothesis: we have observed ubiquitylation patterns but *Pp*RMR2 does not ubiquitylate these proteins. Moreover, it does not ubiquitylate itself, as it happens for many E3 ligases. However, the assay should be improved by adding a negative control such as *Pp*RMR2 without the RING domain: this deletion would prevent the activity of *Pp*RMR2 as E3 ligase.

The two HUWE1- and UBR4-type E3 ligases were also identified by Hybrigenics, but because of their huge size (11.7 and 15.6 Kb coding sequences respectively), we decided to knockout the genes by CRISPR/Cas9 technology, instead of cloning them.

HUWE1 is a HECT-domain E3 ligase that regulates in mammals diverse proteins such as c-MYC, p53 and MCL-1 (Kao *et al.*, 2018). It can act both as oncogene via MYC K48-linked ubiquitylation (Peter *et al.*, 2014; Adhikary *et al.*, 2005) and tumor suppressor via MYC K63-linked ubiquitylation (Myant *et al.*, 2017). The animal UBR4 contains a zinc finger-like domain and it is involved in membrane morphogenesis, cell survival, Ca^{2+} signaling, proteasomal degradation, autophagy (Nakatani *et al.*, 2005; Belzil *et al.* 2013; Tasaki *et al.*, 2013; Rinschen *et al.*, 2016). It has been shown that the E3 ligases can be regulated through self-catalyzed ubiquitylation (Lorick *et al.*, 1999) and/or exogenous ubiquitylation by another E3 ligase (Zaaroor-Regev *et al.*, 2010; Fang *et al.*, 2001; Ballar *et al.*, 2010).

Since we think that *Pp*RMRs are involved in vacuolar transport, we hypothesize that they could modulate the activity of HUWE1 or UBR4, and that this regulation might affect vacuolar trafficking in the line *Pp*WT/Ci-Card. Unfortunately, we could not confirm this hypothesis because of the issues encountered during the generation of CRISPR/Cas9 constructions. In addition, the interaction of *Pp*RMR2 with these E3 ligases and with the proteasome subunits N2, N3, N9 (candidates found by Y2H screening) could indicate that *Pp*RMR2 regulates the proteasomal degradation of HUWE1 or UBR4.

We detected a morphological phenotype for the *Pp*RMR-KO mutants. We noticed that the leafy gametophores developed differently in *Pp*1KO, *Pp*3KO and *Pp*5KO lines: after an extended growth (2 months) on regular NH_4 medium, gametophores were small and short in *Pp*WT, big and long in mutants.

Under salt stress conditions, *Pp*WT did not develop any gametophores at concentrations of 50, 100 and 200 mM NaCl. We thus suppose that *Pp*RMRs, maybe acting as E3 ligases, have a negative effect on leafy shoots development. This is only a hypothesis: the assay should be repeated, and several parameters should be measured, such as the index of multiplication, the protonemal radius, the

chlorophyll and phenolic content, the presence of secondary protonema and leafy gametophores after recovery.

Independently on *Pp*RMRs involvement in ubiquitylation, proteins should be extracted from gametophores of *Pp*WT and *Pp*KO lines, and a proteomic analysis through MS should be done. These proteome profiles should be then compared with the ones from mosses exposed to increasing NaCl concentration (both *Pp*WT and mutants). In this way, we could find out the substrates which interact with *Pp*RMRs or are regulated by them in normal conditions and under salt stress conditions. Differences could emerge in each mutant, meaning that each *Pp*RMR can interact with different substrates. The identification of these substrates would then be essential to understand the role of *Pp*RMRs as E3 ligases and which process they regulate during salt stress response.

It would also be interesting to test *Pp*RMRs response to other abiotic stresses such as temperature and drought. For instance, analysis through Y2H screening revealed that many RING E3 ligases are involved in several stress responses in plants (Liu *et al.*, 2016; Cho *et al.*, 2017).

5.3 *Pp*RMRs as vacuolar receptors

In Angiosperms, vacuolar receptors bind to the VSD of the vacuolar proteins and carry them to protein storage vacuole (PSV) or lytic vacuole (LV). It has been thought that VSRs and RMRs are involved in protein sorting to LV and PSV respectively (Paris *et al.*, 1997; Cao *et al.*, 2000). The PA of VSRs binds the ssVSD of certain proteins (Jiang *et al.*, 2000; Ahmed *et al.*, 2000), whereas in RMRs the function of PA is still unclear. The role of the linker following the TM domain has not been described in *Pp*RMRs, while in *A. thaliana* it is necessary for homodimerization or heterodimerization between *At*RMR1 and *At*RMR2 (Occhialini *et al.*, 2016).

Although the presence of a PSV in moss has not been proven yet, the targeting of the fusion protein Ci-Card to the central vacuole of *P. patens* was demonstrated to depend on *Pp*RMRs (Fahr, 2017). Surprisingly, the sorting phenotype in *Pp*WT/Ci-Card was altered by the overexpression of WT *Pp*RMR2, as well as by the mutation of the two histidines in the RINGH2 domain or of crucial lysines in the cytosolic tail. On the contrary, the line expressing the truncated *Pp*RMR2ΔSer (lacking the Serine-Rich motif) showed a vacuolar fluorescence. This pattern was not reproduced in *Pp*5KO/Ci-Card which displayed an ER fluorescence for all the constructions tested.

This indicates that *Pp*RMR2 without the Serine-Rich motif is still functional and probably more stable than the WT version, and these results also underline the importance of *Pp*RMRs cooperation.

The study of *Pp*RMRs *in vivo* would allow us to answer our questions and would help us to localize these proteins in moss. Endogenous *Pp*RMRs are not detectable by Western Blot, and the expression

of *Pp*RMR2 under the control of a strong promoter such as the HSP has not been successful. The overexpression of a fluorescent construct (such as GFP-*Pp*RMR2) in *P. patens* leaves would be recommended.

However, the study of vacuolar transport in moss protonema brought us interesting results, even if we have never worked "directly" on *Pp*RMRs.

It would be useful to study the effect of *Pp*RMR2ΔSer in *Pp*1KO/Ci-Card (Δrmr2) or *Pp*3KO/Ci-Card (Δrmr1/3/5) which have been shown to have the same phenotype as *Pp*5KO/Ci-Card (Fahr, 2017). In case of complementation of the phenotype, other mutated versions could be tested such as the one without the PA, or without the linker which is important for *At*RMR1 and *At*RMR2 dimerization in *A. thaliana*. This would allow us to understand whether certain domains are essential for the proper functioning of *Pp*RMRs or for promoting the cardosin targeting to the moss central vacuole.

Chapter 6

Material and methods

6.1 Plant material and culture conditions

6.1.1 *In vitro* cultures

Physcomitrella patens (*Grandsen* strain) protonema was plated, under sterile conditions, on autoclaved *Pp*NH_4-agar medium (**Table 6.1**) in 9 cm diameter *Petri* dishes, and grown in a phytotron (25 °C, discontinuous light, 16/8 h light/dark photoperiod). Just before plating, a cellophane disk was placed on the solid medium in order to make the material collection easier. Every week, protonema was collected and fragmented using a polytron blender, resuspended in sterile Milli-Q H_2O, then stored at 4 °C or re-plated on a solid medium (Schaefer and Zrÿd, 2001).

$CaNO_3$ $4H_2O$	800 mg
$MgSO_4$ $7H_2O$	250 mg
$FeSO_4$ $7H_2O$	12.5 mg
NH_4 tartrate	500 mg
1000X Microelements	1 ml
1000X Phosphate buffer	1 ml
Agar	7 g
Milli-Q H_2O	Adjust to 1 L

Table 6.1. *Pp*NH_4-agar medium composition

6.1.2 Heat-shock on moss protonema

The HS promoter of the constructions expressed in the transgenic lines used in this project, had to be induced by heat-shock before confocal microscope observations or protein extraction. Moss protonema was grown on *Pp*NH_4-agar medium for 7-9 days. The sample was then collected in a sterile tube filled with 10 ml of 45 °C pre-heated sterile Milli-Q H_2O, and incubated for a heat-shock in bain-marie at 45 °C, for 5 min. The protonema was transferred into a *Petri* dish to let the temperature cool down, then it was moved to *Pp*NH_4-agar medium and placed in the phytotron for 24 h or 48 h.

6.1.3 Protoplast isolation and stable transformation

The protocol of Scahefer *et al*. (1991) was followed.

Six- or seven-day-old moss protonema was digested by 1% driselase in 8.5% mannitol for 45 min, then this suspension was kindly mixed every 20 min. After 45 min, it was filtered through a stainless-steel sieve mesh and moved into a sterile tube. This was centrifuged at 500 rpm for 7 min, the supernatant was removed, and 8.5% mannitol was added to the pellet. The cells were gently resuspended and centrifuged twice. After the last wash, the pellet was resuspended in MMM solution freshly prepared [9.8 ml of 8.5% mannitol + 100 µl of 1.5 M $MgCl_2$ + 100 µl of 0.5 M MES (MES has pH 5.6 adjusted with 1 N KOH)]. 300 µl of this suspension (protoplasts + MMM) were transferred into a sterile tube containing 12-15 µg of plasmid DNA (isolated from *E.coli* according to Macherey-Nagel maxiprep protocol). After gentle mixing, 300 µl of PEG solution (**Table 6.2**) were added. Protoplast suspension was quickly mixed with PEG solution and incubated at 45 °C for 5 min. After heat-shock, 10 minutes at RT were required to let the temperature cool down. Protoplasts were diluted with *Pp*NH_4-mannitol-glucose liquid medium (**Table 6.3**): 300 µl every minute, 5 times, then 1 ml every minute, 5 times. They remained at RT, overnight in the dark. The next day, 3 ml of protoplast suspension were mixed with 3 ml of top layer (**Table 6.4**); 2 ml of this mix were plated on *Pp*NH_4-agar-mannitol-glucose *Petri* dishes, and these plates were placed in the phytotron for seven days. The cellophane disk was then transferred to a selective medium and, after one week, to a regular *Pp*NH_4 medium. The transfer from selective to regular medium continued for 2 weeks more until the clones were grown enough to be genotyped.

7% Mannitol + 0.1 M $CaNO_3$	10 ml
PEG 4000	4g
Adjust to pH 7.2 with 0.1 M Tris-HCl, pH 8	

Table 6.2. PEG solution composition

$CaNO_3$ $4H_2O$	800 mg
$MgSO_4$ $7H_2O$	250 mg
$FeSO_4$ $7H_2O$	12.5 mg
NH_4 tartrate	500 mg
1000X Microelements	1 ml
1000X Phosphate buffer	1 ml
Mannitol	66 g
Glucose	5 g
Milli-Q H_2O	Adjust to 1 L

Table 6.3. *Pp*NH_4-mannitol-glucose liquid medium composition

Mannitol	4.25 g
Agar	0.7 g
Milli-Q H_2O	Adjust to 50 ml

Table 6.4. Top layer composition

6.2 Techniques related to nucleic acids

6.2.1 Total RNA extraction from *P. patens* and cDNA synthesis

100 mg of 7-day-old protonema were collected in a 1.5 ml tube and quickly submerged in liquid nitrogen. The frozen sample was powdered using pre-chilled mortar and pestle. The powder obtained was transferred into a new 1.5 ml tube, then the RNA isolation continued according to the protocol of Macherey-Nagel (NucleoSpin®, RNA Plant). After quantification of RNA by a NanoDrop spectrophotometer, 500 ng were used to perform a reverse transcription (kit Takara).

6.2.2 Genomic DNA extraction

At least 100 mg of 7-8-day-old protonema were collected and fragmented in a 1.5 ml tube where few grains of quartz sand and 100 µl of extraction buffer (**Table 6.5**) were added. A pestle adapted to a polytron was used for the fragmentation. The protonema was ground for 30 sec in the extraction buffer, at RT. This step was repeated twice more. Samples were centrifuged at full speed for 5 min, then the supernatant was transferred in a new 1.5 ml tube. After adding 1 volume of chloroform to the supernatant, samples were vortexed for 5-10 sec and centrifuged at 13000 rpm for 5 min. The hydrophilic phase was recovered and transferred into a new 1.5 ml tube. After adding 200 µl of isopropanol, samples were well mixed and left at RT for 10 min. Then they were centrifuged at 13000 rpm for 10 min, the supernatant was removed, and the pellet washed with 400-600 µl of 75% ethanol by centrifugation for 10 min. The supernatant was removed, and the pellet was dried at 55 °C. This was resuspended in 50 µl of Milli-Q H_2O containing RNAse (20 µg/ml). Samples were then incubated at 55°C for 10 min, vortexed and centrifuged to remove the insoluble particles. NanoDrop was used to estimate the DNA concentration, then samples were diluted to 10 ng/µl and stored at -20 °C or directly used for PCR analysis.

	Final Concentration	Stock Concentration
Tris-HCl, pH 7.5	200 mM	1 M
NaCl	250 mM	5 N
EDTA, pH 8	25 mM	0.5 M
SDS	0.5%	20%
β-mercapto-EtOH	10 mM	1 M
ddH_2O	Adjust to 50 ml	

Table 6.5. gDNA extraction buffer composition

6.2.3 PCR

In a 0.2 ml sterile tube, the following mix was prepared on ice: forward and reverse primers (Microsynth, 0.5 µM final concentration), 5X Colorless GoTaq® Flexi Buffer or 5X Green GoTaq® Flexi Buffer (1X final concentration), 1 or 1.25 units (depending on the final volume) of DNA polymerase (GoTaq®, or Phusion® or Q5® High-Fidelity DNA polymerase), 10 ng of DNA, dNTPs (0.2 mM final concentration) in a final volume of 20 or 50 µl adjusted with sterile Milli-Q H_2O.

6.2.4 Agarose gel electrophoresis and DNA purification

Agarose was weighed and added to 0.5X TBE buffer (**Table 6.6**). 0.8% (w/v) agarose was used to resolve big DNA fragments (> 500 bp), while 1.5%-2% was used to separate the small ones (between 100 and 500 bp). Using a microwave oven, the agarose was completely dissolved in TBE. Once the solution cooled down to 50-55 °C, Midori Green dye was added (10 µl in 50 ml), and after mixing, the agarose was poured into a gel tray where a comb was previously placed. When the agarose was solidified, the electrophoresis could be performed at 100 V for about 30 min. The DNA was visualized and photographed by placing the gel on a UV-transilluminator. In case of DNA purification, a specific agarose was used, called D-1: after visualization, the band of interest was cut with a scalpel, and the gel slice was weighed in a 1.5 ml tube. DNA purification was performed using the Wizard® SV Gel and PCR Clean-Up System protocol (Promega®).

Tris base	108 g
Boric acid	55 g
EDTA 0.5 M, pH 8	40 ml
ddH_2O	Adjust to 1 L

Table 6.6. 10X TBE buffer composition

6.3 Constructions used for cloning

6.3.1 POG1 constructs

The original plasmid pPOG1 was provided by M. Hasebe. It contained a Gateway cassette which was removed and replaced by *Pp*RMR2 cDNA previously subcloned in pGEM®-T easy vector. All the constructs based on pPOG1 were obtained using the Q5® Site-directed mutagenesis kit (NEB®).

6.3.2 pET21b constructs

The cDNA of interest (DUSP, N2, N3, N9 or COPG) was amplified by PCR and subcloned in the linearized pJET1.2/blunt vector (Termo Fisher) which harbors the ampicillin resistance and accepts inserts from 6 bp to 10 Kb. The insert was then cloned in the reporter vector pET21b.

6.3.3 DNA digestion

1-40 µg of DNA were digested using 1 unit of restriction enzyme per µg of DNA, restriction buffer (1X final concentration) and Milli-Q H_2O, in a total volume of 20 or 200 µl depending on the amount of DNA digested. After mixing all the reagents in a 1.5 ml tube, the mix was incubated at 37 °C for 2 or 4 h, or overnight. Some restriction enzymes needed to be inactivated at 65 °C for 20 min.

6.3.4 DNA precipitation

2 volumes of 100% ethanol were added into a 1.5 ml tube containing the DNA. Samples were placed on ice for 10 min, then they were centrifuged at full speed for 30 min, at 4 °C. The supernatant was discarded, and the pellet washed with 1 volume of 70% ethanol by centrifugation for 10 min. After discarding the supernatant, the pellet was air-dried at RT for 10 min, then it was dissolved in Milli-Q H_2O. DNA was quantified using the NanoDrop.

6.3.5 Ligation of a DNA fragment into a vector

In a 1.5 ml tube, 200 ng of vector (50 ng in the case of pJET1.2) were mixed with the insert in a 3 insert:1 vector molar ratio. 0.5-1 µl of T4 DNA ligase (Promega® or Termo Fisher) and 2X ligation buffer (final concentration 1X) were added, in a final volume of 15 µl adjusted with Milli-Q H_2O. The reaction occurred at RT, for 2 h in the dark (30 min in the case of pJET1.2 vector).

6.3.6 *E. coli* transformation by heat-shock

Competent cells of *E. coli* (XL1/BL21/DH5α) were transformed with 1-10 ng of purified plasmid DNA or with 15 µl of DNA ligation mixture, and incubated on ice for 15 min. The tube containing the bacterial suspension was heated at 42 °C for 90 sec, then it was placed on ice for 3 min. Finally, the bacterial suspension was plated on LB-agar medium containing a selective antibiotic, and incubated overnight at 37 °C.

6.3.7 Plasmid DNA extraction: miniprep (1.2.3 alkaline lysis)

A single bacterial colony was inoculated in LB liquid medium containing antibiotic, and incubated overnight at 37 °C, under shaking. The morning after, 1.5 ml of bacterial suspension was centrifuged at 12000 x g for 3 min. The supernatant was discarded and the pellet was resuspended in 150 µl of buffer 1 (25 mM Tris-HCl pH 8 + 50 mM glucose + 10 mM EDTA pH 8) + 2 µl of RNase (10 mg/ml). This suspension was incubated for 3 min at RT. 200 µl of buffer 2 (0.2 M NaOH + 1% SDS) were added into the tube, and this was strongly mixed by inversion until the solution became homogenous and transparent. The sample was incubated for 5 min on ice. 150 µl of chilled buffer 3 (3 M KOAc + 5 M acetic acid) were added into the sample, this was vortexed for 5 sec and incubated for 5 min on ice. Then it was centrifuged for 5 min at 12000 x g. The supernatant was transferred into a new 1.5 ml tube, and here 400 µl of chloroform + isoamyl alcohol (48:2) were added. After mixing, the tube was centrifuged for 5 min at 12000 x g. The upper aqueous phase was collected in a new 1.5 ml tube, then DNA was precipitated with 900 µl of 100% ethanol. The sample was mixed by inversion, incubated at RT for 10 min and centrifuged for 15 min at 12000 x g. The pellet, containing the DNA, was washed with 900 µl of 70% ethanol by centrifugation for 5 min at 12000 x g. Then it was dried at 65°C for 5 min, resuspended in 40-50 µl of Milli-Q H_20 + RNase (20 µg/ml) and incubated again at 65 °C for 5-10 min. DNA concentration was estimated using the NanoDrop.

6.4 CRISPR/Cas9 technology

Vectors

The entry vector used was pENTR-PpU6p-sgRNA (kanamycin resistance). The destination vector used was pMH-Cas9 (ampicillin bacterial resistance, hygromycin plant resistance). It was propagated with chloramphenicol, in DB3.1 competent cells, because of the presence of the Gateway cassette. The vectors were provided by the Bezanilla laboratory (Department of Biological Sciences, Dartmouth College — Hanover, New Hampshire, USA).

Protospacer design

Protospacers were designed using the website http://crispor.tefor.net/

6.4.1 Cloning steps (Bezanilla's protocol with minor changes)

The entry vector pENTR-PpU6p-sgRNA was digested using the following reagents: 2 µl of miniprep plasmid, 3 µl of Cutsmart buffer (1X final concentration), 0.5 µl of BsaI, 24.5 µl of ddH_2O. Samples were incubated at 37 °C for 1 h, or overnight for a complete digestion. After checking the size by agarose gel electrophoresis, the DNA was purified and quantified for ligation.

The two complementary protospacers were annealed as follows: the forward and the reverse primers were resuspended with ddH_2O to 100 µM; primers were then mixed with 1:1 ratio and this mix was incubated at 98 °C, for 3 min. The annealed product was diluted 100-fold.

6.4.2 Ligation of the protospacer into BsaI digested entry vector

The tube containing the instant sticky-end ligase master mix (NEB®) was transferred on ice. In another tube, 100 ng of linearized entry vector were combined with a 3-fold molar excess of protospacer, and the volume was adjusted to 5 µl with ddH_2O. Here, 5 µl of instant sticky-end ligase master mix were added, and after mixing by pipetting 7-10 times, this tube was incubated at RT for 5-10 min. Then the sample was ready to transform *E. coli* cells. DH5α (or XL1) competent cells were transformed, plated on LB-Kan medium and incubated overnight at 37 °C. Colonies from overnight incubation were picked for miniprep. Consequently, digestion with BsaI was done. Plasmids that had inserted the protospacer could not be cut by BsaI (because the BsaI site disappears after ligation). These were sequenced with M13F sequencing primer.

6.4.3 Obtain the destination vector with your protospacer

LR reaction was performed. In a 1.5 ml tube, the following reagents were mixed: 1-7 µl (50-150 ng) of entry clone (protospacer + entry vector), 1 µl of destination vector (150 ng/µl), TE buffer pH 8 (1 M Tris-HCl pH 8 + 0.5 M EDTA pH 8) to 8 µl. LR clonase II enzyme mix (Termo Fisher) was thawed on ice for about 2 min, then it was vortexed briefly. 2 µl of LR Clonase II mix were added to the reaction and the tube was mixed by brief vortexing. The reaction was incubated at 25 °C for 1 h. 1 µl of proteinase K solution was added to the sample to stop the reaction. The sample was vortexed and incubated at 37 °C for 10 min. DH5α competent cells were transformed with the LR reaction product, plated on LB-Amp plates, and incubated overnight at 37 °C. Colonies from overnight incubation were picked for miniprep. A DNA digestion was done (AflII and SacI enzymes were used) and the positive clones were picked for sequencing.

6.4.4 Plant selection

For single gene targeting, protoplasts were transformed with 15 µg of plasmid and plated onto PRMB plates (**Table 6.7**) with cellophane disk, without top layer. After 4 days, the cellophane disk was moved onto *Pp*NH_4 + hygromycin plates where it was kept for 7 days to ensure the death of the untransformed protoplasts. After 7 days, the cellophane disk was moved to a regular *Pp*NH_4 medium, thus the transformed clones lost the destination plasmid. Once they grew enough, they were genotyped with primers that cover at least 400 bp (200 bp upstream, 200 bp downstream). T7 endonuclease I was used to check if the target gene was mutated or not before sequencing.

Solution B (25 g $MgSO_4$ $7H_2O$ in 1 L Milli-Q H_2O)	10 ml
Solution C (25 g KH_2PO_4 in 1L Milli-Q H_2O, pH 6.5 adjusted with 4 M KOH)	10 ml
Solution D (101 g KNO_3 in 1 L Milli-Q H_2O)	10 ml
Trace element solution (Hoagland's A-Z trace element solution)	1 ml
$FeSO_4$ $7H_2O$	12.5 mg
D-mannitol	60 g
di-ammonium (+) tartrate	920 g
Agar	7 g
Milli-Q H_2O	to 1 L
Add 10 ml of $CaCl_2$ 1M to the sterile medium before pouring	

Table 6.7. PRMB (Protoplast Regeneration Medium-Bottom layer) composition

6.5 Protein techniques

6.5.1 Total protein extraction from *P. patens* in SDS-Sample Buffer

At least 100 mg of 7-8-day-old protonema were collected in a 1.5 ml tube on ice; after adding 250 µl of 2X SDS-sample buffer (4X SDS-SB in the **Table 6.8**) + Protease inhibitor cocktail [Pic from Sigma-Aldrich® (0.5 µl of Pic per 100 µl of 2X SB)] and few grains of quartz sand, samples were ground for 30-40 sec using a polytron blender. This step was repeated twice. Samples were heated for 5 min at 100°C and centrifuged for 15 min at 16000 rpm. The supernatant was transferred into a new 1.5 ml tube, stored at -20 °C or directly used for SDS-PAGE. Protein concentration was quantified according to the Bradford method (Bradford, 1976).

2 M Tris-HCl, pH 6.8	1 ml
DTT	617 mg
20% SDS	4 ml
Bromophenol blue	40 mg
Glycerin	4 ml
ddH_2O	Adjust to 10 ml

Table 6.8. 4X SDS-SB composition

6.5.2 Microsomal fractionation

According to Jabnoune *et al.* (2013) with minor changes.

At least 100 mg of 7-8-day-old protonema were collected in a 1.5 ml tube on ice. After adding few grains of quartz sand and 400 µl of ice-cold extraction buffer (100 mM Tris-HCl pH 7.5 + 400 mM sucrose + 1 mM EDTA + 2X Pic), samples were fragmented for 30-40 sec using a polytron. This step was repeated twice. After 20 min of incubation on ice, samples were centrifuged at 1000 x g, at 4 °C for 5 min and the pellet was discarded. Samples were then centrifuged at 8000 x g, at 4 °C for 15 min and the pellet was removed. Samples were ultracentrifuged at 150000 x g, at 4 °C for 1 h. The microsomal pellet was resuspended in 2X SB, heated at 100 °C for 5 min and analysed by Western Blot.

6.5.3 Immunoprecipitation

Protein A Sepharose beads preparation

100 mg of protein A sepharose beads were resuspended in 10 ml of 1X PBS in a centrifuge tube and incubated for 15 min, at 4 °C, under light shaking. Beads were centrifuged down at 500 rpm, at 4 °C for 5 min and the supernatant was discarded. This procedure was repeated twice. The beads were resuspended in 10 ml of 1X PBS and stored at 4 °C (10X PBS composition is shown in **Table 6.9**).

1.37 M NaCl	80 g
27 mM KCl	2 g
0.1 M Na_2HPO_4 $2H_2O$	17.8 g
17.6 mM KH_2PO_4	2.4 g
ddH_2O	Adjust to 1 L

Table 6.9. 10X PBS composition

Sample preparation

Proteins were extracted from at least 100 mg of 7-8-day-old protonema ground in 1X PBS (500 µl of 1X PBS per 100 mg of protonema) + Pic (0.5 µl of Pic per 100 µl of 1X PBS) + a pinch of PVPP [Poly(vinylpolypyrrolidone, Sigma-Aldrich®)] + few grains of quartz sand. Samples were kept on ice during grinding. They were centrifuged at 16000 rpm, at 4 °C, for 15 min. The supernatant was collected in a 12 ml tube and filtered through a 0.22 µm syringe filter.

After adding anti-Ub antibody (1:800 v/v) to the supernatant containing the total protein extracts, samples were incubated for 2 h at 4 °C, with gentle agitation.

After the first incubation, 100 µl of protein A sepharose beads were added to the samples (using tips with the end cut off), then these were incubated with gentle rocking for 2 h at 4 °C. They were centrifuged at 500 rpm for 1 min, at 4 °C, and the supernatant was discarded. Pellet was washed 5 times with 1X PBS by centrifugation at 500 rpm, at 4 °C, for 1 min (the 1X PBS starting volume was 10 ml, then it was reduced after each wash and transferred into a 1.5 ml tube). After the last centrifugation, the supernatant was carefully removed, and the pellet was resuspended in 2 volumes of 2X SB. Samples were heated at 100°C for 5 min and stored at -20 °C or directly analysed by Western Blot using anti-Ub antibody (1:6000, from Agrisera).

6.5.4 *In vitro* ubiquitylation assay

The E2 Screening kit UBPBio (http://www.ubpbio.com/index.php/e2-screening-kit.html) was used for this assay. For each reaction, a mixture containing the following reagents was prepared: 100 nM E1 activating enzyme, 2 µM E2 conjugating enzyme (29 different human E2 enzymes were tested), 2 µM E3 ligase (GST-*Pp*RMR2), 50 µM ubiquitin, 2 µM substrate (GST-*Pp*RMR2, N3-His, N9-His, DUSP-His or COPG-His, each cloned in pET21b vector), 2 mM ATP, 2 µl of 10X ubiquitylation buffer, in a final volume of 20 µl adjusted with Milli-Q H_2O. As controls, similar reactions were prepared in the absence of either E1 or E2 or E3 or substrate or ubiquitin. The mixture was incubated at 25 °C for 2 h. The reaction was stopped by adding 2X SB and boiling the samples at 100 °C for 5 min. After SDS-PAGE, proteins were detected by Western Blot with the respective antibodies.

6.5.5 Inhibitors of ubiquitin-dependent degradation

The inhibitors ALLN, E64 and MG132 (Merck) were dissolved in DMSO and heated at 40 °C for 10 min before use. At least 200 mg of 7-8-day-old moss protonema were collected and transferred in 5 ml of *Pp*NH_4 liquid medium containing 2.5 µM of ALLN or E64 or MG132 or all the three inhibitors together. Samples were incubated at 15 °C for 4 h with gentle shaking.

After incubation, the moss was collected, then total proteins were extracted in 1X PBS. Protein extraction was followed by immunoprecipitation in presence of anti-Ub antibody (diluted 1:800) and protein A sepharose beads. Samples were analysed by Western Blot analysis with anti-Ub antibody (diluted 1:6000).

6.5.6 GST- and His-tagged proteins purification

Preparation of the beads

The glutathione-agarose resin (Sigma-Aldrich®) was resuspended in 10 ml of sterile Milli-Q H_2O and incubated at 4 °C overnight, under rotary shaking. The morning after, the resin was washed 5 times in 10 ml of 1X PBS (500 rpm, 5 min) and stored at 4°C in a final volume of 5 ml 1X PBS.

Nickel-nitrilotriacetic acid (Ni-NTA)-agarose resin (QIAGEN) was ready for use.

Gravity flow purification of soluble GST-PpRMR2 under native conditions

E.coli BL21 (DE3) cells were transformed with pGEX_GST-*Pp*RMR2 by heat-shock and grown on LA solid medium (LB + Ampicillin) at 37 °C, overnight. The day after, a single colony was resuspended in 20 ml of LA liquid medium and incubated at 37 °C with shaking (190-200 rpm), overnight. The day after, 500 ml of LA were inoculated with 10 ml of the overnight pre-culture and incubated at 37 °C with shaking, until the OD_{600} reached 0.5-0.6. Once the desired OD was reached, IPTG (final concentration 0.5 or 1

mM) was added to induce the expression of GST-*Pp*RMR2, then the culture was incubated for 3 h, at 37 °C with shaking. After 3 h, the bacterial culture was centrifuged at 10000 rpm for 45 min at 4˚C. The pellet was dissolved in 10 ml of lysis buffer pH 8 (50 mM Tris-HCl + 300 mM NaCl + Pic added freshly) and the suspension obtained was sonicated on ice (40 sec, pause 1 min, 3 times). This lysate was ultracentrifuged at 20000 rpm, for 1 h, at 4 °C. The supernatant was filtered through a 0.42 µm syringe filter and incubated with 500 µl of glutathione-agarose beads during 2 h with light rotary shaking. For the affinity chromatography, the mixture (lysate + beads) was transferred into a pre-equilibrated Poly-Prep® chromatography column (Bio-Rad) and the flow-through was collected. The resin which settled down the column was washed 5 times with 1X PBS by centrifugation at 400 rpm for 5 min. The protein was eluted with elution buffer pH 8 (50 mM Tris-HCl + 10 mM free reduced glutathione). The eluate was dialyzed against a buffer pH 8 (50 mM Tris-HCl + 300 mM NaCl) using an Amicon® Ultra centrifugal filter or a regenerated cellulose (RC) membrane. All the steps of purifications were done at 4 °C.

Gravity flow purification of soluble His-tagged proteins under native conditions

E.coli BL21 (DE3) cells were transformed with pET21b_protein-His by heat-shock and grown on LA solid medium (LB + Ampicillin) at 37 °C, overnight. The day after, a single colony was resuspended in 20 ml of LA liquid medium and incubated at 37 °C with shaking (190-200 rpm), overnight. The next morning, 500 ml of LA were inoculated with 10 ml of the overnight pre-culture and incubated at 37 °C with shaking, until the OD_{600} reached 0.5-0.6. Once the desired OD was reached, IPTG (final concentration 1 mM) was added to induce the expression of protein-His, then the bacterial culture was incubated for 3 h, at 37 °C with shaking. After induction, the culture was centrifuged at 10000 rpm for 45 min at 4˚C. The pellet was dissolved in 10 ml of lysis buffer pH 8 (50 mM NaH_2PO_4 + 300 mM NaCl + 10 mM imidazole + Pic added freshly) and the suspension obtained was sonicated on ice (40 sec, pause 1 min, 3 times) or lysed by French press. This lysate was ultracentrifuged at 20000 rpm, for 1 h, at 4 °C. The supernatant was filtered through a 0.42 µm syringe filter and incubated with 500 µl of Ni-NTA agarose beads (QIAGEN) for 2 h with light rotary shaking. The lysate + beads were transferred into a pre-equilibrated Poly-Prep® chromatography column (Bio-Rad) and the flow-through was collected. The resin which settled down the column was washed 5 times with wash buffer pH 8 (50 mM NaH_2PO_4 + 300 mM NaCl + 20 mM imidazole) by centrifugation at 400 rpm for 5 min. The protein was eluted with elution buffer pH 8 (50 mM NaH_2PO_4 + 300 mM NaCl + 250 mM imidazole). The eluate was dialyzed against a buffer pH 8 (50 mM NaH_2PO_4 + 300 mM NaCl), using an Amicon® Ultra centrifugal filter or a regenerated cellulose (RC) membrane. All the steps of purification were done at 4 °C.

Gravity flow purification of insoluble His-tagged proteins under native conditions

The procedure is the same as the one described above. The modifications are the following: 0.5% (w/v) DDM was added to the lysis buffer and elution buffer; 0.1% (v/v) Triton X-100 was added to the wash buffer. Bacterial cells were lysed by high pressure using the French press instead of sonication.

6.5.7 SDS-PAGE

The SDS-PAGE was performed using the Mini PROTEAN® 3 system (Bio-Rad). The gel is composed of a running gel (according to the protein size, 7% - 10% - 12% or 18% of acrylamide/bisacrylamide mix; **Table 6.10**) and a stacking gel (4% acrylamide/bisacrylamide; **Table 6.11**). For the electrophoresis, 1X running buffer (**Table 6.12**) was used. A current of 20 mA was applied until the samples reached the running gel; then it was increased to 35 mA. The electrophoresis was stopped when the blue dye was close to the bottom of the gel.

Milli-Q H_2O	1185 µl
2 M Tris-HCl, pH 8.8	1735 µl
Acryl/Bis-acryl (30%)	2000 µl
20% SDS	25 µl
10% APS	50 µl
Temed	5 µl

Table 6.10. Running gel composition (12% acrylamide)

Milli-Q H_2O	1470 µl
0.5 M Tris-HCl, pH 6.8	625 µl
Acryl/Bis-acryl (30%)	335 µl
20% SDS	12.5 µl
Bromophenol Blue	30 µl
10% APS	25 µl
Temed	2.5 µl

Table 6.11. Stacking gel composition (4% acrylamide)

250 mM Tris base	30.28 g
1.92 M Glycine	144.13 g
SDS	10 g
ddH_2O	Adjust to 1 L

Table 6.12. 10X Running buffer composition

6.5.8 Western Blot

After SDS-PAGE, the Mini Trans-Blot® cell (Bio-Rad) was used to transfer proteins to a nitrocellulose membrane (GE Healthcare Amersham). The "sandwich", prepared in a cassette, consisted of sponge pad, Whatman paper, gel, membrane, Whatman paper, sponge pad, orienting the gel towards the cathode (-) and the membrane on the side of the anode (+). All the system was submerged in 1X transfer buffer (**Table 6.13**), and an electric field (100 V, for 1 h - 1 h 30 min at 4 °C) was applied. Once the transfer was finished, the nitrocellulose membrane was removed from the cassette and incubated for 5 min in Amido Black solution (**Table 6.14**) with shaking, then in a destaining solution (**Table 6.15**) which was changed every 10 minutes, until the background became completely clear. The membrane was washed in 1X TBS solution (**Table 6.16**), then in 1X TBS + 0.1% Tween 20, 10 minutes each wash. It was incubated for 1 h at RT in a blocking solution (3% BSA in 1X TBS), then incubated overnight at 4°C with the primary antibody (diluted in 3% BSA; the antibody anti-RMR2 was diluted 1:3000; the antibody anti-Ub 1:6000; the antibody anti-GST from Abcam and anti-His from Termo Fisher were diluted 1:4000). After incubation, the membrane was washed 10 min in 1X TBS, 2x10 min in 1X TBS + 0.1% Tween 20, and incubated for 1 h at RT with the secondary antibody (diluted in 5% milk; secondary antibody against anti-RMR2, anti-GST and anti-His antibodies were diluted 1:3000; the one against anti-Ub was diluted 1:6000). Once the incubation was completed, the membrane was washed 10 min in 1X TBS and 2x10 min in 1X TBS + 0.1% Tween 20. The bands were revealed with the ECL detection kit (Advansta) using an Amersham Image 600 instrument.

480 mM Tris base	58 g
390 M Glycine	29.28 g
13 mM SDS	3.75 g
ddH_2O	Adjust to 1 L

Table 6.13. 10X Transfer buffer composition

Ethanol	450 ml
Acetic acid	100 ml
Amido Black	1 g
ddH_2O	Adjust to 1 L

Table 6.14. Amido Black composition

Ethanol	400 ml
Acetic acid	100 ml
ddH_2O	Adjust to 1 L

Table 6.15. Destaining solution composition

200 mM Tris base	24 g
1.5 M NaCl	87.66 g
pH	Adjust to 7.6 with HCl
ddH_2O	Adjust to 1 L

Table 6.16. 10X TBS composition

6.6 The Yeast 2-Hybrid (Y2H) system

This assay, performed by Hybrigenics company (France), is used to detect protein-protein interactions in yeast cells, via cDNA library screening. The protein of interest is called bait and it is fused to the DNA Binding Domain (DBD), while the interaction partners present in the cDNA library are defined preys, fused to the Activation Domain (AD). The bait binds the upstream activating sequence (UAS) of the promoter (**Figure 6.1**). The interaction between the bait and the potential prey reconstitutes a functional transcription factor (Gal4), driving to a reporter gene expression. The most used reporter genes are HIS3 for the selection of the yeast on a medium lacking histidine, and LacZ for selection by colorimetric assay.

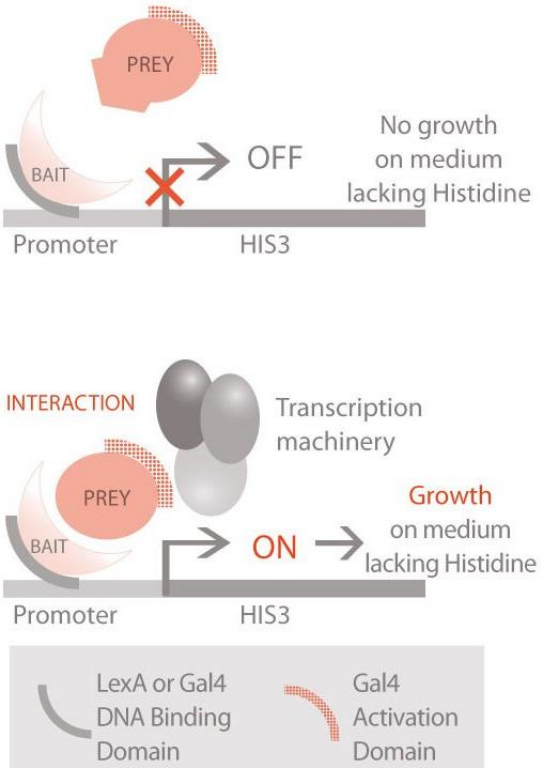

Figure 6.1. Yeast 2-Hybrid System. The interaction of two proteins reconsitutes an active transcription factor and enables yeast growth. Bait: protein of interest. Prey: protein partner of the bait (from www.hybrigenics.com). In our case, the bait is either the luminal or the cytosolic domain of *Pp*RMR2.

Acknowledgements

First, I want to thank my supervisor Prof. Jean-Marc Neuhaus who gave me the opportunity to work in the laboratory of Cell and Molecular Biology and contributed to my PhD project.

I also thank the co-director of my thesis, Prof. Felix Kessler, for his support especially in the last period of my PhD.

Thanks to Dr. Didier Schaefer who answered all my questions and allowed me to know this special plant that is the moss.

I am thankful to the technician of my laboratory, Sophie Marc-Martin who taught me to clone and helped me in several experiments.

A special thank goes to Dr. Guillaume Gouzerh and Dr. Shanmugabalaji Venkatasalam who helped me in confocal microscopy. Many thanks for the interesting scientific discussions we had together.

I want to acknowledge Prof. Erika Isono, who kindly suggested me to test the UBPBio E2 kit for my *in vitro* ubiquitylation assays.

I thank all the members of the laboratory of Cell and Molecular Biology for the nice friendly moments we spent together, moments that I also shared with the teams of Plant Pathology and Plant Physiology in Neuchâtel: I have appreciated a lot your advice, help and encouragement.

Thanks to Prof. Gian Pietro Di Sansebastiano who suggested me to come to Switzerland for this work experience from which I have learnt a lot.

I am deeply grateful to my family for their unconditional love and support: from the South of Italy, you have been so close to me during these years.

Annexes

1. Primers

5'PIG1_bR.fw	ATCTAGACCCAGGTAGGACCC
3'PIG1_bL.rev	TAGCAGAGTTGTTAGGAAATCA
COPG_NdeI.fw	TTCCATATGGCGTCGCTCCCGCCCGC
COPG_NotI.rev	CTTGCGGCCGCGGAGTTGATGATATCATGAATAATGTC
DUSP_NdeI.fw	TTCCATATGGCAGACATAGCAGAAGCTGAGC
DUSP_NotI.rev	CTTGCGGCCGCCTGTAGTTCCTCCTCACTGTC
EF-1 alpha.fw	GTGTTCTAAGAGTGACAACCGCTACG
EF-1 alpha.rev	GCTCATAGTGCATCAAAATGTG
N2_XbaI.fw	TTCTCTAGAATGACGGTGGTGAGCACGG
N2_XhoI.rev	CTTCTCGAGAGGAACATATTCAAAAGGCTCAGG
N3_NdeI.fw	TTCCATATGACTGTGGTGCCTCCAATC
N3_NotI.rev	CTTGCGGCCGCAAAGTCATCATCATCTTCCTCAGC
N9_NdeI.fw	TTCCATATGGCGGCGTTGCAATATTTG
N9_NotI.rev	CTTGCGGCCGCAACAGTCATAAGGTCCGGGG
pPOG1.fw	GCGCACTAGTGTGATCCTGTAGATTTGGCCATC
pPOG1.rev	GCGCCTCGAGCTTCGATTACCTGCAAAAACTC
RMR1.fw	ATCCAGATGGTGGTGAG
RMR1.rev	GCATAATTTAGGATCCACCAGGTC
RMR2.fw	TGGCGAAAAGCTGAGGTTG
RMR2.rev	AGTAGTTTCGTCCGGTGAAGC
RMR3.fw	GCATAGATCAGTGGCTACTCACGCGGA
RMR3.rev	AAGTTAACACAGATCTTCTCCCGA
RMR4.fw	TAGAGGACTATGAGAGCGGACAA
RMR4.rev	AGAGCCTACAGGTGAGGTTTGAG
RMR5.fw	TGCGACTCTTACCTTGTCAGC
RMR5.rev	ATCTGAAGGCGATGATTGGAT
RMR2ΔSer.fw	ACTAGTGTGATCCTGTAGATTTG
RMR2ΔSer.rev	TTATCTTTTGCAGACTGGGCAG
RMR2_K295R.fw	CCCAGTCTGCAGGAGAGATGCCC
RMR2_K295R.rev	CAGAAAGGTTTACGGGTTG
RMR2_K301R.fw	TGCCCAATCCAGGGTTGATAAGC
RMR2_K301R.rev	TCTCTTTTGCAGACTGGG
RMR2_RINGH273R.fw	GCCCTGTCAAAGGGAGTTCCATCTTGAC
RMR2_RINGH273R.rev	AGCAACCTCAGCTTTTCG
RMR2_RINGH276R.fw	AAGGGAGTTCAGGCTTGACTGTATTGATCAATGG
RMR2_RINGH276R.rev	TGACAGGGCAGCAACCTC
RMR2_XhoI.fw	GCGCTCGAGATGCCGTCCCTCGTCGTCGAG
RMR2_SpeI.rev	GCGACTAGTTTAGCAGAGATCTTCGGAACC
T7pro.fw	TAATACGACTCACTATAGGG
T7ter.rev	GCTCAGCGGTGGCAGCAGCC
TrbcS.rev	GTAGGATTCTGGTGTGTGG

2. Vectors

The vectors pGEM®-T easy (Promega®) and pJET1.2/blunt (Termo Fisher), both carrying the ampicillin resistance, were used for subcloning. The insert cDNA subcloned in the first vector was destined to pPOG1, while the insert subcloned in pJET1.2/blunt was then cloned in pET21b (from Merck). Both pPOG1 and pET21b harbor the ampicillin resistance.

pPOG1 was provided by M. Hasebe: it carries a Gateway cassette flanked by EF-1α promoter and TerbcS terminator. The constructions obtained from this plasmid were addressed to PIG loci of moss genome; the targeting sequences for these loci are PIG1bR and PIG1bL. The antibiotic resistance for transgenic plants is the hygromycin B.

3. Cloning

POG1-RMR2: the Gateway cassette was removed from the matrix plasmid pPOG1 by Q5® Site-directed mutagenesis kit (NEB®). The plasmid was amplified by PCR using the primers pPOG1.fw and pPOG1.rev which allowed to add XhoI/SpeI restriction sites. The cDNA sequence of *Pp*RMR2 was amplified by PCR using the primers RMR2_XhoI.fw and RMR2_SpeI.rev, it was then subcloned in pGEM®-T easy vector. The restriction enzymes XhoI/SpeI were used to cut RMR2 fragment which was then cloned in pPOG1 previously deprived of the Gateway cassette and linearized by XhoI/SpeI.

From POG1-RMR2, all the other constructions were generated by Q5® Site-directed mutagenesis.

POG1-RMR2ΔSer: the cDNA of *Pp*RMR2 was amplified using the primers RMR2ΔSer.fw and RMR2ΔSer.rev which were designed to delete the Serine-Rich motif.

POG1-RMR2_RINGR2: four primers were designed to replace the two histidines of the RINGH2 domain by two arginines. The cDNA of *Pp*RMR2 was first amplified using the primers RMR2_RINGH273R.fw and RMR2_RINGH273R.rev (273 is the position of the histidine in the amino acid sequence of RMR2). The resulting mutated RMR2 was amplified by PCR using the primers RMR2_RINGH276R.fw and RMR2_RINGH276R.rev (276 is the position of the other histidine in the amino acid sequence of RMR2). The resulting construct was called POG1-RMR2_RINGR2.

POG1-RMR2_K295R: the cDNA of *Pp*RMR2 was amplified using the primers RMR2_K295R.fw and RMR2_K295R.rev (295 is the position of the lysine in the amino acid sequence of RMR2 which has been replaced by arginine).

POG1-RMR2_K301R: the cDNA of *Pp*RMR2 was amplified using the primers RMR2_K301R.fw and RMR2_K301.rev (301 is the position of the lysine in the amino acid sequence of RMR2 which has been replaced by arginine).

Each construction POG1 was linearized by the enzyme MssI (also called PmeI), before protoplast transformation.

pET21b_DUSP: the cDNA sequence of DUSP was amplified by PCR using the primers DUSP_NdeI.fw and DUSP_NotI.rev. Then it was subcloned in pJET1.2/blunt. The amplified insert was cut using the enzymes NdeI/NotI and cloned in the final vector pET21b which was previously linearized by NdeI/NotI.

pET21b_N2: the cDNA of N2 was amplified using the primers N2_XbaI.fw and N2_XhoI.rev. Then it was subcloned in pJET1.2/blunt. The amplified insert was cut using the enzymes XbaI/XhoI and cloned in the final vector pET21b which was previously linearized by the same restriction enzymes.

pET21b_N3: the cDNA sequence of N3 was amplified using the primers N3_NdeI.fw and N3_NotI.rev. Then it was subcloned in pJET1.2/blunt. The amplified insert was cut by the enzymes NdeI/NotI and cloned in the final vector pET21b which was previously linearized by the same restriction enzymes.

pET21b_N9: the cDNA of N9 was amplified using the primers N9_NdeI.fw and N9_NotI.rev. Then it was subcloned in pJET1.2/blunt. The amplified insert was cut using the enzymes NdeI/NotI and cloned in the final vector pET21b which was previously linearized by the same restriction enzymes.

pET21b_COPG: the cDNA sequence of COPG was amplified using the primers COPG_NdeI.fw and COPG_NotI.rev. Then it was subcloned in pJET1.2/blunt. The amplified insert was cut by the enzymes NdeI/NotI and cloned in the final vector pET21b which was previously linearized by the same restriction enzymes.

4. Maps of plasmids and vectors

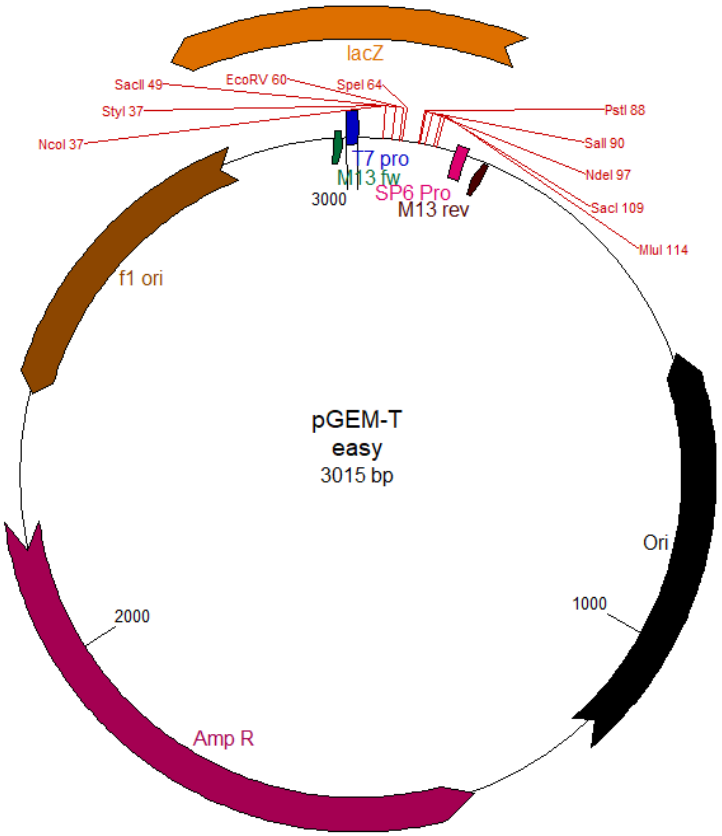

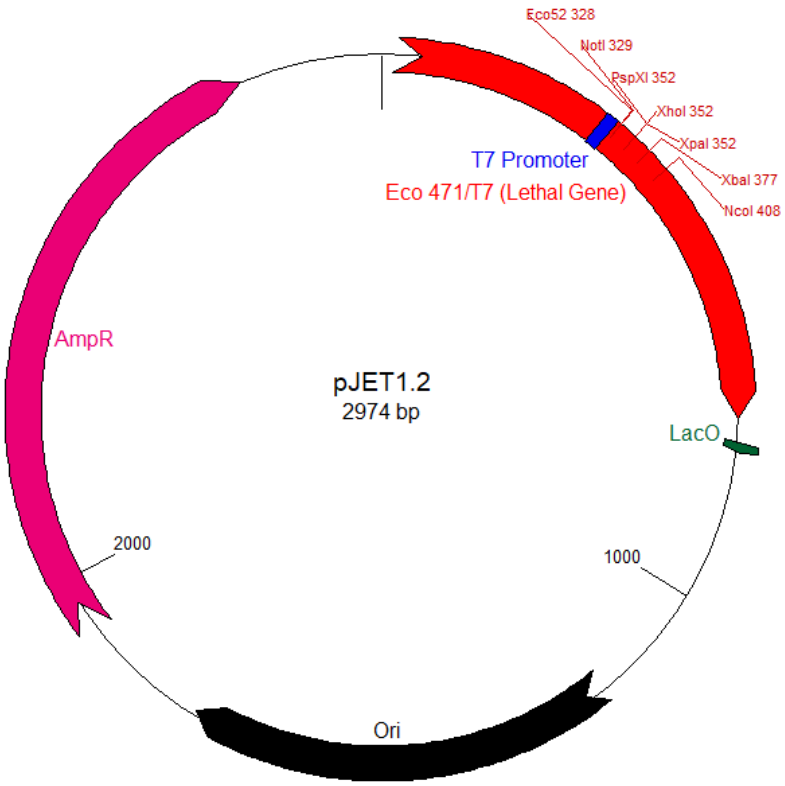

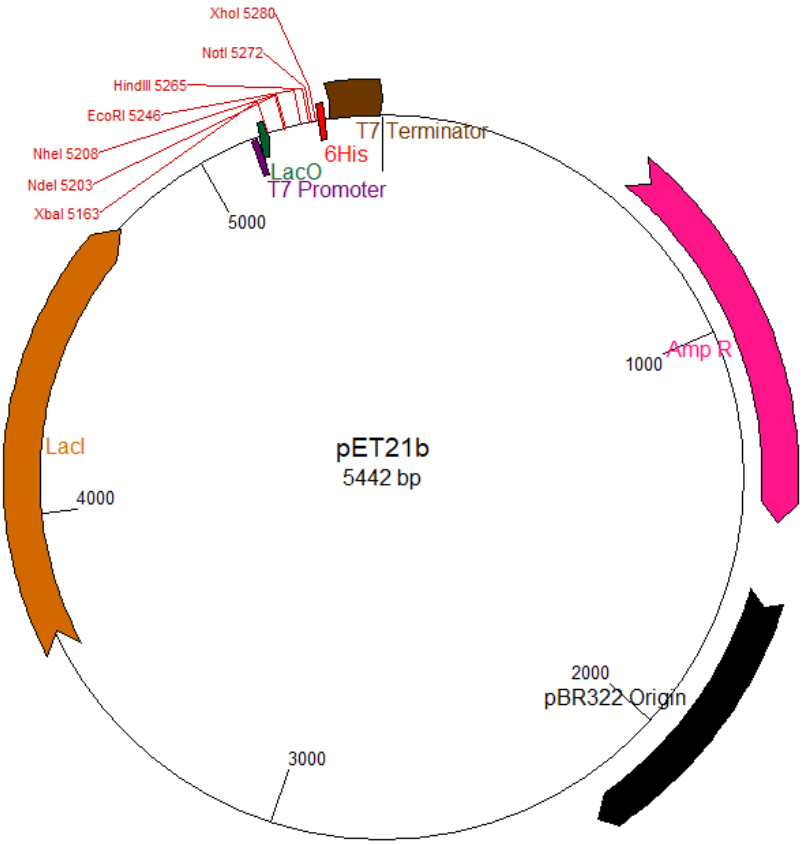
XhoI 5280
NotI 5272
HindIII 5265
EcoRI 5246
NheI 5208
NdeI 5203
XbaI 5163
T7 Terminator
6His
LacO
T7 Promoter
5000
1000
Amp R
LacI
pET21b
5442 bp
4000
2000
pBR322 Origin
3000

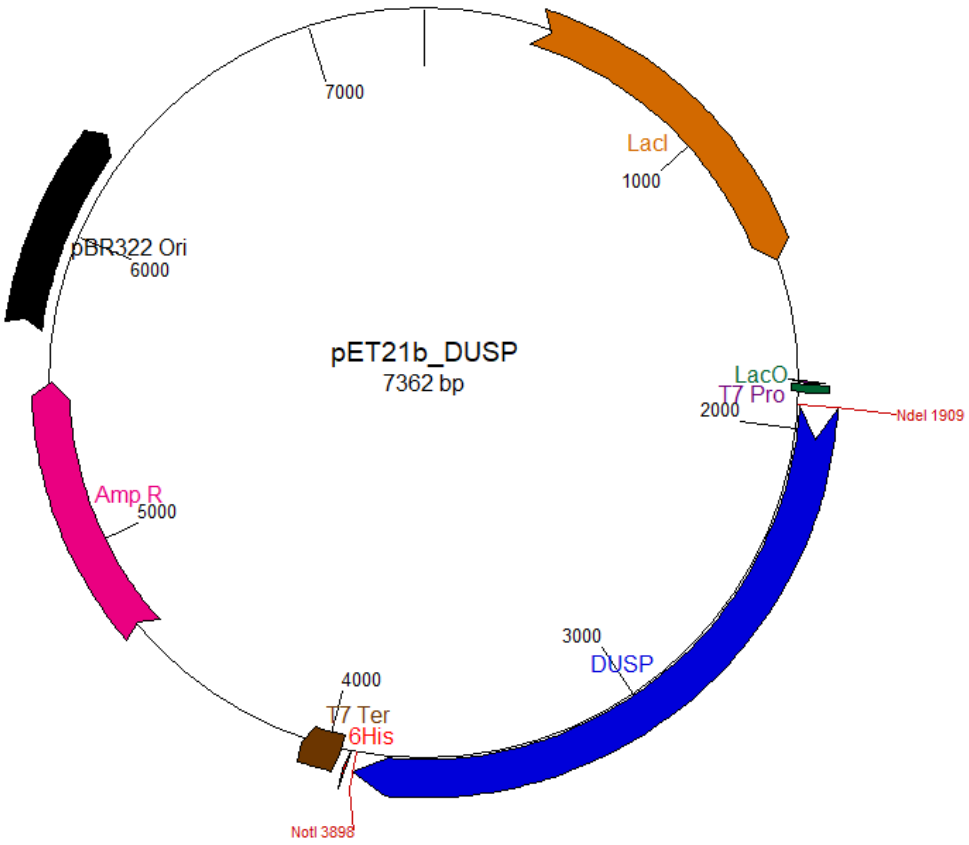
7000
LacI
1000
pBR322 Ori
6000
pET21b_DUSP
7362 bp
LacO
T7 Pro
2000
NdeI 1909
Amp R
5000
3000
DUSP
4000
T7 Ter
6His
NotI 3898

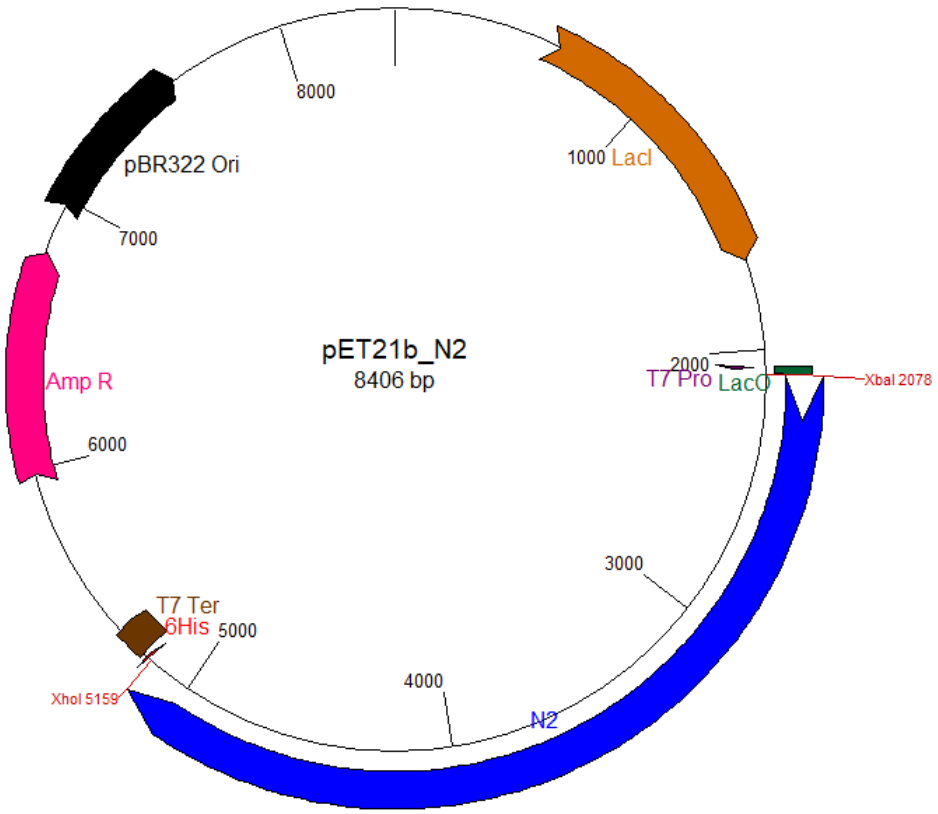
pET21b_N2
8406 bp
8000
1000
LacI
pBR322 Ori
7000
Amp R
6000
2000
T7 Pro
LacO
XbaI 2078
3000
T7 Ter
6His
5000
XhoI 5159
4000
N2

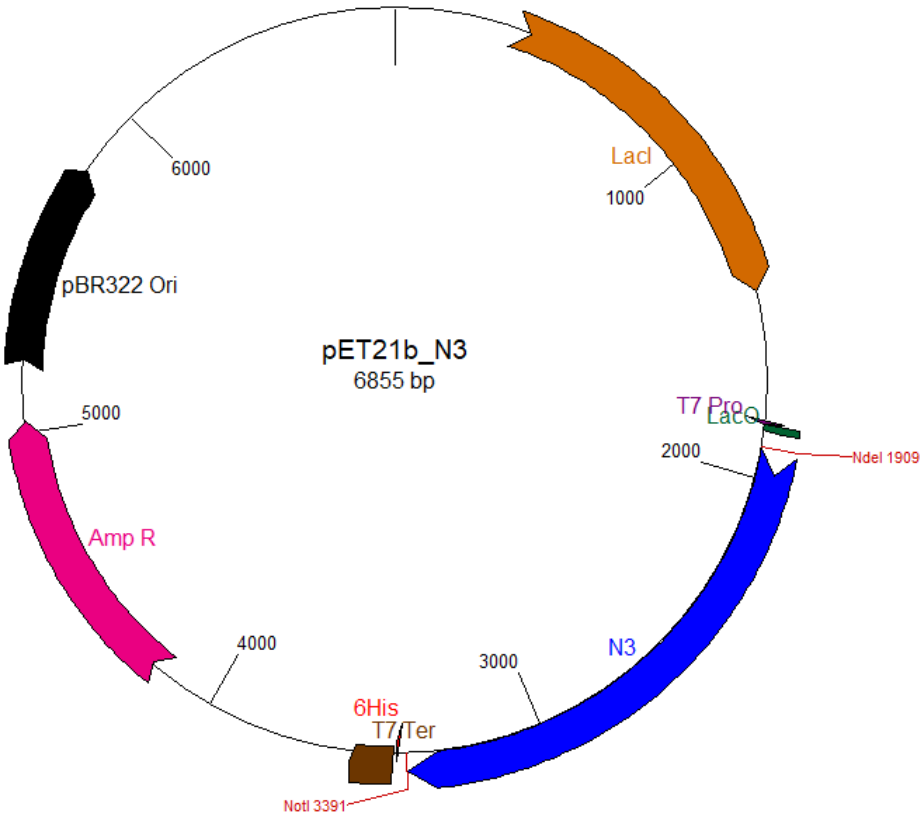
pET21b_N3
6855 bp
6000
LacI
1000
pBR322 Ori
5000
T7 Pro
LacO
2000
NdeI 1909
Amp R
4000
3000
N3
6His
T7 Ter
NotI 3391

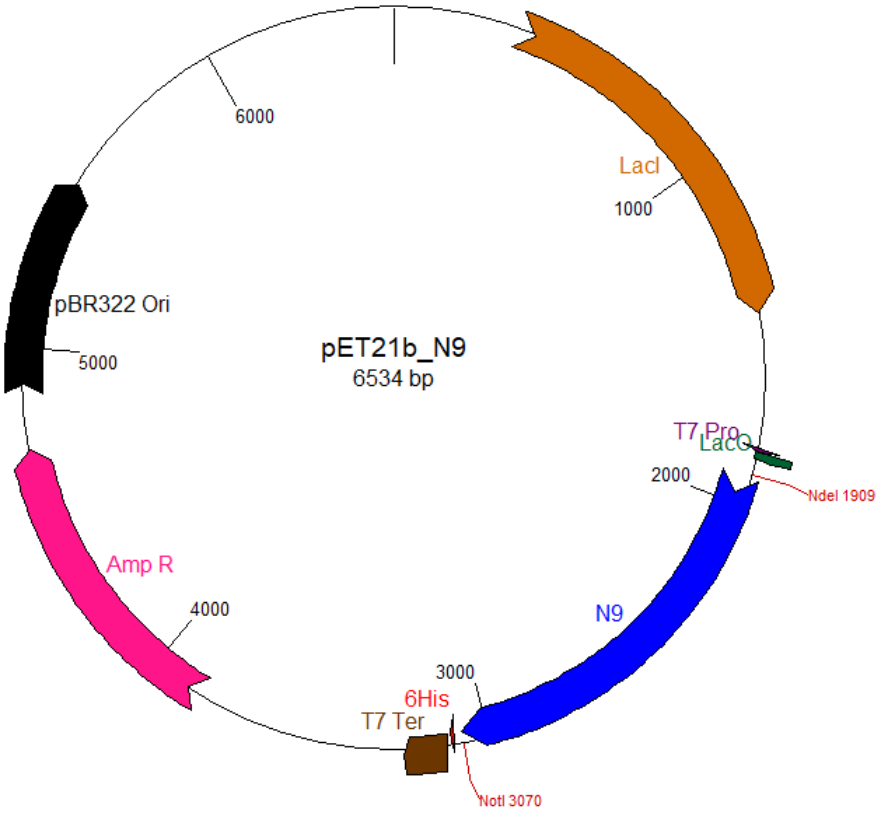
pET21b_N9
6534 bp
6000
LacI
1000
pBR322 Ori
5000
T7 Pro
LacO
2000
NdeI 1909
Amp R
4000
N9
3000
6His
T7 Ter
NotI 3070

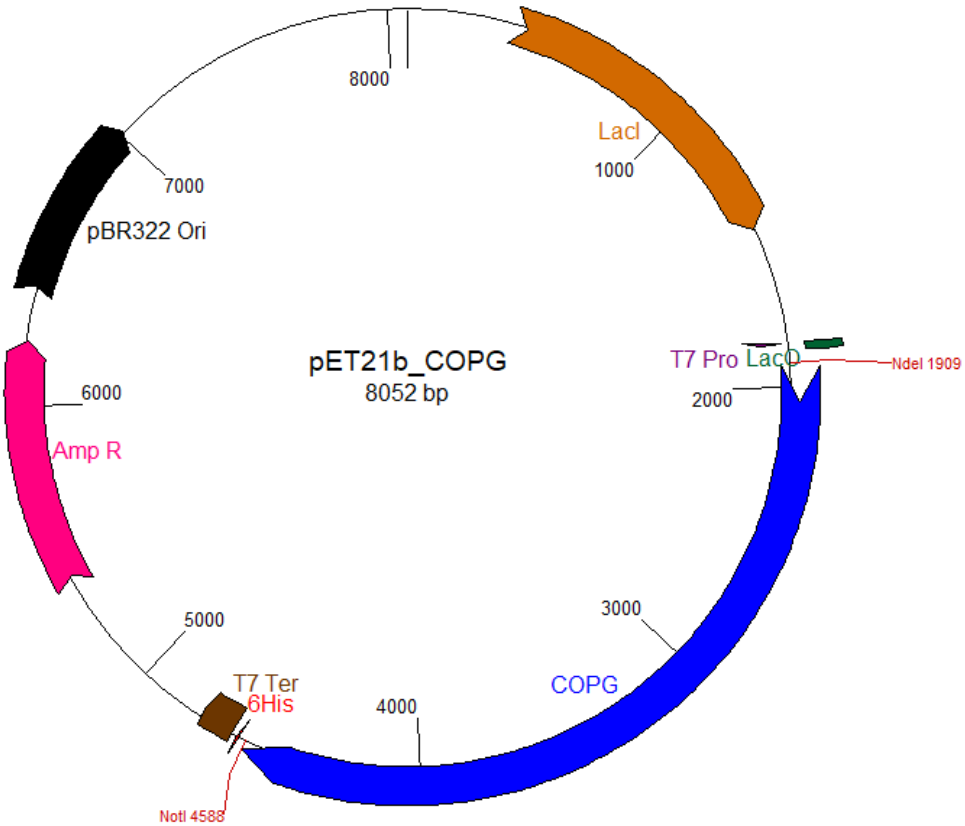
pET21b_COPG
8052 bp
8000
LacI
1000
7000
pBR322 Ori
T7 Pro LacO
NdeI 1909
2000
6000
Amp R
5000
3000
T7 Ter
6His
COPG
4000
NotI 4588

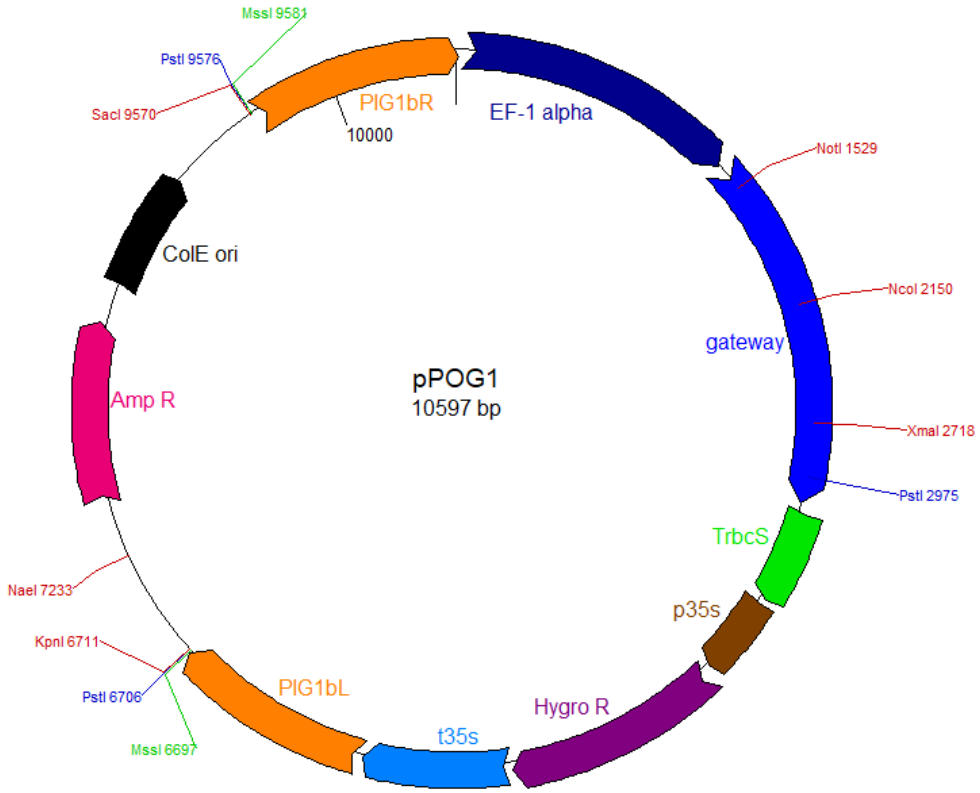
MssI 9581
PstI 9576
SacI 9570
PIG1bR
10000
EF-1 alpha
NotI 1529
ColE ori
NcoI 2150
gateway
pPOG1
10597 bp
Amp R
XmaI 2718
PstI 2975
TrbcS
NaeI 7233
p35s
KpnI 6711
PstI 6706
PIG1bL
Hygro R
MssI 6697
t35s

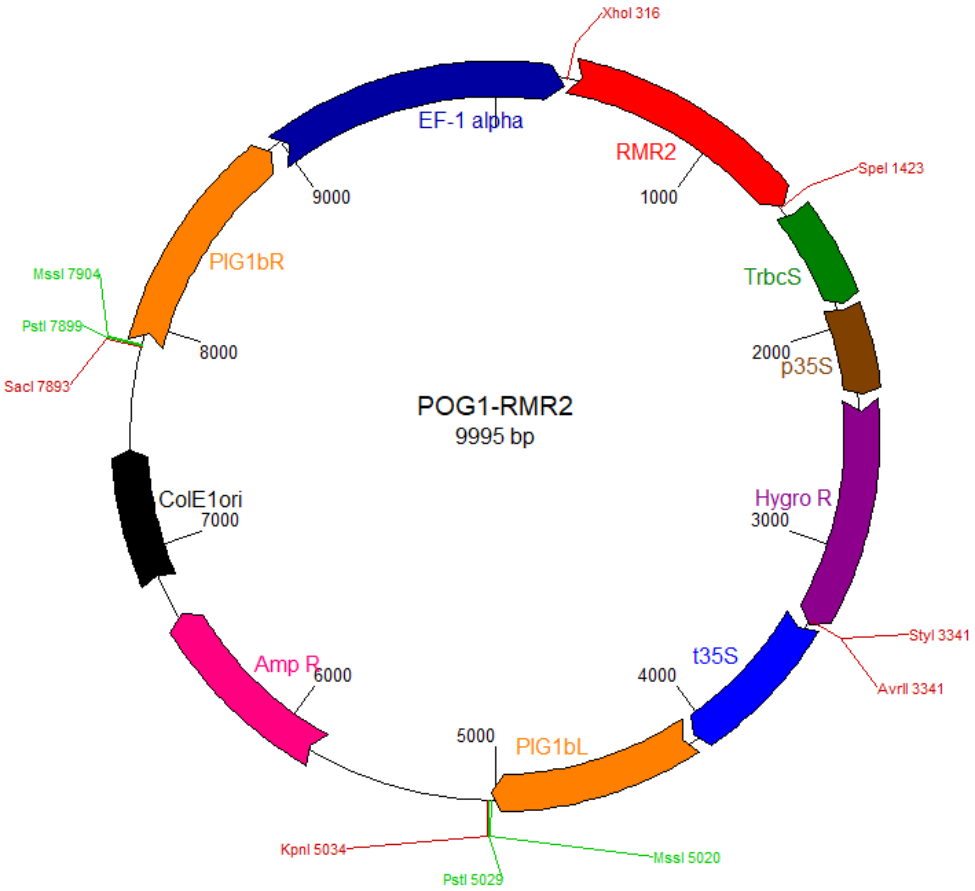
XhoI 316
EF-1 alpha
RMR2
9000
1000
SpeI 1423
PIG1bR
TrbcS
MssI 7904
PstI 7899
8000
2000
p35S
SacI 7893
POG1-RMR2
9995 bp
ColE1ori
7000
Hygro R
3000
StyI 3341
t35S
Amp R
6000
4000
AvrII 3341
5000
PIG1bL
KpnI 5034
MssI 5020
PstI 5029

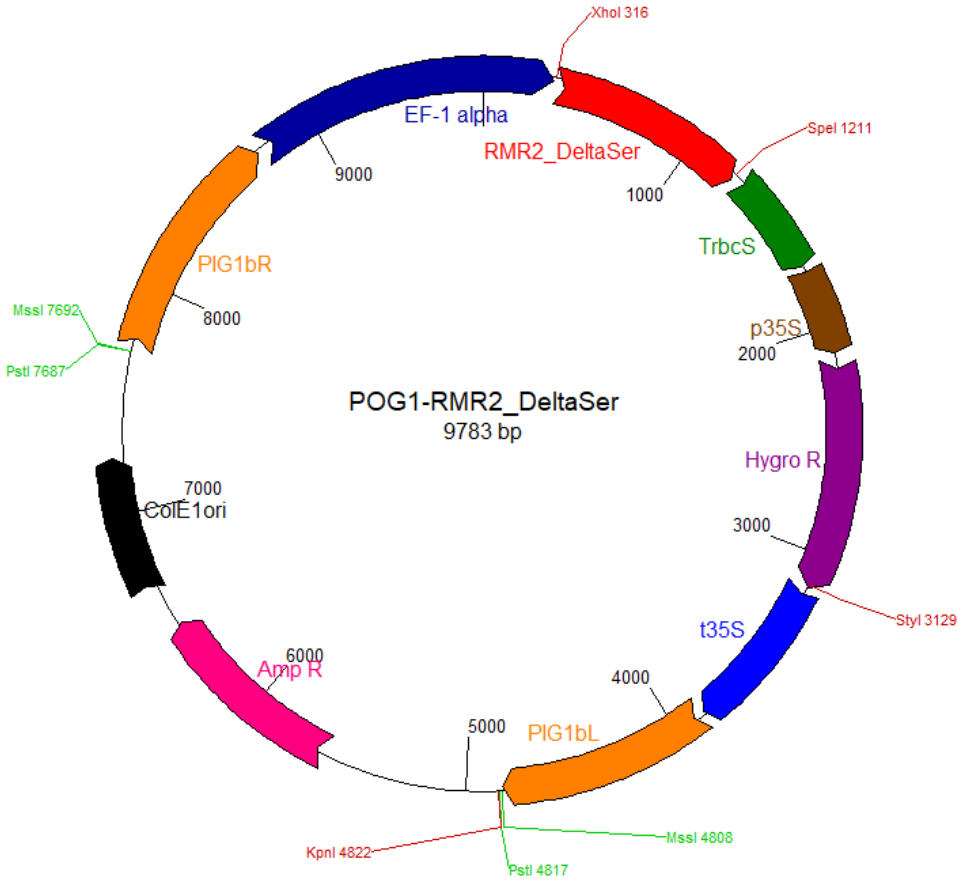
XhoI 316
EF-1 alpha
RMR2_DeltaSer
SpeI 1211
9000
1000
TrbcS
PIG1bR
p35S
MssI 7692
8000
2000
PstI 7687
POG1-RMR2_DeltaSer
9783 bp
Hygro R
7000
ColE1ori
3000
StyI 3129
t35S
6000
Amp R
4000
5000
PIG1bL
KpnI 4822
MssI 4808
PstI 4817

5. Alignments

The full-length amino acid sequences of *Pp*RMR1, *Pp*RMR2, *Pp*RMR3, *Pp*RMR4, *Pp*RMR5, *At*RMR2 and *Os*RMR1 have been aligned using Clustal Omega tool.

```
PpRMR5 MPSVVGESGFLSRITNQKEVMVSLACLSLVILTLLFGHGSAAVLLFNTKNESRSFPDMEA 60
PpRMR3 MPSVSGESGLLDRIGSQREVVVSLGCLSLVLLTLLFGRGSADVLLLNTRNESRSFPDMEA 60
PpRMR4 MPSVAGESGLLERITSQREVMVSLGCLSLVLLTLFFGRGSADVLLLNTRNESRSFPDMEA 60
PpRMR1 MPSVVAEAGFASRIMSYREIMISLAGLCLVLLTLLIGRVNSAVILLAGTNETWSFPDVES 60
PpRMR2 MPSLVVETGLVSRIMNHRELMISLAGLSLVLLTLLLGRVNSAVILLTESNESWSFPDTEA 60
AtRMR2 -------------MNR--------ALVLLLYVCTVSCLASSKVILMRNNITLSFDDIEA 38
OsRMR1 ---------------------------------------------MGTNLTLSFDDVEA 14
                                                      * : ** * *:

PpRMR5 AFTPSIPSGGVAGILHEANPLDACSPLKNLIPKGEP-LPPFVLVSRGSCNFDKKVKNAQD 119
PpRMR3 AFARPIPDEGVSGILHVANPLDACTPLKNDIPKGER-LPPFVVISRGTCNFDKKVRNAQK 119
PpRMR4 AFARPVPDEGVTGILHVANPLDACAPLKNHIPEGEP-LVPFVVISRGTCNFDKKVKNAQV 119
PpRMR1 RFAPRVPTAGVGGVLYASNPLDACSPLLNVSTPGKGSAPAFLLVQRGVCNFEIKVRLAQE 120
PpRMR2 SFSPRIPTTGIVGVLHASNPLDACSPLTNVSRQGQTLFSDFLLVERGVCNFEVKVWNAQE 120
AtRMR2 NFAPSVKGTGEIGVVYVAEPLDACQNLMNKPEQSSNETSPFVLIVRGGCSFEEKVRKAQR 98
OsRMR1 SFAPGVKGSGFEGVVYTAEPLDACSPLTSKAEK--GPPSPFALIIRGGCTFDEKVKNAQD 72
        *:  :   *  *::: ::***** * .           * :: ** *.*: **  **

PpRMR5 AGFQAAIVYNSMDFVGDLV----------------------IMSGSPEGIDIYAVFVSWL 157
PpRMR3 AGFQAAIVYNTIDFIDELV----------------------TMSGSDEDIDIYAVFVSWI 157
PpRMR4 AGFQAAIVYNTMDFTDEMI----------------------TMSGSAEDIDIYAVFVSWN 157
PpRMR1 AGFAAVIVYNDQD-DRELV----------------------TMSGNPVNIHAYAVFVSKY 157
PpRMR2 AGFEAVIIYNNQN-DHELV----------------------TMSGSSNDIHAYSVFVSKV 157
AtRMR2 AGFKAAIIYDNED-RGTLIA---------------------MAGNSGGIRIHAVFVTKE 135
OsRMR1 AGFKAAIVYDNEN-SGVLISIHLALFRLWGHMVLHYLTLKFTVAGSSGGIHIYAVFISKA 131
       *** *.*:*:  :    ::                       ::*.  .*  ::**::

PpRMR5 TGQALLGAVGDNN-TCTLVPYIEDTAWSIMVVSSISLLAISAVLSTFFFVRRHSLRHRGS 216
PpRMR3 TGQALLGAVGENN-TCTLLPAVKDNAWSITVFSSITFLAVSAVLSTFFFVRRDRLRGLGS 216
PpRMR4 TGQALLGAVGDNNVTCTLQAAAEDTAWSIMAVSSISLLAVSAVLSTFFFVRRHRLRHLGS 217
PpRMR1 SGEFLLKYAGDVGATCHIMPAFENTAWSVMAVSFISLLAVSSVLATFFFVRQHRLRHLSA 217
PpRMR2 TGEFLLKYADDKGATCYIMPAFENTAWSVMAVSFISLLAVSSVLVTFFFVRQHRIQHLSA 217
AtRMR2 TGEVLKEYAGFPDTKVWLIPSFENSAWSIMAVSFISLLAMSAVLATCFFVRRHRIRRRTS 195
OsRMR1 SGEVLKKFSGHTDVEVWILPAFENSAWSIMAISFISLLAMSAVLATCFFVRRHHIRRDRP 191
       :*: *    .  .    :    ::.***: ..* *::**:*:** * ****:. ::

PpRMR5 RL-LSREPSGMNARDVHALPTLIFKAVGG--AATGEMCAICLEDYESGEKLRLLPCQHDF 273
PpRMR3 RL-LSRELSRMDARDVDALPTFVFKGAGSDEAGTGETCAICLEDYESGEKLRHLPCHHDF 275
PpRMR4 RF-LSREPSGMNARDVQALPTFIFEDAGGDGAATGETCAICLEDYESGQKLRHLPCDHDF 276
PpRMR1 RY-LLREPAGMSVKEVNALPSLIFKCVE-DGKCTSETCVVCLEDYIPGERLRLLPCQHEF 275
PpRMR2 RF-LPKEPAGMSVKEVNTLPSFVFKHIE-DGKGTSETCAICLEDYVAGEKLRLLPCQHEF 275
AtRMR2 RSSRVREFHGMSRRLVKAMPSLIFSSFH-EDNTTAFTCAICLEDYTVGDKLRLLPCCHKF 254
OsRMR1 RIPEAREFHGMSSQLVKAMPSLIFTKVQ-EDNCTSSMCAICLEDYKVGEKLRVLPCRHKF 250
       *    :*   *. : *.::*:::*         *.  *.:*****  *::** *** *.*
```

```
PpRMR5 HVGCIDQWLLTRRRFCPICKQDASSAPVHPSATETTPLLVAPSH-IFSVPATASA----A 328
PpRMR3 HVGCIDQWLLTRKPFCPICKQDANVTPAYPAATETTPLLVSPV---VSIPVTSSA----A 328
PpRMR4 HVGCIDQWLLTRRPFCPICKQDANAAPRHQAATETTPLLVPPAGRAVPVPSMSSA----A 332
PpRMR1 HLDCIDQWLTLRKPFCPVCKRDAQSQVHEPVATETTPLMAAVG-RALGGGSIRVGTSILS 334
PpRMR2 HLDCIDQWLTTRKPFCPVCKRDAQSKVDKPVATETTPLLAAVG-RALGVGESRVGTPMN- 333
AtRMR2 HAACVDSWLTSWRTFCPVCKRDARTSTGEPPASESTPLLSSAASSFTSSS-LHS-----S 308
OsRMR1 HAACVDLWLTTWRTFCPVCKRDASTGIPDPPASETTPLLSSAVRLPSQSSSFRS-----S 305
       *  *:* **   : ***:**:**        *:*:***:

PpRMR5 TQTSP------VGSPTI---QTIQSSPSDVSGENLC---------------------- 355
PpRMR3 TQTSP------VASPAD---HTPESSYANVSGEDLC---------------------- 355
PpRMR4 TQTSP------VGSPGV---HTTQSLPANVAGEDLC---------------------- 359
PpRMR1 ARSSPLFTTSVINSPNDTPDTRIFSLSYPDGGEDLC---------------------- 370
PpRMR2 --SSPLFAP-TGASPDETTDTRIFSLSSPDGSEDLC---------------------- 366
AtRMR2 VRSSALLIGPSLGSLP-----TSISFSPAYASSSY-IRQSFQ-------SSSNRRSPPIS 355
OsRMR1 VAASP---PRPISRRP-----SSQSISRIYAASVTCLHQSILRYASPHMSHSGYASPSPH 357
         :*                  *     ...

PpRMR5 ------------------------------------------------------------ 355
PpRMR3 ------------------------------------------------------------ 355
PpRMR4 ------------------------------------------------------------ 359
PpRMR1 ------------------------------------------------------------ 370
PpRMR2 ------------------------------------------------------------ 366
AtRMR2 VSRSSVDLRQ---QAASPSPSPSQRSYISHMAS---------P----------------Q 387
OsRMR1 VSSSYVSNSGYGSSSYYLGSSSQHRSYLRRCGESGPSLSTMAPQSPQQSQLRHGGESDIN 417


PpRMR5 ------------------------------------------------------------ 355
PpRMR3 ------------------------------------------------------------ 355
PpRMR4 ------------------------------------------------------------ 359
PpRMR1 ------------------------------------------------------------ 370
PpRMR2 ------------------------------------------------------------ 366
AtRMR2 SLGYPTISPFNTRYMSPYRPSPSNASPAMAGSSNYPLNPLRYSESAGTFSPYASANSLPD 447
OsRMR1 LAGASSGQSFRQSYLRHCADSEVNLAGASSGQSFRQSYLRHCADSDASLSAMASAQSLPG 477


PpRMR5 - 355
PpRMR3 - 355
PpRMR4 - 359
PpRMR1 - 370
PpRMR2 - 366
AtRMR2 C 448
OsRMR1 C 478
```

Bibliography

Adhikary S, Marinoni F, Hock A *et al*. "The ubiquitin ligase HectH9 regulates transcriptional activation by Myc and is essential for tumor cell proliferation" Cell, 123:409-421 (2005)

Ahmed SU, Bar-Peled M and Raikhel NV "Cloning and subcellular location of an *Arabidopsis* receptor-like protein that shares common features with protein-sorting receptors of eukaryotic cells" Plant Physiol, 114:325-336 (1997)

Ahmed SU, Rojo E, Kovaleva V *et al*. "The plant vacuolar sorting receptor *At*ELP is involved in transport of NH_2-terminal propeptide-containing vacuolar proteins in *Arabidopsis thaliana*" J Cell Biol, 149:1335-1344 (2000)

Ahn HK, Kang YW, Lim HM, Hwang I and Pai HS "Physiological functions of the COPI complex in higher plants" Mol Cells, 38:866-875 (2015)

Albert S, Schaffer M, Beck F *et al*. "Proteasomes tether to two distinct sites at the nuclear pore complex" Proc Natl Acad Sci USA, 114:13726-13731 (2017)

Amemiya Y, Azmi P and Seth A: "Autoubiquitination of BCA2 RING E3 ligase regulates its own stability and affects cell migration" Mol Cancer Res, 6:1385-1396 (2008)

An F, Zhao Q, Ji Y *et al*. "Ethylene-induced stabilization of ETHYLENE INSENSITIVE3 and EIN3-LIKE1 is mediated by proteasomal degradation of EIN3 binding F-box 1 and 2 that requires EIN2 in *Arabidopsis*" Plant Cell, 22:2384-2401 (2010)

Anandasabapathy N, Ford GS, Bloom D *et al*. "GRAIL: an E3 Ubiquitin ligase that inhibits cytokine gene transcription is expressed in anergic $CD4^+$ T cells" Immunity, 18:535-547 (2003)

Andrade MA, Petosa C, O'Donoghue SI *et al*. "Comparison of ARM and HEAT protein repeats" J Mol Biol, 309:1-18 (2001)

Antonny B, Beraud-Dufour S, Chardin P and Chabre M "N-terminal hydrophobic residues of the G-protein ADP-ribosylation factor-1 insert into membrane phospholipids upon GDP to GTP exchange" Biochemistry, 36:4675-4684 (1997)

Araújo WL, Tohge T, Ishizaki K *et al*. "Protein degradation - an alternative respiratory substrate for stressed plants" Trends Plant Sci, 16:489-498 (2011)

Aridor M, Weissman J, Bannykh S *et al*. "Cargo selection by the COPII budding machinery during export from the ER" J Cell Biol, 141:61-70 (1998)

Ariizumi, T, Lawrence PK and Steber CM "The role of two F-box proteins, SLEEPY1 and SNEEZY, in *Arabidopsis* gibberellin signaling" Plant Physiol, 155:765-775 (2011)

Asher G, Reuven N and Shaul Y "20S proteasomes and protein degradation by default" Bioessays, 28:844-849 (2006)

Asher G and Shaul Y "p53 proteasomal degradation: poly-ubiquitination is not the whole story" Cell Cycle, 4:1015-1018 (2005)

Asher G, Tsvetkov P, Kahana C and Shaul Y "A mechanism of ubiquitin-independent proteasomal degradation of the tumor suppressors p53 and p73" Genes Dev, 19:316-321 (2005)

Avila EL, Brown M, Pan S *et al*. "Expression analysis of *Arabidopsis* vacuolar sorting receptor 3 reveals a putative function in guard cells" J Exp Bot, 59:1149-1161 (2008)

Ayachi S "Study of moss vacuoles and functional characterization of the putative vacuolar receptors, the RMR proteins" (PhD Thesis, 2012)

Aziz M, Yang WL, Matsuo S *et al*. "Upregulation of GRAIL is associated with impaired CD4 T cell proliferation in sepsis" J Immunol, 192:2305-2314 (2014)

Bachmair A, Finley D and Varshavsky A "In vivo half-life of a protein is a function of its amino-terminal residue" Science, 234:179-186 (1986)

Bachmair A, Novatchkova M, Potuschak T and Eisenhaber F "Ubiquitylation in plants: a post-genomic look at a post-translational modification" Trends Plant Sci, 6:463-470 (2001)

Bae H and Kim WT "Classification and interaction modes of 40 rice E2 ubiquitin-conjugating enzymes with 17 rice ARM-U-box E3 ubiquitin ligases" Biochem Biophys Res Commun, 444:575-580 (2014)

Bailly E and Reed SI "Functional characterization of rpn3 uncovers a distinct 19S proteasomal subunit requirement for ubiquitin-dependent proteolysis of cell cycle regulatory proteins in budding yeast" Mol Cell Biol, 19:6872-6890 (1999)

Baker SJ and Reddy EP "Cloning of murine G1RP, a novel gene related to *Drosophila melanogaster* g1" Gene, 248:33-40 (2000)

Ballar P, Ors AU, Yang H and Fang S "Differential regulation of CFTRDeltaF508 degradation by ubiquitin ligases gp78 and Hrd1" Int J Biochem Cell Biol, 42:167-173 (2010)

Bandmann V and Homann U "Clathrin-independent endocytosis contributes to uptake of glucose into BY-2 protoplasts" Plant J, 70:578-584 (2012)

Barberon M, Dubeaux G, Kolb C, Isono E *et al*. "Polarization of IRON-REGULATED TRANSPORTER 1 (IRT1) to the plant-soil interface plays crucial role in metal homeostasis" Proc Natl Acad Sci USA, 111:8293-8298 (2014)

Barberon M, Zelazny E *et al*. "Monoubiquitin-dependent endocytosis of the iron regulated transporter 1 (IRT1) transporter controls iron uptake in plants" Proc Natl Acad Sci USA, 108:E450-E458 (2011)

Barlowe C, Orci L, Yeung T *et al*. "COPII: a membrane coat formed by Sec proteins that drive vesicle budding from the endoplasmic reticulum" Cell, 77:895-907 (1994)

Bassham DC, Brandizzi F, Otegui MS and Sanderfoot AA "The secretory system of *Arabidopsis*" The *Arabidopsis* Book, 6:e0116 (2008)

Beck R, Ravet M, Wieland FT and Cassel D "The COPI system: Molecular mechanisms and function" FEBS Lett, 583:2701-2709 (2009)

Bednarek SY and Raikhel NV "The barley lectin carboxyl-terminal propeptide is a vacuolar protein sorting determinant in plants" Plant Cell, 3:1195-1206 (1991)

Bednarek SY, Wilkins TA, Dombrowski JE and Raikhe NV "A carboxyl-terminal propeptide is necessary for proper sorting of barley lectin to vacuoles of tobacco" Plant Cell, 2:1145-1155 (1990)

Belzil C, Neumayer G, Vassilev AP *et al*. "A Ca^{2+}-dependent mechanism of neuronal survival mediated by the microtubule-associated protein p600" J Biol Chem, 288:24452-24464 (2013)

Besche HC, Sha Z, Kukushkin NV *et al*. "Autoubiquitination of the 26S proteasome on Rpn13 regulates breakdown of ubiquitin conjugates" EMBO J, 33:1159-1176 (2014)

Bielli A, Haney CJ, Gabreski G *et al*. "Regulation of Sar1 NH_2 terminus by GTP binding and hydrolysis promotes membrane deformation to control COPII vesicle fission" J Cell Biol, 171:919-924 (2005)

Bitterlich M, Krügel U, Boldt-Burisch K *et al*. "Interaction of brassinosteroid functions and sucrose transporter SlSUT2 regulate the formation of arbuscular mycorrhiza" Plant Signal Behav, 9(10):e970426 (2014)

Bocock JP, Carmicle S, Chhotani S *et al*. "The PA-TM-RING protein RING finger protein 13 is an endosomal integral membrane E3 ubiquitin ligase whose RING finger domain is released to the cytoplasm by proteolysis" FEBS J, 276:1860-1877 (2009)

Bocock JP, Carmicle S, Sircar M and Erickson AH "Trafficking and proteolytic processing of RNF13, a model PA-TM-RING family endosomal membrane ubiquitin ligase" FEBS J, 278:69-77 (2010)

Bolte S, Talbot C, Boutte Y *et al*. "FM-dyes as experimental probes for dissecting vesicle trafficking in living plant cells" J Microsc, 214:159-173 (2004)

Borchers AG, Hufton AL, Eldridge AG *et al*. "The E3 ubiquitin ligase GREUL1 anteriorizes ectoderm during *Xenopus* development" Dev Biol, 251:395-408 (2002)

Borden KL and Freemont PS "The RING finger domain: a recent example of a sequence-structure family" Curr Opin Struct Biol, 6:395-401 (1996)

Bouchard ML and Côté S "The *Drosophila melanogaster* developmental gene g1 encodes a variant zinc-finger-motif protein" Gene, 125:205-209 (1993)

Bradford MM "A rapid and sensitive method for the quantitation of microgram quantities of protein utilizing the principle of protein-dye binding" Anal Biochem, 72:248-254 (1976)

Bremser M, Nickel W, Schweikert M *et al*. "Coupling of coat assembly and vesicle budding to packaging of putative cargo receptors" Cell, 96:495-506 (1999)

Breyton C, Tribet C, Olive J *et al*. "Dimer to monomer conversion of the cytochrome b_6f complex. Causes and consequences" J Biol Chem, 272:21892-21900 (1997)

Brown CK, Gu ZY, Matsuka YV, Purushothaman SS *et al*. "Structure of the streptococcal cell wall C5a peptidase" Proc Natl Acad Sci USA, 102:18391-18396 (2005)

Brown JC, Jolliffe NA, Frigerio L and Roberts LM "Sequence-specific, Golgi-dependent vacuolar targeting of castor bean 2S albumin" Plant J, 36:711-719 (2003)

Brukhin V, Gheyselinck J, Gagliardini V *et al*. "The RPN1 subunit of the 26S proteasome in *Arabidopsis* is essential for embryogenesis" Plant Cell, 17:2723-2737 (2005)

Bryksa BC, Bhaumik P, Magracheva E *et al*. "Structure and mechanism of the saposin-like domain of a plant aspartic protease" J Biol Chem, 286:28265-28275 (2011)

Brzovic PS, Rajagopal P, Hoyt DW *et al*. "Structure of a BRCA1-BARD1 heterodimeric RING-RING complex" Nat Struct Biol, 8:833-837 (2001)

Bueso E, Rodriguez L, Lorenzo-Orts L *et al*. "The single-subunit RING-type E3 ubiquitin ligase RSL1 targets PYL4 and PYR1 ABA receptors in plasma membrane to modulate abscisic acid signaling" Plant J, 80:1057-1071 (2014)

Cao X, Rogers SW, Butler J, Beevers L and Rogers JC "Structural requirements for ligand binding by a probable plant vacuolar sorting receptor" Plant Cell, 12:493-506 (2000)

Cardona-López X, Cuyas L, Marín E *et al*. "ESCRT-III-associated protein ALIX mediates high-affinity phosphate transporter trafficking to maintain phosphate homeostasis in *Arabidopsis*" Plant Cell, 27:2560-2581 (2015)

Carvalho P, Goder V and Rapoport TA "Distinct ubiquitin-ligase complexes define convergent pathways for the degradation of ER proteins" Cell, 126:361-373 (2006)

Castelli S and Vitale A "The phaseolin vacuolar sorting signal promotes transient, strong membrane association and aggregation of the bean storage protein in transgenic tobacco" J Exp Bot, 56:1379-1387 (2005)

Chartron JW, Hunt KCL and Frydman J "Cotranslational signal-independent SRP preloading during membrane targeting" Nature, 536:224-228 (2016)

Chen HF, Chuang HC and Tan TH "Regulation of Dual-Specificity Phosphatase (DUSP) ubiquitination and protein stability" Int J Mol Sci, 20:2668 (2019)

Chen X, Irani NG and Friml J "Clathrin-mediated endocytosis: the gateway into plant cells" Curr Opin Plant Biol, 14:674-682 (2011)

Cheng MC, Hsieh EJ *et al*. "*Arabidopsis* RGLG2, functioning as a RING E3 ligase, interacts with *At*ERF53 and negatively regulates the plant drought stress response" Plant Physiol, 158: 363-375 (2012)

Cho SK, Ryu MY, Kim JH *et al*. "RING E3 ligases: key regulatory elements are involved in abiotic stress responses in plants" BMB Rep, 50:393-400 (2017)

Choo YS and Zhang Z "Detection of protein ubiquitination" J Vis Exp, 30:1293 (2009)

Choo YY and Hagen T "Mechanism of cullin3 E3 ubiquitin ligase dimerization" PLoS One, 7(7):e41350 (2012)

Christensen DE, Brzovic PS and Klevit RE "E2-BRCA1 RING interactions dictate synthesis of mono- or specific polyubiquitin chain linkages" Nat Struct Mol Biol, 14:941-948 (2007)

Contento AL and Bassham DC "Structure and function of endosomes in plant cells" J Cell Sci, 125:3511-3518 (2012)

Contreras I, Yang Y, Robinson DG and Aniento F "Sorting signals in the cytosolic tail of plant p24 proteins involved in the interaction with the COPII coat" Plant Cell Physiol, 45:1779-1786 (2004)

Ćosić M, Vujičić MM, Sabovljević MS and Sabovljević AD "Effects of salt on selected bryophyte species tested under controlled conditions" Botanica Serbica, 44:27-35 (2020)

Cosson P and Letourneur F "Coatomer interaction with di-lysine endoplasmic reticulum retention motifs" Science, 263:1629-1631 (1994)

d'Azzo, Bongiovanni A and Nastasi T "E3 Ubiquitin ligases as regulators of membrane protein trafficking and degradation" Traffic, 6:429-441 (2005)

Dale EC and Ow DW "Gene transfer with subsequent removal of the selection gene from the host genome" Proc Natl Acad Sci USA, 88:10558-10562 (1991)

daSilva LL, Foresti O and Denecke J "Targeting of the plant vacuolar sorting receptor BP80 is dependent on multiple sorting signals in the cytosolic tail" Plant Cell, 18:1477-1497 (2006)

daSilva LL, Snapp EL, Denecke J *et al*. "Endoplasmic reticulum export sites and Golgi bodies behave as single mobile secretory units in plant cells" Plant Cell, 16:1753-1771 (2004)

Davis MI, Bennett MJ, Thomas LM and Bjorkman PJ "Crystal structure of prostate-specific membrane antigen, a tumor marker and peptidase" Proc Natl Acad Sci USA, 102:5981-5986 (2005)

Dawaliby R, Trubbia C, Delporte C *et al*. "Allosteric regulation of G protein-coupled receptor activity by phospholipids" Nat Chem Biol, 12:35-39 (2016)

De Hoff PL, Brill LM and Hirsch AM "Plant lectins: the ties that bind in root symbiosis and plant defense" Mol Genet Genomics, 282:1-15 (2009)

De Marchis F, Bellucci M and Pompa A "Unconventional pathways of secretory plant proteins from the endoplasmic reticulum to the vacuole bypassing the Golgi complex" Plant Signal Behav, 8(8):e25129 (2013)

De Marcos Lousa C, Gershlick DC and Denecke J "Mechanisms and concepts paving the way towards a complete transport cycle of plant vacuolar sorting receptors" Plant Cell, 24:1714-1732 (2012)

DeMarini DJ, Papa FR, Swaminathan S *et al*. "The yeast SEN3 gene encodes a regulatory subunit of the 26 S proteasome complex required for ubiquitin-dependent protein degradation in vivo" Mol Cell Biol, 15:6311-6321 (1995)

Debnath DK, Basaiawmoit RV, Nielsen KL and Otzen DE "The role of membrane properties in Mistic folding and dimerisation" Protein Eng Des Sel, 24:89-97 (2011)

del Pozo JC, Dharmasiri S, Hellmann H *et al*. "AXR1-ECR1-dependent conjugation of RUB1 to the *Arabidopsis* Cullin *At*CUL1 is required for auxin response" Plant Cell, 14:421-433 (2002)

Denison C, Kirkpatrick DS and Gygi SP "Proteomic insights into ubiquitin and ubiquitin-like proteins" Curr Opin Chem Biol, 9:69-75 (2005)

Deshaies RJ and Joazeiro CA "RING domain E3 ubiquitin ligases" Annu Rev Biochem, 78:399-434 (2009)

Deshar R, Moon S, Yoo W *et al*. "RNF167 targets Arl8B for degradation to regulate lysosome positioning and endocytic trafficking" FEBS J, 283:4583-4599 (2016)

Dettmer J, Hong-Hermesdorf A, Stierhof YD and Schumacher K "Vacuolar H^+-ATPase activity is required for endocytic and secretory trafficking in *Arabidopsis*" Plant Cell, 18:715-730 (2006)

Dhillon AS, Hagan S, Rath O and Kolch W "MAP kinase signalling pathways in cancer" Oncogene, 26:3279-3290 (2007)

Di Sansebastiano GP, Paris N *et al*. "Specific accumulation of GFP in a non-acidic vacuolar compartment via a C-terminal propeptide-mediated sorting pathway" Plant J, 15:449-457 (1998)

Di Sansebastiano GP, Paris N, Marc-Martin S and Neuhaus JM "Regeneration of a lytic central vacuole and of neutral peripheral vacuoles can be visualized by green fluorescent proteins targeted to either type of vacuoles" Plant Physiol, 126:78-86 (2001)

Donaldson JG, Cassel D, Kahn RA and Klausner RD "ADP-ribosylation factor, a small GTP-binding protein, is required for binding of the coatomer protein beta-COP to Golgi membranes" Proc Natl Acad Sci USA, 89:6408-6412 (1992)

Dörr JM, Koorengevel MC, Schäfer M *et al*. "Detergent-free isolation, characterization, and functional reconstitution of a tetrameric K^+ channel: the power of native nanodiscs" Proc Natl Acad Sci USA, 111:18607-18612 (2014)

Dosztányi Z, Csizmók V *et al*. "The pairwise energy content estimated from amino acid composition discriminates between folded and intrinsically unstructured proteins" J Mol Biol, 347:827-839 (2005)

Dove KK and Klevit RE "RING-Between-RING E3 Ligases: Emerging themes amid the variations" J Mol Biol, 429:3363-3375 (2017)

Downes BP, Stupar RM, Gingerich DJ and Vierstra RD "The HECT ubiquitin-protein ligase (UPL) family in *Arabidopsis*: UPL3 has a specific role in trichome development" Plant J, 35:729-742 (2003)

Driouich A, Follet-Gueye ML, Bernard S *et al*. "Golgi-mediated synthesis and secretion of matrix polysaccharides of the primary cell wall of higher plants" Front Plant Sci, 3:79 (2012)

Duda DM, Scott DC, Calabrese MF *et al*. "Structural regulation of cullin-RING ubiquitin ligase complexes" Curr Opin Struct Biol, 21:257-264 (2011)

Duden R, Griffiths G, Frank R *et al*. "Beta-COP, a 110 kd protein associated with non-clathrin-coated vesicles and the Golgi complex, shows homology to beta-adaptin" Cell, 64:649-665 (1991)

Duplan V and Rivas S "E3 ubiquitin-ligases and their target proteins during the regulation of plant innate immunity" Front Plant Sci, 5:42 (2014)

Dyachok J, Zhu L, Liao F *et al*. "SCAR mediates light-induced root elongation in *Arabidopsis* through photoreceptors and proteasomes" Plant Cell, 23:3610-3626 (2011)

Effantin G, Rosenzweig R, Glickman MH and Steven AC "Electron microscopic evidence in support of solenoid models of proteasomal subunits Rpn1 and Rpn2" J Mol Biol, 386:1204-1211 (2009)

Eiyama A and Okamoto K "PINK1/Parkin-mediated mitophagy in mammalian cells" Curr Opin Cell Biol, 33:95-101 (2015)

Ellgaard L, McCaul N, Chatsisvili A and Braakman I "Co- and post-translational protein folding in the ER" Traffic, 17:615-638 (2016)

Emr S, Glick BS, Linstedt AD *et al*. "Journeys through the Golgi--taking stock in a new era" J Cell Biol, 187:449-453 (2009)

Epimashko S, Meckel T, Fischer-Schliebs E *et al*. "Two functionally different vacuoles for static and dynamic purposes in one plant mesophyll leaf cell" Plant J, 37:294-300 (2004)

Esmann M "Solubilized ($Na^+ + K^+$)-ATPase from shark rectal gland and ox kidney -- an inactivation study" Biochim Biophys Acta, 857:38-47 (1986)

Eugster A, Frigerio G, Dale M and Duden R "COP I domains required for coatomer integrity, and novel interactions with ARF and ARF-GAP" Embo J, 19:3905-3917 (2000)

Eugster A, Frigerio G, Dale M and Duden R "The alpha- and beta'-COP WD40 domains mediate cargo-selective interactions with distinct di-lysine motifs" Mol Biol Cell, 15:1011-1023 (2004)

Fahr N "The functions of RMR proteins in the *Physcomitrella patens* secretory pathway" (PhD thesis, 2017)

Fan L, Li R, Pan J *et al*. "Endocytosis and its regulation in plants" Trends Plant Sci, 20:388-397 (2015)

Fang S, Ferrone M, Yang C *et al*. "The tumor autocrine motility factor receptor, GP78, is a ubiquitin protein ligase implicated in degradation from the endoplasmic reticulum" Proc Natl Acad Sci USA, 98:14422-14427 (2001)

Fang S and Weissman AM "A field guide to ubiquitylation" Cell Mol Life Sci, 61:1546-1561 (2004)

Fath S, Mancias JD, Bi X and Goldberg J "Structure and organization of coat proteins in the COPII cage" Cell, 129:1325-1336 (2007)

Fatimababy AS, Lin YL, Usharani R *et al*. "Cross-species divergence of the major recognition pathways of ubiquitylated substrates for ubiquitin/26S proteasome-mediated proteolysis" FEBS J, 277:796-816 (2010)

Faulstich D, Auerbach S, Orci L *et al*. "Architecture of coatomer: molecular characterization of delta-COP and protein interactions within the complex" J Cell Biol, 135:53-61 (1996)

Fiedler K, Veit M, Stamnes MA and Rothman JE "Bimodal interaction of coatomer with the p24 family of putative cargo receptors" Science, 273:1396-1399 (1996)

Flückiger R, De Caroli M, Piro G, Dalessandro G *et al*. "Vacuolar system distribution in *Arabidopsis* tissues, visualized using GFP fusion proteins" J Exp Bot, 54:1577-1584 (2003)

Foresti O and Denecke J "Intermediate organelles of the plant secretory pathway: identity and function" Traffic, 9:1599-1612 (2008)

Foresti O, Gershlick DC, Bottanelli F *et al*. "A recycling-defective vacuolar sorting receptor reveals an intermediate compartment situated between prevacuoles and vacuoles in tobacco" Plant Cell, 22:3992-4008 (2010)

Frank W, Ratnadewi D and Reski R "*Physcomitrella patens* is highly tolerant against drought, salt and osmotic stress" Planta, 220:384-394 (2005)

Frankel EB and Audhya A "ESCRT-dependent cargo sorting at multivesicular endosomes" Semin Cell Dev Biol, 74:4-10 (2018)

Frigerio L, De Virgilio M, Prada A *et al*. "Sorting of phaseolin to the vacuole is saturable and requires a short C-terminal peptide" Plant Cell, 10:1031-1042 (1998)

Frigerio L, Foresti O, Hernández Felipe D *et al*. "The C-terminal tetrapeptide of phaseolin is sufficient to target green fluorescent protein to the vacuole" J Plant Physiol, 158:499-503 (2001)

Frigerio L, Hinz G and Robinson DG "Multiple vacuoles in plant cells: rule or exception?" Traffic, 9:1564-1570 (2008)

Geldner N, Hyman DL, Wang X *et al*. "Endosomal signaling of plant steroid receptor kinase BRI1" Genes Dev, 21:1598-1602 (2007)

Ghilarducci K "Caractérisation fonctionnelle de l'interaction entre l'ubiquitine E3 ligase RNF167 et des enzymes conjugatrices de l'ubiquitine" Univeristé du Québec à Montréal; pp. 101 (2019)

Glickman MH, Rubin DM, Fried VA and Finley D "The regulatory particle of the *Saccharomyces cerevisiae* proteasome" Mol Cell Biol, 18:3149-3162 (1998)

Gommel DU, Memon A, Heiss A *et al*. "Recruitment to Golgi membranes of ADP-ribosylation factor 1 is mediated by the cytoplasmic domain of p23" EMBO J, 20:6751-6760 (2001)

Gorbea C, Taillandier D and Rechsteiner M "Mapping subunit contacts in the regulatory complex of the 26 S proteasome S2 and S5b form a tetramer with ATPase subunits S4 and S7" Biol Chem, 275:875-882 (2000)

Griffiths G and Simons K "The *trans* Golgi network: sorting at the exit site of the Golgi complex" Science, 234:438-443 (1986)

Gu Y, Zavaliev R and Dong X: "Membrane trafficking in plant immunity" Mol Plant, 10:1026-1034 (2017)

Guais A, Siegrist S, Solhonne B *et al*. "h-Goliath, paralog of GRAIL, is a new E3 ligase protein, expressed in human leukocytes" Gene, 374:112-120 (2006)

Gulati S, Jamshad M, Knowles TJ *et al*. "Detergent-free purification of ABC (ATP-binding-cassette) transporters" Biochem J, 461:269-278 (2014)

Gupta R, Huang Y, Kieber J and Luan S "Identification of a dual-specificity protein phosphatase that inactivates a MAP kinase from *Arabidopsis*" Plant J, 16:581-589 (1998)

Hamid R, Khan MA, Ahmad M *et al*. "Chitinases: An update" J Pharm Bioallied Sci, 5:21-29 (2013)

Han L, Mason M, Risseeuw EP *et al*. "Formation of an SCF(ZTL) complex is required for proper regulation of circadian timing" Plant J, 40:291-301 (2004)

Haney CH and Long SR "Plant flotillins are required for infection by nitrogen-fixing bacteria" Proc Natl Acad Sci USA, 107:478-483 (2010)

Hanna J and Finley D "A proteasome for all occasions" FEBS Lett, 581:2854-2861 (2007)

Hanton SL, Bortolotti LE, Renna L *et al*. "Crossing the divide--transport between the endoplasmic reticulum and Golgi apparatus in plants" Traffic, 6:267-277 (2005)

Hanton SL, Matheson LA and Brandizzi F "Seeking a way out: export of proteins from the plant endoplasmic reticulum" Trends Plant Sci, 11:335-343 (2006)

Hara-Kuge S, Kuge O, Orci L *et al*. "En bloc incorporation of coatomer subunits during the assembly of COP-coated vesicles" J Cell Biol, 124:883-892 (1994)

Hara-Nishimura I, Shimada T, Hatano K *et al*. "Transport of storage proteins to protein storage vacuoles is mediated by large precursor-accumulating vesicles" Plant Cell, 10:825-836 (1998)

Harmon F, Imaizumi T and Gray WM "CUL1 regulates TOC1 protein stability in the *Arabidopsis* circadian clock" Plant J, 55:568-579 (2008)

Harrison-Lavoie KJ, Lewis VA, Hynes GM *et al*. "A 102 kDa subunit of a Golgi-associated particle has homology to beta subunits of trimeric G proteins" EMBO J, 12:2847-2853 (1993)

Harter C and Wieland FT "A single binding site for dilysine retrieval motifs and p23 within the γ subunit of coatomer" Proc Natl Acad Sci USA, 95:11649-11654 (1998)

Hatakeyama S and Kei-ichi IN "U-box proteins as a new family of ubiquitin ligases" Biochemical and biophysical research communications, 302:635-645 (2003)

Hazard A and Montemagno C "Improved purification for thermophilic F1F0 ATP synthase using n-dodecyl beta-D-maltoside" Arch Biochem Biophys, 407:117-124 (2002)

He J, Kulkarni K, da Fonseca PC *et al*. "The structure of the 26S proteasome subunit Rpn2 reveals its PC repeat domain as a closed toroid of two concentric α-helical rings" Structure, 20:513-521 (2012)

Hepler PK, Vidali L and Cheung AY "Polarized cell growth in higher plants" Annu Rev Cell Dev Biol, 17:159-187 (2001)

Herberth S, Shahriari M, Bruderek M *et al*. "Artificial ubiquitylation is sufficient for sorting of a plasma membrane ATPase to the vacuolar lumen of *Arabidopsis* cells" Planta, 236:63-77 (2012)

Herman EM "Endoplasmic reticulum bodies: solving the insoluble" Curr Opin Plant Biol, 11:672-679 (2008)

Hicke L, Yoshihisa T and Schekman R "Sec23p and a novel 105-kDa protein function as a multimeric complex to promote vesicle budding and protein transport from the endoplasmic reticulum" Mol Biol Cell, 3:667-676 (1992)

Hicks GR, Rojo E *et al*. "Germinating pollen has tubular vacuoles, displays highly dynamic vacuole biogenesis, and requires VACUOLESS1 for proper function" Plant Physiol, 134:1227-1239 (2004)

Hiller MM, Finger A, Schweiger M and Wolf DH "ER degradation of a misfolded luminal protein by the cytosolic ubiquitin-proteasome pathway" Science, 273:1725-1728 (1996)

Hinshaw JE "Dynamin and its role in membrane fission" Annu Rev Cell Dev Biol, 16:483-519 (2000)

Hinz G, Colanesi S, Hillmer S *et al*. "Localization of vacuolar transport receptors and cargo proteins in the Golgi apparatus of developing *Arabidopsis* embryos" Traffic, 8:1452-1464 (2007)

Hirst J, Barlow LD *et al*. "The fifth adaptor protein complex" PLoS Biol, 9(10):e1001170 (2011)

Hoffmann B, Proust E, Belcram K *et al*. "Strigolactones inhibit caulonema elongation and cell division in the moss *Physcomitrella patens*" PLoS One, 9(6):e99206 (2014)

Hofmann K "Ubiquitin-binding domains and their role in the DNA damage response" DNA Repair (Amst), 8:544-556 (2009)

Hohe A, Egener T, Lucht JM *et al*. "An improved and highly standardised transformation procedure allows efficient production of single and multiple targeted gene-knockouts in a moss, *Physcomitrella patens*" Curr Genet, 44:339-347 (2004)

Holwerda BC, Padgett HS and Rogers JC "Proaleurain vacuolar targeting is mediated by short contiguous peptide interactions" Plant Cell, 4:307-318 (1992)

Hong Z, Jin H, Tzfira T and Li J "Multiple mechanism-mediated retention of a defective brassinosteroid receptor in the endoplasmic reticulum of *Arabidopsis*" Plant Cell, 20:3418-3429 (2008)

Huang CY and Tan TH "DUSPs, to MAP kinases and beyond" Cell Biosci, 2:24 (2012)

Huang S, Nelson CJ, Li L *et al.* "INTERMEDIATE CLEAVAGE PEPTIDASE55 modifies enzyme amino termini and alters protein stability in *Arabidopsis* mitochondria" Plant Physiol, 168:415-427 (2015)

Hsu VW, Lee SY and Yang JS "The evolving understanding of COPI vesicle formation" Nat Rev Mol Cell Biol, 10:360-364 (2009)

Huibregtse JM, Scheffner M, Beaudenon S and Howley PM "A family of proteins structurally and functionally related to the E6-AP ubiquitin-protein ligase" Proc Natl Acad Sci USA, 92:2563-2567 (1995)

Hunter PR, Craddock CP *et al*. "Fluorescent reporter proteins for the tonoplast and the vacuolar lumen identify a single vacuolar compartment in *Arabidopsis* cells" Plant Physiol, 145:1371-1382 (2007)

Huotari J and Helenius A "Endosome maturation" EMBO J, 30:3481-3500 (2011)

Hüttner S and Strasser R "Endoplasmic reticulum-associated degradation of glycoproteins in plants" Front Plant Sci, 3:67 (2012)

Ibl V and Stoger E "The formation, function and fate of protein storage compartments in seeds" Protoplasma, 249:379-392 (2011)

Imai Y, Soda M and Takahashi R "Parkin suppresses unfolded protein stress-induced cell death through its E3 ubiquitin-protein ligase activity" J Biol Chem, 275:35661-35664 (2000)

Inada N and Ueda T "Membrane trafficking pathways and their roles in plant-microbe interactions" Plant Cell Physiol, 55:672-686 (2014)

Isasa M, Katz EJ, Kim W *et al*. "Monoubiquitination of RPN10 regulates substrate recruitment to the proteasome" Mol Cell, 38:733-745 (2010)

Isono E and Nagel MK "Deubiquitylating enzymes and their emerging role in plant biology" Front Plant Sci, 5:56 (2014)

Ito Y, Toyooka K *et al*. "The *trans*-Golgi network and the Golgi stacks behave independently during regeneration after brefeldin A treatment in tobacco BY-2 cells" Plant Cell Physiol, 58:811-821 (2017)

Jabnoune M, Secco D, Lecampion C *et al*. "A rice *cis*-natural antisense RNA acts as a translational enhancer for its cognate mRNA and contributes to phosphate homeostasis and plant fitness" Plant Cell, 25:4166-4182 (2013)

Janska H, Kwasniak M and Szczepanowska J "Protein quality control in organelles - AAA/FtsH story" Biochim Biophys Acta, 1833:381-387 (2013)

Jarosch E, Taxis C, Volkwein C *et al*. "Protein dislocation from the ER requires polyubiquitination and the AAA-ATPase Cdc48" Nat Cell Biol, 4:134-139 (2002)

Jarsch IK, Konrad SSA, Konrad TF *et al*. "Plasma membranes are subcompartmentalized into a plethora of coexisting and diverse microdomains in *Arabidopsis* and *Nicotiana benthamiana*" Plant Cell, 26:1698-1711 (2014)

Jauh GY, Fischer AM, Grimes HD *et al*. "δ-Tonoplast intrinsic protein defines unique plant vacuole functions" Proc Natl Acad Sci USA, 95:12995-12999 (1998)

Jauh GY, Phillips TE and Rogers JC "Tonoplast intrinsic protein isoforms as markers for vacuolar functions" Plant Cell, 11:1867-1882 (1999)

Jiang L, Phillips TE, Rogers SW and Rogers JC "Biogenesis of the protein storage vacuole crystalloid" J Cell Biol, 150:755-770 (2000)

Jiang X, Coffino P and Li X "Development of a method for screening short-lived proteins using green fluorescent protein" Genome Biol, 5(10):R81 (2004)

Jiang YH and Beaudet AL "Human disorders of ubiquitination and proteasomal degradation" Curr Opin Pediatr, 16:419-426 (2004)

Jin H, Li S and Villegas A Jr "Down-regulation of the 26S proteasome subunit RPN9 inhibits viral systemic transport and alters plant vascular development" Plant Physiol, 142:651-661 (2006)

Jin H, Yan Z, Nam K and Li J "Allele-specific suppression of a defective brassinosteroid receptor reveals a physiological role of UGGT in ER quality control" Mol Cell, 26:821-830 (2007)

Jin L, Williamson A, Banerjee S *et al*. "Mechanism of ubiquitin-chain formation by the human anaphase-promoting complex" Cell, 133:653-665 (2008)

Jin X, Cheng H, Chen J and Zhu D "RNF13: an emerging RING finger ubiquitin ligase important in cell proliferation" FEBS J, 278:78-84 (2011)

Joazeiro CA and Weissman AM "RING finger proteins: mediators of ubiquitin ligase activity" Cell, 102:549-552 (2000)

Johanson U, Karlsson M, Johansson I *et al*. "The complete set of genes encoding major intrinsic proteins in *Arabidopsis* provides a framework for a new nomenclature for major intrinsic proteins in plants" Plant Physiol, 126:1358-1369 (2001)

Joukov V, Chen J, Fox EA *et al*. "Functional communication between endogenous BRCA1 and its partner, BARD1, during *Xenopus laevis* development" Proc Natl Acad Sci USA, 98:12078-12083 (2001)

Jue D, Sang X, Lu S *et al*. "Genome-wide identification, phylogenetic and expression analyses of the ubiquitin-conjugating enzyme gene family in maize" PLoS One, 10(11):e0143488 (2015)

Kajava AV "What curves alpha-solenoids? Evidence for an alpha-helical toroid structure of Rpn1 and Rpn2 proteins of the 26 S proteasome" J Biol Chem, 277:49791-49798 (2002)

Kajava AV, Gorbea C, Ortega J *et al*. "New HEAT-like repeat motifs in proteins regulating proteasome structure and function" J Struct Biol, 146:425-430 (2004)

Kalchman MA, Graham RK, Xia G *et al*. "Huntingtin is ubiquitinated and interacts with a specific ubiquitin-conjugating enzyme" J Biol Chem, 271:19385-19394 (1996)

Kamadurai HB, Qiu Y, Deng A *et al*. "Mechanism of ubiquitin ligation and lysine prioritization by a HECT E3" eLife, 2:e00828 (2013)

Kamisugi Y, Schlink K, Rensing SA, Schween G *et al*. "The mechanism of gene targeting in *Physcomitrella patens*: homologous recombination, concatenation and multiple integration" Nucleic Acids Res, 34:6205-6214 (2006)

Kang BH, Nielsen E, Preuss ML *et al*. "Electron tomography of RabA4b- and PI-4Kβ1-labeled *Trans* Golgi network compartments in *Arabidopsis*" Traffic, 12:313-329 (2011)

Kanyuka K, Praekelt U, Franklin KA *et al*. "Mutations in the huge *Arabidopsis* gene BIG affect a range of hormone and light responses" Plant J, 35:57-70 (2003)

Kao SH, Wu HT and Wu KJ "Ubiquitination by HUWE1 in tumorigenesis and beyond" J Biomed Sci, 25:67 (2018)

Keren-Kaplan T, Zeev Peters L, Levin-Kravets O *et al*. "Structure of ubiquitylated-Rpn10 provides insight into its autoregulation mechanism" Nat Commun, 7:12960 (2016)

Kervinen J, Tobin GJ, Costa J *et al*. "Crystal structure of plant aspartic proteinase prophytepsin: inactivation and vacuolar targeting" EMBO J, 18:3947-3955 (1999)

Keyse SM "An emerging family of dual specificity MAP kinase phosphatases" Biochim Biophys Acta, 1265:152-160 (1995)

Kim DH, Eu YJ, Yoo CM *et al*. "Trafficking of phosphatidylinositol 3-phosphate from the *trans*-Golgi network to the lumen of the central vacuole in plant cells" Plant Cell, 13:287-301 (2001)

Kim DY, Scalf M, Smith LM and Vierstra RD "Advanced proteomic analyses yield a deep catalog of ubiquitylation targets in *Arabidopsis*" Plant Cell, 25:1523-1540 (2013)

Kim HJ, Oh SA, Brownfield L *et al*. "Control of plant germline proliferation by SCF(FBL17) degradation of cell cycle inhibitors" Nature, 455:1134-1137 (2008)

Kim ST, Lee YJ, Tasaki T *et al*. "The N-recognin UBR4 of the N-end rule pathway is required for neurogenesis and homeostasis of cell surface proteins" PLoS One, 13(8):e0202260 (2018)

Kirchhausen T "Clathrin" Annu Rev Biochem, 69:699-727 (2000)

Kirsch T, Paris N, Butler JM *et al*. "Purification and initial characterization of a potential plant vacuolar targeting receptor" Proc Natl Acad Sci USA, 91:3403-3407 (1994)

Knowles TJ, Finka R, Smith C *et al*. "Membrane proteins solubilized intact in lipid containing nanoparticles bounded by styrene maleic acid copolymer" J Am Chem Soc, 131:7484-7485 (2009)

Kominami K, Okura N *et al*. "Yeast counterparts of subunits S5a and p58 (S3) of the human 26S proteasome are encoded by two multicopy suppressors of nin1-1" Mol Biol Cell, 8:171-187 (1997)

Kors S, Geijtenbeek K, Reits E and Schipper-Krom S "Regulation proteasome activity by (post-) transcriptional mechanisms" Front Mol Biosci, 6:48 (2019)

Kraft E, Stone SL, Ma L *et al*. "Genome analysis and functional characterization of the E2 and RING-type E3 ligase ubiquitination enzymes of *Arabidopsis*" Plant Physiol, 139:1597-1611 (2005)

Krawitz P, Haffner C, Fluhrer R *et al*. "Differential localization and identification of a critical aspartate suggest non-redundant proteolytic functions of the presenilin homologues SPPL2b and SPPL3" J Biol Chem, 280:39515-39523 (2005)

Kuge O, Hara-Kuge S, Orci L *et al*. "Zeta-COP, a subunit of coatomer, is required for COP-coated vesicle assembly" J Cell Biol, 123:1727-1734 (1993)

Kurokawa K, Suda Y and Nakano A "Sar1 localizes at the rims of COPII-coated membranes in vivo" J Cell Sci, 129:3231-3237 (2016)

Kwon YT, Lévy F and Varshavsky A "Bivalent inhibitor of the N-end rule pathway" J Biol Chem, 274:18135-18139 (1999)

Kwon YT, Reiss Y, Fried VA *et al*. "The mouse and human genes encoding the recognition component of the N-end rule pathway" Proc Natl Acad Sci USA, 95:7898-7903 (1998)

Kyriakis JM and Avruch J "Mammalian mitogen-activated protein kinase signal transduction pathways activated by stress and inflammation" Physiol Rev, 81:807-869 (2001)

Lam SK, Tse YC, Robinson DG and Jiang L "Tracking down the elusive early endosome" Trends Plant Sci, 12:497-505 (2007)

LaMontagne ED, Collins CA, Peck SC and Heese A "Isolation of microsomal membrane proteins from *Arabidopsis thaliana*" Current Protocols in Plant Biology, 1:217-234 (2016)

Langhans M, Förster S, Helmchen G and Robinson DG "Differential effects of the brefeldin A analogue (6R)-hydroxy-BFA in tobacco and *Arabidopsis*" J Exp Bot, 62:2949-2957 (2011)

Lederkremer GZ, Cheng, Y, Petre BM *et al*. "Structure of the Sec23p/24p and Sec13p/31p complexes of COPII" Proc Natl Acad Sci USA, 98:10704-10709 (2001)

Lee JH and Kim WT "Regulation of abiotic stress signal transduction by E3 ubiquitin ligases in *Arabidopsis*" Mol Cells, 31:201-208 (2011)

Lee SC, Bennett BC, Hong WX *et al*. "Steroid-based facial amphiphiles for stabilization and crystallization of membrane proteins" Proc Natl Acad Sci USA, 110:E1203-E1211 (2013)

Lee SC, Knowles T, Postis V *et al*. "A method for detergent-free isolation of membrane proteins in their local lipid environment. Nat Protoc, 11:1149-1162 (2016)

Lee SY, Ramirez J, Franco M *et al*. "Ube3a, the E3 ubiquitin ligase causing Angelman syndrome and linked to autism, regulates protein homeostasis through the proteasomal shuttle Rpn10" Cell Mol Life Sci, 71:2747-2758 (2014)

Leitner J, Petrášek J, Tomanov K *et al*. "Lysine63-linked ubiquitylation of PIN2 auxin carrier protein governs hormonally controlled adaptation of *Arabidopsis* root growth" Proc Natl Acad Sci USA, 109:8322-8327 (2012)

Lerner DR and Raikhel NV "Cloning and characterization of root-specific barley lectin" Plant Physiol, 91:124-129 (1989)

Lerner RS, Seiser RM, Zheng T *et al*. "Partitioning and translation of mRNAs encoding soluble proteins on membrane-bound ribosomes" RNA, 9:1123-1137 (2003)

Li J, Han Y, Zhao Q *et al*. "The E3 ligase *At*RDUF1 positively regulates salt stress responses in *Arabidopsis thaliana*" PLoS One, 8(8):e71078 (2013)

Li L, Nelson C, Fenske R, Trösch J *et al*. "Changes in specific protein degradation rates in *Arabidopsis thaliana* reveal multiple roles of Lon1 in mitochondrial protein homeostasis" Plant J, 89:458-471 (2017)

Li L, Nelson CJ, Solheim C *et al*. "Determining degradation and synthesis rates of *Arabidopsis* proteins using the kinetics of progressive ^{15}N labeling of two-dimensional gel-separated protein spots" Mol Cell Proteomics, 11(6):M111.010025 (2012)

Li LM, Lü SY and Li RJ "The *Arabidopsis* endoplasmic reticulum associated degradation pathways are involved in the regulation of heat stress response" Biochem Biophys Res Commun, 487:362-367 (2017)

Li N and Li Y "Signaling pathways of seed size control in plants" Curr Opin Plant Biol, 33:23-32 (2016)

Li R, Liu P, Wan Y *et al*. "A membrane microdomain-associated protein, *Arabidopsis* Flot1, is involved in a clathrin-independent endocytic pathway and is required for seedling development" Plant Cell, 24:2105-2122 (2012)

Lin JT, Lineberry NB, Kattah MG *et al*. "Naive CD4 T cell proliferation is controlled by mammalian target of rapamycin regulation of GRAIL expression" J Immunol, 182:5919-5928 (2009)

Lineberry N, Su L, Soares L and Fathman CG "The single subunit transmembrane E3 ligase gene related to anergy in lymphocytes (GRAIL) captures and then ubiquitinates transmembrane proteins across the cell membrane" J Biol Chem, 283:28497-28505 (2008)

Lineberry NB, Su LL, Lin JT *et al*. "Cutting edge: The transmembrane E3 ligase GRAIL ubiquitinates the costimulatory molecule CD40 ligand during the induction of T cell anergy" J Immunol, 181:1622-1626 (2008)

Liu J, Wang F, Mao J *et al*. "High-sensitivity N-glycoproteomic analysis of mouse brain tissue by protein extraction with a mild detergent of N-dodecyl β-D-maltoside" Anal Chem, 87:2054-2057 (2015)

Liu J, Zhang C, Wei C *et al*. "The RING finger ubiquitin E3 ligase *Os*HTAS enhances heat tolerance by promoting H_2O_2-induced stomatal closure in rice" Plant Physiol, 170:429-443 (2016)

Liu JX and Howell SH "Endoplasmic reticulum protein quality control and its relationship to environmental stress responses in plants" Plant Cell, 22:2930-2942 (2010)

Liu JX and Howell SH "Managing the protein folding demands in the endoplasmic reticulum of plants" New Phytol, 211:418-428 (2016)

Liu Y, Kahn RA and Prestegard JH "Structure and membrane interaction of myristoylated ARF1" Structure, 17:79-87 (2009)

Liu YC "The E3 ubiquitin ligase Itch in T cell activation, differentiation, and tolerance" Semin Immunol, 19:197-205 (2007)

Loo TW and Clarke DM "Rapid purification of human P-glycoprotein mutants expressed transiently in HEK 293 cells by nickel-chelate chromatography and characterization of their drug-stimulated ATPase activities" J Biol Chem, 270:21449-21452 (1995)

Lorenz S "Structural mechanisms of HECT-type ubiquitin ligases" Biol Chem, 399:127-145 (2018)

Lorick KL, Jensen JP, Fang S *et al*. "RING fingers mediate ubiquitin-conjugating enzyme (E2)-dependent ubiquitination" Proc Natl Acad Sci USA, 96:11364-11369 (1999)

Lovering R, Hanson IM, Borden KL *et al*. "Identification and preliminary characterization of a protein motif related to the zinc finger" Proc Natl Acad Sci USA, 90:2112-2116 (1993)

Lucas JI, Arnau V and Marín I "Comparative genomics and protein domain graph analyses link ubiquitination and RNA metabolism" J Mol Biol, 357:9-17 (2006)

Luirink J and Sinning I "SRP-mediated protein targeting: structure and function revisited" Biochim Biophys Acta, 1694:17-35 (2004)

Luo F, Fong YH, Zeng Y *et al*. "How vacuolar sorting receptor proteins interact with their cargo proteins: crystal structures of apo and cargo-bound forms of the protease-associated domain from an *Arabidopsis* vacuolar sorting receptor" Plant Cell, 26:3693-3708 (2014)

Luschnig C and Vert G "The dynamics of plant plasma membrane proteins: PINs and beyond" Development, 141:2924-2938 (2014)

Lussier MP, Herring BE, Nasu-Nishimura Y *et al*. "Ubiquitin ligase RNF167 regulates AMPA receptor-mediated synaptic transmission" Proc Natl Acad Sci USA, 109:19426-19431 (2012)

Lynes EM and Simmen T "Urban planning of the endoplasmic reticulum (ER): how diverse mechanisms segregate the many functions of the ER" Biochim Biophys Acta, 1813:1893-1905 (2011)

Mace PD, Linke K, Feltham R *et al*. "Structures of the cIAP2 RING domain reveal conformational changes associated with ubiquitin-conjugating enzyme (E2) recruitment" J Biol Chem, 283:31633-31640 (2008)

Mahon P and Bateman A "The PA domain: a protease-associated domain" Protein Sci, 9:1930-1934 (2000)

Maor R, Jones A, Nühse TS *et al*. "Multidimensional protein identification technology (MudPIT) analysis of ubiquitinated proteins in plants" Mol Cell Proteomics, 6:601-610 (2007)

Marín I "RBR ubiquitin ligases: diversification and streamlining in animal lineages" J Mol Evol, 69:54-64 (2009)

Marín I and Ferrús A "Comparative genomics of the RBR family, including the Parkinson's disease-related gene parkin and the genes of the *Ariadne* subfamily" Mol Biol Evol, 19:2039-2050 (2002)

Marín I, Lucas JI, Gradilla AC and Ferrús A "Parkin and relatives: the RBR family of ubiquitin ligases" Physiol Genomics, 17:253-263 (2004)

Marino D, Peeters N and Rivas S "Ubiquitination during plant immune signaling" Plant Physiol, 160:15-27 (2012)

Markson G, Kiel C, Hyde R, Brown S *et al*. "Analysis of the human E2 ubiquitin conjugating enzyme protein interaction network" Genome Res, 19:1905-1911 (2009)

Marmor M and Yarden Y "Role of protein ubiquitylation in regulating endocytosis of receptor tyrosine kinases" Oncogene, 23:2057-2070 (2004)

Marques AJ, Glanemann C, Ramos PC and Dohmen RJ "The C-terminal extension of the beta7 subunit and activator complexes stabilizes nascent 20 S proteasomes and promotes their maturation" J Biol Chem, 282:34869-34876 (2007)

Martínez-Menárguez JA, Geuze HJ, Slot JW and Klumperman J "Vesicular tubular clusters between the ER and Golgi mediate concentration of soluble secretory proteins by exclusion from COPI-coated vesicles" Cell, 98:81-90 (1999)

Martins S, Dohmann EM, Cayrel A *et al*. "Internalization and vacuolar targeting of the brassinosteroid hormone receptor BRI1 are regulated by ubiquitination" Nat Commun, 6:6151 (2015)

Marty F "Plant vacuoles" Plant Cell, 11:587-599 (1999)

Maruyama S, Miyajima N, Bohgaki M *et al*. "Ubiquitylation of epsilon-COP by PIRH2 and regulation of the secretion of PSA" Mol Cell Biochem, 307:73-82 (2008)

Maspero E, Valentini E, Mari S *et al*. "Structure of a ubiquitin-loaded HECT ligase reveals the molecular basis for catalytic priming" Nat Struct Mol Biol, 20:696-701 (2013)

Matheson LA, Hanton SL and Brandizzi F "Traffic between the plant endoplasmic reticulum and Golgi apparatus: to the Golgi and beyond" Current Opinion in Plant Biology, 9:601-609 (2006)

Mazzucotelli E, Belloni S, Marone D *et al*. "The E3 Ubiquitin ligase gene family in plants: regulation by degradation" Curr Genomics, 7:509-522 (2006)

McCaffrey K and Braakman I "Protein quality control at the endoplasmic reticulum" Essays Biochem, 60:227-235 (2016)

Metzger MB, Pruneda JN, Klevit RE and Weissman AM "RING-type E3 ligases: Master manipulators of E2 ubiquitin-conjugating enzymes and ubiquitination" Biochim Biophys Acta, 1843:47-60 (2014)

Miao Y and Zentgraf U "A HECT E3 ubiquitin ligase negatively regulates *Arabidopsis* leaf senescence through degradation of the transcription factor WRKY53" Plant J, 63:179-188 (2010)

Mishkind ML, Palevitz BA, Raikhel NV and Keegstra K "Localization of wheat germ agglutinin--like lectins in various species of the *Gramineae*" Science, 220:1290-1292 (1983)

Moon J, Parry G and Estelle M "The ubiquitin-proteasome pathway and plant development" Plant Cell, 16:3181-3195 (2004)

Morett E and Bork P "A novel transactivation domain in parkin" Trends Biochem Sci, 24:229-231 (1999)

Morrison KA, Akram A *et al*. "Membrane protein extraction and purification using styrene-maleic acid (SMA) copolymer: effect of variations in polymer structure" Biochem J, 473:4349-4360 (2016)

Mousavi SA, Malerød L *et al*. "Clathrin-dependent endocytosis" Biochem J, 377:1-16 (2004)

Muñoz FF, Mendieta JR, Pagano MR *et al*. "The swaposin-like domain of potato aspartic protease (StAsp-PSI) exerts antimicrobial activity on plant and human pathogens" Peptides, 31:777-785 (2010)

Munro S and Pelham HR "A C-terminal signal prevents secretion of luminal ER proteins" Cell, 48:899-907 (1987)

Myant KB, Cammareri P *et al*. "HUWE1 is a critical colonic tumour suppressor gene that prevents MYC signalling, DNA damage accumulation and tumour initiation" EMBO Mol Med, 9:181-197 (2017)

Nakamura M, Toyota M *et al*. "An *Arabidopsis* E3 ligase, SHOOT GRAVITROPISM9, modulates the interaction between statoliths and F-actin in gravity sensing" Plant Cell, 23:1830-1848 (2011)

Nakano A, Brada D and Schekman R "A membrane glycoprotein, Sec12p, required for protein transport from the endoplasmic reticulum to the Golgi apparatus in yeast" J Cell Biol, 107:851-863 (1988)

Nakano A and Muramatsu M "A novel GTP-binding protein, Sar1p, is involved in transport from the endoplasmic reticulum to the Golgi apparatus" J Cell Biol, 109:2677-2691 (1989)

Nakatani Y, Konishi H, Vassilev A *et al*. "p600, a unique protein required for membrane morphogenesis and cell survival" Proc Natl Acad Sci USA, 102:15093-15098 (2005)

Nam SE and Paetzel M "Structure of signal peptide peptidase A with C-termini bound in the active sites: insights into specificity, self-processing and regulation" Biochemistry, 52:8811-8822 (2013)

Nawkar GM, Lee ES, Shelake RM *et al*. "Activation of the transducers of unfolded protein response in plants" Front Plant Sci, 9:214 (2018)

Nelson CJ, Li L, Jacoby RP and Millar AH "Degradation rate of mitochondrial proteins in *Arabidopsis thaliana* cells" J Proteome Res, 12:3449-3459 (2013)

Neuhaus JM, Pietrzak M and Boller T "Mutation analysis of the C-terminal vacuolar targeting peptide of tobacco chitinase: low specificity of the sorting system, and gradual transition between intracellular retention and secretion into the extracellular space" Plant J, 5:45-54 (1994)

Neuhaus JM and Rogers JC "Sorting of proteins to vacuoles in plant cells" Plant Mol Biol, 38:127-144 (1998)

Neuhaus JM, Sticher L, Meins F Jr and Boller T "A short C-terminal sequence is necessary and sufficient for the targeting of chitinases to the plant vacuole" Proc Natl Acad Sci USA, 88:10362-10366 (1991)

Nickel W, Brügger B and Wieland FT "Vesicular transport: the core machinery of COPI recruitment and budding" J Cell Sci, 115:3235-3240 (2002)

Nickel W, Sohn K *et al*. "p23, a major COPI-vesicle membrane protein, constitutively cycles through the early secretory pathway" Proc Natl Acad Sci USA, 94:11393-11398 (1997)

Obradovic Z, Peng K, Vucetic S *et al*. "Exploiting heterogeneous sequence properties improves prediction of protein disorder" Proteins, 61:176-182 (2005)

Occhialini A, Gouzerh G, Di Sansebastiano GP and Neuhaus JM: "Dimerization of the vacuolar receptors *At*RMR1 and-2 from *Arabidopsis thaliana* contributes to their localization in the *trans*-Golgi Network" Int J Mol Sci, 17:1661 (2016)

Oda Y, Hirata A, Sano T *et al*. "Microtubules regulate dynamic organization of vacuoles in *Physcomitrella patens*" Plant Cell Physiol, 50:855-868 (2009)

Ohta M and Takaiwa F "*Os*Hrd3 is necessary for maintaining the quality of endoplasmic reticulum-derived protein bodies in rice endosperm" J Exp Bot, 66:4585-4593 (2015)

Okamoto T "Transport of proteases to the vacuole: ER export bypassing Golgi?" The Plant Endoplasmic Reticulum, 4:125-139 (2006)

Okita TW and Rogers JC "Compartmentation of proteins in the endomembrane system of plant cells" Annu Rev Plant Physiol Plant Mol Biol, 47:327-350 (1996)

Olsen GJ, Matsuda H, Hagstrom and Overbeek R "fastDNAmL: a tool for construction of phylogenetic trees of DNA sequences using maximum likelihood" Comput Appl Biosci, 10:41-48 (1994)

Oluwole AO, Danielczak B, Meister A *et al*. "Solubilization of membrane proteins into functional lipid-bilayer nanodiscs using a diisobutylene/maleic acid copolymer" Angew Chem Int Ed Engl, 56:1919-1924 (2017)

Orwick-Rydmark M, Lovett JE, Graziadei A *et al*. "Detergent-free incorporation of a seven-transmembrane receptor protein into nanosized bilayer Lipodisq particles for functional and biophysical studies" Nano Lett, 12:4687-4692 (2012)

Otegui MS and Reyes FC "Endosomes in plants" Nature Education, 3:23 (2010)

Ovecka M, Lang I, Baluska F *et al*. "Endocytosis and vesicle trafficking during tip growth of root hairs" Protoplasma, 226:39-54 (2005)

Paciorek T, Zazímalová E, Ruthardt N *et al*. "Auxin inhibits endocytosis and promotes its own efflux from cells" Nature, 435:1251-1256 (2005)

Paris N, Rogers SW, Jiang L *et al*. "Molecular cloning and further characterization of a probable plant vacuolar sorting receptor" Plant Physiol, 115:29-39 (1997)

Paris N, Stanley CM, Jones RL and Rogers JC "Plant cells contain two functionally distinct vacuolar compartments" Cell, 85:563-572 (1996)

Park JH, Oufattole M and Rogers JC "Golgi-mediated vacuolar sorting in plant cells: RMR proteins are sorting receptors for the protein aggregation/membrane internalization pathway" Plant Science, 172:728-745 (2007)

Park M, Lee D, Lee GJ and Hwang I "*At*RMR1 functions as a cargo receptor for protein trafficking to the protein storage vacuole" J Cell Biol, 170:757-767 (2005)

Park SH and Blackstone C "Further assembly required: construction and dynamics of the endoplasmic reticulum network" EMBO Rep, 11:515-521 (2010)

Park SY and Guo X "Adaptor protein complexes and intracellular transport" Biosci Rep, 34(4):e00123 (2014)

Passmore LA and Barford D "Getting into position: the catalytic mechanisms of protein ubiquitylation" Biochem J, 379:513-525 (2004)

Paul MJ and Frigerio L "Coated vesicles in plant cells" Semin Cell Dev Biol, 18:471-478 (2007)

Pedersen JT and Palmgren M "Why do plants lack sodium pumps and would they benefit from having one?" Funct Plant Biol, 44:473-479 (2017)

Pelham HR and Rothman JE "The debate about transport in the Golgi--two sides of the same coin?" Cell, 102:713-719 (2000)

Perazza D, Herzog M, Hülskamp M *et al*. "Trichome cell growth in *Arabidopsis thaliana* can be derepressed by mutations in at least five genes" Genetics, 152:461-476 (1999)

Pereira C, Pereira S and Pissarra J: "Delivering of proteins to the plant vacuole--an update" Int J Mol Sci, 15:7611-7623 (2014)

Pereira C, Pereira S, Satiat-Jeunemaitre B and Pissarra J "Cardosin A contains two vacuolar sorting signals using different vacuolar routes in tobacco epidermal cells" Plant J, 76:87-100 (2013)

Peter S, Bultinck J, Myant K *et al*. "Tumor cell-specific inhibition of MYC function using small molecule inhibitors of the HUWE1 ubiquitin ligase. EMBO Mol Med, 6:1525-1541 (2014)

Petroski MD and Deshaies RJ "Function and regulation of cullin-RING ubiquitin ligases" Nat Rev Mol Cell Biol, 6:9-20 (2005)

Pfeffer SR "How the Golgi works: a cisternal progenitor model" 107:19614-19618 (2010)

Phillipson BA, Pimpl P, daSilva LL *et al*. "Secretory bulk flow of soluble proteins is efficient and COPII dependent" Plant Cell, 13:2005-2020 (2001)

Pickart CM and Eddins MJ "Ubiquitin: structures, functions, mechanisms" Biochim Biophys Acta, 1695:55-72 (2004)

Pickrell AM and Youle RJ "The roles of PINK1, parkin, and mitochondrial fidelity in Parkinson's disease" Neuron, 85:257-273 (2015)

Pimpl P, Movafeghi A, Coughlan S *et al*. "In situ localization and in vitro induction of plant COPI-coated vesicles" Plant Cell, 12:2219-2236 (2000)

Prelich G "Gene overexpression: uses, mechanisms and interpretation" Genetics, 190:841-854 (2012)

Price JC, Guan S, Burlingame A *et al*. "Analysis of proteome dynamics in the mouse brain" Proc Natl Acad Sci USA, 107:14508-14513 (2010)

Prigge MJ and Bezanilla M "Evolutionary crossroads in developmental biology: *Physcomitrella patens*" Development, 137:3535-3543 (2010)

Pruneda JN, Stoll KE, Bolton LJ *et al*. "Ubiquitin in motion: structural studies of the ubiquitin-conjugating enzyme∼ubiquitin conjugate" Biochemistry, 50:1624-1633 (2011)

Quatrano RS, McDaniel SF, Khandelwal A *et al*. "*Physcomitrella patens*: mosses enter the genomic age" Curr Opin Plant Biol, 10:182-189 (2007)

Raffaele S, Bayer E, Lafarge D *et al*. "Remorin, a *solanaceae* protein resident in membrane rafts and plasmodesmata, impairs *potato virus X* movement" Plant Cell, 21:1541-1555 (2009)

Rahighi S, Ikeda F, Kawasaki M *et al*. "Specific recognition of linear ubiquitin chains by NEMO is important for NF-kappaB activation" Cell, 136:1098-1109 (2009)

Raiborg C and Stenmark H "The ESCRT machinery in endosomal sorting of ubiquitylated membrane proteins" Nature, 458:445-452 (2009)

Ramalho-Santos M, Pissarra J, Veríssimo P *et al*. "Cardosin A, an abundant aspartic proteinase, accumulates in protein storage vacuoles in the stigmatic papillae of *Cynara cardunculus* L" Planta, 203:204-212 (1997)

Reid DW and Nicchitta CV "Diversity and selectivity in mRNA translation on the endoplasmic reticulum" Nat Rev Mol Cell Biol, 16:221-231 (2015)

Rensing SA, Lang D, Zimmer AD *et al*. "The *Physcomitrella* genome reveals evolutionary insights into the conquest of land by plants" Science, 319:64-69 (2008)

Repetto G, del Peso A and Zurita JL "Neutral red uptake assay for the estimation of cell viability/cytotoxicity" Nat Protoc, 3:1125-1131 (2008)

Reski R "Development, genetics and molecular biology of mosses" Botanica Acta, 111:1-15 (1998)

Reynolds GD, Wang C, Pan J and Bednarek SY "Inroads into internalization: five years of endocytic exploration" Plant Physiol, 176:208-218 (2018)

Richardson LG, Howard AS, Khuu N *et al*. "Protein-protein interaction network and subcellular localization of the *Arabidopsis thaliana* ESCRT machinery" Front Plant Sci, 2:20 (2011)

Richter S, Müller L, Stierhof YD *et al*. "Polarized cell growth in *Arabidopsis* requires endosomal recycling mediated by GBF1-related ARF exchange factors" Nat Cell Biol, 14:80-86 (2012)

Rinschen MM, Bharill P, Wu X *et al*. "The ubiquitin ligase Ubr4 controls stability of podocin/MEC-2 supercomplexes" Hum Mol Genet, 25:1328-1344 (2016)

Robinson DG and Aniento F "A model for ERD2 function in higher plants" Front Plant Sci, 11:343 (2020)

Robinson DG, Brandizzi F, Hawes C and Nakano A "Vesicles versus tubes: is endoplasmic reticulum-Golgi transport in plants fundamentally different from other eukaryotes?" Plant Physiol, 168:393-406 (2015)

Robinson DG and Neuhaus JM "Receptor-mediated sorting of soluble vacuolar proteins: myths, facts, and a new model" J Exp Bot, 67:4435-4449 (2016)

Rosenzweig R, Bronner V, Zhang D *et al*. "Rpn1 and Rpn2 coordinate ubiquitin processing factors at proteasome" J Biol Chem, 287:14659-14671 (2012)

Rosenzweig, R, Osmulski PA, Gaczynska M and Glickman MH "The central unit within the 19S regulatory particle of the proteasome" Nat Struct Mol Biol, 15:573-580 (2008)

Rosquete MR, Davis DJ and Drakakaki G "The plant *Trans*-Golgi network: not just a matter of distinction" Plant Physiol, 176:187-198 (2018)

Rothman JE "Mechanisms of intracellular protein transport" Nature, 372:55-63 (1994)

Rothman JE and Wieland FT "Protein sorting by transport vesicles" Science, 272:227-234 (1996)

Rotin D and Kumar S "Physiological functions of the HECT family of ubiquitin ligases" Nat Rev Mol Cell Biol, 10:398-409 (2009)

Ruiz-May E, Kim SJ, Brandizzi F and Rose JK "The secreted plant N-glycoproteome and associated secretory pathways" Front Plant Sci, 3:117 (2012)

Runeberg-Roos P and Saarma M "Phytepsin, a barley vacuolar aspartic proteinase, is highly expressed during autolysis of developing tracheary elements and sieve cells" Plant J, 15:139-145 (1998)

Rusten TE and Stenmark H "How do ESCRT proteins control autophagy?" J Cell Sci, 122:2179-2183 (2009)

Ryan PE, Davies GC, Nau MM and Lipkowitz S "Regulating the regulator: negative regulation of Cbl ubiquitin ligases" Trends Biochem Sci, 31:79-88 (2006)

Saalbach G, Jung R, Kunze G *et al*. "Different legumin protein domains act as vacuolar targeting signals" Plant Cell, 3:695-708 (1991)

Sabovljević M and Sabovljević A "Contribution to the coastal bryophytes of the Northern Mediterranean: are there halophytes among bryophytes?" Phytologia Balcanica, 13:131-135 (2007)

Sadowski M and Sarcevic B "Mechanisms of mono- and poly-ubiquitination: Ubiquitination specificity depends on compatibility between the E2 catalytic core and amino acid residues proximal to the lysine" Cell Div, 5:19 (2010)

Sadowski M, Suryadinata R, Tan AR *et al*. "Protein monoubiquitination and polyubiquitination generate structural diversity to control distinct biological processes" IUBMB Life, 64:136-142 (2012)

Saeki Y "Ubiquitin recognition by the proteasome" J Biochem, 161:113-124 (2017)

Saito C and Ueda T "Chapter 4: functions of RAB and SNARE proteins in plant life" Int Rev Cell Mol Biol, 274:183-233 (2009)

Sakai T, Mochizuki S, Haga K *et al*. "The wavy growth 3 E3 ligase family controls the gravitropic response in *Arabidopsis* roots" Plant J, 70:303-314 (2012)

Salvat C, Wang G, Dastur A *et al*. "The -4 phenylalanine is required for substrate ubiquitination catalyzed by HECT ubiquitin ligases" J Biol Chem, 279:18935-18943 (2004)

Šamaj J, Müller J, Beck M *et al*. "Vesicular trafficking, cytoskeleton and signalling in root hairs and pollen tubes" Trends Plant Sci, 11:594-600 (2006)

Sanderfoot AA, Ahmed SU, Marty-Mazars D *et al*. "A putative vacuolar cargo receptor partially colocalizes with *At*PEP12p on a prevacuolar compartment in *Arabidopsis* roots" Proc Natl Acad Sci USA, 95:9920-9925 (1998)

Sarikas A, Hartmann T and Pan ZQ "The cullin protein family" Genome Biol, 12:220 (2011)

Sato K and Nakano A "Mechanisms of COPII vesicle formation and protein sorting" FEBS Lett, 581:2076-2082 (2007)

Sauer B "Functional expression of the cre-lox site-specific recombination system in the yeast *Saccharomyces cerevisiae*" Mol Cell Biol, 7:2087-2096 (1987)

Sawasdikosol S, Pratt JC, Meng W *et al*. "Adapting to multiple personalities: Cbl is also a RING finger ubiquitin ligase" Biochim Biophys Acta, 1471:M1-M12 (2000)

Scabone CM, Frigerio L and Petruccelli S "A fluorescent reporter protein containing *At*RMR1 domains is targeted to the storage and central vacuoles in *Arabidopsis thaliana* and tobacco leaf cells" Plant Cell Rep, 30:1823-1833 (2011)

Schaaf A, Reski R and Decker EL "A novel aspartic proteinase is targeted to the secretory pathway and to the vacuole in the moss *Physcomitrella patens*" Eur J Cell Biol, 83:145-152 (2004)

Schaefer DG and Zrÿd JP "Efficient gene targeting in the moss *Physcomitrella patens* Plant J, 11:1195-1206 (1997)

Schaefer DG and Zrÿd JP "The moss *Physcomitrella patens*, now and then" Plant Physiol, 127:1430-1438 (2001)

Schaefer DG, Zryd JP, Knight CD and Cove DJ "Stable transformation of the moss *Physcomitrella patens*" Mol Gen Genet, 226:418-424 (1991)

Scheffner M, Huibregtse JM, Vierstra RD and Howley PM "The HPV-16 E6 and E6-AP complex functions as a ubiquitin-protein ligase in the ubiquitination of p53" Cell, 75:495-505 (1993)

Scheuring D, Künzl F, Viotti C *et al*. "Ubiquitin initiates sorting of Golgi and plasma membrane proteins into the vacuolar degradation pathway" BMC Plant Biol, 12:164 (2012)

Scheuring D, Viotti C, Krüger F *et al*. "Multivesicular bodies mature from the *trans*-Golgi network/early endosome in *Arabidopsis*" Plant Cell, 23:3463-3481 (2011)

Schmidt O and Teis D "The ESCRT machinery" Curr Biol, 22:R116-R120 (2012)

Schöneberg J, Lee IH, Iwasa JH and Hurley JH "Reverse-topology membrane scission by the ESCRT proteins" Nat Rev Mol Cell Biol, 18:5-17 (2017)

Schreiber A, Stengel F, Zhang Z *et al*. "Structural basis for the subunit assembly of the anaphase-promoting complex" Nature, 470:227-232 (2011)

Schwanhäusser B, Busse D, Li N *et al*. "Global quantification of mammalian gene expression control" Nature, 473:337-342 (2011)

Serafini T, Stenbeck G, Brecht A *et al*. "A coat subunit of Golgi-derived non-clathrin-coated vesicles with homology to the clathrin-coated vesicle coat protein beta-adaptin" Nature, 349:215-220 (1991)

Seroogy CM, Soares L, Ranheim EA, SU L *et al*. "The gene related to anergy in lymphocytes, an E3 ubiquitin ligase, is necessary for anergy induction in CD4 T cells" J Immunol, 173:79-85 (2004)

Shan SO, Schmid SL and Zhang X "Signal recognition particle (SRP) and SRP receptor: a new paradigm for multistate regulatory GTPases" Biochemistry, 48:6696-6704 (2009)

Shen Y, Wang J, Ding Y *et al*. "The rice RMR1 associates with a distinct prevacuolar compartment for the protein storage vacuole pathway" Mol Plant, 4:854-868 (2011)

Shimada T, Fuji K, Tamura K *et al*. "Vacuolar sorting receptor for seed storage proteins in *Arabidopsis thaliana*" Proc Natl Acad USA, 100:16095-16100 (2003)

Shimada T, Kuroyanagi M, Nishimura M and Hara-Nishimura I "A pumpkin 72-kDa membrane protein of precursor-accumulating vesicles have characteristics for a vacuolar sorting receptor" Plant Cell Physiol, 38:1414-1420 (1997)

Shringarpure R, Grune T, Mehlhase J and Davies KJ "Ubiquitin conjugation is not required for the degradation of oxidized proteins by proteasome" J Biol Chem, 278:311-318 (2003)

Sigismund S, Algisi V, Nappo G *et al*. "Threshold-controlled ubiquitination of the EGFR directs receptor fate" EMBO J, 32:2140-2157 (2013)

Silva-Alvim FAL, An J, Alvim JC *et al.* "Predominant Golgi-residency of the plant K/HDEL receptor is essential for its function in mediating ER retention" Plant Cell, 30:2174-2196 (2018)

Simões I and Faro C "Structure and function of plant aspartic proteinases" Eur J Biochem, 271:2067-2075 (2004)

Smalle J, Kurepa J, Yang P, Babiychuk E *et al*. "Cytokinin growth responses in *Arabidopsis* involve the 26S proteasome subunit RPN12" Plant Cell, 14:17-32 (2002)

Smalle J, Kurepa J, Yang P, Emborg TJ *et al.* "The pleiotropic role of the 26S proteasome subunit RPN10 in *Arabidopsis* growth and development supports a substrate-specific function in abscisic acid signaling" Plant Cell, 15:965-980 (2003)

Smalle J and Vierstra RD "The ubiquitin 26S proteasome proteolytic pathway" Annu Rev Plant Biol, 55:555-590 (2004)

Sohn K, Orci L, Ravazzola M, Amherdt M *et al*. "A major transmembrane protein of Golgi-derived COPI-coated vesicles involved in coatomer binding" J Cell Biol, 135:1239-1248 (1996)

Soss SE, Yue Y, Dhe-Paganon S and Chazin WJ "E2 conjugating enzyme selectivity and requirements for function of the E3 ubiquitin ligase CHIP" J Biol Chem, 286:21277-21286 (2011)

Sparkes IA, Frigerio L, Tolley N and Hawes C "The plant endoplasmic reticulum: a cell-wide web" Biochem J, 423:145-155 (2009)

Stanley P "Golgi glycosylation" Cold Spring Harb Perspect Biol, 3(4):a005199 (2011)

Stefano G, Renna L, Chatre L *et al*. "In tobacco leaf epidermal cells, the integrity of protein export from the endoplasmic reticulum and of ER export sites depends on active COPI machinery" Plant J, 46:95-110 (2006)

Stenbeck G, Harte C *et al*. "beta'-COP, a novel subunit of coatomer" EMBO J, 12:2841-2845 (1993)

Stewart MD, Ritterhoff T *et al*. "E2 enzymes: more than just middle men" Cell Res, 26:423-440 (2016)

Sticher L, Hinz U, Meyer AD and Meins F Jr "Intracellular transport and processing of a tobacco vacuolar β-1,3-glucanase" Plant, 188:559-565 (1992)

Stoebel DM, Dean AM and Dykhuizen DE "The cost of expression of *Escherichia coli* lac operon proteins is in the process, not in the products" Genetics, 178:1653-1660 (2008)

Stone SL "Role of the ubiquitin proteasome system in plant response to abiotic stress" Int Rev Cell Mol Biol, 343:65-110 (2018)

Stone SL, Hauksdóttir H, Troy A *et al*. "Functional analysis of the RING-type ubiquitin ligase family of *Arabidopsis*" Plant Physiol, 137:13-30 (2005)

Stone SL, Williams LA, Farmer LM *et al*. "KEEP ON GOING, a RING E3 ligase essential for *Arabidopsis* growth and development, is involved in abscisic acid signalling" Plant Cell, 18:3415-3428 (2006)

Su L, Lineberry N *et al*. "A novel E3 ubiquitin ligase substrate screen identifies Rho guanine dissociation inhibitor as a substrate of gene related to anergy in lymphocytes" J Immunol, 177:7559-7566 (2006)

Sutter JU, Sieben C, Hartel A *et al*. "Abscisic acid triggers the endocytosis of the *Arabidopsis* KAT1 K^+ channel and its recycling to the plasma membrane" Curr Biol, 17:1396-1402 (2007)

Svozil J, Hirsch-Hoffmann M *et al*. K "Protein abundance changes and ubiquitylation targets identified after inhibition of the proteasome with syringolin A" Mol Cell Proteomics, 13:1523-1536 (2014)

Swanson SJ, Bethke PC and Jones RL "Barley aleurone cells contain two types of vacuoles: characterization of lytic organelles by use of fluorescent probes" Plant Cell, 10:685-698 (1998)

Takeuchi J, Fujimuro M, Yokosawa H *et al*. "Rpn9 is required for efficient assembly of the yeast 26S proteasome" Mol Cell Biol, 19:6575-6584 (1999)

Tanaka K "The proteasome: overview of structure and functions" Proc Jpn Acad Ser B Phys Biol Sci, 85:12-36 (2009)

Tang YC and Amon A "Gene copy-number alterations: a cost-benefit analysis" Cell, 152:394-405 (2013)

Tanigawa G, Orci L, Amherdt M *et al*. "Hydrolysis of bound GTP by ARF protein triggers uncoating of Golgi-derived COP-coated vesicles" J Cell Biol, 123:1365-1371 (1993)

Tasaki T, Kim ST, Zakrzewska A *et al*. "UBR box N-recognin-4 (UBR4), an N-recognin of the N-end rule pathway, and its role in yolk sac vascular development and autophagy" Proc Natl Acad Sci USA, 110:3800-3805 (2013)

Tasaki T, Mulder LC, Iwamatsu A *et al*. "A family of mammalian E3 ubiquitin ligases that contain the UBR box motif and recognize N-degrons" Mol Cell Biol, 25:7120-7136 (2005)

Tasaki T, Sriram SM *et al*. "The N-end rule pathway" Annu Rev Biochem, 81:261-289 (2012)

Thrower JS, Hoffman L, Rechsteiner M and Pickart CM "Recognition of the polyubiquitin proteolytic signal" EMBO J, 19:94-102 (2000)

Törmäkangas K, Hadlington JL, Pimpl P *et al*. "A vacuolar sorting domain may also influence the way in which proteins leave the endoplasmic reticulum" Plant Cell, 13:2021-2032 (2001)

Toyooka K, Goto Y, Asatsuma S *et al*. "A mobile secretory vesicle cluster involved in mass transport from the Golgi to the plant cell exterior" Plant Cell, 21:1212-1229 (2009)

Toyooka K, Okamoto T and Minamikawa T "Mass transport of proform of a KDEL-tailed cysteine proteinase (SH-EP) to protein storage vacuoles by endoplasmic reticulum-derived vesicle is involved in protein mobilization in germinating seeds" J Cell Biol, 148:453-464 (2000)

Tranque P, Crossin KL, Cirelli C *et al*. "Identification and characterization of a RING zinc finger gene (C-RZF) expressed in chicken embryo cells" Proc Natl Acad Sci USA, 93:3105-3109 (1996)

Traub LM "Tickets to ride: selecting cargo for clathrin-regulated internalization" Nat Rev Mol Cell Biol, 10:583-596 (2009)

Tse YC, Mo B, Hillmer S *et al*. "Identification of multivesicular bodies as prevacuolar compartments in *Nicotiana tabacum* BY-2 cells" Plant Cell, 16:672-693 (2004)

Turek I, Tischer N, Lassig R and Trujillo M "Multi-tiered pairing selectivity between E2 ubiquitin-conjugating enzymes and E3 ligases" J Biol Chem, 293:16324-16336 (2018)

Turjanski AG, Vaqué JP and Gutkind JS "MAP kinases and the control of nuclear events" Oncogene, 26:3240-3253 (2007)

Uldrijan S, Pannekoek WJ and Vousden KH "An essential function of the extreme C-terminus of MDM2 can be provided by MDMX" EMBO J, 26:102-112 (2007)

van der Lee R, Lang B, Kruse K *et al*. "Intrinsically disordered segments affect protein half-life in the cell and during evolution" Cell Rep, 8:1832-1844 (2014)

van der Reijden BA, Erpelinck-Verschueren CA *et al*. "TRIADs: a new class of proteins with a novel cysteine-rich signature" Protein Sci, 8:1557-1561 (1999)

van Dijk JR, Yamazaki Y and Palmer RH "Tumour-associated mutations of PA-TM-RING ubiquitin ligases RNF167/RNF13 identify the PA domain as a determinant for endosomal localization" Biochem J, 459:27-36 (2014)

Van Hoewyk D "Defects in endoplasmic reticulum-associated degradation (ERAD) increase selenate sensitivity in *Arabidopsis*" Plant Signal Behav, 13(4):e1171451 (2018)

van Wijk KJ "Protein maturation and proteolysis in plant plastids, mitochondria, and peroxisomes" Annu Rev Plant Biol, 66:75-111 (2015)

Vander Kooi CW, Ohi MD, Rosenberg JA *et al*. "The Prp19 U-box crystal structure suggests a common dimeric architecture for a class of oligomeric E3 ubiquitin ligases" Biochemistry, 45:121-130 (2006)

Varedi K SM, Ventura AC, Merajver SD and Lin XN "Multisite phosphorylation provides an effective and flexible mechanism for switch-like protein degradation" PLoS One, 5(12):e14029 (2010)

Vavouri T, Semple JI, Garcia-Verdugo R and Lehner B "Intrinsic protein disorder and interaction promiscuity are widely associated with dosage sensitivity" Cell, 138:198-208 (2009)

Verchot J "How does the stressed out ER find relief during virus infection?" Curr Opin Virol, 17:74-79 (2016)

Verdecia MA, Joazeiro CA, Wells NJ *et al.* "Conformational flexibility underlies ubiquitin ligation mediated by the WWP1 HECT domain E3 ligase" Mol Cell, 11:249-259 (2003)

Verma R, Aravind L, Oania R *et al*. "Role of Rpn11 metalloprotease in deubiquitination and degradation by the 26S proteasome" Science, 298:611-615 (2002)

Vida TA and Emr SD "A new vital stain for visualizing vacuolar membrane dynamics and endocytosis in yeast" J Cell Biol, 128:779-792 (1995)

Vieira M, Pissarr J, Veríssimo P *et al*. "Molecular cloning and characterization of cDNA encoding cardosin B, an aspartic proteinase accumulating extracellularly in the transmitting tissue of *Cynara cardunculus* L" Plant Mol Biol, 45:529-539 (2001)

Vierstra RD "The ubiquitin-26S proteasome system at the nexus of plant biology" Nat Rev Mol Cell Biol, 10:385-397 (2009)

Vildanova MS, Wang W and Smirnova EA "Specific organization of Golgi apparatus in plant cells" Biochemistry (Mosc), 79:894-906 (2014)

Viotti C, Bubeck J, Stierhof YD *et al*. "Endocytic and secretory traffic in *Arabidopsis* merge in the *trans*-Golgi network/early endosome, an independent and highly dynamic organelle" Plant Cell, 22:1344-1357 (2010)

Vitale A and Chrispeels MJ “Sorting of proteins to the vacuoles of plant cells” Bioessays, 14:151-160 (1992)

Voorhees RM and Hegde RS “Structures of the scanning and engaged states of the mammalian SRP-ribosome complex” eLife, 4:e07975 (2015)

Voss M, Schroder B and Fluhrer R “Mechanism, specificity and physiology of signal peptide peptidase (SPP) and SPP-like proteases” Biochim Biophys Acta, 1828:2828-2839 (2013)

Wada T and Penninger J “Mitogen-activated protein kinases in apoptosis regulation” Oncogene 23:2838-2849 (2004)

Wang H, Rogers JC and Jiang L “Plant RMR proteins: unique vacuolar sorting receptors that couple ligand sorting with membrane internalization” FEBS J, 278:59-68 (2011)

Wang H, Tse YC, Law AH *et al*. “Vacuolar sorting receptors (VSRs) and secretory carrier membrane proteins (SCAMPs) are essential for pollen tube growth” Plant J, 61:826-838 (2010)

Wang L, Li H, Lv X *et al*. “Spatiotemporal dynamics of the BRI1 receptor and its regulation by membrane microdomains in living *Arabidopsis* cells” Mol Plant, 8:1334-1349 (2015)

Wang Q, Zhao Y *et al*. “Single-particle analysis reveals shutoff control of the *Arabidopsis* ammonium transporter AMT1;3 by clustering and internalization” Proc Natl Acad Sci USA, 110:13204-13209 (2013)

Wang S, Kurepa J and Smalle JA “The *Arabidopsis* 26S proteasome subunit RPN1a is required for optimal plant growth and stress responses” Plant Cell Physiol, 50:1721-1725 (2009)

Wang T, Liu NS, Seet LF and Hong W “The emerging role of VHS domain-containing Tom1, Tom1L1 and Tom1L2 in membrane trafficking” Traffic, 11:1119-1128 (2010)

Wang X, Yang P, Gao Q *et al*. “Proteomic analysis of the response to high-salinity stress in *Physcomitrella patens*” Planta, 228:167-177 (2008)

Ward JJ, Sodhi JS, McGuffin LJ *et al*. “Prediction and functional analysis of native disorder in proteins from the three kingdoms of life” J Mol Biol, 337:635-645 (2004)

Waters MG, Serafini T and Rothman JE “Coatomer: a cytosolic protein complex containing subunits of non-clathrin-coated Golgi transport vesicles” Nature, 349:248-251 (1991)

Weissman AM, Shabek N and Ciechanover A “The predator becomes the prey: regulating the ubiquitin system by ubiquitylation and degradation” Nat Rev Mol Cell Biol, 12:605-620 (2011)

Wendler P, Lehmann A, Janek K *et al*. “The bipartite nuclear localization sequence of Rpn2 is required for nuclear import of proteasomal base complexes via karyopherin alphabeta and proteasome functions” J Biol Chem, 279:37751-37762 (2004)

Wenzel DM, Lissounov A, Brzovic PS and Klevit RE “UBCH7 reactivity profile reveals parkin and HHARI to be RING/HECT hybrids” Nature, 474:105-108 (2011)

Westrate LM, Lee JE, Prinz WA and Voeltz GK “Form follows function: the importance of endoplasmic reticulum shape” Annu Rev Biochem, 84:791-811 (2015)

Whitelegge JP, le Coutre J, Lee JC *et al*. "Toward the bilayer proteome, electrospray ionization-mass spectrometry of large, intact transmembrane proteins" Proc Natl Acad Sci USA, 96:10695-10698 (1999)

Whiting CC, Su LL, Lin JT and Fathman CG "GRAIL: a unique mediator of CD4 T-lymphocyte unresponsiveness" FEBS J, 278:47-58 (2011)

Wiener R, DiBello AT, Lombardi PM *et al*. "E2 ubiquitin-conjugating enzymes regulate the deubiquitinating activity of OTUB1" Nat Struct Mol Biol, 20:1033-1039 (2013)

Wiggins CM, Tsvetkov P, Johnson M *et al*. "BIM(EL), an intrinsically disordered protein, is degraded by 20S proteasomes in the absence of poly-ubiquitylation" J Cell Sci, 124:969-977 (2011)

Wilbur JD, Hwang PK and Brodsky FM "New faces of the familiar clathrin lattice" Traffic, 6:346-350 (2005)

Windheim M, Peggie M and Cohen P "Two different classes of E2 ubiquitin-conjugating enzymes are required for the mono-ubiquitination of proteins and elongation by polyubiquitin chains with a specific topology" Biochem J, 409:723-729 (2008)

Worden EJ, Dong KC and Martin A "An AAA motor-driven mechanical switch in Rpn11 controls deubiquitination at the 26S proteasome" Mol Cell, 67:799-811 (2017)

Wu H, Carvalho P and Voeltz GK "Here, there, and everywhere: The importance of ER membrane contact sites" Science, 3:361(6401):eaan5835 (2018)

Wu PY, Hanlon M, Eddins M *et al*. "A conserved catalytic residue in the ubiquitin-conjugating enzyme family" EMBO J, 22:5241-5250 (2003)

Wu X and Rapoport TA "Mechanistic insights into ER-associated protein degradation" Curr Opin Cell Biol, 53:22-28 (2018)

Xia T, Li N, Dumenil J, Li J *et al*. "The ubiquitin receptor DA1 interacts with the E3 ubiquitin ligase DA2 to regulate seed and organ size in *Arabidopsis*" Plant Cell, 25:3347-3359 (2013)

Xiang L, Etxeberria E and Van den Ende W "Vacuolar protein sorting mechanisms in plants" FEBS J, 280:979-993 (2013)

Xu P, Hankins HM, MacDonald C *et al*. "COPI mediates recycling of an exocytic SNARE by recognition of a ubiquitin sorting signal" eLife 6:e28342 (2017)

Yamada HY and Gorbsky GJ "Tumor suppressor candidate TSSC5 is regulated by UbcH6 and a novel ubiquitin ligase RING105" Oncogene, 25:1330-1339 (2006)

Yamazaki Y, Schönherr C, Varshney GK *et al*. "Goliath family E3 ligases regulate the recycling endosome pathway via VAMP3 ubiquitylation" EMBO J, 32:524-537 (2013)

Yang CY, Chiu LL, Chang CC *et al*. "Induction of DUSP14 ubiquitination by PRMT5-mediated arginine methylation" FASEB J, 32(12):fj201800244RR (2018)

Yang XY, Chen WP, Rendahl AK *et al*. "Measuring the turnover rates of *Arabidopsis* proteins using deuterium oxide: an auxin signaling case study" Plant J, 63:680-695 (2010)

Yoshida A, Sakai N, Uekusa Y *et al*. "Morphological changes of plasma membrane and protein assembly during clathrin-mediated endocytosis" PLoS Biol, 16(5):e2004786 (2018)

Zaaroor-Regev D, de Bie P, Scheffner M *et al*. "Regulation of the polycomb protein Ring1B by self-ubiquitination or by E6-AP may have implications to the pathogenesis of Angelman syndrome" Proc Natl Acad Sci USA, 107:6788-6793 (2010)

Zhang H, Cui F, Wu Y *et al*. "The RING finger ubiquitin E3 ligase SDIR1 targets SDIR1-INTERACTING PROTEIN1 for degradation to modulate the salt stress response and ABA signaling in *Arabidopsis*" Plant Cell, 27:214-227 (2015)

Zhang Q, Fan L, Hou F *et al*. "New insights into the RNA-binding and E3 ubiquitin ligase activities of Roquins" Sci Rep, 5:15660 (2015)

Zhang Q, Meng Y, Zhang L *et al*. "RNF13: a novel RING-type ubiquitin ligase over-expressed in pancreatic cancer" Cell Res, 19:348-357 (2009)

Zhang Q, Wang K, Zhang Y *et al*. "The myostatin-induced E3 ubiquitin ligase RNF13 negatively regulates the proliferation of chicken myoblasts" FEBS J, 277:466-476 (2010)

Zoghbi ME, Cooper RS and Altenberg GA "The lipid bilayer modulates the structure and function of an ATP-binding cassette exporter" J Biol Chem, 291:4453-4461 (2016)

Zouhar J, Muñoz A and Rojo E "Functional specialization within the vacuolar sorting receptor family: VSR1, VSR3 and VSR4 sort vacuolar storage cargo in seeds and vegetative tissues" Plant J, 64:577-588 (2010)